

Development of Analytical Methodology for Neurochemical Investigations

David J. Fischer

M.S., University of Kansas, 2006

M.S., Saint Louis University, 2003

B.S., Saint Louis University, 2001

Submitted to the Department of Pharmaceutical Chemistry and the Faculty of the Graduate School of the University of Kansas in partial fulfillment of the requirements for the degree of Doctor of Philosophy.

Date Approved

This dissertation is dedicated to my mother Rosemarie and my father William. Your support, encouragement, and undying love has given me the courage and inspiration to pursue my dreams.

Abstract

David J. Fischer
Department of Pharmaceutical Chemistry
University of Kansas

Neurochemical Applications of Microchip Electrophoresis

The development of sensitive and selective analytical tools has facilitated the investigation of complex neurological pathways and enhanced our understanding of neurodegenerative diseases. The development of sensitive analytical methodology for the determination of neurotransmitters and proteins related to neurodegenerative disease is described. The goal of the work performed in the first part of this dissertation was to develop analytical methodology for the analysis of catecholamine neurotransmitters (NTs) by microchip electrophoresis with electrochemical (EC) detection. Much of this work focused on the fabrication and characterization of the novel carbon-based electrode material, pyrolyzed photoresist. The fabrication of pyrolyzed photoresist film (PPF) electrodes was optimized for use in microchip electrophoresis and analytical performance was characterized using catecholamine NTs. In addition, an extensive comparison of the analytical performance of several commonly used electrode materials and electrode alignment schemes and the PPF electrode material was performed. Aspects such as sensitivity, limit of detection (LOD), resolution, reproducibility, and ease of fabrication were examined.

In addition to the development of EC detection methods for catecholamine NTs, analytical methods for the determination of myc-tagged proteins were

developed. The development of an electrophoretic immunoaffinity assay for the detection of a myc-tagged protein expressed in cell culture is described. While this is a general assay that can be applied to a variety of myc-tagged proteins, mutant huntingtin protein (mHtt) was used as a specific example. The development and optimization of capillary and microchip electrophoresis assays were performed for this purpose. In addition, the results obtained using these methods were directly compared to traditional analysis by Western blotting. The long term goal of this project is integrate both of these assays into a single lab-on-a-chip device capable of detecting NT release and mHtt protein in single cells.

Acknowledgements

My graduate school experience at the University of Kansas has been enriched through the interaction with many wonderful people. The completion of my Ph.D. would not have been possible without their friendship and support, for which I am truly grateful. I would like to first thank my friend and advisor Susan Lunte. I am very fortunate to have had such an understanding and patient advisor. Your consummate enthusiasm for new projects and ideas always lifted my spirits and inspired me to work harder. The compassion you showed was a reminder that you cared about us as individuals not just as employees. Taken collectively, these experiences have facilitated my development as a scientist as well as a person. I feel extremely fortunate to have worked for you and can only hope that my future employers are as pleasant to work for as you have been.

It is often said that graduate students inevitably turn out like their advisor. As such, I have had the fortune of working with a great group of people over the years. I want to thank many previous students and postdocs who not only took time to instruct me in the lab but were also friends: Bryan Huynh, Nathan Lacher, Walter (Van) Vandaveer, and Barb Fogarty. I also need to thank all of the current lab members (Pradyot Nandi, Courtney Kuhnline, Tom Linz, Anne Regel, Jessica Creamer, and Ryan Grigsby) for being such great coworkers and friends. I thank you for the many discussions about or relating to food, the many trips to the Chinese buffet, and numerous outings to enjoy a frosty beverage while discussing the finer points of life.

Much of what I have accomplished would not have been possible without the friendship of Pradyot Nandi. Throughout the years, you have always been someone I could turn to for help or advice. There is no doubt that I would have had a much tougher time getting through classes and prelim exams if it were not for your help. I also thank you for being a great coworker who was quick to give guidance or instruction, and thank you for being a great friend that I could always count on for advice or to simply listen. I must also acknowledge the extremely valuable contribution our postdoc, Matt Hulvey, has made to our lab in the past two years. I cannot think of anyone else who is as eager to learn and volunteer his time help others. I appreciate all the great conversations we had about music, science, and life in general during those long days and late nights in the lab.

I must also thank the faculty and staff of the Pharmaceutical Chemistry Department who work diligently to shape and mold young minds. It has been invaluable learning from faculty who possess such a wealth of experience and success. Of course, nothing would be possible without the wonderful staffs in both Pharm Chem and HBC who facilitate everyday operations. I would like to especially thank Nancy Helm for putting up with all of my inane questions and problems.

Finally, I would like to express my deepest appreciation for my family. This dissertation has been dedicated to you as a symbol of my gratitude. Throughout my life you have encouraged me to reach beyond my grasp. You always challenged me to be more than I thought I could be and inspired me to pursue my dreams. I am truly blessed to have had two loving, supportive, and wonderful parents and sister to

help guide my journey though this life. I would not know where I would be; let alone who I would be without your love and support.

Table of Contents

Chapter 1: Thesis Objective and Summary	1
1.1 Research Objective	2
1.2 Chapter Summaries	4
1.3 References	11
Chapter 2: Review of EC Detection for Microchip Electrophoresis	12
2.1 Introduction	13
2.2 Electrochemical Detection Modes for Microchip Electrophoresis	14
2.2.1 Amperometric detection	14
2.2.2 Conductimetric Detection	18
2.2.3 Voltammetric detection	21
2.3 Instrumental Design	23
2.3.1 Microchip Materials	23
2.3.2 Electrode Materials and Fabrication	24
2.3.3 Amperometric Detection: Isolation of the Detector from the Separation Voltage	27
2.3.3.1 End-Channel Alignment	31
2.3.3.2 In-Channel Alignment	34
2.3.3.3 Off-channel Alignment	36
2.3.3.4 Summary	39
2.3.4 Related Electrochemical Detection Modes: Conductimetric Detection	40
2.3.4.1 Contact Conductivity Detection	41
2.3.4.2 Contactless Conductivity Detection	46
2.4 Applications	50
2.4.1 Neurotransmitters and Related Compounds	51
2.4.2 Enzyme and Immunoassays	56
2.4.3 Clinical Assays	60
2.4.4 Environmental Applications	65
2.5 Conclusions and Future Directions	70
2.6 References	72

Chapter 3: Pyrolyzed Photoresist Carbon Electrodes for Microchip Electrophoresis with Dual-Electrode Amperometric Detection	79
3.1 Introduction	80
3.2 Materials and Methods	82
3.2.1 Materials and Reagents	82
3.2.2 Fabrication of PDMS Microchips	83
3.2.3 Electrode Fabrication	84
3.2.4 Chip Construction	86
3.2.5 Electrophoresis Procedure	86
3.2.6 Electrochemical Detection	87
3.3 Results and Discussion	88
3.3.1 Electrode Comparison	88
3.3.2 Electrode Evaluation	89
3.3.3 Dual-Electrode Detection	91
3.4 Conclusions	97
3.5 References	98
Chapter 4: Amperometric Detection in Microchip Electrophoresis Devices: Effect of Electrode Material and Alignment on Analytical Performance	100
4.1 Introduction	101
4.2 Materials and Methods	106
4.2.1 Materials and Reagents	106
4.2.2 PDMS Fabrication	107
4.2.3 Pyrolyzed Carbon Electrode Fabrication	108
4.2.4 Carbon Fiber Electrode Fabrication	109
4.2.5 Carbon Ink Electrode Fabrication	110
4.2.6 Palladium Electrode Fabrication	112
4.2.7 Chip Construction	113
4.2.8 Electrophoresis Procedure	114
4.2.9 Electrochemical Detection	115
4.3 Results and Discussion	117
4.3.1 Comparison of Electrode Fabrication and Alignment	117
4.3.2 Comparison of Electrode Sensitivity	123
4.3.3 Comparison of Limit of Detection	129

4.3.4 In-channel EC EC Detection	133
4.4 Conclusions	134
4.5 References	137
Chapter 5: Part I: Conclusion and Direction of Future Research	140
5.1 Conclusion of Part I	141
5.2 Future Research Directions	144
5.2.1 Serpentine Separation Channels	145
5.2.2 Single Cell Analysis	147
5.2.3 Miniaturization and Integration of Supporting Instrumentation	151
5.3 References	154
Chapter 6: Review of Electrophoretic Methods of Protein Analysis	156
6.1 Introduction	156
6.2 Modes and Methods of Capillary Electrophoresis	161
6.2.1 Sample Preparation	161
6.2.1.1 Preconcentration	161
6.2.1.2 Derivatization	165
6.2.2 Detection Methods	168
6.2.2.1 Ultraviolet Absorbance	168
6.2.2.2 Laser Induced Fluorescence	169
2.2.2.3 Mass Spectrometry	171
6.2.3 Methods of Surface Modification	172
6.2.3.1 Dynamic Wall Coating	174
6.2.3.2 Static Wall Coating	177
6.2.4 Capillary Zone Electrophoresis	179
6.2.5 Micellar Electrokinetic Chromatography	187
6.2.6 Capillary Gel Electrophoresis	195

6.3	Special Electrophoretic Techniques	210
6.3.1	Isoelectric Focusing	210
6.3.2	Affinity Capillary Electrophoresis	212
6.4	Applications of Capillary and Microchip Electrophoresis	216
6.4.1	Analysis of Brain and Cerebrospinal Proteins	216
6.4.2	Analysis of Proteins in Blood and Urine	218
6.5	Conclusions	221
6.6	References	222
Chapter 7:	Development of an Electrophoretic Immunoaffinity Assay for myc-Tagged Proteins: Application to Mutant Huntingtin Protein	234
7.1	Introduction	235
7.2	Materials and Methods	239
7.2.1	Materials and Reagents	239
7.2.2	Cell Culture System	240
7.2.3	Immunoblot Procedure	242
7.2.4	Sample Preparation	244
7.2.4.1	Sample Derivatization Using NDA/CN ⁻	244
7.2.4.2	Immunoaffinity Sample Preparation	245
7.2.5	Capillary Electrophoresis with Laser Induced Detection	245
7.2.6	Microchip Electrophoresis with Laser Induced Detection	246
7.2.6.1	Microchip Fabrication	246
7.2.6.2	Electrophoresis Procedure for NDA Derivatized Samples	249
7.2.6.3	Electrophoresis Procedure for Immunoaffinity Experiments	250
7.2.6.4	Laser Induced Detection for Microchip Electrophoresis	250
7.3	Results and Discussion	251
7.3.1	Detection of mHtt by Immunoblotting	252
7.3.2	Detection of NDA Derivatized mHtt	255
7.3.2.1	Capillary Electrophoresis with Laser Induced	

	Fluorescence	256
7.3.2.2	Microchip Electrophoresis with Laser Induced Fluorescence	258
7.3.3	Detection of mHtt using an Electrophoretic Immunoaffinity Assay	265
7.3.3.1	Capillary Electrophoresis with Laser Induced Fluorescence	266
7.3.3.2	Microchip Electrophoresis with Laser Induced Fluorescence	270
7.4	Conclusions: Comparison of Analytical Performance	274
7.5	References	281
Chapter 8: Part II: Conclusion and Direction of Future Research		284
8.1	Conclusion of Part II	286
8.2	Future Research Directions	291
8.2.1	Immunoaffinity using an Alternate Fluorophore	291
8.2.2	Calmodulin Affinity Assay for Huntingtin Protein	293
8.2.3	Photoaffinity Capture of Calmodulin-binding Proteins	297
8.3	References	301

List of Figures and Tables

Chapter 2

- Figure 2.1 Schematic of common PAD waveforms.
- Figure 2.2 Schematic of a typical C⁴D detector.
- Figure 2.3 Schematic of linear sweep voltammetry and differential pulse voltammetry waveforms.
- Figure 2.4 Comparison of electropherograms for separation and detection of neurotransmitters at a cellulose-DNA-modified vs. unmodified electrode.
- Figure 2.5 Photograph of 3-dimensional electrodes for EC detection with microchip electrophoresis.
- Figure 2.6 Schematic of the three most commonly utilized electrode alignments for microchip EC detection: end-channel alignment, off-channel alignment, and in-channel alignment.
- Figure 2.7 Crescent electrodes with sheath-flow supported electrophoresis for end-channel detection.
- Figure 2.8 In silico modeling of the analyte plug shape resulting from end-channel detection.
- Figure 2.9 Dual-channel microchip for in-channel EC detection.
- Figure 2.10 Electropherograms for the contact conductivity detection of amino acids, peptides, and proteins.
- Figure 2.11 Layout and schematic of a 16 channel contact conductivity detection microchip.
- Figure 2.12 Design and layout of a of a microchip utilizing a bubble cell for contact conductivity detection
- Figure 2.13 Design of a polyester-toner microchip with integrated detection electrodes.
- Figure 2.14 Schematic of a microfabricated low temperature co-fired ceramic device for C⁴D.

- Figure 2.15 Separation of chiral neurotransmitters using microchip electrophoresis with EC detection.
- Figure 2.16 Schematic of bilayer microchip utilizing pneumatically actuated valves for on-line microdialysis sampling with EC detection.
- Figure 2.17 Multiprotein electrical detection protocol based on different inorganic colloid nanocrystal tracers.
- Figure 2.18 Schematic of the biochip used for simultaneous immunological and enzymatic assays.
- Figure 2.19 Microchip device for point-of-care analysis of lithium with integrated sampling from a glass capillary.
- Figure 2.20 Picture of a three electrode paper-based microfluidic device with EC detection.

Chapter 3

- Figure 3.1 Schematic of the photolithographic fabrication procedure used for the PPF electrodes
- Figure 3.2 Direct comparison of a PPF and a carbon fiber electrode using cyclic voltammetry.
- Table 3.1 Normalized sensitivity values for a PPF and a carbon fiber electrode.
- Figure 3.3 Direct comparison of a PPF and a carbon fiber electrode using amperometric detection.
- Figure 3.4 Dual-electrode EC detection of neurotransmitters at a PPF electrode.
- Figure 3.5 Reproducibility of dual-electrode EC detection at a PPF electrode.

Chapter 4

- Figure 4.1 Schematic of the three most commonly utilized electrode alignments for microchip EC detection: end-channel alignment, off-channel alignment, and in-channel alignment.

- Figure 4.2 Pinnacle Technology, Inc. wireless, isolated potentiostat used for in-channel electrochemical detection.
- Figure 4.3 Electropherograms depicting the effect of electrode alignment on resolution and peak shape.
- Table 4.1 Calculated values for the effect of electrode alignment on resolution and peak shape.
- Figure 4.4 Graphical representation and the equations used to calculate peak tailing and peak skew.
- Table 4.2 Normalized sensitivity values for the EC detection of dopamine.
- Table 4.3 Normalized sensitivity values for the EC detection of dopamine, norepinephrine, and catechol.
- Figure 4.5 EC response of CAT at three different end-channel carbon electrodes which depict the differences in the signal-to-noise ratio.
- Table 4.4 Concentration and mass limits of detection for dopamine, norepinephrine, and catechol.
- Table 4.5 Qualitative assessment of electrode performance for various electrode materials and alignments.

Chapter 5

- Figure 5.1 Microchip with serpentine channels and an expanded view of the optimized asymmetric turn profile.
- Figure 5.2 Schematic of an idealized single cell analysis device showing the multiple integrated functions.
- Figure 5.3 Proposed fully integrated μ -TAS device for on-line, on-animal, in vivo microdialysis sampling with in-channel EC detection.

Chapter 6

- Figure 6.1 Depiction of the steps involved in a two-step probing protocol used for Western blot analysis.

- Figure 6.2 Schematic diagrams of a short-channel and long-channel CE-ESI-MS microchip.
- Figure 6.3 Separation of calmodulin by CZE-UV using a boric acid BGE.
- Figure 6.4 Separation of calmodulin by CZE-UV using a phosphate BGE.
- Figure 6.5 Separation of calmodulin by CZE-UV using a tris BGE.
- Figure 6.6 Time course oxidation study of calmodulin.
- Figure 6.7 Oxidation and reduction study of calmodulin.
- Figure 6.8 Separation of calmodulin by MEKC-UV.
- Figure 6.9 MEKC of several proteins utilizing microchip electrophoresis with LIF detection and the effect of separation length on resolution and plate number.
- Figure 6.10 Geometrical layout of the microchip used for 2-dimensional separations.
- Figure 6.11 Separation of a molecular weight ladder using CGE-UV.
- Table 6.1 Concentration and mass sensitivity values of CGE-UV for the detection of a molecular weight ladder.
- Figure 6.12 Linear relationship observed between the log of the molecular weight and the inverse electrophoretic mobility.
- Figure 6.13 Separation and detection of MLCK using CGE-UV compared to analysis by SDS-PAGE.
- Figure 6.14 Separation and detection of eNOS using CGE-UV compared to analysis by SDS-PAGE.
- Figure 6.15 Separation of a mixture of four model proteins separated by CGE-UV.
- Figure 6.16 Schematic of the all-glass microchip used for μ CGE-LIF.
- Figure 6.17 Replicate injections of 500 nM Oregon Green labeled CaM with μ CGE-LIF.

- Figure 6.18 Replicate injections of 500 nM MLCK with μ CGE-LIF.
- Figure 6.19 Replicate injections of 250 nM MLCK and 250 nM CaM with μ CGE-LIF.
- Figure 6.20 Illustration of the preparation of an immunoaffinity capillary and steps of an immunoaffinity assay.

Chapter 7

- Table 7.1 Materials needed to make the resolving gel for Western blot analysis.
- Figure 7.1 Schematic of the two types of all-PDMS microchips used for microchip electrophoresis with LIF detection.
- Figure 7.2 Western blot analysis of vector control (VC) and mutant huntingtin (mHtt) transfected cells.
- Figure 7.3 CE separation and LIF detection of the mHtt insoluble fraction of transfected cells which had been derivatized with NDA.
- Figure 7.4 CE separation and LIF detection of the mHtt insoluble fraction of transfected cells *versus* the VC insoluble fraction which had been derivatized with NDA.
- Figure 7.5 CE separation and LIF detection of the mHtt insoluble fraction of transfected cells *versus* the soluble mHtt fraction which had been derivatized with NDA.
- Figure 7.6 Microchip electrophoresis with LIF detection of the mHtt insoluble fraction of transfected cells which had been derivatized with NDA.
- Figure 7.7 Microchip electrophoresis with LIF detection of the mHtt insoluble fraction of transfected cells *versus* the soluble mHtt fraction which had been derivatized with NDA.

- Figure 7.8 Microchip electrophoresis with LIF detection of the mHtt insoluble fraction of transfected cells *versus* the VC insoluble fraction which had been derivatized with NDA
- Figure 7.9 CE separation and LIF detection of standard solutions of FITC labeled anti-myc mAb.
- Figure 7.10 Calibration curve of the resulting peak area of the FITC labeled anti-myc mAb plotted *versus* the concentration
- Figure 7.11 Electropherogram of the myc-tagged mHtt immunoassay performed using CE-LIF.
- Figure 7.12 Electropherogram of the myc-tagged mHtt immunoassay performed using CE-LIF.
- Figure 7.13 Microchip electrophoresis with LIF detection of standard solutions of FITC labeled anti-myc mAb.
- Figure 7.14 Calibration curve of the resulting peak area of the FITC labeled anti-myc mAb plotted *versus* the concentration.
- Figure 7.15 Electropherogram of the myc-tagged mHtt immunoassay performed using microchip electrophoresis with LIF detection.
- Figure 7.16 Electropherogram of the myc-tagged mHtt immunoassay performed using microchip electrophoresis with LIF detection.
- Table 7.2 Qualitative comparison of the analytical performance of the three methods examined.

Chapter 8

- Figure 8.1 Comparison of the spectral properties of several fluorescein-based dyes and Alexa Fluor 488.
- Figure 8.2 Calmodulin affinity assay protocol.
- Figure 8.3 Schematic of the procedure for photo-reactive protein cross-linking.

List of Abbreviations

CE	capillary electrophoresis
ME	microchip electrophoresis
SDS-PAGE	sodium dodecyl sulfate polyacrylamide gel electrophoresis
MW	molecular weight
MD	microdialysis
HPLC	high performance liquid chromatography
LC	liquid chromatography
LOD	limit of detection
LOQ	limit of quantitation
S/N	signal to noise ratio
HDV	hydrodynamic voltammetry
CV	cyclic voltammetry
PAD	pulsed amperometric detection
iPAD	integrated pulsed amperometric detection
(C ⁴ D)	contactless conductivity detection
SV	sinusoidal voltammetry
AC	alternating current
Hz	Hertz
I _p	peak current
pI	isoelectric point

BGE	background electrolyte
BA	boric acid
PPF	pyrolyzed photoresist film
CZE	capillary zone electrophoresis
MEKC	micellar electrokinetic chromatography
CGE	capillary gel electrophoresis
μ CGE	microchip gel electrophoresis
ITP	isotachophoresis
ACE	affinity capillary electrophoresis
EMMA	electrophoretically mediated microanalysis assay
FAS	field-amplified stacking
FASS	field-amplified sample stacking
FASI	field-amplified sample injection
IEF	isoelectric focusing
CAs	carrier ampholytes
EC	electrochemical detection
CE-EC	capillary electrophoresis with electrochemical detection
LIF	laser-induced fluorescence
LED	light emitting diode
UV	ultraviolet
PMT	photomultiplier tube
MS	mass spectrometry

LC-MS	liquid chromatography with mass spectrometric detection
MALDI	matrix-assisted laser desorption ionization
TOF	time-of-flight
ESI	electrospray ionization
EOF	electroosmotic flow
CMC	critical micelle concentration
LOD	limit of detection
HV	high voltage
HVPS	high voltage power supply
PDMS	poly(dimethylsiloxane)
PMMA	poly(methyl methacrylate)
PET	polyethyleneterephthalate
PE	polyethylene
PT	polyester-toner
PUMA	polyurethane methacrylate
LTCC	low temperature co-fired ceramics
μ -TAS	micro total analysis system
TES	N-tris[hydroxymethyl]methyl-2-aminoethane sulfonic acid
SDS	sodium dodecyl sulfate
PEO	poly(ethylene oxide)
PEG	poly(ethylene glycol)
IPA	isopropyl alcohol

ACN	acetonitrile
DMF	N-N'-dimethylformamide
FITC	fluorescein isothiocyanate
BODIPY	boron-dipyrromethene
DMF	dimethylformamide
β -ME	β -mercaptoethanol
OPA	o-phthalic dicarboxaldehyde
NDA/CN	naphthalene-2,3-dicarboxaldehyde/cyanide ion
CBI	1-cyanobenz(f)isoindole
POC	point of care
NdYAG	neodymium-doped yttrium aluminum garnet
DNA	deoxyribonucleic acid
RNA	ribonucleic acid
SWCNT	single-wall carbon nanotube
MWCNT	multiwall carbon nanotube
AuNPs	gold nanoparticle
GCE	glassy carbon electrode
CNS	central nervous system
NT	neurotransmitter
DA	dopamine
NE	norepinephrine
CAT	catechol

AA	ascorbic acid
Epi	epinephrine
HVA	homovanillic acid
MT	methoxytyramine
L-DOPA	L-dopamine
CaM	calmodulin
CaMBPs	calmodulin binding proteins
MLCK	myosin light chain kinase
eNOS	endothelial nitric oxide synthase
HD	Huntington's disease
mHtt	mutant huntingtin protein
VC	vector control
TG	transglutaminase
BSA	bovine serum albumin
mAb	monoclonal antibody
kDa	kilodaltons
HEK	human embryonic kidney
SCD	sulfated β -cyclodextrin
CA	cellulose acetate
5-HIAA	5-hydroxyindole acetic acid
3D	three-dimensional
2D	two-dimensional

Chapter 1

Thesis Objective and Summary

1.1 Research Objective

Neurodegeneration is a condition of the brain in which neurons suffer a progressive loss of structure or function, often leading to cell death. This term can be used to describe a variety of diseases which include Alzheimer's, Parkinson's, Huntington's, as well as amyotrophic lateral sclerosis (Lou Gehrig's Disease). Neurodegeneration encompasses a host of complications leading to loss of coordination, speech, cognition, and in many cases leads to dementia and/or death [1-2]. Many neurodegenerative diseases, such as Huntington's disease are caused by genetic mutations [3]; however various mechanisms such as mitochondrial dysfunction [4-5], protein degradation [6-7], misfolding [8-9], and aggregation [10-12] have also been implicated. In addition, these conditions can have a profound impact on neurotransmitter (NT) storage and release [13-16]. In many diseases, neurons in brain regions responsible for NT synthesis and storage (such as the substantia nigra) are severely damaged. Deterioration of these pathways can lead to the loss of proper neuronal communication and function which may proceed or accompany cell death.

Despite the wealth of knowledge of these processes, many fundamental questions regarding neurodegenerative diseases remain unanswered. Many of the techniques such as Western blot analysis, immunofluorescence, and high performance liquid chromatography with detection by mass spectrometry (HPLC-MS) which are employed to study proteins involved in disease pathogenesis are often time

consuming and labor intensive. For this reason, there are two major objectives of this research. The first objective is to develop sensitive and selective analytical methods for the electrochemical (EC) detection of catecholamine neurotransmitters (NTs) in conjunction with microchip electrophoresis. The second objective is to develop sensitive and selective analytical methods for the analysis of proteins involved in neurodegeneration. Specifically, mutant huntingtin protein which is involved in the progression of Huntington's disease was used as a model protein. Assays using capillary and microchip electrophoresis with laser induced fluorescence (LIF) detection were developed.

In the first part of this dissertation, the fabrication of novel carbon-based electrode materials for the EC detection of NTs was explored. Carbon-based electrodes are of interest in EC detection due to their low cost, large potential window, and low background noise. In addition, many of the commonly used carbon electrodes such as carbon fiber and carbon ink cannot be microfabricated and are time consuming to produce. For these reasons, a novel approach to creating a microfabricated carbon-based electrode for EC detection was investigated. Once fabrication of pyrolyzed photoresist film (PPF) electrodes was optimized, analytical performance was characterized and compared to alternate electrode materials. It was determined that PPF electrodes were an excellent electrode material which offered superior analytical performance. A concentration limit of detection of ~ 75 nM and a mass limit of detection of ~ 25 amol was achieved for the detection of dopamine.

These values are in the range of biologically relevant concentrations of dopamine in the brain.

The second part of this dissertation focused on the development of an immunoaffinity assay for the analysis of myc-tagged proteins, with specific application to myc-tagged mHtt protein. Both capillary and microchip electrophoresis were utilized in the development of an analytical method that required very little reagent or sample volume. In addition, a fluorescein isothiocyanate (FITC) labeled anti-myc monoclonal antibody (mAb) improved the sensitivity and selectivity of the assay as compared to derivatization with NDA/CN⁻. To assess performance, the results of the newly developed assay were compared to traditional Western Blot analysis. It was determined that both types of analysis have unique advantages and disadvantages. Western blotting provides the greatest resolution between aggregate forms of mHtt. However, the electrophoretic immunoassay provides a high-throughput alternative that drastically reduces analysis time, limits of detection, as well as reagent and sample consumption. Using microchip electrophoresis, a mass limit of detection of ~4.5 pg was achieved for the detection of mHtt.

1.2 Chapter Summaries

1.2.1 Chapter 2

This chapter is a comprehensive review of the use of EC detection with microchip electrophoresis (ME) [17]. Topics such as the most commonly utilized modes of EC detection, fabrication strategies for electrodes and microchips, and

integration of electrodes into microfluidic devices are detailed. In addition, the use of microchip electrophoresis with EC detection for a variety of applications is discussed. While microchip electrophoresis with EC detection has been employed for a variety of applications, recent advances in some of the most common uses including the detection of neurotransmitters (NTs) and related compounds, enzyme and immunoassays, clinical assays, and environmental applications are discussed.

1.2.2 Chapter 3

In this chapter, the fabrication and evaluation of the novel carbon-based electrode material pyrolyzed photoresist film (PPF) electrodes for ME with dual-electrode EC detection is described [18]. Carbon electrodes have previously been employed with microchip CE by inserting a carbon fiber or carbon paste into a microchannel on a polymer substrate. An improved approach for fabricating carbon electrodes involves pyrolyzing photolithographically patterned photoresist on fused silica plates. Once the fabrication procedure was optimized, analytical characteristics such as sensitivity, linearity, and reproducibility of the integrated PPF electrodes were evaluated using catecholamines and related compounds including dopamine (DA), 5-hydroxyindole-3-acetic acid (5-HIAA), ascorbic acid (AA), and catechol (CAT). The performance of the PPF electrodes was then directly compared to carbon fiber microelectrodes that are commonly used for EC detection in microfluidic devices. The PPF electrodes exhibited analytical characteristics which were very similar to the carbon fiber electrode material. In addition, the PPF electrodes proved to be linear

between 5 and 500 μM ($r^2 = 0.998$) with a limit of detection (LOD) of 5 μM (S/N = 3) and sensitivity of 9.4 $\text{pA}/\mu\text{M}$. Electrochemical selectivity was further enhanced by employing a dual-electrode configuration for selective detection of species exhibiting chemically reversible redox reactions.

1.2.3 Chapter 4

Chapter four expands the scope of electrode comparison initiated in chapter 3. Not only were many different electrode materials investigated, but the effects of electrode alignment on analytical performance were also examined [19]. Carbon-based electrode materials such as carbon fiber, carbon ink, and pyrolyzed carbon as well as palladium (Pd) metal electrodes were directly compared. There are three commonly utilized electrode alignment schemes for ME: end-, off-, and in-channel alignment. However, the effect of these alignments on analytical performance had never been quantified. Therefore, parameters such as resolution, limit of detection (LOD), and concentration and mass sensitivity were determined through the separation and EC detection of DA, norepinephrine (NE), and CAT mixtures.

It was determined that a PPF electrode used in an end-channel configuration outperformed all other electrode materials and alignments. The PPF electrode yielded the highest sensitivity and lowest limit of detection (LOD) for all analytes tested. Using PPF electrodes in an end-channel configuration, a concentration LOD of 73 nM and a mass LOD of 25 amol was achieved for the detection of DA. Because end-channel alignment is the easiest to implement, this combination of

electrode material and alignment resulted in the best performing and most user friendly EC detection mode examined.

Off-channel EC detection has been shown to substantially reduce band broadening associated with end-channel alignment, resulting in increased sensitivity. However, it was determined that off-channel detection was much less sensitive than end-channel alignment when the same electrode material was directly compared. In contrast, off-channel alignment did result in greater separation efficiency and resolution than end-channel alignment for the closely migrating species DA and NE. The best resolution was achieved using in-channel alignment. This is because the electrode is placed directly in the separation channel without the use of a decoupler. Although this configuration requires the use of specialized electronics (an electrically isolated potentiostat), in-channel alignment resulted in the most dramatic improvement in peak shape and quality of analytical data.

1.2.4 Chapter 5

Chapter 5 summarizes the progress made concerning the fabrication of pyrolyzed photoresist electrodes for the EC detection of neurotransmitters with ME. In addition, experimental variables such as electrode material and alignment were characterized. Regardless of the application, the judicious choice of these two aspects is critical to the success of any experiment utilizing EC with ME. Therefore, the work performed in the first part of this dissertation aimed to reduce uncertainty associated with choosing the proper electrode material and alignment for a specific

application. Future experiments involving PPF electrodes are also outlined in this chapter. There are a variety of exciting possibilities involving the detection of neurotransmitters and neuroactive compounds. The application of microfluidic technology with EC detection for monitoring NTs released from single neurons is described. In addition, the challenges associated with the development of miniaturized supporting instrumentation (potentiostat and high voltage power supply) for the realization of a self-contained micro-total analysis system are discussed.

1.2.5 Chapter 6

Chapter 6 describes the use of electrophoretic separations for the analysis of proteins. This chapter reviews many of the commonly utilized slab gel techniques such as sodium dodecyl sulfate polyacrylamide gel electrophoresis (SDS-PAGE) and Western blot analysis. In addition the use of many different capillary and microchip electrophoresis techniques are discussed which include capillary zone electrophoresis (CZE), micellar electrokinetic chromatography (MEKC), and capillary gel electrophoresis (CGE). Not only are the fundamentals of the techniques described, but the use of these techniques for a variety of applications is reviewed. In addition, specific examples are given for the separation of calmodulin and related calmodulin binding proteins. Recent advances in the utilization of these techniques for the analysis of neural, cerebrospinal, urinary, and blood proteins are discussed.

1.2.6 Chapter 7

In this chapter, the development of a capillary electrophoresis immunoassay for myc-tagged proteins is described. While this technique can be used for any myc-tagged protein, the applicability is demonstrated for the analysis of mutant huntingtin protein which had been expressed in cells in culture. Mutant huntingtin (mHtt) protein is responsible for the neurodegenerative effects observed in individuals suffering from Huntington's disease. Physical symptoms include loss of coordination and balance, slurred speech, and development of involuntary movements. Cognitive abilities such as judgment and memory are also diminished, which ultimately leads to dementia.

Currently, the most popular methods of analyzing mHtt include gel electrophoresis, immunoblotting, immunofluorescence, and HPLC with MS detection. Although these analysis methods can be sensitive, highly selective, and are well characterized, they are often time consuming and labor intensive. Therefore, the goal of this chapter was to develop a microchip electrophoresis-based assay for the analysis of mHtt protein. This chapter describes the development and evaluation of capillary and microchip electrophoresis methodology with laser induced fluorescence (LIF) detection for the detection of mutant huntingtin protein. An immunoaffinity technique was developed through the use of a fluorescently labeled monoclonal antibody (mAb) specific for myc-tagged proteins. The results obtained from these experiments were then compared to those obtained using conventional Western blot

analysis. Analytical parameters such as selectivity, sensitivity, and limit of detection (LOD) were directly compared.

It was determined that both capillary and microchip electrophoresis were well suited for the determination of mHtt in cell lysates. Compared to Western blot analysis, the CE-based immunoaffinity assay reduced the required sample volume by a factor of 4, the required volume of reagents by a factor of 130, and reduced the analysis time from 36 hr to 5 hr. The limit of detection was significantly reduced as well. The mass LOD was determined to be ~490 pg for CE-LIF and ~4.5 pg for ME-LIF. Despite these advantages, CE and ME techniques are not the best analysis methods. Western blot analysis confirmed the presence of monomeric, dimeric, and high-order aggregate forms of mHtt. However, both CE and ME were unable to separate the multiple forms of mHtt present in the sample. In this regard, Western blot analysis has an obvious advantage over both CE and ME.

1.2.7 Chapter 8

This chapter summarizes progress made on the development of a capillary and microchip electrophoresis method for the analysis of myc-tagged proteins. This chapter describes some of the challenges associated with the development of the mHtt assay, and details possible future directions to improve sensitivity and throughput. In addition, the development of a microfluidic device capable of combining the first and second part of this dissertation is described. Recommendations for future projects which integrate EC and LIF detection onto a single device capable of analyzing single cells are given.

1.3 References

- [1] Bates, G., Harper, P. S., Jones, L., *Huntington's Disease, Third Edition. [In: Oxford Monographs on Medical Genetics., 2002; 45]*, 2002.
- [2] Davies, S. W., Turmaine, M., Cozens, B. A., DiFiglia, M., Sharp, A. H., Ross, C. A., Scherzinger, E., Wanker, E. E., Mangiarini, L., Bates, G. P., *Cell* 1997, *90*, 537-548.
- [3] The Huntington's Disease Collaborative Research Group, T. H. s. D. C. R., *Cell* 1993, *72*, 971-983.
- [4] Choo, Y. S., Johnson, G. V. W., MacDonald, M., Detloff, P. J., Lesort, M., *Human Molecular Genetics*. 2004, *13*, 1407-1420.
- [5] Fernandes, H. B., Baimbridge, K. G., Church, J., Hayden, M. R., Raymond, L. A., *Journal of Neuroscience* 2007, *27*, 13614-13623.
- [6] Cummings Jeffrey, L., *Annals of Neurology* 2003, *54*, 147-154.
- [7] Luque, F. A., Jaffe, S. L., *International Review of Neurobiology* 2009, *84*, 151-165.
- [8] Furukawa, Y., Fu, R., Deng, H.-X., Siddique, T., O'Halloran, T. V., *Proceedings of the National Academy of Sciences* 2006, *103*, 7148-7153.
- [9] Boillee, S., Vande Velde, C., Cleveland, D. W., *Neuron* 2006, *52*, 39-59.
- [10] Cooper, A. J. L., Sheu, K.-F. R., Burke, J. R., Strittmatter, W. J., Gentile, V., Peluso, G., Blass, J. P., *Journal of Neurochemistry* 1999, *72*, 889-899.
- [11] Dudek, N. L., Dai, Y., Muma, N. A., *Journal of Neuropathology & Experimental Neurology* 2008, *67*, 355-365.
- [12] Lindner, A. B., Demarez, A., *Biochimica et Biophysica Acta, General Subjects* 2009, *1790*, 980-996.
- [13] Johnson, M. A., Villanueva, M., Haynes, C. L., Seipel, A. T., Buhler, L. A., Wightman, R. M., *Journal of Neurochemistry* 2007, *103*, 2102-2110.
- [14] Johnson, M. A., Rajan, V., Miller, C. E., Wightman, R. M., *Journal of Neurochemistry* 2006, *97*, 737-746.
- [15] Truong, J. G., 2004, p. 119 pp.
- [16] Leonelli, M., Torrao, A. S., Britto, L. R. G., *Brazilian Journal of Medical and Biological Research* 2009, *42*, 68-75.
- [17] Vandaveer IV, W. R., Padas-Farmer, S. A., Fischer, D. J., Frankenfeld, C. N., Lunte, S., M., *Electrophoresis* 2004, *25*, 3528-3549.
- [18] Fischer, D. J., Vandaveer, W. R. I. V., Grigsby, R. J., Lunte, S. M., *Electroanalysis* 2005, *17*, 1153-1159.
- [19] Fischer, D. J., Hulvey, M. K., Regel, A. R., Lunte, S. M., *Electrophoresis* 2009, *30*, 3324-3333.

Chapter 2

Recent Developments in Electrochemical Detection for Microchip Electrophoresis

(Electrophoresis 2004, 25, 3528-3549)
(Encyclopedia of Analytical Chemistry, In preparation)

2.1. Introduction

Miniaturized microfluidic analysis devices have become increasingly popular since the introduction of the micro total analysis system (μ -TAS) by Manz and co-workers almost two decades ago [1-7]. The integration of several processes on a single chip including sample preparation, mixing, separation, and detection has been demonstrated by several research groups [8-14]. The advantages of incorporating multiple functions on a single chip include reduced analysis time, decreased cost and waste, portability, disposability, and the potential for point-of-care use [15-18].

Although the miniaturized format is amenable to a large number of detection techniques, laser-induced fluorescence (LIF) and electrochemical (EC) detection are most commonly employed [19-21]. LIF has remained very popular for microchip electrophoresis due to its high degree of selectivity, sensitivity, and the low limits of detection (LOD) that can be achieved. However, unless the analyte of interest is natively fluorescent, it must be derivatized prior to detection [22-23]. Mass spectrometry (MS) has also been employed as a detection mode for miniaturized devices [24-28]. MS has the advantage of providing a high degree of chemical information with very small sample volumes; however, commercially available systems are not inherently portable and are more expensive than LIF.

Electrochemical (EC) detection offers many advantages which make it a very popular mode of detection for miniaturized analytical systems [15, 25, 29-31]. Many compounds can be detected without the need for derivatization and with comparable sensitivity and selectivity to that of LIF detection. Since many types of electrodes

can be fabricated using the same photolithographic techniques used to make the microchip, an entirely integrated device can be mass produced. In addition, electrodes can be miniaturized without suffering a loss in sensitivity. These advantages typically produce LODs in the low to mid-nanomolar range [32-34].

There are several modes of EC detection some of which include: amperometry, conductimetry, potentiometry, and voltammetry. While amperometry and conductimetry are most widely used, this review will highlight recent developments in the use of these detection modes with microchip electrophoresis. Topics such as microchip format, materials, and fabrication, electrode materials and design, and integration of several distinct processes on a single miniaturized format will be discussed in the following sections.

2.2 Electrochemical Detection Modes for Microchip Electrophoresis

2.2.1 Amperometric Detection

Due to its ease of operation, selectivity, and high degree of sensitivity, amperometry is the most widely used EC detection method for microchip electrophoresis [15, 31, 35-36]. It is performed by applying a fixed, constant potential to a working electrode while monitoring current as a function of time [37]. An auxiliary electrode can be used to complete a typical 3-electrode electrochemical cell; however, this may be omitted for use as a 2-electrode configuration [38-40]. In addition, a 2-electrode configuration can be used without damaging the detection electronics when the currents generated at the electrode are at or below the low microampere range. Above this, an auxiliary electrode should be used. In either

configuration, the resulting signal (current) is directly proportional to the number of moles of analyte oxidized or reduced at the working electrode as described by Faraday's law:

$$i_t = \frac{dQ}{dt} = nF \frac{dN}{dt} \quad \text{Eq. 1}$$

where i_t is the current generated at the working electrode at time t , Q is the charge at the electrode surface, t is time, n is the number of moles of electrons transferred per mole of analyte, N is the number of moles of analyte oxidized or reduced, and F is the Faraday constant (96,485 C/mol). Selectivity can be achieved through careful selection of electrode potential, which is typically empirically determined by hydrodynamic voltammetry (HDV) or cyclic voltammetry (CV) [41-42].

A variation or subset of fixed-potential amperometry is pulsed amperometric detection (PAD) detection. In this technique, the electrode potential is modulated in a simple three potential step waveform. The surface of the electrode is first oxidized at a high positive potential, reactivated at a negative potential, and then set to an optimum detection potential for analysis while signals are collected. Because this technique relies on electrochemical stripping (or cleaning) of the electrode during the oxidation and reactivation steps, the choice of electrode material is critical. Therefore highly stable metals such as gold and platinum are most often used.

As seen in Figure 2.1, there are two main modes in which PAD waveforms can be employed. Mode I is optimum for carbohydrates and aliphatic compounds, while Mode II is better suited for amines and thiol-compounds [43-45]. Mode I (or

PAD at an oxide-free surface), occurs with little or no formation of surface oxides and the background current is caused by charging of the double-layer. In contrast, Mode II oxidizes the adsorbed analytes simultaneously with the surface material. Alternatively, integrated pulsed amperometric detection (iPAD) uses an integrated potential scan for the detection step (Fig. 2.1B). The integration of oxide formation and dissolution during the triangular waveform produces much faster baseline stabilization, leading to less noise.

The placement and geometry of electrodes used for amperometric detection can vary widely depending on the application. Several electrode configurations and alignments exist which will be discussed in detail in section 3.3.

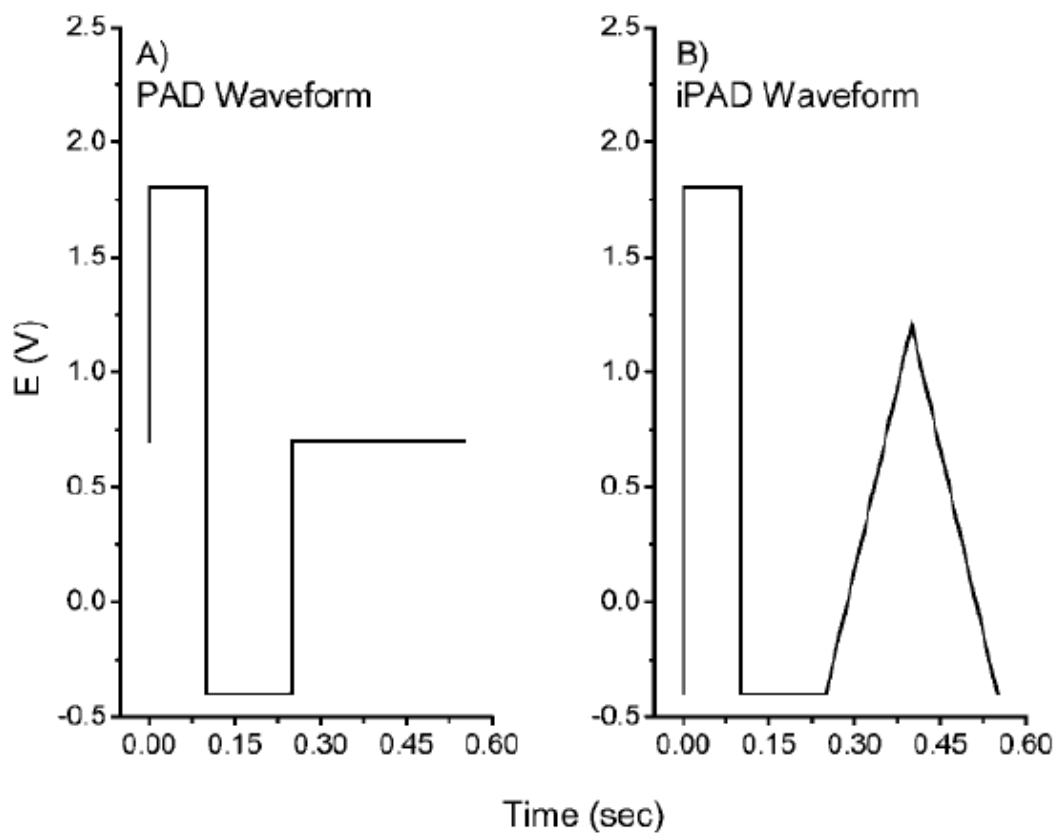


Figure 2.1: Schematic of the pulsed amperometric detection waveform (A) in comparison with the (B) integrated pulsed amperometric detection waveform. Reprinted with permission from [45].

2.2.2 Conductimetric Detection

Although amperometry is the most widely utilized mode of EC detection for microchip electrophoresis, conductimetric detection has become a more widely investigated technique in recent years [46-49]. Unlike amperometry, conductivity detection does not rely on redox reactions occurring at a working electrode. Instead, it measures an electrical signal (conductance) between a set of electrodes. Therefore, conductivity detection is considered a universal detection method since any charged species will give rise to a signal. Conductimetric detection can be carried out in two different methods, contact and contactless mode.

In contact conductivity detection, the electrodes are in galvanic contact with the electrolyte solution and therefore the analytes of interest. With contactless conductivity detection, the electrodes are placed on the external surface of the microfluidic device. Capacitively coupled contactless conductivity detection (C^4D) was originally described by two different groups in 1998, Zemmann *et al.*[50] and Fracassi da Silva and do Logo [51]. This method applies a high frequency alternating current (AC) to an upstream, actuator electrode while signals are collected at a downstream, sensing electrode. As shown in Figure 2.2, the AC field between the electrodes creates a capacitor with the internal electrolyte solution, making it possible to detect changes in conductance.

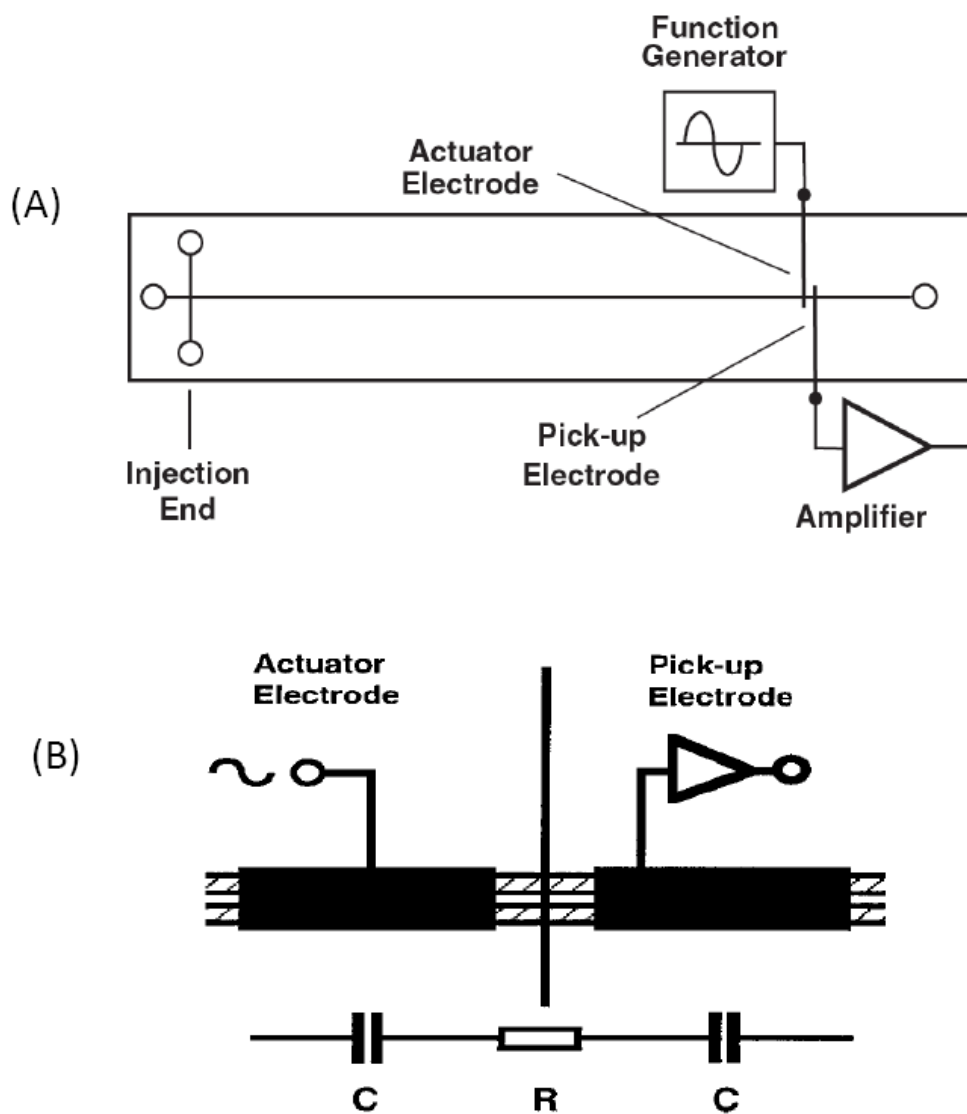


Figure 2.2: (A) Typical arrangement for C⁴D on an electrophoresis microchip. (B) Schematic drawing of a C⁴D detector. Reprinted with permission from [46] and [48].

With either contact or contactless conductivity detection, the sensing electrode measures the conductance of the solution between the electrodes. This relationship is given by Equation 2:

$$L = \frac{A}{d} \sum \lambda_i C_i \quad \text{Eq. 2}$$

where the conductance of the solution (L) is dependent on the electrode area (A), the relative distance between the electrodes (d), the concentrations (C) of all the charge carriers present, and their molar conductivity (λ). Since all charged species will give rise to a signal, one major concern is the background electrolyte (BGE) used for the separation. Highly charged BGE solutions will yield a high background signal resulting in diminished sensitivity and limit of detection (LOD). Therefore low conductivity buffer solutions such as lactic acid, 2-(N-morpholino)ethanesulfonic acid (MES), or N-Tris(hydroxymethyl)methyl-2-aminoethanesulfonic acid (TES) are commonly used to reduce the background signal.

The placement of electrodes for C⁴D is ideally suited as a detection method with miniaturized devices. Because the electrodes are external to the microfluidic network, they can be placed at almost any location; however, electrode alignment can be a critical factor to achieve day-to-day reproducibility. Integration of the electrodes into the microfluidic device will diminish any error associated with electrode alignment. Electrode configuration and integration into microfluidic devices is discussed in more detail in Section 2.3.3.

2.2.3 Voltammetric Detection

While used less extensively than amperometry or conductimetry, the use of voltammetry for microchip electrophoresis has been investigated [47, 52-53]. In its simplest form, voltammetry is performed by measuring the current generated as the applied potential is varied. Many different modes of voltammetry exist, but sinusoidal voltammetry and differential pulse voltammetry are most frequently employed (Fig 2.3). A derivative of linear sweep voltammetry, differential pulse voltammetry utilizes a stair step type of waveform in which the electrode potential is modulated and gradually increased as a function of time [54]. Like PAD, this technique offers some advantages over amperometry. Charging current is minimized which leads to a high degree of sensitivity. In addition, Faradaic current is extracted from the signal which facilitates more accurate measurements. Both of these factors allow for the investigation into the redox properties of extremely small amounts of analyte.

Sinusoidal voltammetry (SV) is an EC detection technique that is very similar to fast-scan cyclic voltammetry (CV). Whereas CV uses a triangular excitation waveform, SV uses a large-amplitude sine wave for excitation while analysis is performed in the frequency domain. Selectivity can be achieved through manipulation of the applied potential window [55] and has been shown to be a sensitive technique for the detection of native amino acids [56], carbohydrates [57], neurotransmitters [55], nucleotides [58], and DNA [59-60]. Electrode configurations and geometries for SV are very similar to those used in amperometry. In addition,

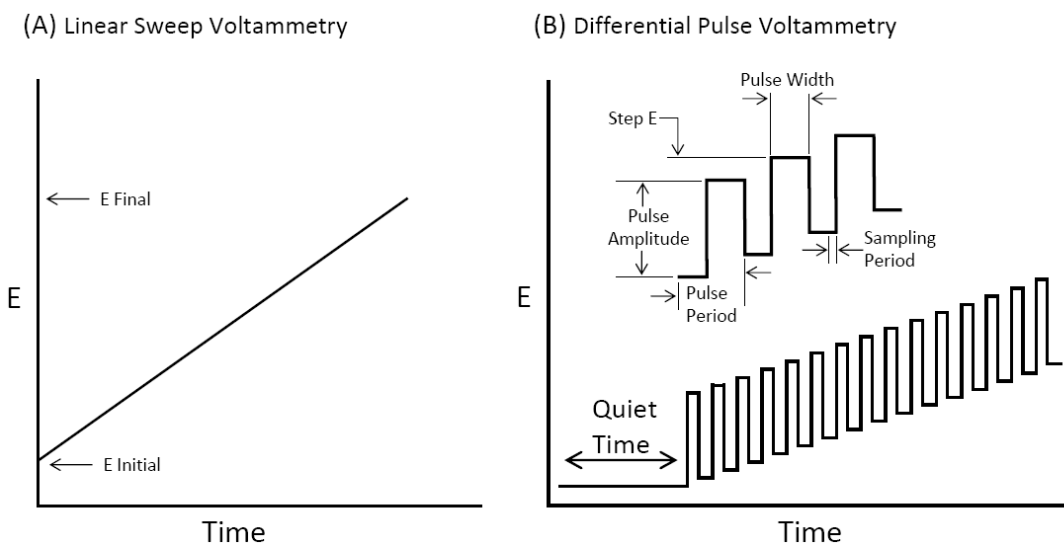


Figure 2.3: Schematic of the linear sweep voltammetry waveform (A) in comparison with the (B) differential pulse voltammetry waveform.

there are no limitations of electrode material so both carbon-based and metal electrodes have been investigated. While numerous publications have demonstrated the applicability of SV for use in miniaturized devices, there have been very few recent publications. Because this review is focused on recent developments in EC detection, the use of SV in microchip electrophoresis will not be covered in the application section.

2.3. Instrumental Design

2.3.1 Microchip Materials

With few exceptions, conventional capillary electrophoresis (CE) is performed in fused silica capillaries [61]. Many of the earliest reports for microchip electrophoresis also utilized glass-like materials such as fused silica, quartz, or soda lime [2, 62]. These substrates are a popular choice due to their high optical clarity, well established fabrication techniques, and are chemically similar to the fused silica capillaries used for CE [63-64]. The planar nature of microfluidic devices, however, permits the use of a variety of substrate materials. Many alternate materials have been explored in order to identify those which were less expensive, easier to fabricate, or have a different surface chemistry than glass devices. Some of the most commonly used materials now include: low-temperature co-fired ceramics [65-66], and many polymeric materials [67] such as poly(ethylene terephthalate) (PET) and polyethylene, poly(methylmethacrylate) (PMMA) [67-69], and poly(dimethylsiloxane) (PDMS) [35, 39, 70-71]. The increased research and use of polymeric materials has led to a better understanding of surface chemistry and how

it affects analytical performance of electrophoretic devices. Work performed by Lacher *et al.* [72] and Coltro *et al.* [73] demonstrated how the microchip substrate material can effect the quality of separation. In addition, much work has been done to chemically or physically modify the surface chemistry of these materials to influence the electrophoretic separation or fabrication of the device [63]. Some of these techniques include: plasma modification of PDMS [22, 74], solvent extraction [75-76], or by employing dynamic [77-78] or static coatings [79-81].

2.3.2 Electrode Materials and Fabrication

The growing popularity of EC detection for microchip electrophoresis has led to the development and incorporation of many different electrode materials and electrode configurations. However, in many cases, the choice of electrode material dictates the design and fabrication method for the microchip device. For example, carbon fibers must be placed manually into a channel fabricated in PDMS. This mandates the use of an all-PDMS device [34, 70]. Metal wires can also be placed in a PDMS channel, but this also dictates the use of an all-PDMS device [35, 82]. Most often, metal electrodes are fabricated in a low-profile, planar format on rigid substrates such as ceramic or glass [31, 83-84]. Therefore, electrode fabrication on these substrates generally requires the use of a hybrid glass-PDMS device.

Perhaps the most important factor to consider when using EC detection is the choice of electrode material. While metal electrodes, such as Au, Pt and Pd, have been used in microfluidic devices for the detection of thiols, carbohydrates, and ROS [15, 32, 85-86], carbon electrodes have been the most popular choice for the detection

of organic analytes, including catecholamines, phenols, and aromatic amines [33, 87-88]. In particular, carbon electrodes are ideal for the detection of catecholamines due to their large potential window, resistance to fouling, low overpotential, low background noise, and favorable electron transfer [34, 87, 89-90]. The most commonly employed carbon-based electrodes are carbon fibers, pastes, and inks [83, 91-92].

Martin and co-workers have developed a new technique to pattern carbon electrodes for microchip devices [40, 92-93]. This process, called micromolding of carbon ink electrodes, uses channels formed in PDMS to define the size and shape of the resulting carbon electrode. In this technique, a slurry of a carbon ink and solvent thinner is vacuumed through a PDMS microchannel and allowed to dry for 1 hr in a 85 °C oven. The PDMS mold is then removed and the electrode is cured for 1 hr at 125 °C. One main advantage of this type of electrode fabrication is that it can be performed inexpensively and without the need for dedicated cleanroom facilities. In addition, the resulting electrodes have shown good sensitivity and linearity for a variety of compounds

This type of carbon ink electrode, however, cannot be fabricated using standard photolithographic procedures. Therefore, their fabrication can be time-consuming and labor-intensive. An alternative carbon-based electrode material that can be fabricated *via* photolithography is pyrolyzed carbon [59, 94-95]. Recent work by Fischer *et al.* has shown that pyrolyzed photoresist film (PPF) electrodes are easily manufactured and exhibit excellent linearity and sensitivity [96].

Boron-doped diamond and carbon nanotube electrodes [97-98] are another type of carbon-based materials which have excellent electrochemical properties [99]. Wang and co-workers have described boron-doped diamond electrodes for the detection of nitroaromatic explosives, organophosphate nerve agents, phenols, and purine-containing compounds [100-102]. Recently, Pumera and co-workers compared the performance of single-wall carbon nanotubes (SWCNT), multiwall carbon nanotube (MWCNT), and graphite powder film detectors on glassy carbon (GC), gold, and platinum electrode surfaces [98]. Using an unmodified glassy carbon electrode (GCE), they showed that dopamine (DA) reaches a maximum detection potential at 0.6 V while a MWCNT modified GCE reaches a maximum detection potential at 0.3 V. The authors attribute this significant shift in detection potential to the electrocatalytic activity of carbon nanotubes. In addition, a MWCNT modified GCE showed increased sensitivity and resolution over an unmodified GCE for the separation and detection of DA and catechol (CAT).

Chemically modified electrodes have also been explored for use in microchip electrophoresis. Chemically modified electrodes contain a surface-bound redox mediator that is used to lower the redox potential for various analytes [15]. Fewer compounds undergo redox processes at lowered detection potentials which can lead to greater selectivity. Cobalt phthalocyanine has been used as a redox mediator in carbon paste electrodes for the detection of thiols [85] and hydrazine compounds [103]. Shiddiky and co-workers demonstrated the use of a conducting polymer-modified electrode that was further functionalized with gold nanoparticles (AuNPs)

for the trace analysis of DNA [104]. When compared to an unmodified electrode, the sensitivity improved approximately 25,000 fold and yielded a LOD of 5.7 amol in a 50 μ L sample of a 20 base pair DNA oligomer.

Johirul *et al.* has demonstrated the use of a cellulose-DNA-modified screen-printed electrode for the analysis of several neurotransmitters (NTs) [105]. As seen in Figure 2.4, the modified electrode displayed a much improved sensitivity for several catecholamine NTs and ascorbic acid. The modification of the electrode also reduced the amount of background noise, leading to a LOD of 32 nM for DA. Recent work by Pai *et al.* has demonstrated the benefits of three-dimensional (3D) electrodes [106]. As seen in Figure 2.5, the 3D gold electrodes are raised approx. 20 μ m from the surface of the glass substrate. The larger surface area of the electrode creates more contact with the analyte of interest. Therefore more analyte is oxidized and a larger signal can be obtained.

2.3.3 Amperometric Detection: Isolation of the Detector from the Separation Voltage

One of the most important issues in the design of a microchip electrophoresis experiment is the isolation of the electrochemical detector from the separation voltage. Failure to properly isolate the electrode will lead to increased noise as well as probable damage to the potentiostat circuitry. Three different electrode alignments are commonly used and are depicted in Figure 2.6. The most prevalent method, end-channel detection, involves placing the electrode 5–20 μ m from the end of the separation channel (Fig. 2.6 A). This allows the separation voltage to dissipate prior

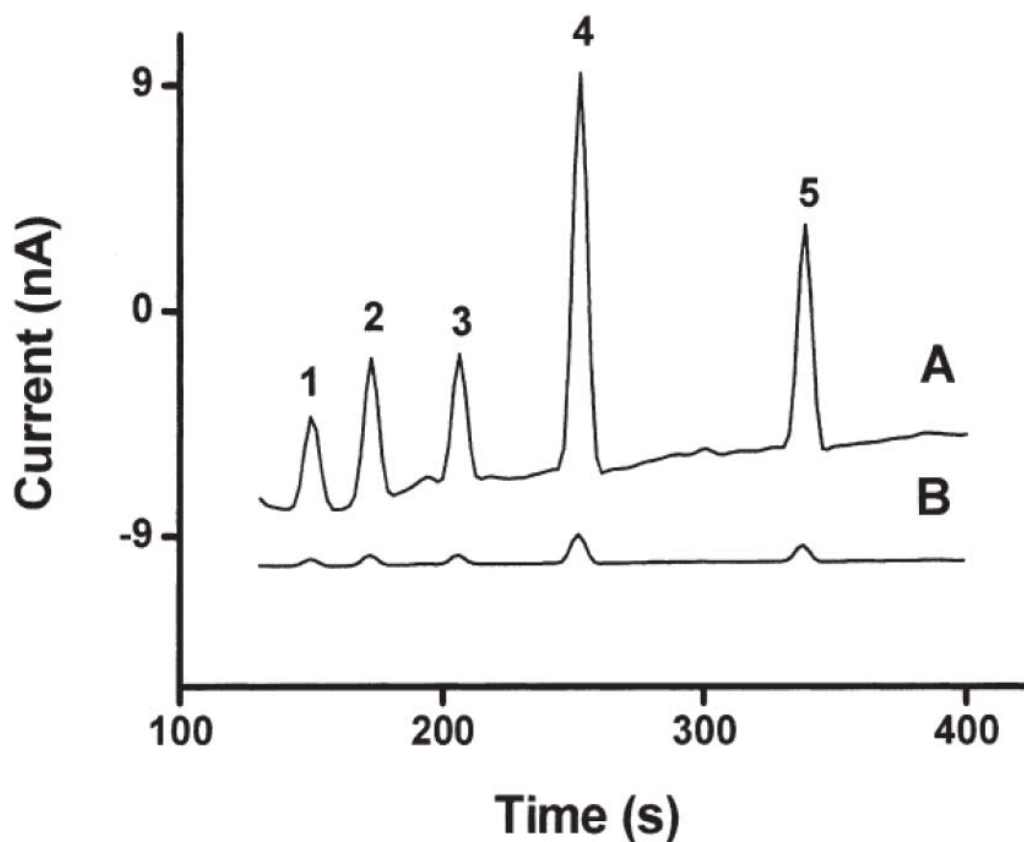


Figure 2.4: Electropherograms for separation and detection of neurotransmitters (A) at a modified electrode, and (B) a bare electrode. Peak assignment and concentration: 1, DA (15 mM); 2, NE (60 mM); 3, L-DOPA (60 mM); 4, DOPAC (60 mM); and 5, AA (60 mM). Detection potential, 0.7 V (vs. Ag/AgCl). Reprinted with permission from [105].

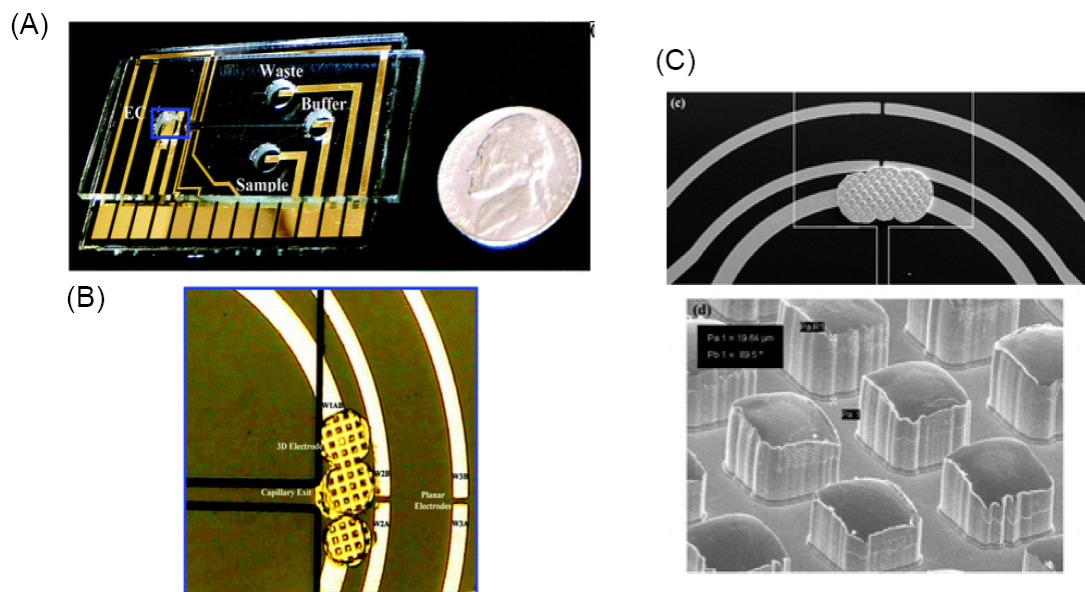


Figure 2.5: Photograph of (A) the entire CE/EC device and (B) a close-up view of the end-channel EC detection setup (top view), (C) Scanning electron microscopy (SEM) images of the final electrodes. Reprinted with permission from [106].

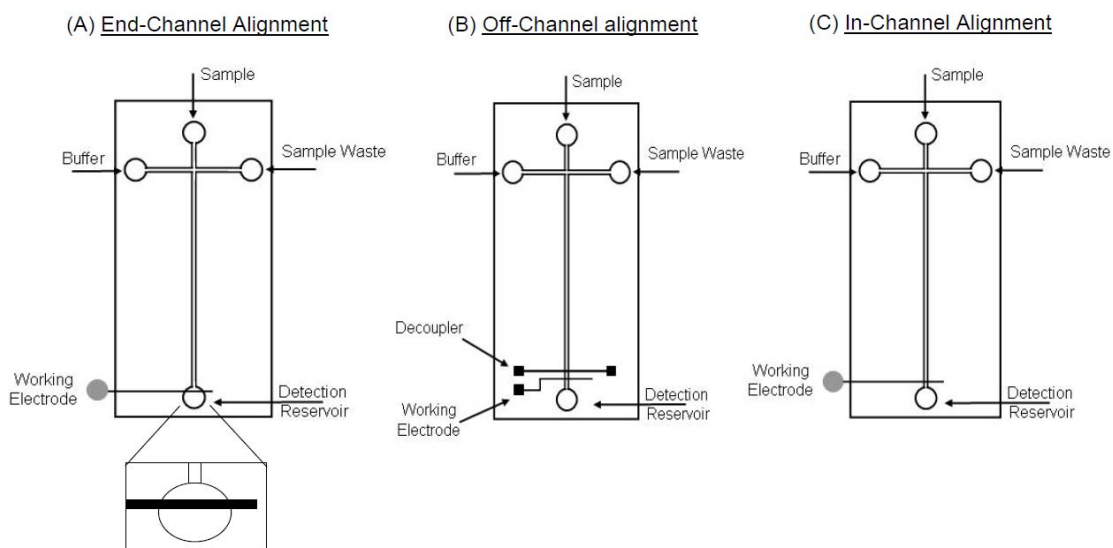


Figure 2.6: Schematic diagram of different electrode alignments for microchip electrophoresis with EC detection: (A) end-channel alignment, (B) off-channel alignment, and (C) in-channel alignment. In-channel alignment is possible only when using an electrically isolated potentiostat.

to reaching the working electrode [107]. An alternative way to isolate the working electrode from the separation voltage is to use a decoupler for off-channel detection (Fig. 2.6 B). In this technique, the decoupler is placed in the separation channel ahead of the working electrode and serves as a path to ground [108-110]. Another approach involves the use of an electrically isolated or “floating” potentiostat for in-channel alignment (Fig. 2.6 C) [111]. In this configuration there is no decoupler, but the working electrode can be placed directly in the separation channel because the potentiostat is not earth-grounded. These three electrode alignments are described in detail below.

2.3.3.1 End-Channel Alignment

Due to its simplicity, end-channel alignment is the most widely utilized alignment for amperometric detection in microchip devices. In this configuration, the working electrode is placed 5–20 μm from the end of the separation channel (Fig. 2.6 A). This allows sufficient dissipation of the separation voltage in the ground reservoir prior to reaching the working electrode. However, since the separation voltage is placed very close to the separation channel exit and the voltage is grounded in the same reservoir, shifts in half-wave potential are observed [42]. Therefore, it is always necessary to construct a hydrodynamic voltammogram (HDV) using the exact separation conditions that will be employed to determine the optimum redox potential. Because the electrode is placed 5-20 μm from the exit of the separation channel, analyte diffusion and dilution occurs before reaching the detection electrode. This can result in lower separation efficiencies and higher background currents than

the other electrode alignments. Positioning the electrode too close to the separation channel can be detrimental as well. Small fluctuations in the separation voltage can produce excess noise, resulting in higher LODs. In extreme cases, the separation voltage can ground through the potentiostat, resulting in severe damage to the electronics [42, 111]. Typical LODs for end-channel detection range in the low micromolar to low nanomolar range [96, 112].

Garcia and Henry have described a straightforward approach to end-channel alignment [82]. PAD was performed using a gold wire which was placed in a micromolded PDMS channel in the same layer as the separation channel. This type of fabrication is easy to perform and reduces variability in alignment distance. The device was completed by irreversibly sealing another layer of PDMS to the channel and electrode layer. Using this technique, the authors were able to efficiently detect underivatized carbohydrates, amino acids, and antibiotics.

As mentioned earlier, one of the major drawbacks associated with end-channel detection is analyte diffusion that occurs between the channel exit and the electrode. Mathies and co-workers have developed a novel sheath-flow design that carries analyte to the electrode more efficiently [113]. The sheath flow channels were placed at a 30° angle relative to the separation channel and were filled with buffer to establish a gravity-driven flow towards the detection electrode (Fig. 2.7). The authors report that this flow was responsible for increasing the velocity of CAT by ~50 $\mu\text{m/s}$ following separation. This stabilization of the analyte velocity allowed the placement

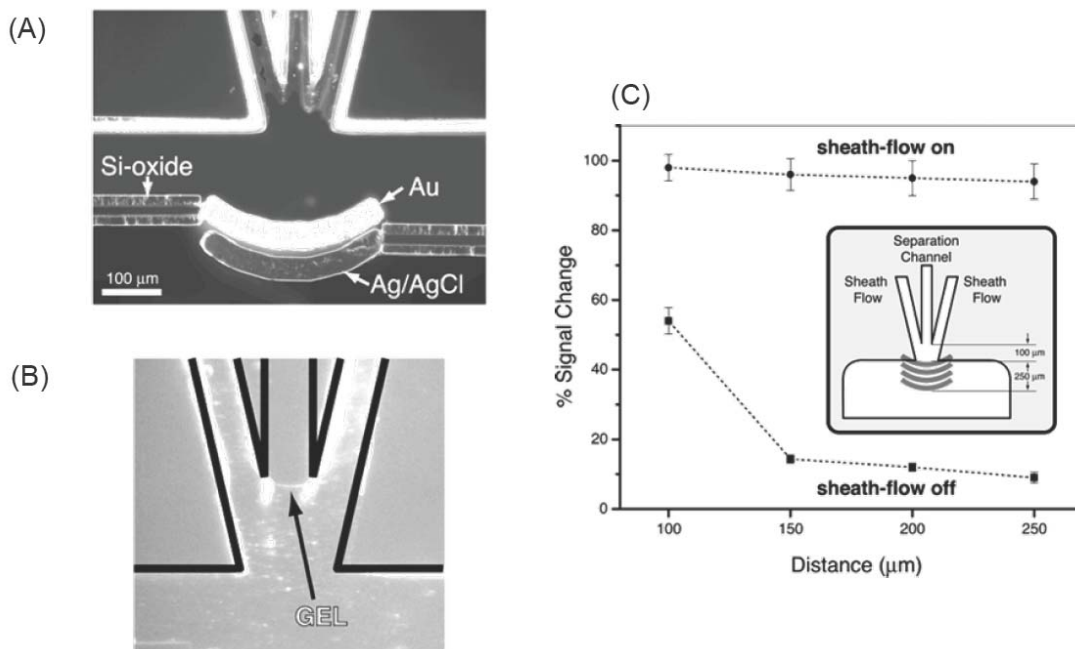


Figure 2.7: Exploded view of crescent electrodes with sheath-flow supported electrophoresis. (A) Photo of the electrodes at the detection region. (B) Separation and sheath-flow channel after gel loading visualized with dark-field microscopy. The arrow indicates the boundary of the sieving matrix. (C) Results of catechol separations presented as relative (%) signal change as a function of electrode distance calculated from triplicate measurements obtained in the (▪) absence and (•) presence of sheath-flow support. Inset: Schematic representation of investigated EC detector configurations with working electrodes placed at a distance of 100, 150, 200, and 250 μm from the separation channel. Reprinted with permission from [113].

of the working electrode as far as 250 μm from the channel exit with very little loss in signal.

Work performed by Baldwin's group noted that the analyte plug takes on a crescent shape or radial pattern as it exits the separation channel [114]. In order to maximize analyte contact with the electrode, the authors designed an electrode to mimic the shape of the analyte plug as it exits the separation channel (Fig. 2.8). This configuration resulted in increased analyte contact and an increase of the signal-to-noise ratio (S/N). In addition, this microchip device was self-contained and portable with integrated high voltage (HV) and detection electrodes.

2.3.3.2 In-Channel Alignment

Another approach for minimizing band broadening associated with end-channel detection is the use of an electrically isolated or "floating" potentiostat for in-channel alignment [111]. In this technique, the electrode is placed directly in the separation channel. Since the potentiostat is not earth-grounded, no damage can be done to the potentiostat or electronics. However, the electrode is heavily influenced by the separation field, and detection potentials must be optimized by constructing a HDV. For example, Martin and co-workers reported as much as a +600 mV shift in half-wave potential for the detection of CAT and found the optimal detection potential of +2.2 V vs. Ag/AgCl. In addition, the use of an electrode placed in-channel significantly reduced the amount of band broadening when compared to end-

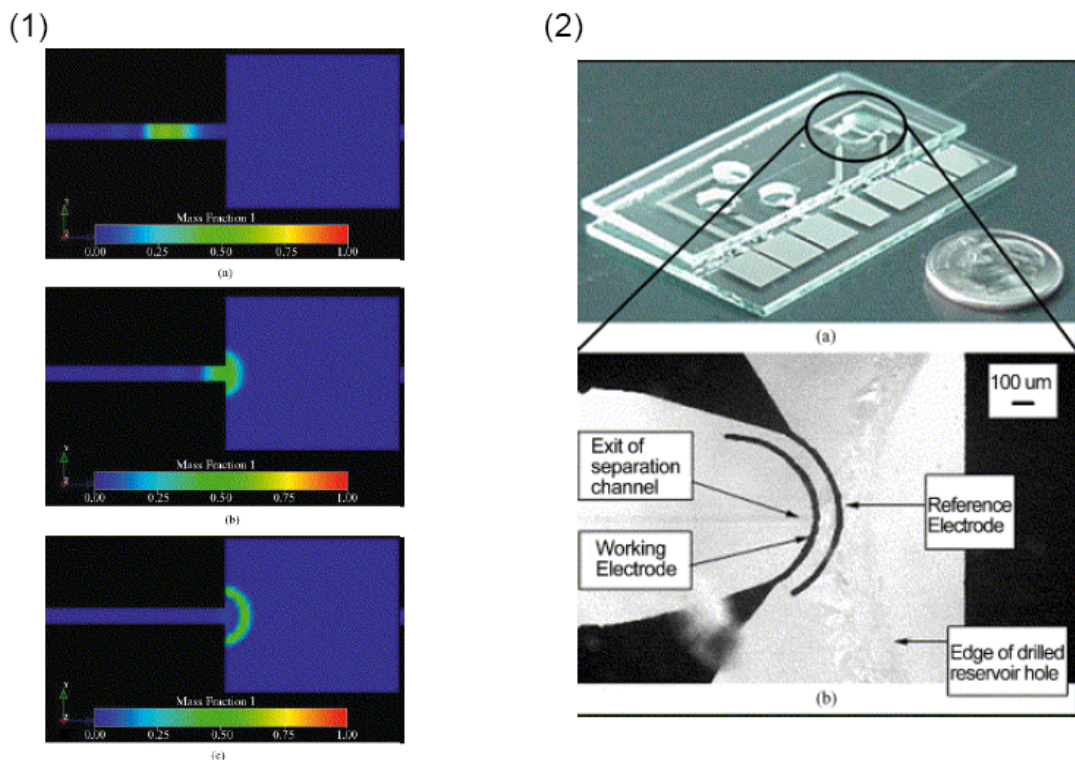


Figure 2.8: (1) Finite element model demonstrating plug shape (a) in the separation channel, (b) exiting the separation channel, and (c) in the detection reservoir; (2) Photographs of (a) entire CE/ED microchip and (b) magnified (30×) top view of the ED cell and electrodes. Reprinted with permission from [114].

channel alignment. This resulted in a 4.6 fold decrease in plate height and a 1.3 fold decrease in peak skew for the detection of catechol.

Recent work by Chen *et al.* described an alternate method of in-channel detection for microchip electrophoresis [115]. Instead of a single separation channel, their work used a dual-channel configuration consisting of two parallel separation and reference channels. The two channels have a common ground and auxiliary electrode, but have a working and reference electrode placed equidistant from the channel outlet (Fig 2.9). In this configuration, only buffer flows through the reference channel and over the reference electrode. The analyte mixture is injected and separated in the separation channel and detected at the working electrode. Because the electrodes are positioned at the same distance from the channel exit, fluctuations in the separation voltage influence both electrodes equally. The signal from the reference channel is then subtracted from the signal obtained from the separation channel, leading to decreased interference and noise. This configuration resulted in a LOD of 1.8 nM for DA at S/N = 3.

2.3.3.2 Off-Channel Alignment

An alternative way to isolate the working electrode from the separation voltage is to use a decoupler for off-channel detection (Fig. 2.6 B). The decoupler is placed in the separation channel ahead of the working electrode and serves as a path to ground [84, 108-109]. The grounding of the separation voltage prior to the working electrode provides a field-free region over the electrode which helps to reduce the amount of background noise. Because the HV is grounded at the

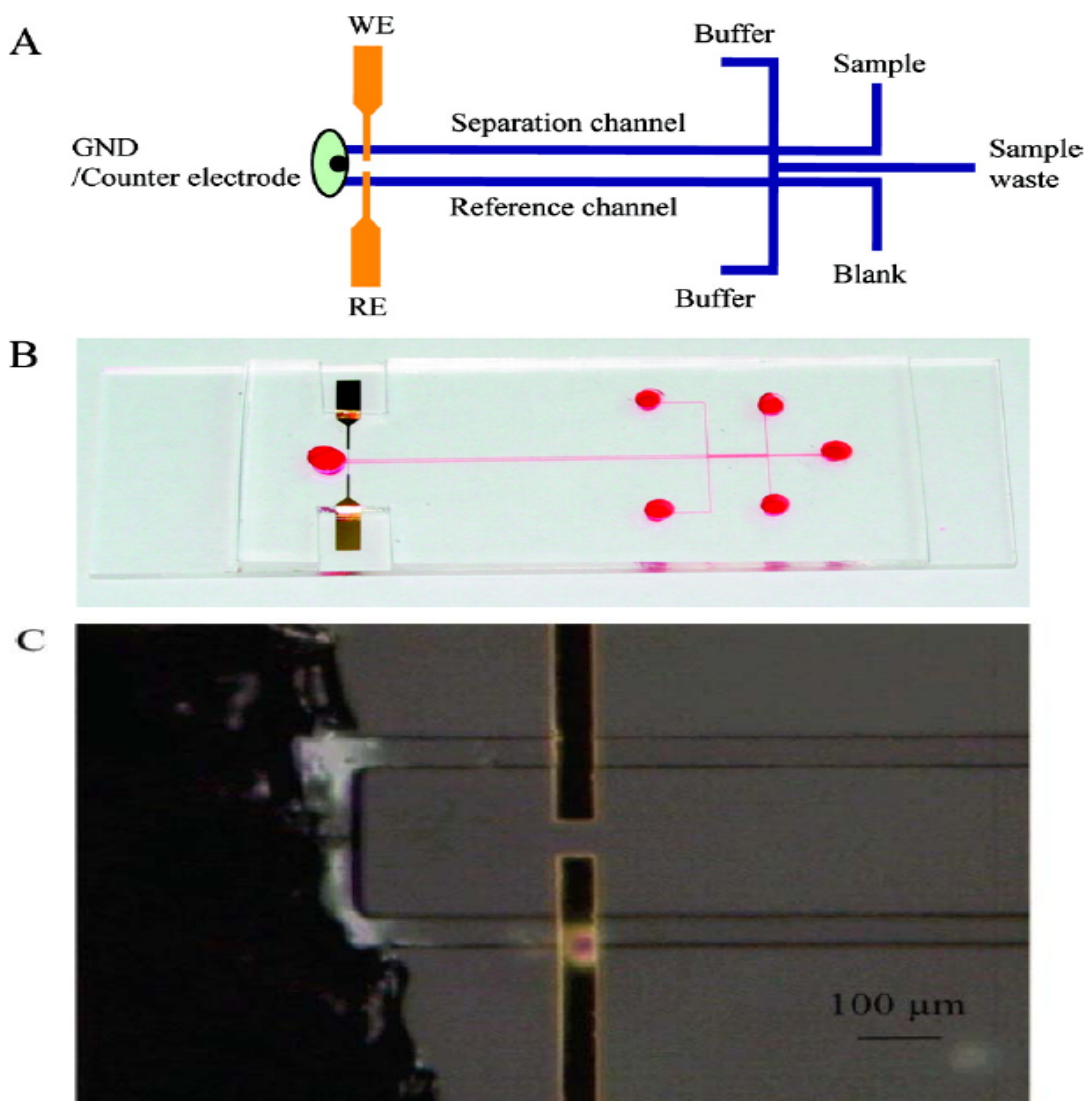


Figure 2.9: (A) Schematic of the microchannel network in the dual channel CE microchip with an in-channel electrochemical detector. The separation and reference channels have the same length: 3 cm. Lengths of all other channels are shown in proportion to those of these two channels. All channels have the same cross section of 50 μm width and 20 μm depth, except the sample waste channel that is double in width. (B) Photograph of the microchip. Channels are filled with red ink for visualization. (C) CCD image of Au electrodes mounted in the exit of dual-channel. Reprinted with permission from [115].

decoupler, there is no electroosmotic flow (EOF) past this point. The EOF generated prior to the decoupler generates a hydrodynamic flow to push analytes past the electrode. However, due to the parabolic flow profile that develops, this change in flow dynamics can cause small amounts of band broadening.

One of the earliest reports detailing the use of a decoupler for microchip electrophoresis was published by Wu and co-workers [110]. The authors reported a microfabricated platinum (Pt) decoupler with integrated auxiliary and pseudo-reference electrode. Both gold (Au) and Pt decoupler materials were investigated, however, it was found that the Pt decoupler offered the best performance. This stems from the ability of the Pt group metals to efficiently absorb the hydrogen gas that results from the electrolysis of H₂O. Using this configuration, the authors were able to achieve a LOD of 125 nM for DA.

Osborn and Lunte demonstrated the use of a cellulose acetate (CA) decoupler for microchip electrophoresis [109]. A CO₂ laser was used to etch 20 small scores placed 75 μ m apart in a glass coverplate. The decoupler was created by casting a thin film of CA in the scored holes. The glass coverplate was then aligned 1 cm from the channel exit and irreversibly sealed to complete the device. The authors report that this device was capable of dissipating currents as high as 60 μ A and had a lifetime of up to 4 months. In addition, the CA decoupler was able to withstand field strengths as high as 1700 V/cm. Citing extremely low noise levels (\sim 1pA) the authors reported a LOD of 25 nM for DA at a carbon fiber electrode.

Lacher and Martin described the use of a palladium (Pd) thin film decoupler for use with microchip devices. In their work, both a Pd decoupler and working electrode were fabricated on glass using standard photolithographic techniques. In their work, the authors investigated the optimum decoupler size and spacing from the working electrode. By characterizing flow profiles and background noise levels, the authors reported an optimum decoupler width of 500 μm and a spacing of 250 μm from the working electrode. If the working electrode was placed closer than this, excess noise was observed. When the electrode was placed farther away (500-1000 μm), noise decreased but resolution was diminished. Using this configuration, the authors were able to achieve a LOD of 500 nM for the detection of DA.

2.3.3.4 Summary

The previous sections detailed the most commonly used techniques to isolate the EC detector from the separation voltage. As described above, each method has its unique advantages and disadvantages. End-channel alignment is the easiest method to implement but suffers from excess band broadening. In-channel alignment mitigates many of the deleterious band broadening effects observed with end-channel alignment, but an electrically isolated or “floating” potentiostat is required. Because there are very few commercial manufacturers of this instrumentation, it must often be built in-house. Off-channel detection offers increased resolution of analytes with decreased noise, but extensive fabrication with expensive metals such as Pt or Pd is required.

In addition, many different types of electrode materials have been used with microchip electrophoresis. Carbon-based materials such as carbon fiber, carbon paste, carbon ink, or pyrolyzed photoresist electrodes can be used. Furthermore, metal electrodes made from gold, platinum, palladium, or even copper have been employed. It is important to remember that the electrode alignment as well as the electrode material contributes to the overall analytical performance of the device. A recent publication by Fischer *et al.* addressed these variables by directly comparing the effects of electrode alignment and material on analytical performance [96].

2.3.4 Related Electrochemical Detection Modes: Conductimetric Detection

The previous sections, which detailed electrode alignment, were described in the context of amperometric detection. However, electrode placement and configuration for conductimetric detection is important as well. As described in section 2.2, conductimetric detection can be performed in either contact or contactless mode. As the name implies, contact conductivity detection places the electrode in direct galvanic contact with the analyte solution. Capacitively coupled contactless conductivity detection (C⁴D) places the electrodes on an external surface of the microchip device. In either case, the electrode geometry and configuration are important considerations when designing an experiment with conductimetric detection.

2.3.4.1 Contact Conductivity Detection

Originally developed for use with conventional CE, contact conductivity detection has been shown to be a quite useful detection method [116-118]. However, contact conductivity detection has been less successful in the microchip format [119]. Fabrication and integration of the electrodes into microfluidic devices is much easier than for conventional CE. A major problem with contact detection in the chip format is the interaction between the HV used for separation and the detection electronics [116]. The high field strengths used in microchips can lead to unwanted electrochemical reactions at the detection electrodes, the electrolysis of water, and increased noise. Despite these issues, contact detection does not suffer from the same problems observed with end-channel amperometric detection. Since the electrodes are placed prior to the detection reservoir, band broadening is not observed.

Several approaches have been used to minimize HV drops at the detection electrodes. Feng and co-workers designed a microchip with an orthogonal channel just before the detection reservoir in which measurements were taken [120]. However, sensitivity was an issue as detection limits for several small ions were only ~1 mM. The same group later designed a double-T detection chip that improved sensitivity and LOD to 10-80 μM [121].

Soper and co-workers demonstrated a contact detector that utilized a 5 kHz bipolar pulse waveform applied to a pair of Pt wire detection electrodes. Using a 3 cm separation channel in an all PMMA device, the authors demonstrated the separation and indirect contact detection of various analytes (Fig. 2.10) [122]. Amino

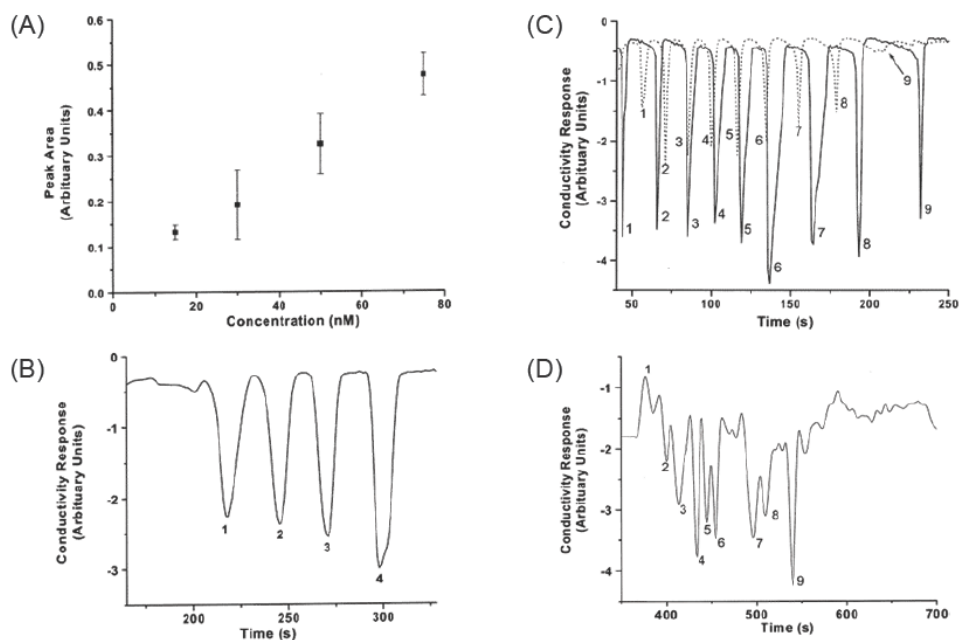


Figure 2.10: (A) Calibration plot for alanine over a concentration range of 15–100 nM. Alanine was electrophoresed using TEAA as the background carrier electrolyte (10 mM, pH 7.0). (B) Free-solution zone electrophoretic separation of 100 μ M amino acid mixture consisting of (1) alanine, (2) valine, (3) glutamine, and (4) tryptophan in an unmodified PMMA microchip using indirect, contact conductivity detection. (C) Free-solution zone electrophoretic separation of a peptide mixture (0.23 μ M total peptide concentration) consisting of (1) bradykinin, (2) bradykinin fragment 1–5, (3) substance P, (4) [Arg8]-vasopressin, (5) luteinizing hormone, (6) bombesin, (7) leucine enkephalin, (8) methionine enkephalin, and (9) oxytocin in an unmodified PMMA microchip. The solid line represents the 3rd electrophoretic run on this chip, and the dotted line is the 35th electrophoretic run on the same chip. (D) MEKC separation of a protein mixture (1.7 μ M total protein concentration with all proteins at similar concentrations within the mixture) in an unmodified PMMA microchip consisting of (2) lysozyme, (3) trypsin inhibitor, (4) carbonic anhydrase, (5) ovalbumin, (6) serum albumin, (7) phosphorylase B, (8) β -galactosidase, and (9) myosin detected using indirect, contact conductivity detection. Benzoic acid (1) was added to the mixture as an internal standard. Electrophoresis conditions: carrier electrolyte 100 μ M TRIS HCl with 1% SDS (pH 9.2); a 3 s injection time; $E = 250$ V/cm for the electrophoresis; detector operated at 5.0 kHz using a bipolar pulse amplitude of ± 0.5 V was used for all data presented. Reprinted with permission from [122].

acids (AA) such as alanine, valine, glutamine and tryptophan with a reported detection limit of 8 nM for alanine. The ability of the device to detect peptides was also demonstrated. A mixture of nine peptides including bradykinin, substance P, luteinizing hormone, leucine enkephalin, and oxytocin was baseline resolved in less than 250 s. In addition, proteins were analyzed using this microchip configuration. The authors demonstrated the ability to separate and detect such proteins as: lysozyme, trypsin inhibitor, serum albumin, and myosin using indirect contact conductivity detection. More recently, the same group detailed efforts to fabricate a multichannel microchip capable utilizing a slightly different detector configuration [123]. The authors demonstrated the fabrication of a 16 channel microchip capable of simultaneous separation and detection of amino acids, peptides, proteins, and DNA (Fig 2.11). By running multiple samples in parallel, all four types of analytes could be analyzed in less than 200 s.

A recent publication by Henry *et al.* outlined a new approach to improve the compatibility between contact conductivity detection and microchip electrophoresis [119]. The authors developed a bubble cell detection zone around the electrodes (Fig. 2.12). Increasing the dimensions of the separation channel decreases the effective field strength of the local environment. Therefore, this configuration decreased unwanted interactions between the HV and detection electrodes leading to decreased noise. In addition, the authors were able to determine that the use of a bubble cell four times as wide as the separation channel led to a decrease of only 3% in separation efficiency. A detection limit of 71 nM, which corresponded to a mass

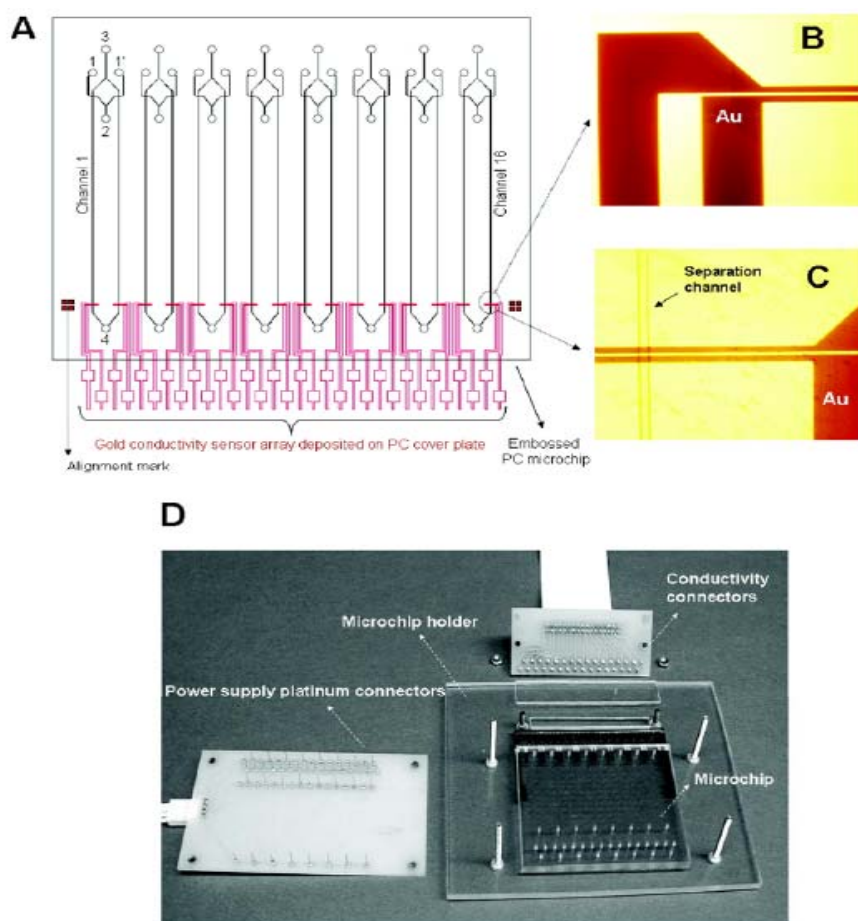


Figure 2.11: (A) Topographical layout of the multichannel microfluidic network. Injection channel length = 9 mm; total separation channel length = 54 mm; effective separation channel length (L_{eff}) = 40 mm; channel width = 60 μm; channel depth = 40 μm. The reservoirs for each microfluidic channel pair are (1) and (1') sample reservoirs; (2) sample waste reservoir; (3) buffer reservoir; (4) buffer waste reservoir. All reservoirs were 1.5 mm in diameter. The center-to-center spacing of each fluidic reservoir was fixed at 9 mm. The line trace shown in red provides a topographical layout of the lithographically printed-Au conductivity sensor array. The outlet end consisted of 16 Au-electrodes (7.62 mm long × 500 μm wide) serving as the conductivity sensors. Shown is the detection region of one Au-electrode pair before (B) and after (C) thermal annealing of the cover plate to the microfluidic chip. Each contact conductivity electrode was 60 μm in diameter with an end-to-end spacing of 5 μm. (D) Photograph showing the microchip and the holder setup with connectors for the high-voltage power supply and conductivity detection units. Reprinted with permission from [123]

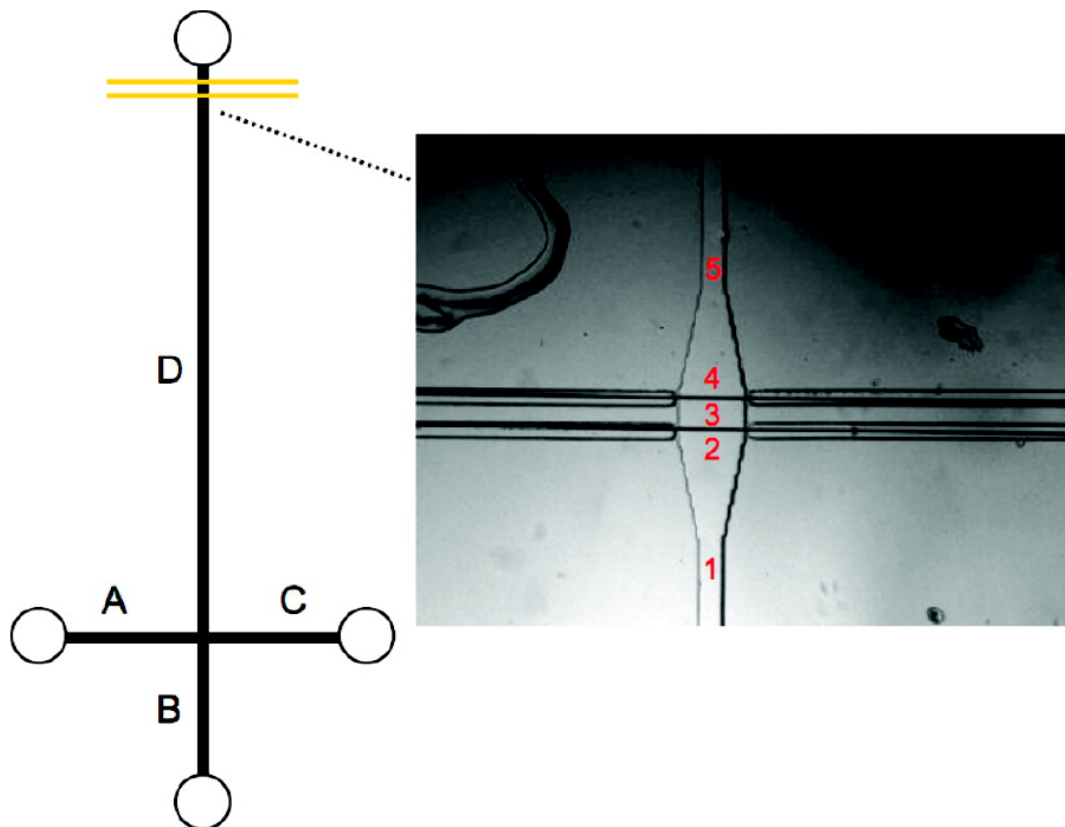


Figure 2.12: Microchip design utilizing a bubble cell for contact conductivity detection used in this work. Gated injected was used for all analyses, and the channel were designated as follows: A = sample waste, B = sample, C = buffer, and D = separation. The numbers designate locations monitored with fluorescent imaging. Reprinted with permission from [119].

detection limit of 89 amol, was achieved for dithionate using a gold plated tungsten wire.

2.3.4.2 Contactless Conductivity Detection

Like contact conductivity detection, contactless conductivity detection was first applied to conventional CE systems [51, 116, 124]. Many of the original designs were constructed by threading the capillary tubing through circular metal rings. A significant improvement was reported independently by Zemmann *et al.* [50] and Fracassi da Silva and do Lago [51]. They reported the use of an axial electrode arrangement in which four tubular electrodes are placed side by side along the capillary axis. A small gap between the electrodes (usually millimeters) defines the detection volume. The terminology used to define this detection method has also evolved over the years. The use of the term contactless conductivity detection lacks precision as it could also refer to inductively coupled methods. Therefore, the use of capacitively coupled contactless conductivity detection (C^4D) has become standard nomenclature. Furthermore, the qualifier “axial” can be added to distinguish the use of this type of electrode design from other configurations such as a radial design.

The use of C^4D has become very popular for microchip electrophoresis in the past several years. This is due to several reasons; namely the fact that ultraviolet (UV) detection is not ideal for small ionic species or easily adopted for the microchip format. However, axial electrodes are much easier to integrate into the planar chip format. The use of C^4D for both CE and microchip electrophoresis can be found in several previously published reviews [46, 48-49, 116].

Electrodes for C^4D are typically utilized in two different approaches. Separate, external electrodes can be used or the electrodes can be integrated into the device. The former is simpler, but the latter facilitates device integration and reproducibility in measurements. Recently, Coltro and co-workers demonstrated the fabrication and integration of aluminum electrodes on a polyester-toner (PT) microchip [125]. Planar electrodes were fabricated in three simple steps: (1) drawing and laser printing the electrode geometry on polyester films, (2) sputtering metal onto the substrates, and (3) removal of the toner layer by a lift-off process. Based on a previous technique [126], the polyester film with integrated detection electrodes (Fig 2.13) was coupled with PT electrophoresis microchannels by lamination at 120 °C in less than 1 min. The authors optimized performance by investigating excitation voltage and excitation frequency for the detection of biologically relevant ions. The authors reported detection limits of 3.1, 4.3, and 7.2 μM for K^+ , Na^+ , and Li^+ , respectively in less than 90 s.

Recent work by Fercher *et al.* described the development of a micromachined C^4D device fabricated in low temperature co-fired ceramics (LTCC) [65]. All features including the microchannels, access holes, as well as liquid inlet and outlet ports were micromachined with a diode pumped Nd:YAG laser. The entire device was constructed from five layers of dielectric ceramic tape which were aligned, laminated, and fired at 850 °C for 90 min. The two silver (Ag) detection electrodes were fabricated by screen printing conductive paste prior to the firing process (Fig 2.14). After firing, the C^4D electronic circuit was placed on top to create a fully

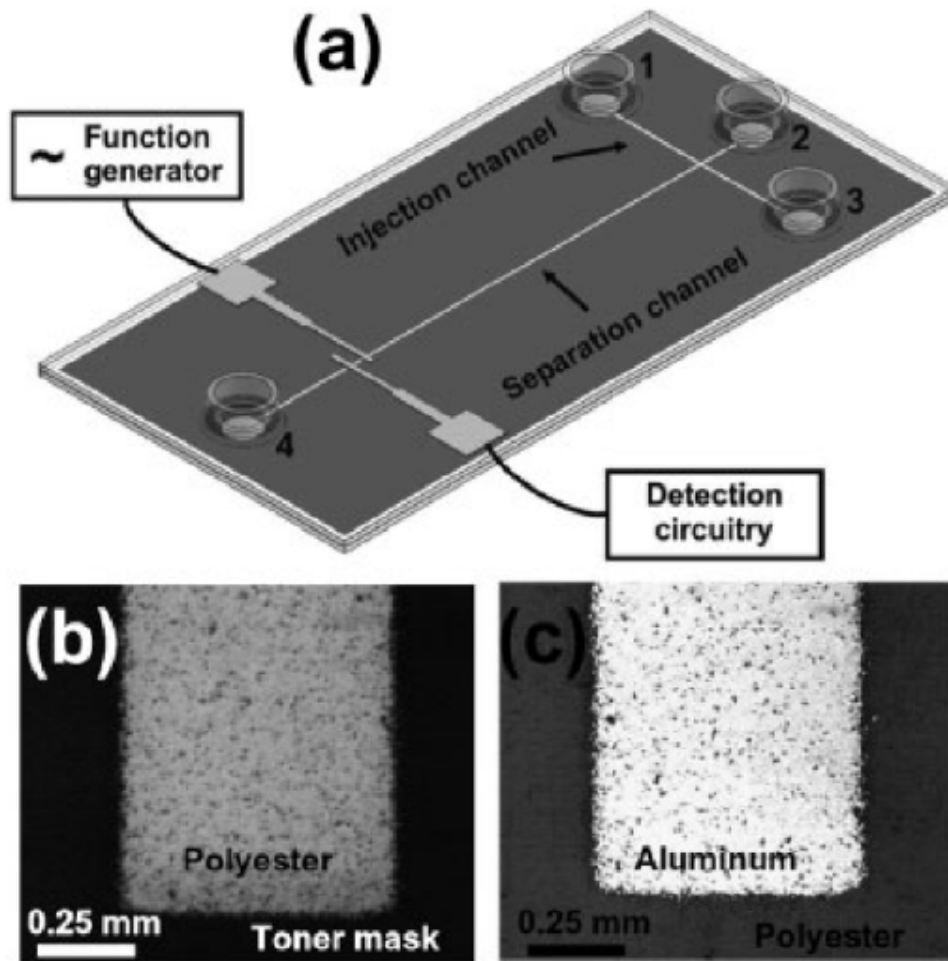


Figure 2.13: Representation of the (a) proposed PT device with integrated electrodes for C^4D and optical micrographics of (b) toner mask and (c) its resulting electrode after sputtering and toner lift-off steps. Reprinted with permission from [125].

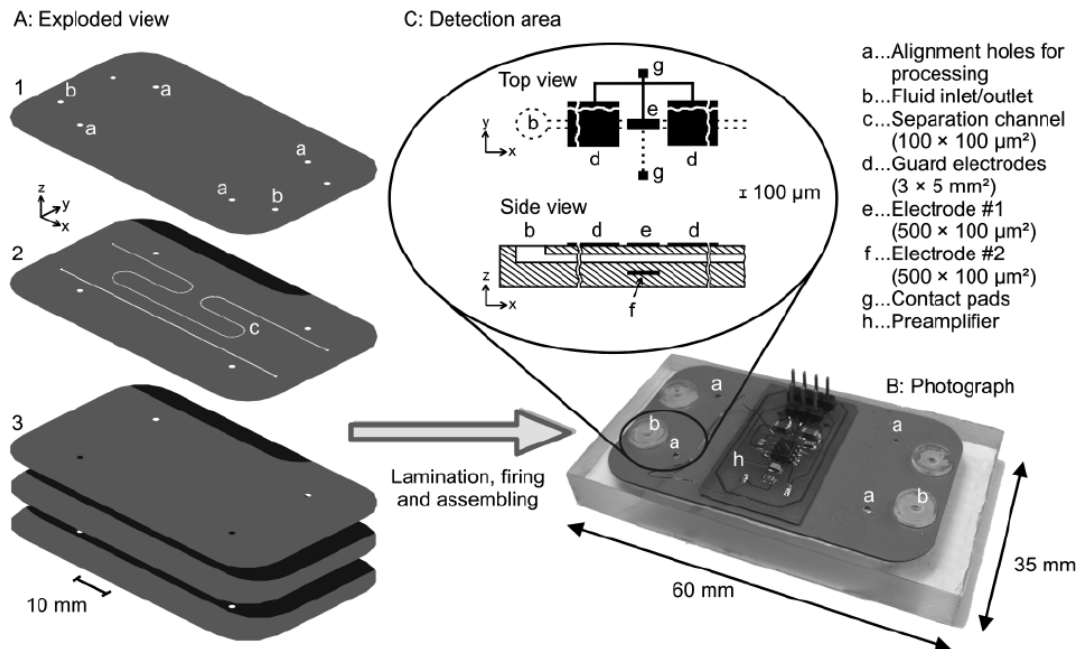


Figure 2.14: Exploded view (A) and photograph (B) of the fabricated LTCC-CE module. A closeup of both the top and side views of the detection area is depicted in inset (C). (1) cover layer; (2) middle layer comprising separation channels; (3) bottom layers for mechanical support. Total device thickness is 500 mm. Temperature sensitive components such as preamplifier and polysiloxane rings were placed after the firing process. Reprinted with permission from [65].

integrated device. Because ceramic has a higher dielectric constant than glass or plastics, this approach exhibits a high degree of sensitivity for organic and inorganic ions. Separation of K^+ , Na^+ and Li^+ was achieved in less than 60 s with a reported LOD of $10 \mu M$ for K^+ .

In an effort to further improve the sensitivity of C^4D in microchip devices, Wang and co-workers developed a novel “hybrid” detector [127]. The detector is based on a “hybrid” arrangement where the receiving electrode is insulated by a thin layer of insulating material and placed in the bulk solution of the detection reservoir whereas the emitting electrode is placed in contact with the solution eluting from the separation channel outlet in a wall-jet arrangement. The device was tested using explosive-related compounds including methylammonium, ammonium, and Na ions. The authors demonstrated that this electrode arrangement produces a low amount of noise and 10-fold improvement in sensitivity when compared to other type of contactless conductivity detectors.

2.4 Applications

Microfluidic electrophoresis devices with electrochemical detection have been used for a variety of applications. The most prevalent research topics include: neurochemistry, enzyme and immunoassays, clinical diagnostics, and environmental assays. Additional information regarding microchip and electrode materials, detection modes, and applications can be found in previous reviews of microfluidic and microchip electrophoresis [7, 11, 24-25, 31, 71, 128].

2.4.1 Neurotransmitters and Related Compounds

The analysis of neurotransmitters (NTs) is a subject matter that has received a tremendous amount of attention. The development of more sensitive and robust analytical tools has facilitated the investigation of complex neurological pathways and enhanced our understanding of neurodegenerative diseases. Due to their widespread presence in the central and peripheral nervous systems, catecholamine NTs have been extensively studied. Accordingly, dopamine (DA) and norepinephrine (NE) [35, 84, 88, 95, 106, 109, 129-132] are often chosen as model analytes because of their biological importance and the fact that they are electroactive at moderate redox potentials [15].

In one of the very first reports of EC detection with microchip electrophoresis, Wooley *et al.* characterized the performance of their device using DA and NE [30]. A few years later, Gawron and co-workers advanced the field of EC detection for microchip electrophoresis through the development of a carbon-based dual-electrode detector [91]. This was the first report of two carbon fiber electrodes for dual-electrode EC detection with microchip electrophoresis. The authors demonstrated the separation and detection of serotonin (5-HT), epinephrine (Epi) and 5-hydroxyindole acetic acid (5-HIAA) in less than 90 sec.

Schwarz and Hauser described the separation and detection of several NTs and metabolites of NTs [133]. The authors demonstrated the separation and amperometric detection of a chiral mixture of DA, several DA precursors, and DA metabolites at a Au wire (Fig 2.15). The separation of a mixture containing DA,

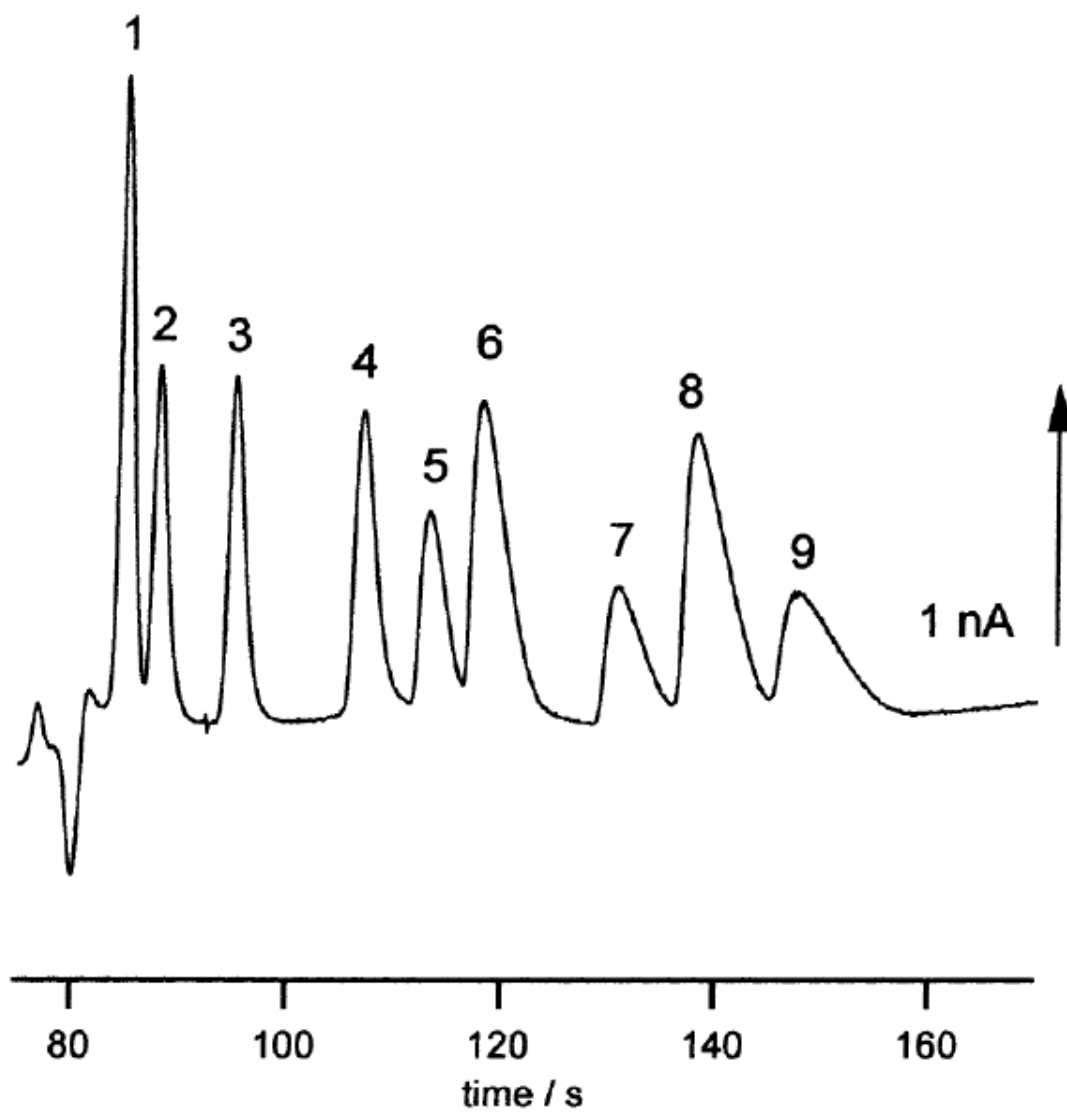


Figure 2.15: Electropherogram for (1) HVA, (2) D-DOPA, (3) L-DOPA, (4) L-CDOPA, (5) D-ME, (6) D-NME, (7) L-ME, (8) MT, and (9) L-NME beside D, A, and NA. Conditions: buffer, 10 mM TRIS, acetic acid, pH 3.0, 8.0 mg/mL SCD, 12 mM 18-crown-6; HV, 4 kV; detection potential, 1700 mV; injection voltage, 1 kV (2 s); concentration, 100 μ M; electrode, Au. Reprinted with permission from [133].

adrenaline (A), noradrenaline (NA), homovanillic acid (HVA), methoxytyramine (MT), L-metanephrine (L-ME), D-metanephrine (D-ME), L-normetanephrine (L-NME), D-normetanephrine (D-NME), and its precursors L-dopamine (L-DOPA) and D-dopamine (D-DOPA), and the related compound L-hydrazinomethylidihydroxyphenylalanine (L-CDOPA) was demonstrated. The authors determined that A, NA, and DA interacted strongly with sulfated β -cyclodextrin (SCD); however, a complete separation of NA and A, and a nonchiral separation of MT, NME, ME, and DA were achieved with the addition of carboxymethylated cyclodextrin and a dendrimer. To achieve a separation of chiral and nonchiral compounds, the authors used a combination of SCD and crown ether in a tris-based buffer at low pH.

More recently, Martin and Mecker reported the integration of microdialysis (MD) sampling with microchip electrophoresis and EC detection for the detection of NTs released from neuronal cells in culture [88]. They described the fabrication, optimization, and application of a microchip device using PDMS-based valves for discrete sample injection, a Pd decoupler and micromolded carbon ink electrodes for off-channel amperometric detection (Fig. 2.16). The authors described the optimization of buffer conditions, valve actuation, and voltage switching to achieve injection from the hydrodynamic flow channel into the electrophoresis channel. The integration of MD and EC detection with microchip electrophoresis (ME) was shown via the separation and detection of DA and CAT standards sampled through a MD probe. To show the ability of this microchip format to monitor a biological system,

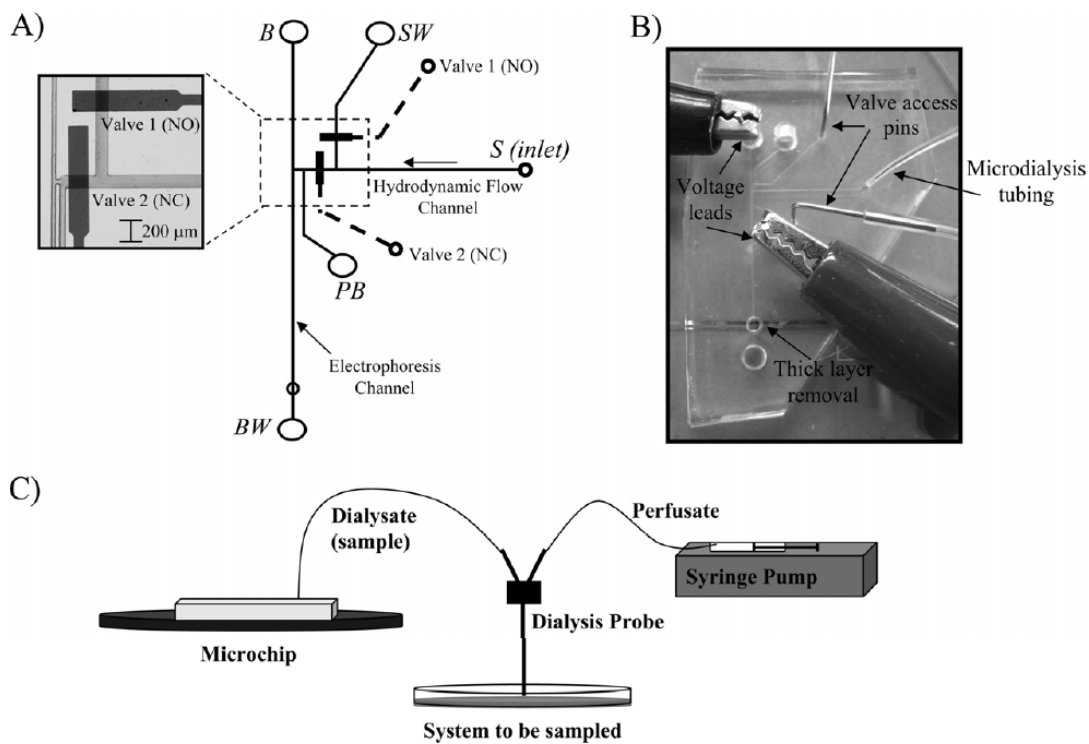


Figure 2.16: (A) Schematic of bilayer microchip with a picture of the valving interface between the hydrodynamic flow and electrophoretic flow. Abbreviations: B, buffer; BW, buffer waste; PB, pushback; SW, sample waste; S, sample; NO, normally open; NC, normally closed. (B) Picture taken on gray background showing how the microdialysis tubing, access pins, and voltage leads are inserted into the microchip. (C) Coupling of the microchip device with microdialysis sampling, associated tubing, and syringe pump. Reprinted with permission from [88].

the authors employed this novel ME/ME/EC device to monitor DA release from cultured neuronal cells. PC 12 cells, which are derived from a pheochromocytoma of the rat adrenal medulla, were grown in a Petri dish and the stimulated release of DA was monitored through the device. The authors were able to detect an average concentration of 29.6 μM DA released by the PC 12 cells which corresponded to ~ 5.5 fmol DA released per cell. This report, demonstrates the ability of a fully integrated device to quantitate analytes samples from a complex biological system.

Vickova and Schwarz developed an analytical method for the determination of several catecholamine NTs and their respective cationic metabolites from brain homogenates [134]. An all glass chip was fitted with a Pt wire, which served as a pseudoreference electrode, and a CNT-modified Au wire as the working electrode. The Au wire was easily functionalized by refluxing CNTs in concentrated nitric acid for 5 hr before dissolving in N-N'-dimethylformamide (DMF). The Au wire was simply dipped in the CNT suspension and allowed to dry at 100 °C which was repeated a total of 10 times. The authors rigorously optimized the BGE in order to achieve a complete separation of DA, Epi, NE, and their O-methoxylated metabolites. It was determined that a 5 mM borate-phosphate buffer containing 10 mM sodium dodecyl sulfate (SDS), and 0.5% (v/v) dendrimer polyamidoamine (PAMAM) dendrimer (with ethylenediamine core generation 1.5), was needed to achieve a separation of all analytes. Limits of detection for DA and Epi were reported to be 1.7 μM and 450 nM respectively. Once the optimal separation conditions were

determined, the method was used for the determination of NTs in mouse brain homogenates in less than 120 s.

2.4.2 Enzyme and Immunoassays

Enzyme and immunoassays have long been one of the standard analysis tools used for biochemistry, molecular biology, and immunology. Owing its name to the immunological reagents it uses, an immunoassay takes advantage of the specific binding of an antibody and its corresponding antigen. The binding constants for the antibody and antigen complex can be as high as 10^{11} M and result in highly selective and sensitive detection [135]. The development of both enzyme and immunoassays for the microchip format has attracted much attention from researchers due to the benefits of fast analysis times, high-throughput, and small reagent volumes needed. In addition, lab-on-a-chip technology has allowed the integration of multiple tasks on a single device including sample preparation, mixing, solid phase extraction, separation, and analyte detection [13, 136-139]. Sample preparation steps can include both chemical and biological derivatization, enzymatic cleaving or conversion, and analyte extraction from samples such as blood or urine. In traditional analyses, antibodies or enzymes are covalently linked to a solid support such as the wells of a microtiter plate. Recently, the use of microbeads or nanoparticles in microfluidic devices has become popular [135, 138]. These spherical substrates have an extremely large surface area-to-volume ratio and can decrease the diffusion distance of reagents. In addition, many types of beads are magnetic, allowing the easy manipulation of bead location with a simple magnet.

The use of inorganic nanocrystal tracers was described by Liu *et al.* for determination of proteins by sandwich immunoassay [140]. While they did not use electrophoretic separation, the authors performed cathodic voltammetric stripping analysis for the simultaneous determination of bovine serum albumin (BSA), β_2 -microglobulin, and C reactive protein. As seen in Figure 2.17, the assay consisted of primary antibodies bound to the inorganic nanocrystals which captured the analyte of interest, followed by binding of the secondary antibody. Each protein binding event yields a distinct voltammetric peak, whose position and size reflects the identity and concentration of the corresponding antigen. This technique resulted in a mass LOD of ~ 7.5 fmol for BSA.

Wang and co-workers described an on-chip enzymatic assay for the separation and detection of organophosphate (OP) nerve agents [141]. The microchip consisted of a pre-column reaction of organophosphorus hydrolase (OPH), the separation of the phosphonic acid products, and detection using $C^{4}D$. The authors optimized the conditions of the enzymatic process, separation, and detection. They were able to perform a complete assay in under 3 min, requiring 1 min for the enzymatic reaction and 1-2 min for the separation and detection of the reaction products. Detection limits of $5 \mu\text{g/mL}$ for paraoxon and $3 \mu\text{g/mL}$ for methyl parathion were achieved.

Wang's lab has also demonstrated the use of a biochip that has integrated both enzymatic and immunochemical assays within the same microchannel [142]. Through the use of pre- and postcolumn reaction steps, this dual function chip allowed for the simultaneous measurement of glucose and insulin (Fig 2.18). The

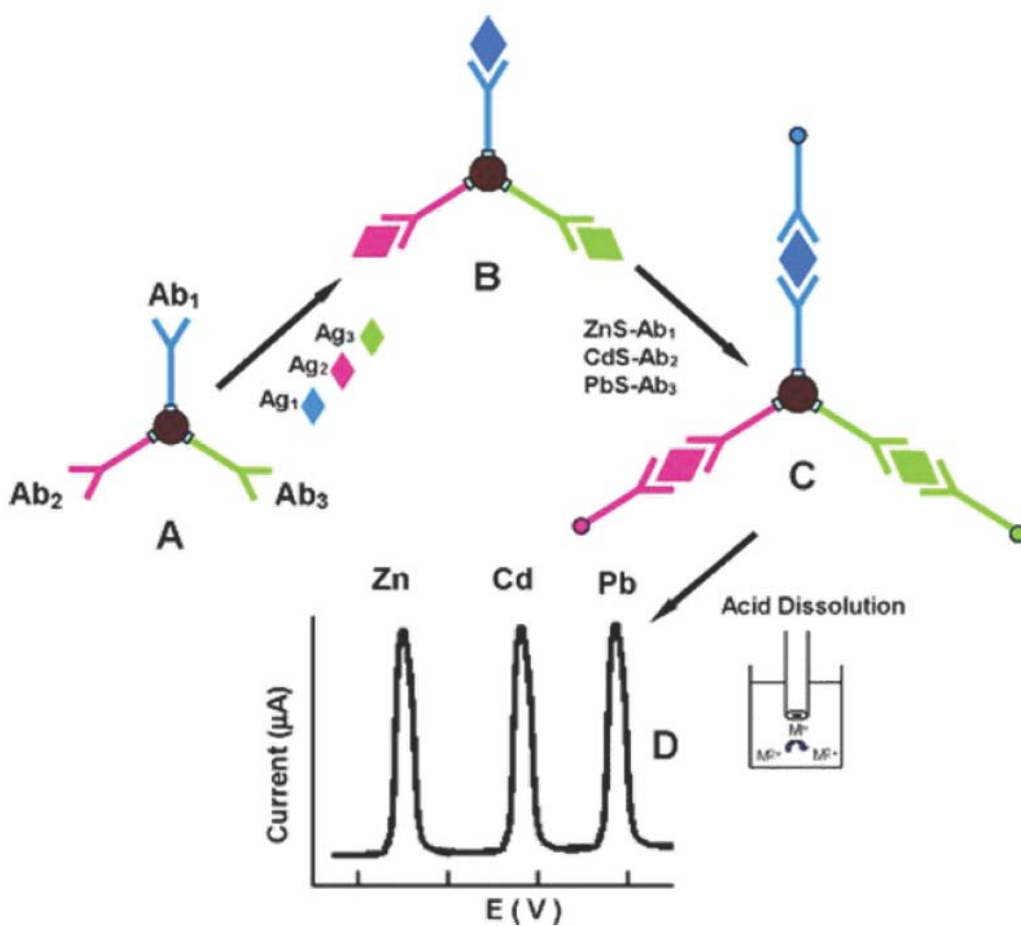


Figure 2.17: Multiprotein electrical detection protocol based on different inorganic colloid nanocrystal tracers. (A) Introduction of antibody-modified magnetic beads; (B) binding of the antigens to the antibodies on the magnetic beads; (C) capture of the nanocrystal-labeled secondary antibodies; (D) dissolution of nanocrystals and electrochemical stripping detection. Reprinted with permission from [140].

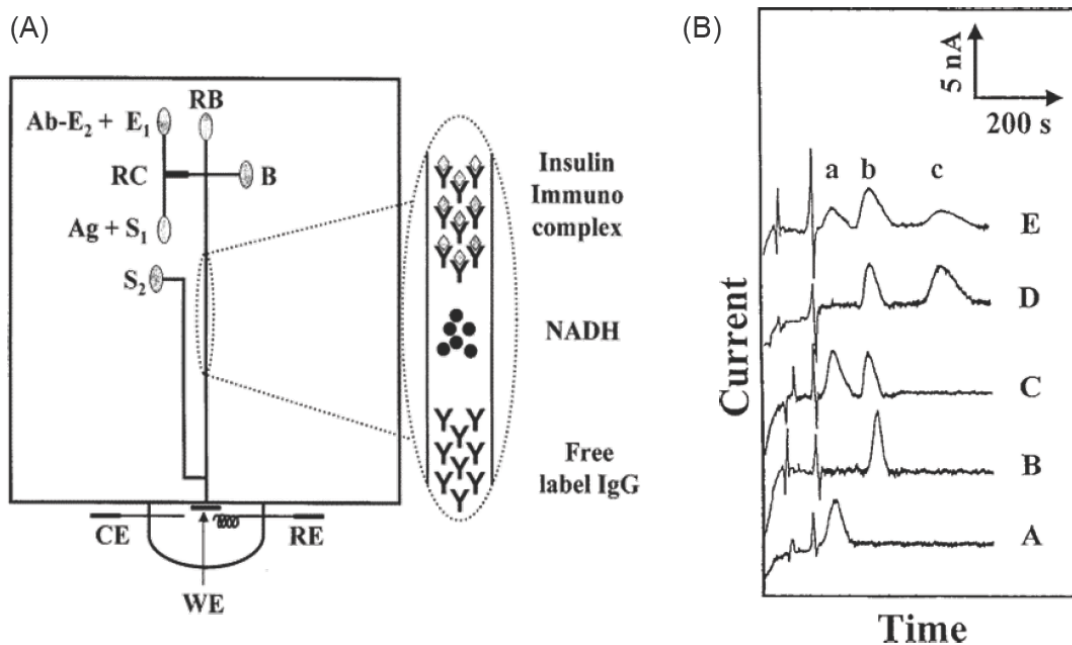


Figure 2.18: (1) Schematic of the biochip used for simultaneous immunological and enzymatic assays. (RB) Running buffer, (Ab-E2) alkaline phosphatase-labeled anti-insulin, (E1) GDH enzyme, (Ag) insulin, (S1) glucose, (RC) reaction chamber, (S2) *p*-NPP, (B) buffer, (WE) working electrode, (CE) counter electrode, and (RE) reference electrode. (2) Electropherograms for the ALP-labeled antibody (1.28×10^{-4} g mL⁻¹) in connection to a postcolumn addition of the *p*-NPP substrate (at 20 mM). (B) Response for 1 mM glucose in the presence of GDH and NAD⁺ (20 U mL⁻¹ and 20 mM, respectively). (C) Same as B but in the presence of ALP-labeled antibody (1.28×10^{-4} g mL⁻¹) and *p*-NP (20 mM). (D) Same as C but in the presence of 1 μ M insulin. (E) Same as D but in the presence of 0.3 nM insulin. Separation and postcolumn voltages, 1500 V; injection, 5 s at 1000 V; detection potential, +1.2 V (vs Ag/AgCl wire). Reprinted with permission from [141].

precolumn reactions involve enzyme-labeled antibody (anti-human insulin) with its antigen (insulin) and the reaction of glucose-dehydrogenase (GDH) with its glucose substrate in the presence of its NAD^+ cofactor. Following the reaction, the free antibody, the antibody-antigen complex, and the NADH product of the enzymatic reaction are electrophoretically separated. Prior to detection, the post-column reaction of an alkaline-phosphatase (ALP) enzyme tag and its substrate p-nitrophenyl phosphate (p-NPP) occurs. Both the NADH and p-nitrophenol (P-NP) products are detected amperometrically at a downstream Au electrode. Despite a large concentration difference between glucose and insulin (mM and nM respectively), the biochip was able to provide independent responses for the corresponding targets. Furthermore, it was demonstrated that this technique could accurately detect both analytes over their clinically relevant ranges: 2.5-7.2 mM for glucose and 36-179 pM for insulin.

2.4.3 Clinical Assays

Coinciding with the development of microfluidic platforms capable of analyzing biologically relevant analytes, was the growth in microchip devices used for clinical analysis. The portability of lab-on-a-chip devices is ideally suited for point-of-care analysis. Traditional analyses can be time consuming, labor intensive, and most must be done off-site. Therefore, the ability of microfluidic devices to integrate multiple processes and process samples in parallel is an attractive alternative. In addition, the small footprint of these devices has led to the

development of microchip capable of clinical point-of-care analyses. Over the past decade, several research groups have demonstrated the analysis of several important clinical markers such as glucose [143-144], DNA [17, 145-146], peptides [147], amino acids [148-149], and renal markers [150]. In addition, several excellent reviews detailing the use of microfluidic devices for clinical analysis have been recently published [151-156].

Used as markers of glomerular filtration rate and therefore kidney function, creatinine, creatine, and uric acid are among the most widely tested analytes for clinical diagnostics. Garcia and Henry demonstrated the use microchip electrophoresis with PAD to detect these three important biomarkers [157]. Creatinine and creatine are not considered electroactive due to the fact that they do not possess any easily oxidizable or reducible functional groups. However, the use of PAD permits the direct EC detection of these otherwise non-electroactive analytes. Using standards, the authors reported LODs of 80 μM , 250 μM , and 270 μM for creatinine, creatine, and uric acid respectively, which are well below physiologically relevant concentrations. In addition, the analysis of creatinine in a real urine sample was demonstrated and validated using a commercial clinical kit based on the Jaffé reaction. The calculated concentrations were 2.20 and 2.12 mM using the Jaffé reaction and the microchip analysis respectively. However, results were obtained in less than 3 min using microchip with PAD compared to ~20 min when using traditional clinical analysis.

Small inorganic ions in human body fluids such as Na^+ , K^+ , Ca^+ , and Mg^+ are also routinely tested for clinical analysis. Determination of these small ions can be particularly challenging due to the fact that they cannot be detected by LIF. Therefore the use of C^4D has become popular for the analysis of small inorganic ions for clinical analyses. Kuban and Hauser recently published a microchip device with integrated C^4D for the separation and detection of several clinically important ions [158]. The authors used an all PMMA microchip and performed several experiments to optimize the size and configuration of the external Cu electrodes. Using standard solutions, the LODs achieved were $1\ \mu\text{M}$ for K^+ , $1.5\ \mu\text{M}$ for Ca^+ , $3\ \mu\text{M}$ Na^+ , $1.75\ \mu\text{M}$ for Mg^+ and $7.5\ \mu\text{M}$ for Li^+ . The use of the device for the clinical analysis of real samples was also demonstrated through the determination of biologically significant ions in both blood and urine. Using no sample preparation other than dilution, the authors were able to demonstrate the detection of the cations NH_4^+ , Na^+ , K^+ , Ca^+ , and Mg^+ , and the anions Cl^- , NO_3^- , SO_4^{2-} , and phosphate in both blood and urine less than 90 s.

Another major important aspect of clinical analysis is the monitoring of therapeutics administered to patients. Because many drugs have a narrow therapeutic window, the routine testing of plasma or serum concentrations is often necessary. Lithium is one of the most widely used and important mood stabilizers that suffers from this problem. While the conventional method for determining the concentration of Li^+ in blood in plasma is quick, it requires $\sim 50\ \mu\text{L}$ of sample [159]. Recently, van den Berg and co-workers have described a novel approach to determine Li^+ in blood

using microchip electrophoresis with $C^{4}D$ [160]. The authors developed a new sample-to-chip interface for sample introduction. Samples were collected from a finger-stick into a glass capillary with an internal volume of only $2 \mu L$. This capillary was then directly inserted into the fully integrated microchip device (Fig 2.19). Because the glass sample collector had an integrated filter membrane, blood cells were excluded from the chip and no sample preparation was necessary. A LOD of $150 \mu M$ was achieved for the detection of Li^{+} . The authors noted that analysis using microchip electrophoresis was less precise than the traditional method (RSD values of 10% and 2.3% respectively); however, the new method was capable of determining concentrations of Li^{+} as well as Na^{+} , Ca^{+} , and Mg^{+} in less than 20 s.

One of the most challenging aspects of clinical analyses is the development of assays which can be used on-site in developing countries. This task is especially difficult because many locations do not have access to trained personnel or advanced instrumentation. For these reasons, the use of paper-based microfluidic devices has gained popularity. These devices are inexpensive, easy to use, disposable, portable, and require little supporting instrumentation. Henry and co-workers recently described the development of a paper-based microfluidic device for the EC detection of glucose, lactate, and uric acid [161]. Many of the previously developed paper microchips utilized colorimetric detection which can have several limitations. The device described by Henry *et al.* increased selectivity by utilizing EC detection with oxidase enzyme reactions (glucose oxidase, lactate oxidase, and uricase) for the determination of glucose, lactate, and uric acid, respectively. Photolithography was

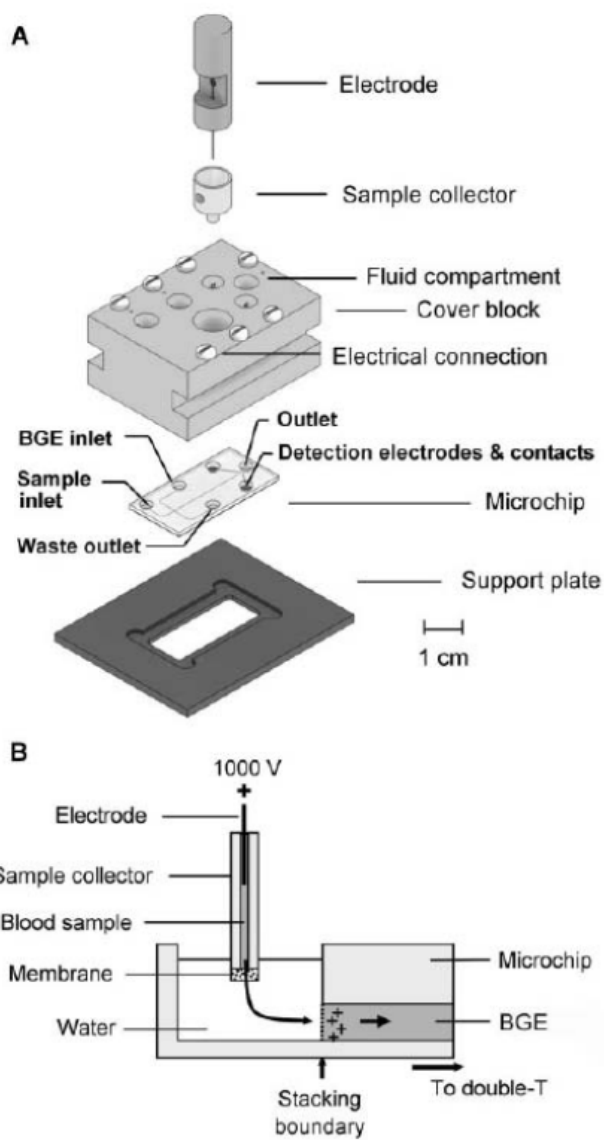


Figure 2.19: (A) Components of the microchip CE system with the Plexiglas sample collector and (B) schematic representation of the sample-to chip interface. Reprinted with permission from [160].

used to make microfluidic channels on filter paper, and screen-printing technology was used to fabricate electrodes. Analysis could be performed on as little as 5 μL of sample which was placed in the center of the paper device (Fig 2.20). The fluid then flowed through the electrode zone for EC detection. The LOD for glucose, lactate, and uric acid were found to be 210 μM , 360 μM , and 1.38 mM, respectively. This device was then used for the accurate determination of glucose and lactate levels in human serum as validated using traditional analysis.

2.4.4 Environmental Applications

The development of new microchip technologies, fabrication strategies, and fully integrated lab-on-a-chip systems has led the use of these devices for environmental monitoring. Microchip electrophoresis has been used to monitor environmental pollutants [162], biological and chemical warfare agents [101, 163], and explosives [127, 164-165]. The use of microfluidic devices allows monitoring and rapid identification of hazardous materials in air or water, which can help protect personal health and safety and prevent contamination of the food supply. Several research labs have investigated the use of lab-on-a-chip devices for these purposes, and several excellent reviews are available [162-163, 166-167].

Recently, Noblitt and co-workers described a microchip device optimized for the separation of atmospheric aerosols, sulfate, nitrate, chloride, and oxalate using contact conductivity detection [168]. Atmospheric samples were collected using an automated annular denuder/filter pack system and subsequently analyzed on chip. The authors performed extensive optimization of the separation conditions to achieve

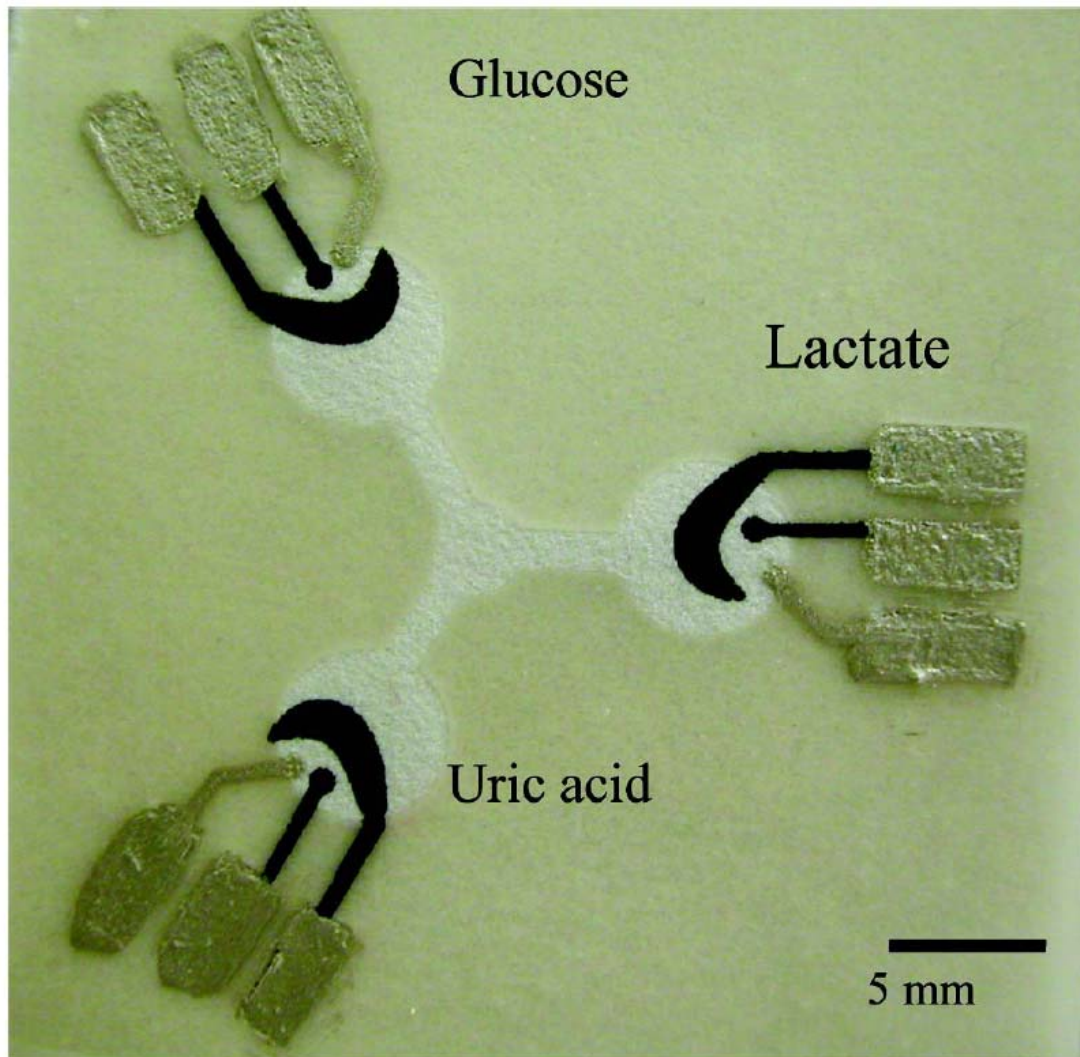


Figure 2.20: Picture of three electrode paper-based microfluidic devices. The hydrophilic area at the center of the device wicks sample into the three separate test zones where independent enzyme reactions occur. The silver electrodes and contact pads are made from Ag/AgCl paste with the black electrode portions being the PB-modified carbon electrodes. The device size is 4 cm × 4 cm. Reprinted with permission from [161].

a suitable separation of all analytes. The approach chosen used a zwitterionic surfactant to modify the mobility of nitrate via MEKC, a BGE with pH in the 4.5–5.0 range to control the migration of weak acids, and a weak counter-EOF to accentuate differences in ionic mobilities. A LOD of 180 nM for oxalate was reported, however when it was injected from a dilute buffer solution, sample stacking lowered the LOD to 19 nM. When using a typical sample size of 20 μL , only 34 pg of oxalic acid is needed to be collected to reach the LOD. Assuming a typical atmospheric concentration of 50 ng m^{-3} and a 1 L min^{-1} collection rate, a sampling time of only 41 s would be required. The future use of an on-chip aerosol sampling method combined with the short migration times observed (~ 60 s) would allow this separation technique make this an ideal candidate for rapid analysis of environmental pollutants.

Another class of compounds that has gained attention as environmental pollutants in recent years are polyphenols and related phenolic compounds. Phenolic compounds have been shown to be toxic, carcinogenic, and immunosuppressive to humans and are considered pollutants by the U.S. Environmental Protection Agency (EPA) [169]. Therefore, their accurate determination in environmental matrices is highly important. Shiddiky *et al.* has recently published a report detailing the development of a μ -TAS device capable of trace analysis of phenolic compounds [170]. The device consisted of three parallel channels. The first channel is for sample preconcentration by field-amplified sample stacking (FASS), the second channel is for field-amplified sample injection (FASI), while the third is for sample separation and EC detection (Fig 2.21). EC detection was performed at a cellulose-

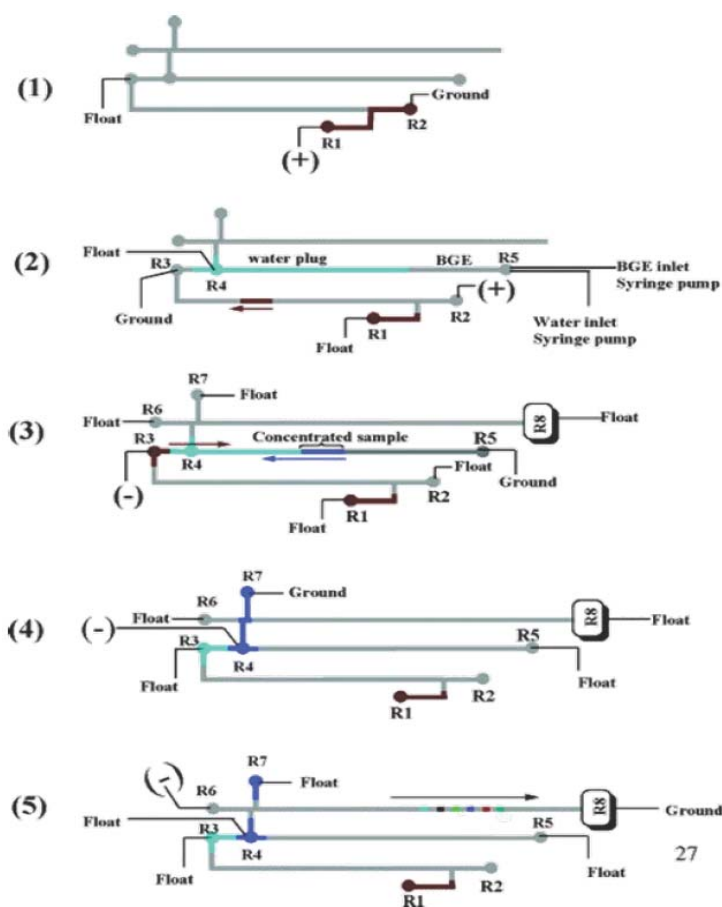


Figure 2.21: Schematic illustration of the sample preconcentration, separation, and electrochemical detection: (1) Sample loading; a voltage of +100 V/cm was applied to R1 while R2 was grounded and R3 was left floating. (2) FASS step: (i) A voltage of +200 V/cm was applied to R2 while R3 was grounded and R1 and R4 were left floating. (ii) Water/BGE injection: during the FASS step, water was injected hydrodynamically from R5 to R4 in channel 2 at a flow rate of 0.1 $\mu\text{L}/\text{min}$ for 2 min. Immediately afterward, the low-pH BGE was injected for 50 s at the same flow rate. (3) FASI step: Initially preconcentrated sample was then injected into channel 2 by applying a voltage of -100 V/cm to R3 with the R5 grounded, leaving all other reservoirs floating. (4) Sample loading and injection: A voltage of -200 V/cm was applied to R4 with R7 grounded and R3, R5, R6, and R8 floating. Injection was effected by applying an injection voltage of -200 V/cm to R4. (5) Separation and detection: MEKC-EC was performed by applying a separation field strength of -250 V/cm to R6 with R8 grounded and R3, R4, R5, and R7 floating. Amperometric detection potential (DP): +1.0 V vs Ag/AgCl. Reprinted with permission from [169].

dsDNA modified screen-printed carbon electrode. Enhanced the signal-to-noise ratios were attributed to the improved electron transfer process through the DNA while diminished passivation was attributed to the presence of the cellulose. All aspects of the analysis (FASS, FASI, and separation were optimized) using standard solutions. It was calculated that the preconcentration factor was increased by 5200-fold as compared to traditional microchip electrophoresis. This high degree of analyte preconcentration was able to yield limits of detection between 100 and 150 pM for several trichlorophenol (TCP) derivatives. The authors used this method to analyze real samples collected from tap water and surface water. The results obtained from the environmental samples showed good correlation to the standards used for optimization (RSD < 3.2%), and the levels detected were below the maximum allowable levels in water mandated by the EPA. Thus, the microchip device and analysis method showed the promise for use as a rapid and sensitive method for detection of environmental pollutants.

In a unique application of environmental analysis, Garcia *et al.* published a report of a mobile system for the detection of phenolic acids [171]. The authors describe the development of a lab-on-a-robot system. It consists of robotics controlled by a wireless global positioning system (GPS), an air pump for environmental sampling, an onboard high voltage power supply (HVPS), and self-contained microchip electrophoresis device using PAD. In order to demonstrate the system was capable of performing the all necessary operations, a testing environment was simulated by placing the system in side a plexiglass box. Atmospheric samples

were collected through an onboard air pump connected to the sample inlet reservoir. All aspects of operation were optimized including the GPS, HVPS, and EC detector. Subsequently, the operation of the robotic unit was demonstrated through the sampling, separation, and detection of atmospheric phenol and ferulic acid. The flexibility of this system demonstrates its ability to perform autonomous environmental testing with near-real time detection of atmospheric pollutants.

2.5 Conclusions and Future Directions

This review has focused on recent developments in employing electrochemical detection for use in microchip electrophoresis. Since the first report of microfluidic devices almost two decades ago, microchip electrophoresis has been extensively researched and developed. Much of this progress is the result of new microfabrication techniques with a variety of materials. In addition, the ability to fabricate electrodes for EC detection on a single microfluidic device has led to the development of fully integrated lab-on-a-chip instrumentation. Due to its ease of operation, simple electronics, and minimal background current contributions, amperometric detection has been the predominant mode of EC detection. However in recent years, advances in conductimetric detection have made it a popular alternative for many environmental and clinical applications. The fabrication and application of miniaturized systems with integrated sample preparation, separation, and detection have been demonstrated. In addition, their use as valuable research tools in areas such as neurochemistry and point-of-care diagnostics has been described. Future directions include integration and automation of all system components to yield

portable, self-contained analytical systems. In addition, the enhancement of sample throughput and detection sensitivity will make microchip electrophoresis with EC an indispensable analytical tool for many areas of research.

2.6 References:

- [1] Manz, A., Graber, N., Widmer, H. M., *Sensors and Actuators B* 1990, *1*, 244-248.
- [2] Manz, A., Harrison, D. J., Verpoorte, E., Fettinger, J. C., Ludi, H., Widmer, H. M., *Journal of Chromatography* 1992, *593*, 253-258.
- [3] Harrison, D. J., Manz, A., Fan, Z., Ludi, H., Widmer, H. M., *Analytical Chemistry* 1992, *64*, 1926-1932.
- [4] Harrison, D. J., Fluri, K., Seiler, K., Fan, Z., Effenhauser, C. S., Manz, A., *Science* 1993, *261*, 895-897.
- [5] Effenhauser, C. S., Manz, A., Widmer, H. M., *Analytical Chemistry* 1993, *65*, 2637-2642.
- [6] Dolnik, V., Liu, S., Jovanovich, S., *Electrophoresis* 2000, *21*, 41-54.
- [7] Ohno, K.-i., Tachikawa, K., Manz, A., *Electrophoresis* 2008, *29*, 4443-4453.
- [8] Wang, J., Chatrathi, M. P., Ibanez, A., Escarpa, A., *Electroanalysis* 2002, *14*, 400-404.
- [9] Wang, J., Chatrathi, M. P., Tian, B., *Analytical Chemistry* 2000, *72*, 5774-5778.
- [10] Wang, J., Chatrathi, M. P., Tian, B., *Analytical Chemistry* 2001, *73*, 1296-1300.
- [11] West, J., Becker, M., Tombrink, S., Manz, A., *Analytical Chemistry* 2008, *80*, 4403-4419.
- [12] Verpoorte, E., de Rooij, N. F., *Proceedings of the IEEE* 2003, *91*, 930-953.
- [13] Haerberle, S., Zengerle, R., *Lab on a Chip* 2007, *7*, 1094-1110.
- [14] Lichtenberg, J., Koster, S., Ceriotti, L., de Rooij, N. F., Verpoorte, E., *Separation Methods in Microanalytical Systems* 2006, 359-431.
- [15] Vandaveer IV, W. R., Pisas-Farmer, S. A., Fischer, D. J., Frankenfeld, C. N., Lunte, S. M., *Electrophoresis* 2004, *25*, 3528-3549.
- [16] Mecker, L. C., Martin, R. S., *Analytical Chemistry* 2008, *80*, 9257-9264.
- [17] Legendre, L. A., Bienvenue, J. M., Roper, M. G., Ferrance, J. P., Landers, J. P., *Analytical Chemistry* 2006, *78*, 1444-1451.
- [18] Iannacone, J. M., Kim, B. Y., King, T. L., Bohn, P. W., Sweedler, J. V., *Biological Applications of Microfluidics* 2008, 451-472.
- [19] Pisas, S. A., Fogarty, B. A., Huynh, B. H., Lacher, N. A., Carlson, B., Martin, R. S., Vandaveer IV, W. R., Lunte, S. M., in: Kutter, J. P., Fintschenko, Y. (Eds.), *Separation Methods in Microanalytical Systems*, Marcel Dekker, New York 2004.
- [20] Johnson, M. E., Landers, J. P., *Electrophoresis* 2004, *25*, 3513-3527.
- [21] Garcia, C. D., Henry, C. S., *Bio-MEMS* 2007, 265-297.
- [22] Huynh, B. H., Fogarty, B. A., Nandi, P., Lunte, S. M., *Journal of Pharmaceutical and Biomedical Analysis* 2006, *42*, 529-534.
- [23] Li, M. W., Martin, R. S., *Analyst* 2008, *133*, 1358-1366.
- [24] Schappler, J., Veuthey, J.-L., Rudaz, S., *Separation Science and Technology* 2008, *9*, 477-521.

- [25] Landers, J. P., Editor, *Capillary and Microchip Electrophoresis and Associated Microtechniques*, 2008.
- [26] Hoffmann, P., Hiusig, U., Schulze, P., Belder, D., *Angewandte Chemie, International Edition* 2007, *46*, 4913-4916.
- [27] Mellors, J. S., Gorbounov, V., Ramsey, R. S., Ramsey, J. M., *Analytical Chemistry* 2008, *80*, 6881-6887.
- [28] Mogensen, K. B., Klank, H., Kutter, J. P., *Electrophoresis* 2004, *25*, 3498-3512.
- [29] Wang, J., *Electroanalysis* 2005, *17*, 1133-1140.
- [30] Woolley, A. T., Lao, K., Glazer, A. N., Mathies, R. A., *Analytical Chemistry* 1998, *70*, 684-688.
- [31] Vickers, J. A., Henry, C. S., *Biological Applications of Microfluidics* 2008, 435-450.
- [32] Vickers, J. A., Henry, C. S., *Electrophoresis* 2005, *26*, 4641-4647.
- [33] Ding, Y., Ayon, A., Garcia, C. D., *Analytica Chimica Acta* 2007, *584*, 244-251.
- [34] Lacher, N. A., Garrison, K. E., Martin, R. S., Lunte, S. M., *Electrophoresis* 2001, *22*, 2526-2536.
- [35] Holcomb, R. E., Kraly, J. R., Henry, C. S., *Analyst* 2009, *134*, 486-492.
- [36] Martin, R. S., *Methods in Molecular Biology* 2006, *339*, 85-112.
- [37] Lunte, S. M., Lunte, C. E., Kissinger, P. T., Heineman, W. R. (Eds.), *Laboratory Techniques in Electroanalytical Chemistry, 2nd Edition.*, pp. 813-853, Marcel Dekker, New York 1996.
- [38] Kissinger, P. T., in: Kissinger, P. T., Heineman, W. R. (Eds.), *Laboratory Techniques in Electroanalytical Chemistry, 2nd Edition.*, Marcel Dekker, New York 1996, pp. 165-194.
- [39] Hulvey, M. K., Martin, R. S., *Analytical and Bioanalytical Chemistry* 2009, *393*, 599-605.
- [40] Hulvey, M. K., Genes, L. I., Spence, D. M., Martin, R. S., *Analyst* 2007, *132*, 1246-1253.
- [41] Lunte, S. M., Lunte, C. E., Kissinger, P. T., Heineman, W. R. (Eds.), *Laboratory Techniques in Electroanalytical Chemistry, 2nd Edition.*, Marcel Dekker, New York, 1996, pp. 813-853.
- [42] Wallenborg, S. R., Nyholm, L., Lunte, C. E., *Analytical Chemistry* 1999, *71*, 544-549.
- [43] LaCourse, W. R., *Pulsed Electrochemical Detection in High-Performance Liquid Chromatography*, 1997.
- [44] Owens, G. S., LaCourse, W. R., *Journal of Chromatography, B: Biomedical Sciences and Applications* 1997, *695*, 15-25.
- [45] Garcia, C. D., Henry, C. S., *Electroanalysis* 2005, *17*, 1125-1131.
- [46] Tanyanyiwa, J., Abad-Villar, E. M., Hauser, P. C., *Electrophoresis* 2004, *25*, 903-908.
- [47] Tanyanyiwa, J., Leuthardt, S., Hauser, P. C., *Electrophoresis* 2002, *23*, 3659-3666.
- [48] Kuban, P., Hauser, P. C., *Electrophoresis* 2009, *30*, 176-188.
- [49] Pumera, M., *Talanta* 2007, *74*, 358-364.

- [50] Zemann, A. J., Schnell, E., Volgger, D., Bonn, G. K., *Analytical Chemistry* 1998, 70, 563-567.
- [51] Silva, J. A. F. d., Lago, C. L. d., *Analytical Chemistry* 1998, 70, 4339-4343.
- [52] Kumar, S. S., Mathiyarasu, J., Phani, K. L., Jain, Y. K., Yegnaraman, V., *Electroanalysis* 2005, 17, 2281-2286.
- [53] Hebert, N. E., Kuhr, W. G., Brazill, S. A., *Electrophoresis* 2002, 23, 3750-3759.
- [54] Ridgway, T. H. K., P. T.; Heineman, W. R. (Eds.), *Laboratory Techniques in Electroanalytical Chemistry, 2nd Edition., Marcel Dekker, New York 1996, pp. 141-163.*
- [55] Brazill, S. A., Bender, S. E., Hebert, N. E., Cullison, J. K., Kristensen, E. W., Kuhr, W. G., *Journal of Electroanalytical Chemistry* 2002, 531, 119-132.
- [56] Brazill, S. A., Singhal, P., Kuhr, W. G., *Analytical Chemistry* 2000, 72, 5542-5548.
- [57] Singhal, P., Kawagoe, K. T., Christian, C. N., Kuhr, W. G., *Analytical Chemistry* 1997, 69, 1662-1668.
- [58] Singhal, P., Kuhr, W. G., *Analytical Chemistry* 1997, 69, 3552-3557.
- [59] Hebert, N. E., Snyder, B., McCreery, R., Kuhr, W. G., Brazill, S. A., *Analytical Chemistry* 2003, 75, 4265-4271.
- [60] Singhal, P., Kuhr, W. G., *Analytical Chemistry* 1997, 69, 4828-4832.
- [61] Anon, *Capillary Electrophoresis: Theory and Practice, 2nd ed. by Patrick Camilleri, 1999.*
- [62] Jacobson, S. C., Hergenroder, R., Koutny, L. B., Ramsey, J. M., *Analytical Chemistry* 1994, 66, 1114-1118.
- [63] Henry, C. S., Dressen, B. M., *Handbook of Capillary and Microchip Electrophoresis and Associated Microtechniques (3rd Edition) 2008, 1441-1457.*
- [64] Wang, J., Tian, B., Sahlin, E., *Analytical Chemistry* 1999, 77, 5436-5440.
- [65] Fercher, G., Smetana, W., Vellekoop, M. J., *Electrophoresis* 2009, 30, 2516-2522.
- [66] Henry, C. S., Zhong, M., Lunte, S. M., Kim, M., Bau, H., Santiago, J., *Analytical Communications* 1999, 36, 305-308.
- [67] Papautsky, I., *Bio-MEMS* 2007, 117-140.
- [68] Chen, Y., Duan, H., Zhang, L., Chen, G., *Electrophoresis* 2008, 29, 4922-4927.
- [69] Nikcevic, I., Lee, S. H., Piruska, A., Ahn, C. H., Ridgway, T. H., Limbach, P. A., Wehmeyer, K. R., Heineman, W. R., Seliskar, C. J., *Journal of Chromatography, A* 2007, 1154, 444-453.
- [70] Martin, R. S., Gawron, A. J., Lunte, S. M., Henry, C. S., *Analytical Chemistry* 2000, 72, 3196-3202.
- [71] Madou, M. J., *Fundamentals of microfabrication: The science of minaturization, CRC Press 2002.*
- [72] Lacher, N. A., de Rooij, N. F., Verpoorte, E., Lunte, S. M., *Journal of ChromatographyA* 2003, 1004, 225-235.
- [73] Coltro, W. K. T., Lunte, S. M., Carrilho, E., *Electrophoresis* 2008, 29, 4928-4937.

- [74] Martin, I. T., Dressen, B., Boggs, M., Liu, Y., Henry, C. S., Fisher, E. R., *Plasma Processes and Polymers* 2007, 4, 414-424.
- [75] Lee, J. N., Park, C., Whitesides, G. M., *Analytical Chemistry* 2003, 75, 6544-6554.
- [76] Vickers, J. A., Caulum, M. M., Henry, C. S., *Analytical Chemistry* 2006, 78, 7446-7452.
- [77] Roman, G. T., McDaniel, K., Culbertson, C. T., *Analyst* 2006, 131, 194-201.
- [78] Nagata, H., Tabuchi, M., Hirano, K., Baba, Y., *Electrophoresis* 2005, 26, 2247-2253.
- [79] Roman Gregory, T., Culbertson Christopher, T., *Langmuir : the ACS journal of surfaces and colloids* 2006, 22, 4445-4451.
- [80] Luo, Y., Huang, B., Wu, H., Zare, R. N., *Analytical Chemistry* 2006, 78, 4588-4592.
- [81] Chen, G., Xu, X., Lin, Y., Wang, J., *Chemistry--A European Journal* 2007, 13, 6461-6467, S6461/6461-S6461/6465.
- [82] Garcia, C. D., Henry, C. S., *Analytical Chemistry* 2003, 75, 4778-4783.
- [83] Mecker, L. C., Martin, R. S., *Electrophoresis* 2006, 27, 5032-5042.
- [84] Lacher, N. A., Lunte, S. M., Martin, R. S., *Analytical Chemistry* 2004, 76, 2482-2491.
- [85] Kuhnline, C. D., Gangel, M. G., Hulvey, M. K., Martin, R. S., *Analyst* 2006, 131, 202-207.
- [86] Amatore, C., Arbault, S., Bouton, C., Drapier, J.-C., Ghandour, H., Koh, A. C. W., *ChemBioChem* 2008, 9, 1472-1480.
- [87] Zachek, M. K., Hermans, A., Wightman, R. M., McCarty, G. S., *Journal of Electroanalytical Chemistry* 2008, 614, 113-120.
- [88] Mecker, L. C., Martin, R. S., *Analytical Chemistry* 2008, 80, 9257-9264.
- [89] McCreery, R. L., Cline, K. K., in: Kissinger, P. T., Heineman, W. R. (Eds.), *Laboratory Techniques in Electroanalytical Chemistry*, Marcel Dekker, New York 1996, pp. 293-332.
- [90] McCreery, R., L.,; Cline K., K., *Laboratory Techniques in Electroanalytical Chemistry, 2nd Edition. Edited by Peter T. Kissinger (Purdue University) and William R. Heineman (University of Cincinnati), 1996, pp. 293-332.*
- [91] Gawron, A. J., Martin, R. S., Lunte, S. M., *Electrophoresis* 2001, 22, 242-248.
- [92] Kovarik, M. L., Torrence, N. J., Spence, D. M., Martin, R. S., *Analyst* 2004, 129, 400-405.
- [93] Kovarik, M. L., Li, M. W., Martin, R. S., *Electrophoresis* 2005, 26, 202-210.
- [94] Kim, J., Song, X., Kinoshita, K., Madou, M., White, R., *Journal of The Electrochemical Society* 1998, 145, 2314-2319.
- [95] Fischer, D. J., Vandaveer, W. R. I. V., Grigsby, R. J., Lunte, S. M., *Electroanalysis* 2005, 17, 1153-1159.
- [96] Fischer, D. J., Hulvey, M. K., Regel, A. R., Lunte, S. M., *Electrophoresis* 2009, 30, 3324-3333.
- [97] Chen, G., *Talanta* 2007, 74, 326-332.
- [98] Pumera, M., Merkoci, A., Alegret, S., *Electrophoresis* 2007, 28, 1274-1280.

- [99] Chen, G., *Talanta* 2007, 74, 326-332.
- [100] Wang, J., Chen, G., Muck, A., Jr., Shin, D., Fujishima, A., *Journal of Chromatography A* 2004, 1022, 207-212.
- [101] Wang, J., Chen, G., Chatrathi, M. P., Fujishima, A., Tryk, D. A., Shin, D., *Analytical Chemistry* 2003, 75, 935-939.
- [102] Kim, D. Y., Merzougui, B., Swain, G. M., *Chemistry of Materials* 2009, 21, 2705-2713.
- [103] Siangproh, W., Chailapakul, O., Laocharoensuk, R., Wang, J., *Talanta* 2005, 67, 903-907.
- [104] Shiddiky, M. J. A., Shim, Y.-B., *Analytical Chemistry* 2007, 79, 3724-3733.
- [105] Johirul, M., Shiddiky, A., Kim, R.-E., Shim, Y.-B., *Electrophoresis* 2005, 26, 3043-3052.
- [106] Pai, R. S., Walsh, K. M., Crain, M. M., Roussel, T. J., Jr., Jackson, D. J., Baldwin, R. P., Keynton, R. S., Naber, J. F., *Analytical Chemistry* 2009, 81, 4762-4769.
- [107] Huang, X., Zare, R. N., Sloss, S., Ewing, A. G., *Analytical Chemistry* 1991, 63, 189-192.
- [108] Wallingford, R. A., Ewing, A. G., *Analytical Chemistry* 1987, 59, 1762-1766.
- [109] Osbourn, D. M., Lunte, C. E., *Analytical Chemistry* 2003, 75, 2710-2714.
- [110] Wu, C.-C., Wu, R.-G., Huang, J.-G., Lin, Y.-C., Chang, H.-C., *Analytical Chemistry* 2003, 75, 947-952.
- [111] Martin, R. S., Ratzlaff, K. L., Huynh, B. H., Lunte, S. M., *Analytical Chemistry* 2002, 74, 1136-1143.
- [112] Manica, D. P., Mitsumori, Y., Ewing, A. G., *Analytical Chemistry* 2003, 75, 4572-4577.
- [113] Ertl, P., Emrich, C. A., Singhal, P., Mathies, R. A., *Analytical Chemistry* 2004, 76, 3749-3755.
- [114] Keynton, R. S., Roussel, T. J., Crain, M. M., Jackson, D. J., Franco, D. B., Naber, J. F., Walsh, K. M., Baldwin, R. P., *Analytica Chimica Acta* 2004, 507, 95-105.
- [115] Chen, C., Hahn, J. H., *Analytical Chemistry* 2007, 79, 7182-7186.
- [116] Guijt, R. M., Evenhuis, C. J., Macka, M., Haddad, P. R., *Electrophoresis* 2004, 25, 4032-4057.
- [117] Huang, X., Pang, T. K. J., Gordon, M. J., Zare, R. N., *Analytical Chemistry* 1987, 59, 2747-2749.
- [118] Dasgupta, P. K., Bao, L., *Analytical Chemistry* 1993, 65, 1003-1011.
- [119] Noblitt, S. D., Henry, C. S., *Analytical Chemistry* 2008, 80, 7624-7630.
- [120] Feng, H.-T., Wei, H.-P., Li Sam, F. Y., *Electrophoresis* 2004, 25, 909-913.
- [121] Tay, E. T. T., Law, W. S., Sim, S. P. C., Feng, H., Zhao, J. H., Li, S. F. Y., *Electrophoresis* 2007, 28, 4620-4628.
- [122] Galloway, M., Stryjewski, W., Henry, A., Ford, S. M., Llopis, S., McCarley, R. L., Soper, S. A., *Analytical Chemistry* 2002, 74, 2407-2415.
- [123] Shadpour, H., Hupert, M. L., Patterson, D., Liu, C., Galloway, M., Stryjewski, W., Goettert, J., Soper, S. A., *Analytical Chemistry* 2007, 79, 870-878.

- [124] Gas, B., Demjanenko, M., Vacik, J., *Journal of Chromatography* 1980, 192, 253-257.
- [125] Coltro, W. K. T., da Silva, J. A. F., Carrilho, E., *Electrophoresis* 2008, 29, 2260-2265.
- [126] Coltro, W. K. T., Carrilho, E., *Handbook of Capillary and Microchip Electrophoresis and Associated Microtechniques (3rd Edition)* 2008, 1169-1184.
- [127] Wang, J., Chen, G., Muck, A., *Talanta* 2009, 78, 207-211.
- [128] Garcia, C. D., Henry, C. S., *Bio-MEMS* 2007, 265-297.
- [129] Liu, Y., Vickers, J. A., Henry, C. S., *Analytical Chemistry* 2004, 76, 1513-1517.
- [130] Chen, Z., Goa, Y., Lin, J., Su, R., Xie, Y., *Journal of Chromatography A* 2004, 1038, 239-245.
- [131] Muck, A., Jr., Wang, J., Jacobs, M., Chen, G., Chatrathi, M. P., Jurka, V., Vyborny, Z., Spillman, S. D., Sridharan, G., Schoening, M. J., *Analytical Chemistry* 2004, 76, 2290-2297.
- [132] Huang, W.-H., Cheng, W., Zhang, Z., Pang, D.-W., Wang, Z.-L., Cheng, J.-K., Cui, D.-F., *Analytical Chemistry* 2004, 76, 483-488.
- [133] Schwarz, M. A., Hauser, P. C., *Analytical Chemistry* 2003, 75, 4691-4695.
- [134] Vlckova, M., Schwarz, M. A., *Journal of Chromatography, A* 2007, 1142, 214-221.
- [135] Kuramitz, H., *Analytical and Bioanalytical Chemistry* 2009, 394, 61-69.
- [136] Chatrathi, M. P., Collins, G. E., Wang, J., *Methods in Molecular Biology (Totowa, NJ, United States)* 2007, 385, 215-224.
- [137] Moser, A. C., Hage, D. S., *Electrophoresis* 2008, 29, 3279-3295.
- [138] Sato, K., Kitamori, T., *Handbook of Capillary and Microchip Electrophoresis and Associated Microtechniques (3rd Edition)* 2008, 1013-1019.
- [139] Chatrathi, M. P., Collins, G. E., Wang, J., *Methods in Molecular Biology (Totowa, NJ, United States)* 2007, 385, 215-224.
- [140] Liu, G., Wang, J., Kim, J., Jan, M. R., Collins, G. E., *Analytical Chemistry* 2004, 76, 7126-7130.
- [141] Wang, J., Chen, G., Muck Jr, A., Chatrathi, M. P., Mulchandani, A., Chen, W., *Anal. Chim. Acta* 2004, 505, 183-187.
- [142] Wang, J., Ibanez, A., Prakash Chatrathi, M., *Journal of the American Chemical Society* 2003, 125, 8444-8445.
- [143] Wang, J., Chatrathi, M. P., Ibanez, A., *Analyst* 2001, 126, 1203-1206.
- [144] Wang, J., Chatrathi, M. P., Tian, B., Polsky, R., *Analytical Chemistry* 2000, 72, 2514-2518.
- [145] Dewald, A. H., Poe, B. L., Landers, J. P., *Expert Opinion on Medical Diagnostics* 2008, 2, 963-977.
- [146] Price, C. W., Leslie, D. C., Landers, J. P., *Lab on a Chip* 2009, 9, 2484-2494.
- [147] Pasas, S. A., Lacher, N. A., Davies, M. I., Lunte, S. M., *Electrophoresis* 2002, 23, 759-766.

- [148] Tay, E. T. T., Law, W. S., Sim, S. P. C., Feng, H., Zhao, J. H., Li, S. F. Y., *Electrophoresis* 2007, 28, 4620-4628.
- [149] Wang, J., Chen, G., *Talanta* 2003, 60, 1239-1244.
- [150] Wang, J., Chatrathi, M. P., *Analytical Chemistry* 2003, 75, 525-529.
- [151] Verpoorte, E., *Electrophoresis* 2002, 23, 677-712.
- [152] Ferrance, J. P., *Handbook of Capillary and Microchip Electrophoresis and Associated Microtechniques (3rd Edition)* 2008, 1037-1063.
- [153] Castano-Alvarez, M., Fernandez-Abedul, M. T., Costa-Garcia, A., *Comprehensive Analytical Chemistry* 2007, 49, 827-872.
- [154] Sato, K., Mawatari, K., Kitamori, T., *Lab on a Chip* 2008, 8, 1992-1998.
- [155] Belluzo, M. S., Ribone, M. E., Lagier, C. M., *Sensors* 2008, 8, 1366-1399.
- [156] Li Sam, F. Y., Kricka Larry, J., *Clinical chemistry* 2006, 52, 37-45.
- [157] Garcia, C. D., Henry, C. S., *Analyst* 2004, 129, 579-584.
- [158] Kuban, P., Hauser, P. C., *Lab on a Chip* 2008, 8, 1829-1836.
- [159] Glazer, W. M., Sonnenberg, J. G., Reinstein, M. J., Akers, R. F., *Journal of Clinical Psychiatry* 2004, 65, 652-655.
- [160] Vrouwe, E. X., Luttge, R., Vermes, I., van den Berg, A., *Clinical Chemistry* 2007, 53, 117-123.
- [161] Dungchai, W., Chailapakul, O., Henry, C. S., *Analytical Chemistry* 2009, 81, 5821-5826.
- [162] Chen, G., Lin, Y., Wang, J., *Current Analytical Chemistry* 2006, 2, 43-50.
- [163] Wang, J., *Analytica Chimica Acta* 2004, 507, 3-10.
- [164] Hilmi, A., Luong, J. H. T., *Environmental Science & Technology* 2000, 34, 3046-3050.
- [165] Pumera, M., Wang, J., *Jala* 2002, 7, 47-49.
- [166] Pumera, M., *Electrophoresis* 2006, 27, 244-256.
- [167] Mora, M. F., Garcia, C. D., *Biological Applications of Microfluidics* 2008, 245-261.
- [168] Noblitt, S. D., Schwandner, F. M., Hering, S. V., Collett, J. L., Jr., Henry, C. S., *Journal of Chromatography, A* 2009, 1216, 1503-1510.
- [169] Richardson, S. D., Ternes, T. A., *Analytical Chemistry* 2005, 77, 3807-3838.
- [170] Shiddiky, M. J. A., Park, H., Shim, Y.-B., *Analytical Chemistry* 2006, 78, 6809-6817.
- [171] Berg, C., Valdez, D. C., Bergeron, P., Mora, M. F., Garcia, C. D., Ayon, A., *Electrophoresis* 2008, 29, 4914-4921.

Chapter 3

Pyrolyzed Photoresist Carbon Electrodes for Microchip Electrophoresis with Dual-Electrode Amperometric Detection

(Electroanalysis, 2005, 17(13), 1153-1159)

3.1 Introduction

Over the past decade, there has been an increasing trend toward the miniaturization of analytical instrumentation [1-5]. The microfabricated format permits integration of several laboratory processes on a single microchip [6, 7]. The advantages associated with these miniaturized systems include increased speed of analysis and throughput, precision and accuracy, portability, reduced cost and waste, disposability, and the potential for on-site use [5, 8]. Numerous detection modes have been employed in conjunction with microchip devices including mass spectrometry (MS), laser-induced fluorescence (LIF), and optical measurements [9, 10].

Electrochemical (EC) detection is ideally suited for miniaturized analytical systems and has been used frequently with microchip electrophoresis (ME) devices [11, 12]. Electrochemistry has several advantages as a detection method including sensitivity, selectivity, and the ability to miniaturize both the detector and the control instrumentation. In addition, many types of microelectrodes can be fabricated using common photolithographic procedures.

Both metal and carbon-based electrodes have been used as working electrodes for microchip CE [12-19]. Carbon has been the most popular material for use with conventional (capillary-based) CE-EC and liquid chromatography/electrochemistry [20, 21]. Carbon electrodes have a larger potential window, lower overpotential and background noise, and foul less easily than most metal electrodes [20, 22]. The most common types of carbon-based electrodes employed in the microchip format are

carbon fibers, paste, and ink [13-16]. Although these electrodes have performed well as detectors for microchip electrophoresis systems, they are not fabricated photolithographically and, hence, are not amenable to mass production as are the other components of the microchip.

Photoresist has been used extensively in the microelectronics industry for the production of integrated circuits. One of the attractive features of photoresist is that it can be patterned on silicon and glass surfaces with micron-to-submicron resolution. Lyons *et al.* initially showed the advantages of using pyrolyzed photoresist for integrated circuit production [23, 24]. Recently, several investigators have explored the use of pyrolyzed photoresist for the production of carbon film electrodes [25-28].

In their first report concerning the electrochemistry of pyrolyzed photoresist film (PPF) electrodes, Kim *et al.* showed that when pyrolysis was performed at high temperatures ($\geq 700^{\circ}\text{C}$), the electrocatalytic behavior of the carbon films was improved [25]. The resulting carbon films exhibited electrochemical behaviors similar to that of glassy carbon electrodes [25]. Later, Madou and coworkers showed that pyrolyzed photoresist films displayed lower background currents and possessed a smoother surface and a lower oxygen/carbon atomic (O/C) ratio than that of glassy carbon electrodes [26]. The smoothness and low O/C ratio resulted in lower capacitance and background current [28]. In addition, these electrodes were shown to only weakly absorb methylene blue, which is known to physisorb strongly to most carbon surfaces [28]. Lastly, the use of interdigitated PPF electrodes for cyclic voltammetric measurements was investigated by KostECKI *et al.* [27].

Recently, PPF electrodes have been evaluated as detectors for microchip CEEC [17, 29]. The PPF electrodes have several potential advantages for microchip CE. They are more robust than fibers and paste and can be fabricated photolithographically to create a truly integrated separation and detection system. The first report of the use of a PPF electrode with microchip CEEC was published by Hebert *et al.* in 2003. In this report, sinusoidal voltammetry was employed for the detection of four neurotransmitters [17].

In the work presented here, the use of PPF electrodes for microchip CE with amperometric detection is described. In particular, the performance of the PPF electrodes is compared directly with that of carbon fiber electrodes for the detection of biogenic amines and ascorbate. The development of a dual-electrode detector using PPF electrodes is also described. This is the first report of a PPF-based dual-electrode detector for microchip CEEC.

3.2 Materials and Methods

3.2.1 Materials and Reagents

The following chemicals were used as received: AZ 1518 positive photoresist and AZ 300 MIF developer (Clariant Corp., Somerville, NJ); SU-8 10 negative photoresist and Nano SU-8 developer (MicroChem Corp., Newton, MA); 100-mm Si wafers (Silicon, Inc., Boise, ID); Sylgard 184 (Ellsworth Adhesives, Germantown, WI); dopamine (DA), catechol, ascorbic acid (AA), boric acid (BA) and 5-hydroxyindole-3-acetic acid (5-HIAA) (Sigma-Aldrich, St. Louis, MO); 2-propanol (IPA), acetone, 1

mL syringes, and Pt wire (22 gauge) (Fisher Scientific); high temperature fused silica glass plates (4 in. × 2.5 in. × 0.085 in.; Glass Fab Inc., Rochester, NY); 33 μm carbon fibers (Avco Specialty Materials, Lowell, MA); conductive epoxy (ITW Chemtronics, Kennesaw, GA); 0.22 μm Teflon filters (Osmonics, Inc., Minnetonka, MN); NANOpure water (Labconco, Kansas City, MO); Cu wire (22 gauge; Westlake Hardware, Lawrence, KS).

3.2.2 Fabrication of PDMS Microchips

The fabrication of PDMS-based microfluidic devices has been described previously [30, 31]. Briefly, SU-8 10 negative photoresist was spin coated (500 rpm for 5 s, then 2000 rpm for 30 s) on a 100-mm silicon wafer using a Cee 100 spincoater (Brewer Science, Rolla, MO). A design containing the desired structures was created using Freehand 10 (Macromedia Inc., San Francisco, CA) and transferred to a transparency film at a resolution of 2400 dpi (Jostens, Topeka, KS). Following a prebake process (40°C for 5 min, 65°C for 5 min, then 95°C for 2 min), the negative film mask was placed over the coated wafer and exposed to a near-UV flood source (4 min, 5.6 W/cm², Autoflood 1000, Optical Associates, Milpitas, CA). Following the exposure, the wafer was postbaked at 95°C for 2 min. Subsequently, the wafer was allowed to cool to room temperature and then developed in Nano SU-8 developer, rinsed with acetone and IPA, and then dried under nitrogen. The thickness of the raised photoresist, which corresponded to the depth of the PDMS channels, was measured with a profilometer (Alpha Step-200, Tencor Instruments, Mountain View, CA). PDMS microstructures were made by casting a 10:1 mixture of PDMS

elastomer and curing agent, respectively, against the silicon master. After curing at 75°C for 1.5 h, the PDMS was removed from the master, yielding the desired negative relief pattern. The same simple T design was used for all studies reported and contained both the separation and injection channels. The dimensions were 5.5 cm from the T intersection to the end of separation channel and 1.4 cm from the T intersection to the sample and buffer reservoirs. Holes for the reservoirs were created in the polymer with a single hole punch. The width and depth of the PDMS microchannels were 30 μm and 17 μm , respectively.

3.2.3 Electrode Fabrication

The PPF electrodes used for these studies were fabricated (Fig. 3.1) by first spin coating AZ 1518 positive photoresist on a fused silica glass plate (100 rpm for 20 s then 2000 rpm for 20 s). The coated plates were prebaked at 95°C for 1 min, covered with the desired positive film mask, and exposed to a near-UV flood source (9 s at 5.6 W/cm²). After exposure the plate was developed in AZ 300 MIF developer for 20 s, rinsed with NANOpure water, and dried under nitrogen. The plates underwent a subsequent postbake at 90°C for 1 min. A Lindberg/Blue M Three-Zone Tube Furnace (Cole-Parmer) was utilized for pyrolysis. The furnace was fitted with quartz end caps with connections to heat-resistant polytetrafluoroethylene extruded Teflon tubing (Fisher Scientific) and was continuously flushed with nitrogen at 5 psi to provide an inert atmosphere. The temperature of the furnace started under ambient conditions and was increased at the rate of 5.5°C/min to 925°C, held for 1 h, and then allowed to cool to room temperature. The width of the electrodes was 40 μm and the

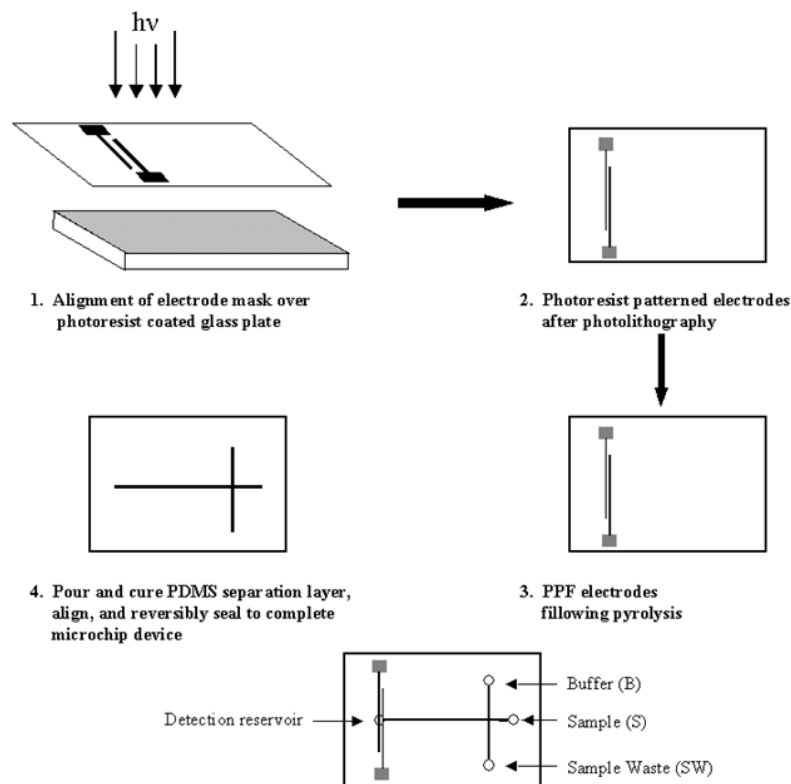


Figure 3.1 Schematic of the photolithographic fabrication procedure used for the PPF electrodes (images not to scale). (1) alignment of electrode mask over photoresist covered glass plate; (2) photoresist patterned electrodes after photolithography; (3) PPF electrode following pyrolysis; (4) pour and cure PDMS separation layer, align, and reversibly seal to complete microchip device.

height was determined with a profilometer to be 0.5 μm . Conductive epoxy (ITW Chemtronics) was used to bond copper wires to the electrode contact pads to provide electrical connection. Fabrication of the PDMS carbon fiber electrode channel and placement of the carbon fiber was based on previously described work [13].

3.2.4 Chip Construction

The layer of PDMS containing the separation channel was aligned and reversibly sealed to the glass electrode plate by bringing the two substrates into conformal contact with one another. This was achieved after extensive cleaning of the surfaces with IPA and drying with N_2 . The first working electrode was aligned within 5–20 μm of the exit of the separation channel, with the aid of a light microscope, in an end-channel configuration. The second electrode was positioned 30 μm from the first; this distance was predetermined by the fabrication procedure. End-channel detection allows sufficient decoupling of the high-voltage (HV) separation field from the working electrodes. For all studies described here, end-channel detection was employed.

3.3.5 Electrophoresis Procedure

Capillary electrophoresis (CE) was carried out in unmodified PDMS microchannels using two Spellman CZE 1000R HV power supplies (Spellman High Voltage Electronics, Hauppauge, NY). The electrophoresis buffer used for all data presented was 25 mM boric acid at pH 9.2. The buffer was degassed (Fisher Ultrasonic Cleaner, Fisher Scientific) and filtered with a 0.22- μm Teflon filter before

use. The PDMS channels were flushed with buffer after applying a vacuum. This process was continued until no air bubbles were observed. Stock solutions (1 mM) of DA, AA, catechol, and 5-HIAA were prepared daily in NANOpure water. Samples were made prior to use by diluting with buffer. Electrophoresis was performed by applying a high voltage (+1880 V) at the buffer reservoir (B) and a fraction of this high voltage (+1250 V) at the sample reservoir (S) while the sample waste (SW) and detection reservoirs were left at ground (Figure 3.1). For all data presented, a gated injection method [32, 33] was used for introduction of the sample plug and was achieved by allowing the high voltage at B to float for 5 s before it was returned to +1880 V.

3.2.6 Electrochemical Detection

Electrochemical detection was accomplished using either a CHI 802A electrochemical analyzer (CH Instruments Inc., Austin, TX) or a LC-4CE potentiostat (Bioanalytical Systems, West Lafayette, IN). When using the CHI bipotentiostat, signals were collected while operating in either “*amperometric i-t mode*” for separations or “*cyclic voltammogram mode*” for EC response and were analyzed using the built-in software package. Experiments performed with the BAS system used an analog-to-digital converter (DA-5, Bioanalytical Systems) for signal collection while data were analyzed using the accompanying Chromgraph software (Bioanalytical Systems). Experiments were performed in either three-electrode mode for single electrode detection or four-electrode mode for dual-electrode detection. A Pt wire auxiliary electrode (22 gauge) and Ag/AgCl reference electrode (CH

Instruments) were placed in the detection reservoir to complete the electrochemical cell. The first working electrode (E_1) was held at a fixed potential of +900 mV (vs. Ag/AgCl); when operating in dual-detection mode, the second working electrode (E_2) was held at a fixed potential of -100 mV (vs. Ag/AgCl).

3.3 Results and Discussion

3.3.1 Electrode Comparison

Carbon-based electrodes such as carbon fibers, ink, and paste have been successfully used in the microchip format. The major disadvantage of these electrodes is that, in most cases, the fabrication and alignment of the electrodes on the chip must be accomplished manually and is labor intensive. This precludes the use of these electrodes for mass production. PPF electrodes are an attractive alternative to fibers, inks and pastes since they are produced by photolithography. This makes it possible to produce the carbon-based electrodes using the same microfabrication equipment and procedures that are employed for chip fabrication. The use of photolithographic methods also provides better precision of electrode dimensions and placement.

Carbon fibers have been used successfully by our laboratory for microchip CEEC [13]. These electrodes are well characterized and have been shown to exhibit good electrochemical properties for a variety of biological compounds. However, carbon fibers also suffer from the disadvantages described above. In particular, the fiber must be inserted manually into the detection plate, a procedure that cannot be

easily automated. One goal of this work was to directly compare the performance of the PPF electrodes with carbon fibers in the microchip format.

For the initial evaluation of the electrodes, cyclic voltammetry was performed on dopamine (DA), catechol, and ascorbic acid (AA) using both a carbon fiber and a PPF electrode. To determine the relative sensitivity of the two electrodes for both species, a four-point calibration curve ($n = 3$) was generated and is shown in Figure 3.2 along with Table 3.1 which contains the sensitivity values for each analyte. Both electrodes exhibited a linear response for the response vs. concentration curves. After normalizing for surface area, the carbon fiber electrode exhibited a slightly higher sensitivity for dopamine than did the PPF electrode ($0.925 \text{ pA}/\mu\text{M} * \mu\text{m}^2$ at the PPF electrode vs. $2.22 \text{ pA}/\mu\text{M} * \mu\text{m}^2$ at the carbon fiber), while the sensitivity for ascorbate was very similar ($0.433 \text{ pA}/\mu\text{M} * \mu\text{m}^2$ vs. $0.596 \text{ pA}/\mu\text{M} * \mu\text{m}^2$). In general, it was found that the performance of the PPF electrode was very similar to that of the carbon fiber, making it a good candidate for microchip CEEC.

3.3.2 Electrode Evaluation

The PPF electrode was then evaluated in the microchip CEEC format using end-channel detection. An advantage of PPF electrodes over most other carbon electrodes is that they can be fabricated directly onto a glass substrate. It was observed that the electrode adhered strongly to the glass surface, making it possible to easily remove and clean the PDMS (separation) layer without removing or damaging

the electrode. It was found that the PDMS could be removed, cleaned, and replaced for realignment or reuse in excess of fifteen times without damaging the electrode.

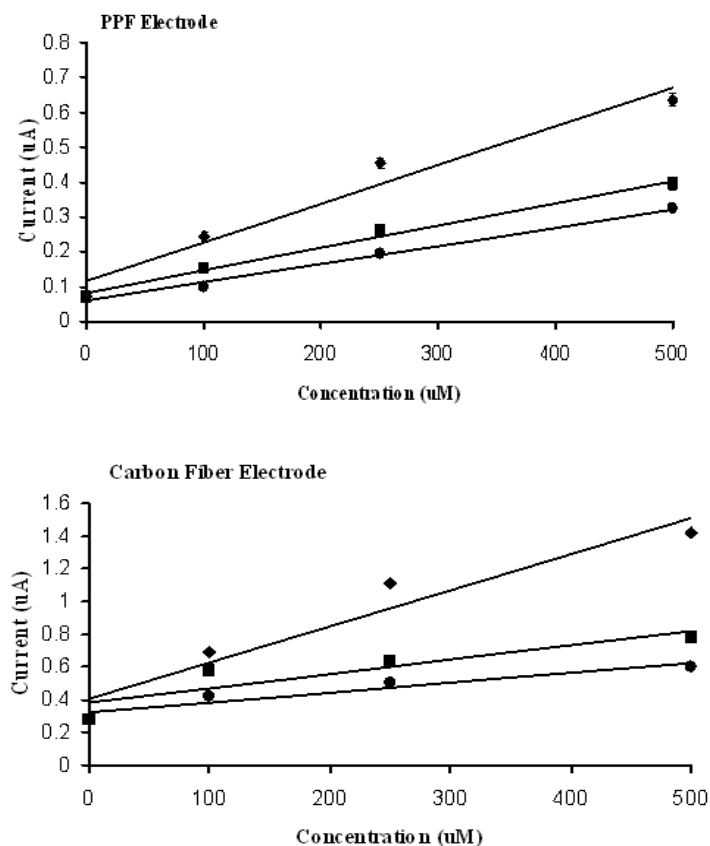


Table 3.1: Normalized Sensitivity ($\text{pA}/\mu\text{M} \cdot \mu\text{m}^2$) for Each Electrode

	PPF Electrode		Carbon Fiber Electrode	
	Sensitivity ($\text{pA}/\mu\text{M} \cdot \mu\text{m}^2$)	Correlation Coefficient R^2	Sensitivity ($\text{pA}/\mu\text{M} \cdot \mu\text{m}^2$)	Correlation Coefficient R^2
Dopamine \blacklozenge	0.925	0.961	2.22	0.930
Catechol \blacksquare	0.533	0.991	0.879	0.813

Figure 3.2 Direct comparison of a PPF and a carbon fiber electrode. Calibration curves for DA (\blacklozenge), catechol (\blacksquare), and AA (\bullet) at a PPF electrode and a carbon fiber electrode. Data points were taken from peak currents generated by cyclic voltammetry. CVs were performed at 0.1 V s^{-1} and swept from -0.5 V to $+1.0 \text{ V}$ and back vs. Ag/AgCl in 25 mM BA buffer, pH 9.2.

The PPF electrode was also found to be fairly robust; typically lasting from two to five days and for more than 100 runs.

Figure 3.3 shows electropherograms obtained for a mixture of dopamine and ascorbate using a carbon fiber (1) and a PPF electrode (2). It can be seen that the carbon fiber and PPF electrodes exhibit very similar behavior for these two compounds. The sensitivity for dopamine was higher than for that of ascorbate at both electrodes. Some peak tailing is observed and can be attributed to an end-channel electrode alignment.

The figures of merit for dopamine were determined using a separate microchip CEEC device utilizing a PPF electrode. The response was found to be linear from 25–500 μM ($r^2 = 0.999$) with a sensitivity of 5.8 pA/ μM . The limit of detection (LOD) was determined experimentally to be 5 μM at S/N = 3 (data not shown).

3.3.3 Dual-Electrode Detection

Dual-electrode detection in a serial mode offers enhanced selectivity for compounds undergoing chemically reversible redox reactions. This configuration has been shown to be useful with conventional CE for the selective detection of many compounds, including catecholamines, phenolic acids, peptides and disulfides [21, 34, 35]. One of the difficulties in performing dual-electrode detection in the capillary format is positioning two electrodes in close proximity to one another. This is

accomplished much more effectively in the planar format used for microchip CEEC.

The deposition of metal electrodes is fairly straightforward and metal-based dual-

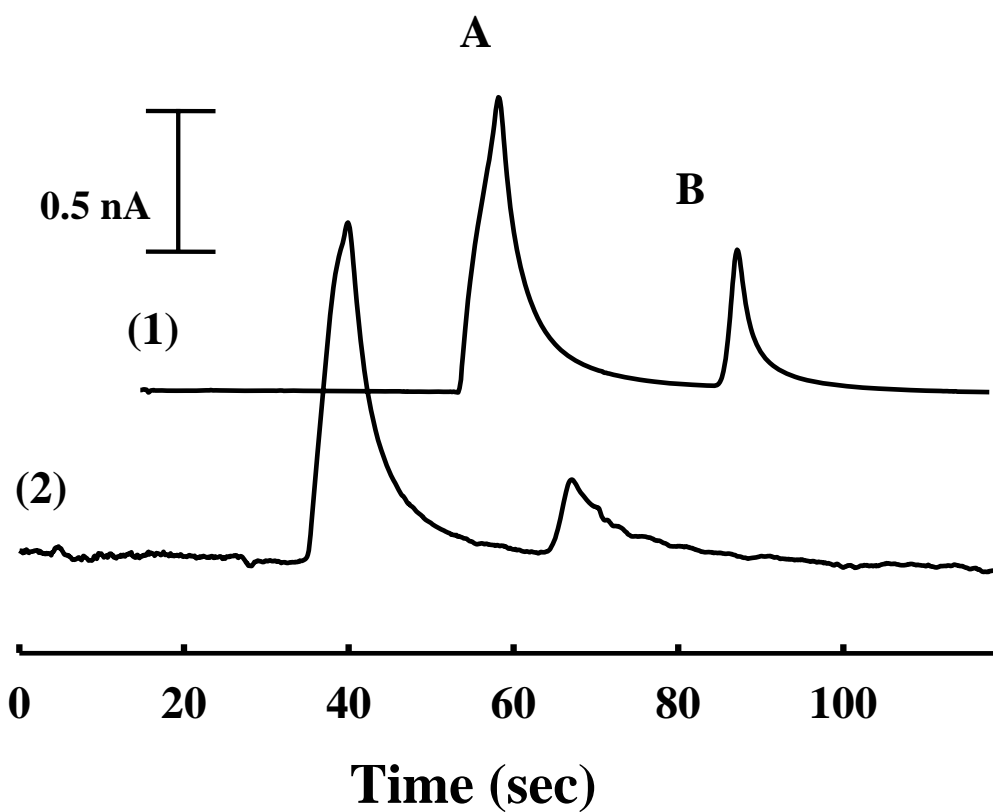


Figure 3.3 Separation and detection of 100 μM DA (A) and 500 μM AA (B) at a carbon fiber (1) and a PPF (2) electrode. Separation conditions: 25 mM boric acid, pH 9.2; applied voltage +1880 V to B, +1250 V to S; 5 s gated injection; $E_1 = +900$ mV vs. Ag/AgCl.

electrode systems have been reported [19]. However, carbon-based dual electrode detectors are much more difficult to fabricate. A dual-electrode detection system using carbon fibers has been developed in our laboratory [13]. However, a major drawback of this approach is the difficulty in manually placing two fibers in close proximity to each other on the chip.

PPF electrodes offer a substantial improvement over carbon fibers for the development and implementation of multiple electrode detection systems. The ability to produce the PPF electrodes using photolithographic methods permits mass production of the microchip device; further streamlining the process while rigidly controlling electrode placement, spacing, and size. This makes the procedure for electrode production much closer to that used for metal electrodes.

Figure 3.4 shows the dual-electrode detection of 5-HIAA and catechol on a microchip. Both compounds are oxidized at the first electrode; however, only catechol shows a significant response at the second electrode. Catechol undergoes a two-electron chemically reversible oxidation. The orthoquinone product generated at the first electrode is detected at the second electrode, which is set at -100 mV vs. Ag/AgCl. In contrast, 5-HIAA is a monophenol and the reaction is not chemically reversible. Thus there is only a minor response observed for 5-HIAA at the second electrode.

A measure of how well the reversible species are detected can be estimated from the collection efficiency (N_e), which is the ratio of the cathodic to anodic response. The collection efficiency for catechol was determined to be 42.2%. This is

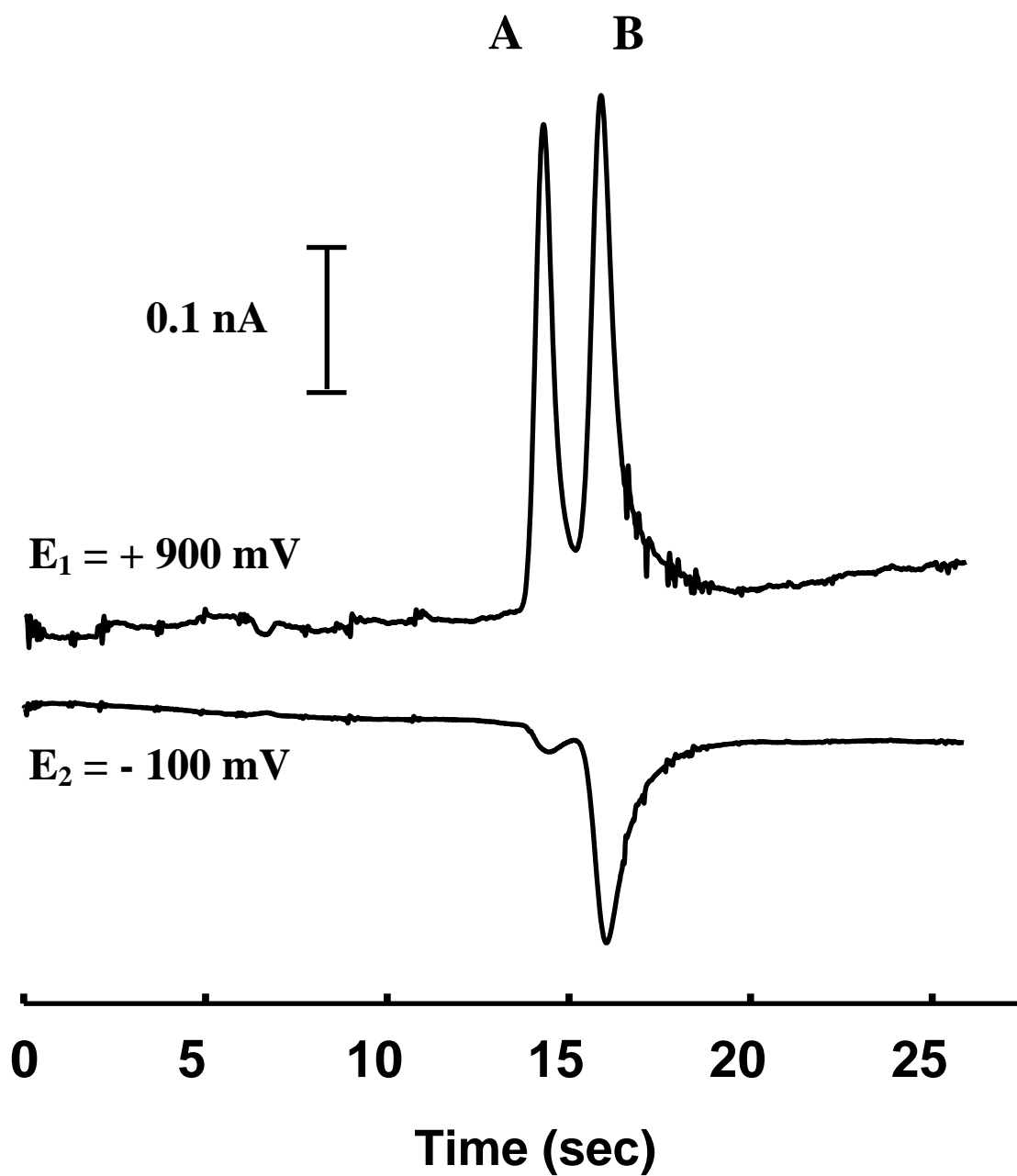


Figure 3.4 Separation and dual-electrode detection of 5-HIAA (A) and catechol (B) at a PPF electrode in serial configuration. Both compounds are $100 \mu\text{M}$. Separation and injection conditions the same as stated in Fig. 3.3. $E_1 = +900$, $E_2 = -100 \text{ mV}$ vs. Ag/AgCl.

considerably higher than reported N_e values for similarly configured dual-electrode detectors for both conventional (25–35%) [21] and microchip CE using gold electrodes (26–29%) [19]. However, this value was very similar to that reported previously for a carbon fiber-based dual-electrode detector (36–43.7%) [13].

The demand placed on microchip devices for high-throughput analyses is quite high. It is therefore important to have a stable and robust detection method. In particular, electrode fouling and response reproducibility is always a concern when employing amperometric detection. It has been demonstrated with other dual-electrode configurations for microchip CEEC that the adsorption of analytes to the electrode surface can be quite significant and detrimental to the chip performance [13, 19].

Figure 3.5 shows the response obtained from fourteen consecutive injections of 500 μM dopamine using the PPF dual-electrode microchip CEEC device. The oxidation of dopamine at E_1 (+900 mV) generated an average response of 4.24 nA while exhibiting a RSD of only 2.24%. The reduction of dopamine at E_2 (–100 mV) had an average response of 0.21 nA with a RSD of 3.50%. The comparatively small response at E_2 can be attributed to the end-channel detection configuration. The second electrode in the series (E_2) is at a much greater distance from the separation channel exit (75–90 μm), which can lead to band broadening and dilution of the analyte plug. Although the RSDs presented here are relatively small and indicate minimal fouling and excellent signal reproducibility, some response variation can be attributed to the manual gated injection method.

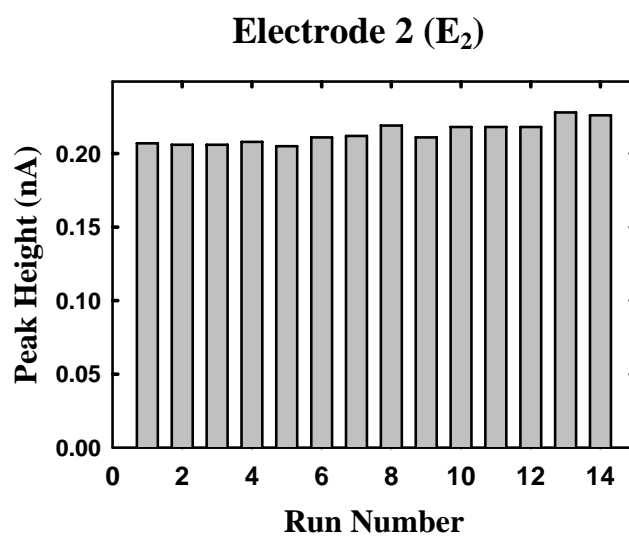
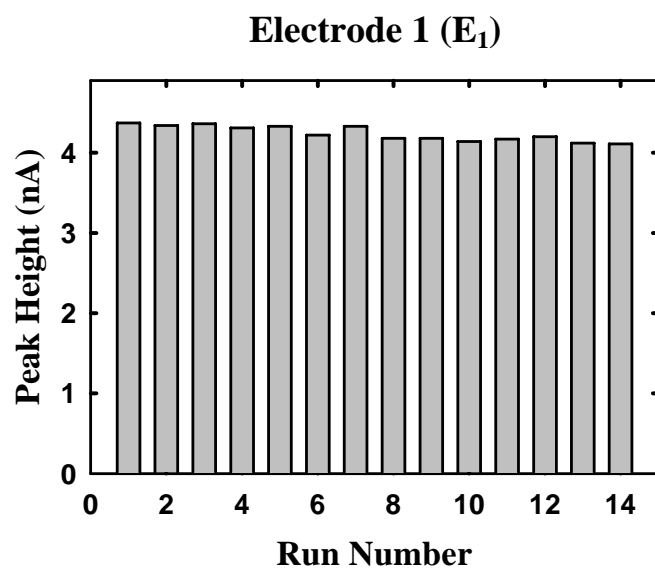


Figure 3.5 Dual-electrode response of fourteen consecutive injections of 500 μM DA. DA was first oxidized at E₁ (+900 mV) then reduced at E₂ (-100 mV). Separation and injection conditions the same as stated in Fig. 3.3.

3.4 Conclusion

An integrated microfabricated carbon-based electrochemical detector has been described. Pyrolyzed photoresist film electrodes demonstrate excellent sensitivity and reproducibility for use as electrochemical detectors with microchip CE. The PPF electrodes have proven to be effective for the detection of several biologically relevant compounds and neurotransmitters. The integrated PPF electrodes are useful for microchip CEEC analyses as well as standard electrochemical techniques such as cyclic voltammetry. In addition, the PPF electrodes exhibit performance comparable to that of carbon fiber electrodes and present an excellent alternative for use with microchip CEEC devices. Photolithographic microfabrication of PPF electrodes permits complete and precise control of electrode configuration and integration into microchip devices. This not only allows electrode integration but permits the fabrication of intricate and complex electrode designs that are also amenable to mass production. Future work will include the development of a palladium decoupler along with a PPF EC detector to allow in-channel EC detection, which will reduce noise and peak tailing while lowering detection limits.

3.5 References

- [1] A. Manz, N. Graber, H. M. Widmer, *Sensors and Actuators B* **1990**, *1*, 244.
- [2] A. Manz, D. J. Harrison, E. Verpoorte, J. C. Fettinger, H. Ludi, H. M. Widmer, *Journal of Chromatography* **1992**, *593*, 253.
- [3] D. J. Harrison, A. Manz, Z. Fan, H. Ludi, H. M. Widmer, *Analytical Chemistry* **1992**, *64*, 1926.
- [4] D. J. Harrison, K. Fluri, K. Seiler, Z. Fan, C. S. Effenhauser, A. Manz, *Science* **1993**, *261*, 895.
- [5] T. Vilknér, D. Janásek, A. Manz, *Analytical Chemistry* **2004**, *76*, 3373.
- [6] R. K. Hanajiri, R. S. Martin, S. M. Lunte, *Analytical Chemistry* **2002**, *74*, 6370.
- [7] J. Wang, M. P. Chatrathi, *Analytical Chemistry* **2003**, *75*, 525.
- [8] W. R. Vandaveer IV, S. A. Pasas-Farmer, D. J. Fischer, C. N. Frankenfeld, S. Lunte, M., *Electrophoresis* **2004**, *25*, 3528.
- [9] S. A. Pasas, B. A. Fogarty, B. H. Huynh, N. A. Lacher, B. Carlson, R. S. Martin, W. R. Vandaveer IV, S. M. Lunte, in *Separation Methods in Microanalytical Systems* (Eds: J. P. Kutter, Y. Fintschenko), Marcel Dekker, New York **2004**, in press.
- [10] K. B. Mogensen, H. Klank, J. P. Kutter, *Electrophoresis* **2004**, *25*, 3498.
- [11] A. T. Woolley, K. Lao, A. N. Glazer, R. A. Mathies, *Analytical Chemistry* **1998**, *70*, 684.
- [12] N. A. Lacher, S. M. Lunte, R. S. Martin, *Analytical Chemistry* **2004**, *76*, 2482.
- [13] A. J. Gawron, R. S. Martin, S. M. Lunte, *Electrophoresis* **2001**, *22*, 242.
- [14] R. S. Martin, A. J. Gawron, B. A. Fogarty, F. B. Regan, E. Dempsey, S. M. Lunte, *Analyst* **2001**, *126*, 277.
- [15] J. Wang, M. Pumera, M. P. Chatrathi, A. Rodriguez, S. Spillman, R. S. Martin, S. M. Lunte, *Electroanalysis* **2002**, *14*, 1251.
- [16] M. L. Kovarik, N. J. Torrence, D. M. Spence, R. S. Martin, *Analyst* **2004**, *129*, 400.
- [17] N. E. Hebert, B. Snyder, R. L. McCreery, W. G. Kuhr, S. A. Brazill, *Analytical Chemistry* **2003**, *75*, 4265.
- [18] P. Ertl, C. A. Emrich, P. Singhal, R. A. Mathies, *Analytical Chemistry* **2004**, *76*, 3749.
- [19] R. S. Martin, A. J. Gawron, S. M. Lunte, C. S. Henry, *Analytical Chemistry* **2000**, *72*, 3196.
- [20] N. A. Lacher, K. E. Garrison, R. S. Martin, S. M. Lunte, *Electrophoresis* **2001**, *22*, 2526.
- [21] M. Zhong, J. Zhou, S. M. Lunte, G. Zhao, D. M. Giolando, J. R. Kirchhoff, *Analytical Chemistry* **1996**, *68*, 203.
- [22] R. L. McCreery, K. K. Cline, in *Laboratory Techniques in Electroanalytical Chemistry* (Eds: P. T. Kissinger, W. R. Heineman), Marcel Dekker, New York **1996**, pp. 293-332.

- [23] A. M. Lyons, *Journal of Non-Crystalline Solids* **1985**, 70, 99.
- [24] A. M. Lyons, L. P. Hale, C. W. Wilkins, Jr., *Journal of Vacuum Science and Technology B* **1985**, 3, 447.
- [25] J. Kim, X. Song, K. Kinoshita, M. Madou, R. White, *Journal of The Electrochemical Society* **1998**, 145, 2314.
- [26] S. Ranganathan, R. L. McCreery, S. M. Majji, M. Madou, *Journal of The Electrochemical Society* **2000**, 147, 277.
- [27] R. Kostecky, X. Y. Song, K. Kinoshita, *Journal of The Electrochemical Society* **2000**, 147, 1878.
- [28] S. Ranganathan, R. L. McCreery, *Analytical Chemistry* **2001**, 73, 893.
- [29] N. E. Hebert, S. A. Brazill, *Lab Chip* **2003**, 3, 241.
- [30] D. C. Duffy, J. C. McDonald, O. J. A. Schueller, G. M. Whitesides, *Analytical Chemistry* **1998**, 70, 4974.
- [31] J. C. McDonald, D. C. Duffy, J. R. Anderson, D. T. Chiu, H. Wu, O. J. A. Schueller, G. M. Whitesides, *Electrophoresis* **2000**, 21, 27.
- [32] S. C. Jacobson, L. B. Koutny, R. Hergenroder, A. W. Moore Jr., J. M. Ramsey, *Analytical Chemistry* **1994**, 66, 3472.
- [33] S. V. Ermakov, S. C. Jacobson, J. M. Ramsey, *Analytical Chemistry* **2000**, 72, 3512.
- [34] M. Zhong, S. M. Lunte, *Analytical Chemistry* **1999**, 71, 251.
- [35] L. A. Holland, N. M. Harmony, S. M. Lunte, *Electroanalysis* **1999**, 11, 327.

Chapter 4

Amperometric Detection in Microchip Electrophoresis Devices: Effect of Electrode Material and Alignment on Analytical Performance

(Electrophoresis, 30(19), 3324-3333, 2009)

4.1 Introduction

A large number of microfabrication methods have been developed for the production of microchip devices since they were first reported in 1992 [1-6]. Microchip electrophoresis is among the most commonly employed formats for lab-on-a-chip devices and offers many potential advantages over liquid chromatography and conventional capillary electrophoresis (CE). These include decreased sample and reagent volumes, higher sample throughput, improved precision, and the possibility for disposable/portable devices. In addition, they are inexpensive and generate minimal chemical waste. The small footprint of the chip along with the ability to integrate several different processes into a single device makes this approach an attractive option for point-of-care use [7-9].

Although the miniaturized format is amenable to a large number of detection techniques, laser-induced fluorescence (LIF) and electrochemical (EC) detection are most commonly employed [10, 11]. LIF detection remains very popular for microchip electrophoresis due to the relative ease of instrumental set-up and the low limits of detection that can be obtained. However, unless the analyte of interest exhibits native fluorescence, the sample must be derivatized either pre-, on-, or postcolumn prior to detection [12, 13].

Electrochemical detection is ideal for many lab-on-a-chip applications. Not only can electroactive analytes be detected without derivatization, the detector can also be miniaturized without a loss in sensitivity. Furthermore, electrodes can be

fabricated using the same photolithographic processes that are employed to produce the fluidic network. While several EC detection methods have been used for microchip electrophoresis, amperometry and conductivity are the most common [14-17]. Conductivity functions as a universal detection method that provides a response for all analytes; however, it lacks a high degree of selectivity and sensitivity [18, 19]. Amperometric detection is much more selective and sensitive than conductivity detection, but it is not universal [20]. Thus, amperometry is well suited for the detection of redox active species such as phenols, reactive oxygen (ROS) and nitrogen species (RNS), thiols, carbohydrates, and catecholamines. [9, 21-23].

One of the major challenges when using EC detection with microchip electrophoresis is decoupling the separation voltage from the detection electrode. Failure to do this properly leads to increased noise as well as probable damage to the potentiostat. The two most commonly used methods of isolating the working electrode from the separation voltage are end-channel and off-channel alignment. With end-channel alignment, the electrode is placed 5–20 μm from the end of the separation channel (Fig. 1A). This allows the separation voltage to dissipate prior to reaching the working electrode [24]. While this alignment is simple and easy to implement in microchip devices, it can lead to peak dispersion and band broadening due to the gap between the channel exit and electrode [25].

An alternative way to isolate the working electrode from the separation voltage is to use a decoupler for off-channel detection (Fig. 1B). The decoupler is placed in the separation channel ahead of the working electrode and serves as a path to ground

[26-28]. Martin *et al.* described a microfabricated Pd decoupler for off-channel detection in a microchip device [29]. It has been shown that this configuration greatly reduces band broadening when compared to end channel detection.

Another approach for minimizing band broadening associated with end-channel detection is the use of an electrically isolated or “floating” potentiostat for in-channel alignment (Fig. 1C) [25, 30]. In this configuration there is no decoupler, but the working electrode can be placed directly in the separation channel because the potentiostat is not earth-grounded. A substantial improvement in peak skew and tailing was observed with this approach as compared to end-channel detection. With this configuration, the working electrode is biased by the separation voltage. Therefore, the choice of applied potential must take into account this voltage bias in order to obtain a reproducible response.

Perhaps the most important factor to consider when using EC detection is the choice of electrode material. While metal electrodes, such as Au, Pt and Pd, have been used in microfluidic devices for the detection of thiols, carbohydrates, and ROS, carbon electrodes have been the most popular choice for the detection of organic analytes, including catecholamines, phenols, and aromatic amines [9, 21-23]. In particular, carbon electrodes are ideal for the detection of catecholamines due to their large potential window, resistance to fouling, low overpotential, low background noise, and favorable electron transfer. [31-34].

The most commonly employed carbon-based electrodes are carbon fibers, pastes, and inks [35-38]. However, these three types of electrodes cannot be

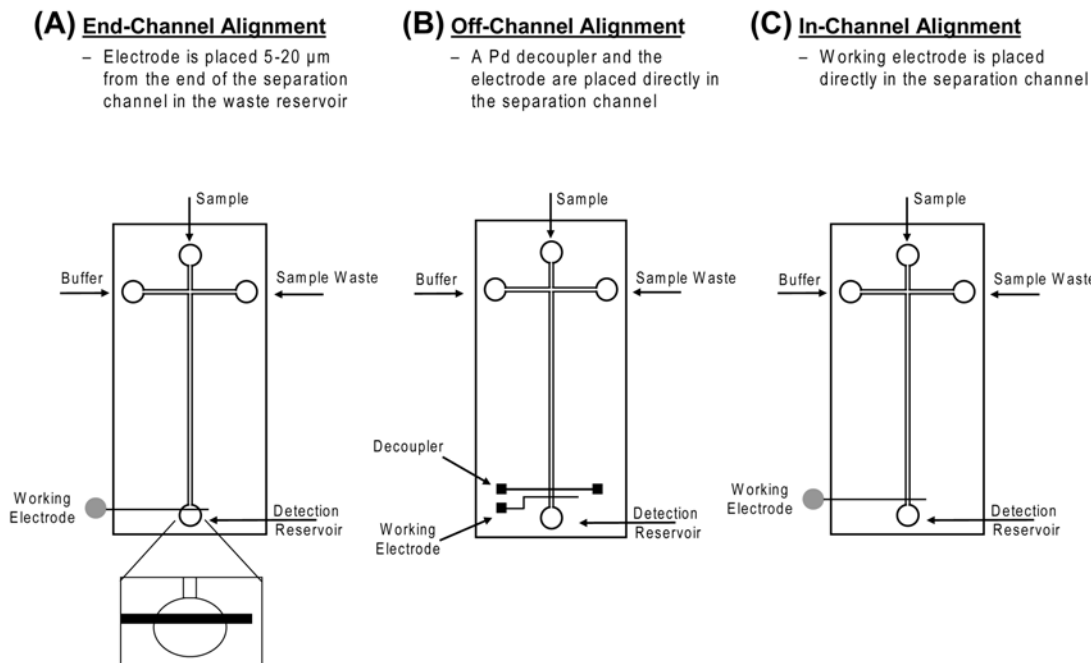


Figure 4.1. Schematic diagram of different electrode alignments for microchip electrophoresis with EC detection: (A) end-channel alignment; (B) off-channel alignment; (C) in-channel alignment. In-channel alignment is only possible when using an electrically isolated potentiostat.

fabricated using standard photolithographic procedures. Therefore, their fabrication can be time-consuming and labor-intensive. An alternative carbon-based electrode material that can be fabricated *via* photolithography is pyrolyzed carbon [39, 40]. Previous work in our lab has shown that pyrolyzed photoresist film (PPF) electrodes are easily manufactured and exhibit excellent linearity and sensitivity [41]. Despite numerous reports detailing the use of carbon or metal-based electrodes, a direct comparison of the different types of materials for the detection of catecholamines has not been reported.

In this study, the fabrication and evaluation of multiple electrode materials and configurations for microchip electrophoresis with electrochemical detection is described. Catechol, dopamine, and norepinephrine are used as model analytes. In particular, the analytical performances of carbon fiber, carbon ink, PPF, and Pd electrodes for the detection of these analytes are directly compared. In addition, end-, off-, and in-channel electrode alignments are evaluated using Pd and carbon ink electrodes. The effect of electrode material and alignment on EC response is directly compared by evaluating the sensitivity and limits of detection (LOD). Factors such as analyte resolution, separation efficiency, and ease of fabrication and implementation are also discussed.

4.2 Materials and Methods

4.2.1 Materials and Reagents

The following chemicals were used as received: AZ 1518 positive photoresist and AZ 300 MIF developer (Clariant Corp., Somerville, NJ, USA); S1818 positive photoresist and Microposit 351 developer (Microchem Corp., Newton, MA, USA); SU-8 10, SU-8 2 negative photoresist and SU-8 developer (MicroChem Corp., Newton, MA, USA); 100 mm and 127 mm Si wafers (Silicon, Inc., Boise, ID, USA); Sylgard 184 (Ellsworth Adhesives, Germantown, WI, USA); dopamine (DA), catechol (CAT), norepinephrine (NE), 1 N NaOH and boric acid (BA) (Sigma-Aldrich, St. Louis, MO, USA); 2-propanol (IPA), acetone, 30% H₂O₂, H₂SO₄, HNO₃, and HCl. In addition, the following were utilized: 1 mL syringes and Pt wire (22 gauge) (Fisher Scientific, Fairlawn, New Jersey, USA); Pd (99.95% purity) and Ti (99.97% purity) targets (2 in. diameter × 0.125 in. thick; Kurt J. Lesker Co., Clairton, PA); Ti etchant (TFTN; Transene Co., Danvers, MA, USA); optical quality borosilicate glass (4 in. × 2.5 in. 0.043 in., Telic Co., Valencia, CA, USA); high temperature fused silica glass plates (4 in. × 2.5 in. × 0.085 in.; Glass Fab, Inc., Rochester, NY, USA); 33 μm diameter carbon fibers (Avco Specialty Materials, Lowell, MA, USA); conductive epoxy (ITW Chemtronics, Kennesaw, GA, USA); carbon ink and solvent thinner (Ercon Inc., Wareham, MA); colloidal silver liquid (Ted Pella, Inc., Redding, CA, USA); 0.22 μm Teflon filters (Osmonics, Inc., Minnetonka, MN, USA); 18.2 MΩ water (Millipore, Kansas City, MO, USA); quick-set epoxy and Cu wire (22 gauge; Westlake Hardware, Lawrence, KS, USA).

4.2.2 PDMS Fabrication

The fabrication of PDMS-based microfluidic devices has been described previously [42, 43]. SU-8 10 negative photoresist (for electrophoresis channels) or SU-8 2 (for electrode channels) was spin coated on a 100 mm silicon (Si) wafer using a Cee 100 spincoater (Brewer Science, Rolla, MO, USA). SU-8 10 was spun at 500 rpm for 5 s, then 2100 rpm for 30 s, while SU-8 2 was spun at 500 rpm for 5 s, then 1200 rpm for 30 s. A design containing the desired structures was created using AutoCad LT 2004 (Autodesk, Inc., San Rafael, CA, USA) and transferred to a transparency film at a resolution of 50,000 dpi (Infinite Graphics Inc., Minneapolis, MN, USA). Following the manufacturer's recommended prebake process, the appropriate negative film mask was placed over the coated wafer, brought into hard contact, and exposed to a near-UV flood source at 21.5 mW/cm^2 (ABM, San Jose, CA, USA) using the suggested exposure dose. Following the UV exposure, both wafers were postbaked and allowed to cool to room temperature. The wafers were then developed in SU-8 developer, rinsed with IPA, and dried under nitrogen. A final hard-curing bake was performed at 175°C for 2 h. The thickness of the raised photoresist, which corresponded to the depth of the PDMS channels, was measured with a surface profiler (Alpha Step-200, Tencor Instruments, Mountain View, CA, USA). PDMS microstructures were made by casting a 10:1 mixture of PDMS elastomer and curing agent, respectively, against the silicon master. The 10:1 ratio of PDMS was used for all analyses, except for off-channel detection with a carbon ink

electrode. To minimize fluid leakage around the off-channel carbon ink electrode, a 20:1 ratio of PDMS was used for the electrophoresis channels. After curing at 75°C for at least 1.5 h, the PDMS was removed from the master, yielding the desired negative relief pattern. A simple “T” device containing a 3.5 cm separation channel (from the T intersection to the end of the separation channel) and 0.75 cm side arms was used for all studies reported. The width and depth of the electrophoresis microchannels were 50 μm and 14 μm , respectively. Final dimensions of the electrode molding channels used were either 20 μm or 50 μm wide and either 3.8 μm or 4.0 μm deep, depending on the type of electrode and alignment used (discussed in Section 2.5). Holes for the reservoirs were created in the polymer with a hole punch.

4.2.3 Pyrolyzed Carbon Electrode Fabrication

Pyrolyzed photoresist electrodes were fabricated based on a previously published technique, using two different types of positive photoresist [41]. AZ 1518 positive photoresist was dynamically coated (100 rpm for 20 s then 2000 rpm for 20 s) on a fused silica glass plate. The coated plate was prebaked at 95°C for 1 min, covered with the desired positive film mask, and exposed to a near-UV flood source (7 s at 21.5 mW/cm²). After exposure, the plate was developed in AZ 300 MIF developer for 20 s, rinsed with 18.2 M Ω water, and dried under N₂. The plates underwent a subsequent postbake at 90°C for 1 min. The second type of positive photoresist used, S1818, was also dynamically coated (100 rpm for 5 s then 3500 rpm

for 30 s) on a fused silica glass plate. The photoresist coated plate was prebaked at 100°C for 1 min prior to UV exposure (7 s at 21.5 mW/cm²). The plate was developed for 30 s in Microposit 351 developer, diluted 1:3.5 (V_{Devl}:V_{H2O}) with 18.2 MΩ H₂O, then rinsed with 18.2 MΩ H₂O and dried under N₂. A final postbake was performed for 10 min at 115 °C.

A Lindberg/Blue M Three-Zone Tube Furnace (Cole-Parmer, Vernon Hills, IL, USA) was utilized for pyrolysis. The furnace was fitted with quartz end caps with connections to heat-resistant polytetrafluoroethylene extruded Teflon tubing (Fisher Scientific) and was continuously flushed with nitrogen at 5 psi to provide an inert atmosphere. The temperature of the furnace started under ambient conditions and was increased at the rate of 5.5 °C/min to 925 °C, held for 1 h, and then allowed to cool to room temperature. The resultant width of the PPF electrodes was 40 μm and the height was determined with a surface profiler to be 0.6 μm. Conductive epoxy (ITW Chemtronics, Kennesaw, GA, USA) was used to bond copper wires to the electrode contact pads to provide electrical connection.

4.2.4 Carbon Fiber Electrode Fabrication

Fabrication of the PDMS carbon fiber electrode channel and placement of the carbon fiber was based on previously described work [9, 42, 44]. Briefly, a 127 cm Si master containing a raised structure 33 μm wide, 33 μm high, and 3.5 cm long was fabricated in the same manner described in Section 2.2. PDMS was cast against this master to yield an electrode channel containing the same dimensions. To increase

rigidity, the PDMS electrode layer was then sealed to a 2.5 in. \times 4 in. glass substrate and a carbon fiber was placed directly in the electrode channel with the aid of a stereoscope. A hole was punched at one end of the electrode channel to provide an access point for an electrical connection. Cu wire was fixed to the substrate using quick-set epoxy, while Ag colloidal liquid (Ted Pella) was used to make electrical contact between the Cu wire and carbon fiber. Hot glue was then used to cover the entire connection, providing additional rigidity and insulation.

4.2.5 Carbon Ink Electrode Fabrication

Two different but related procedures for micromolding carbon ink electrodes were utilized. When used in an end-channel configuration, the carbon ink electrode was embedded in a PDMS channel to facilitate fabrication [45, 46]. Similar to the fabrication of the carbon fiber, a channel that would house the electrode (14.8 μm deep, 50 μm wide, and 2 cm long) was fabricated in PDMS. Holes were punched in the PDMS micromolding channel (4.0 μm deep, 50 μm wide, and 1 cm long) which was then aligned and sealed over the electrode channel with the aid of a stereoscope. When using a carbon ink electrode with a Pd decoupler in an off-channel configuration, a Pd contact pad was used for alignment and electrical connection. In this case, the PDMS micromolding channel (3.8 μm deep, 20 μm wide, and 1 cm long) was aligned so that a portion of the micromold was positioned over the Pd contact pad (50 μm wide).

Once the electrode micromold was aligned and sealed to the electrode substrate, carbon ink electrodes were fabricated based on previously published techniques [36, 38, 45, 47, 48]. Carbon ink and solvent thinner were mixed in either a 0.2% or 0.4% v/w (thinner/ink) ratio. The electrode micromold channel was primed with the solvent thinner, which was allowed to remain in the channel for 60 s. Once the excess solvent was removed from the reservoir, either the 0.2% (v/w) carbon ink solution (for end-channel fabrication) or 0.4% (v/w) carbon ink solution (for off-channel fabrication) was placed in the same reservoir to which the solvent had been added while a vacuum was simultaneously applied to the opposite end of the electrode micromold. When the ink solution had filled the micromold, the entire plate was placed in an 85°C oven. After 1 h, the plate was taken out of the oven, the PDMS micromold was removed, and the plate was placed in a 125°C oven for 1 h. The electrode heights were measured using a surface profiler while the widths were measured using optical microscopy. The resulting electrode fabricated for end-channel alignment measured 50 μm wide, 8 mm long, and 1.1 μm at its tallest point from the PDMS surface. The electrode used for off-channel EC detection was 20 μm wide, 2 mm long, and 0.8 μm tall and was placed 250 μm from the Pd decoupler. This spacing had been previously optimized and was a fixed distance as determined by the fabrication of the Pd contact pad.

4.2.6 Palladium Electrode Fabrication

The Pd electrodes used for both end- and off-channel EC detection consisted of a 200 Å thick titanium (Ti) adhesion layer followed by a 2000 Å thick palladium (Pd) electrode layer deposited on a glass substrate. The Pd decoupler and electrode used for off-channel EC detection were obtained from the Nanofabrication Facility at Stanford University while the Pd electrode used for end-channel detection was fabricated in-house using a previously reported fabrication procedure [29, 38]. (*Caution! Acid piranha and aqua regia solutions, which are used in this procedure, are powerful oxidizers; they should be handled with extreme care.*) Glass substrates used to fabricate end-channel electrodes were cleaned in an acid piranha solution (7:3 H₂SO₄/H₂O₂) for 20 min to remove organic impurities. The glass was rinsed thoroughly with 18.2 MΩ H₂O and dried with N₂ prior to immersion in a base piranha solution (7:3 NH₄OH/H₂O₂) for 20 min. Again, the glass was thoroughly rinsed with 18.2 MΩ H₂O and dried with N₂. The substrates were then placed into a deposition system for metal deposition (Kurt J. Lesker Co.). Deposition thickness was monitored using a quartz crystal deposition monitor (Inficon XTM/2, Leybold Inficon, Syracuse, NY, USA). Ti was deposited at a rate of ~2.0 Å/s to a thickness of ~200 Å while Pd was deposited at a rate of ~2.2 Å/s to a thickness of ~2000 Å.

Positive photoresist (S1818) was used to dynamically coat both plates at 100 rpm for 5 s. The spin coater was then ramped to a final speed of 3500 rpm and held for 30s to yield a photoresist thickness of 2.0–2.2 μm. The photoresist was prebaked at 100°C for 2 min prior to UV exposure using the appropriate positive-tone

transparency mask. After exposure, the plates were developed for ~30 s in Microposit 351 developer diluted 1:3.5 (v:v) with 18.2 M Ω H₂O, then rinsed thoroughly with 18.2 M Ω H₂O and blown dry with N₂. A final post-exposure bake was performed at 100°C for 10 min.

The unexposed or remaining photoresist on the plate serves to protect the underlying metal from the subsequent acid-etching procedure. Pd metal was removed by immersion in 85°C aqua regia (3:1:6 H₂O/HCl/HNO₃) for ~5 s or until no Pd metal could be seen. Ti metal was removed by immersing the plate in Ti etchant (Transene) held at 95°C for ~ 45 s or until no remaining metal could be seen. After completion of the metal etching procedure, the protective photoresist was removed by rinsing the plate with acetone, followed by IPA, and drying with N₂. The final dimension of the Pd electrodes used for end and off-channel experiments measured 40 μ m wide and 50 μ m respectively. Electrical contacts to the electrodes were made by fixing Cu wire on the plate with quick-set epoxy and using colloidal Ag liquid (Ted Pella) between the Cu wire and electrodes.

4.2.7 Chip Construction

Two types of microchip devices were used in these studies. An all-PDMS device was used for experiments employing a carbon fiber and carbon ink (end-channel) electrodes. A PDMS/glass hybrid device was used for all other experiments. The latter device consisted of a glass substrate, upon which the electrode was fabricated, and a layer of PDMS containing the fluid channels. The layer of PDMS

containing the separation channel was aligned and reversibly sealed to the electrode plate by bringing the two substrates into conformal contact with one another. This was achieved after extensively cleaning the electrode substrate with IPA and drying with N₂. For both end-channel and off-channel EC detection using a Pd working electrode, the Pd surface was subjected to nitric acid cleaning prior to analysis. Nitric acid (6 N) was added to a PDMS reservoir and allowed to sit over the electrode for 5 min. The nitric acid was then removed from the reservoir, and the electrode was rinsed with 18.2 MΩ H₂O and dried with N₂. For end-channel EC detection, the working electrode was aligned within 5–20 μm of the exit of the separation channel (Fig. 4.1A). For off-channel detection, the decoupler and working electrode were placed directly in the separation channel, with the working electrode placed 20–30 μm ahead of the end of the channel exit (Fig. 4.1B). For experiments performed in an in-channel configuration, the electrode was also aligned 20–30 μm prior to the end of the separation channel (Fig. 4.1C).

4.2.8 Electrophoresis Procedure

Electrophoresis was carried out in unmodified PDMS microchannels using a programmable Jenway Microfluidic Power Supply (Dunlow, Essex, U.K.). The electrophoresis buffer used for all data presented was 25 mM boric acid at pH 9.2. The buffer was degassed (Fisher Ultrasonic Cleaner, Fisher Scientific) and filtered with a 0.22 μm teflon filter before use. The PDMS channels were first flushed with 0.1 N NaOH for 3–5 min, then rinsed with 18.2 MΩ H₂O, and finally filled with

buffer by applying a vacuum. Stock solutions (10 mM) of DA, NE, and CAT were prepared daily in 18.2 M Ω water. Samples were made prior to use by diluting with buffer. Electrophoresis was performed by applying a high voltage (+1400 V) at the buffer reservoir (B) and a fraction of this high voltage (+1200 V) at the sample reservoir (S) while the sample waste (SW) and detection reservoirs were grounded. The application of these voltages to the PDMS microchip described in section 4.2.2 resulted in a junction potential of 809 V and field strength of 231 V/cm. For all data presented, a gated injection method was used for introduction of the sample plug and was achieved by floating the high voltage at the buffer reservoir for the duration of the injection before returning it to +1400 V. Unless otherwise noted, an injection time of 600 ms was employed for all data presented.

4.2.9 Electrochemical Detection

Electrochemical detection was accomplished using a CHI 802B electrochemical analyzer (CH Instruments Inc., Austin, TX, USA), a BAS Epsilon potentiostat (Bioanalytical Systems, West Lafayette, IN, USA) or a modified model 8151BP 2-Channel wireless potentiostat (Pinnacle Technology Inc., Lawrence, KS, USA) which is shown in Figure 4.2. Each of the three potentiostats required the use of specific data collection and analysis software. When using the CHI potentiostat, the EC response was analyzed using the built-in software package. When using the Epsilon potentiostat, signals were collected and analyzed using Chromgraph software (Bioanalytical Systems). Pinnacle Acquisition Laboratory (PAL) software was used

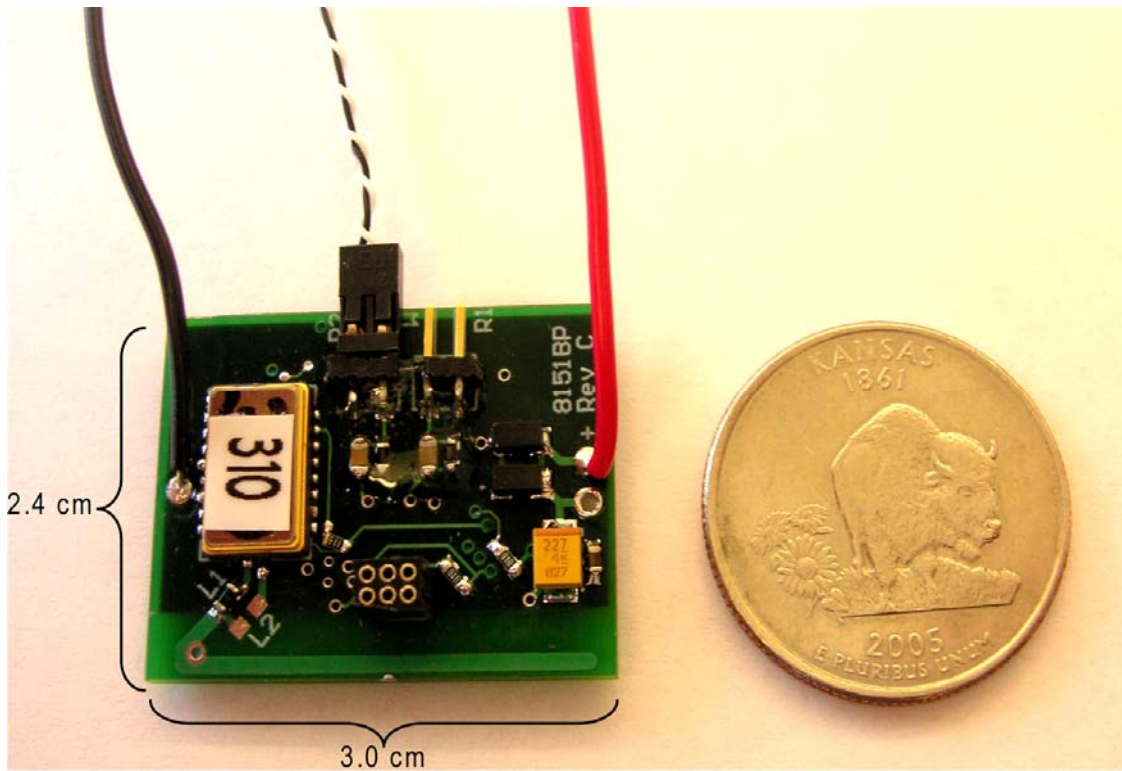


Figure 4.2. Pinnacle Technology, Inc. wireless, isolated potentiostat used for in-channel electrochemical detection.

when the Pinnacle Technology wireless potentiostat was employed. Data was collected at a sampling rate of 10 Hz when using the CHI or BAS potentiostat while a rate of 5 Hz was used when employing the Pinnacle wireless potentiostat. This was because the Pinnacle isolated potentiostat was a prototype model with a maximum sampling rate of 5 Hz. The Pinnacle potentiostat was designed as a two-electrode system capable of compensating for any negative shift in half-wave potential. For experiments employing this potentiostat, a two-electrode format (working vs. Ag/AgCl reference) was used. For all other experiments a three-electrode system (working, Ag/AgCl reference, and Pt wire auxiliary) was used. For all data reported, the working electrode was set at a potential of +900 mV (vs. Ag/AgCl).

4.3 Results and Discussion

4.3.1 Comparison of Electrode Fabrication and Alignment

The growing popularity of EC detection for microchip electrophoresis has led to the development and incorporation of many different electrode materials and electrode configurations. However, in most cases, the choice of electrode material dictates the design and fabrication method for the microchip device. For example, carbon fibers must be placed manually into a channel fabricated in PDMS. This mandates the use of an all-PDMS device with an end-channel electrode alignment (Fig. 4.1A). Palladium decouplers can be fabricated using standard microfabrication methods, and have been shown to significantly reduce band broadening and peak

skew compared to end-channel alignment. Most experiments employing a Pd decoupler employ a Pd working electrode that is deposited on the glass substrate at the same time. An exception to this is a report by Mecker *et al.* who used a Pd decoupler in conjunction with micromolded carbon ink electrodes for the detection of catecholamines [38]. Their approach combined the benefits of off-channel EC detection and carbon-based electrodes. However, this decoupler and working electrode combination is not amenable to mass production since only the Pd decoupler is photolithographically fabricated. Alternatively, the use of in-channel alignment (Fig. 4.1C) further reduces band broadening but requires the use of an electrically isolated potentiostat and specialized electronics that may not be readily available.

When determining which electrode material and/or electrode alignment to use for a particular application, it is important to understand how these variables will affect analytical performance. When using end-channel alignment, it is common practice to align the electrode 5–20 μm from the channel exit. However, dramatic differences in peak height and resolution are observed with only minor changes in alignment distance. Figure 4.3 and Table 4.1 illustrate how electrode alignment can influence peak skew, resolution, and the sensitivity for a given analyte. The equations used to calculate peak skew and tailing factor are illustrated in Figure 4.4. Figure 4.3A shows the electropherogram obtained using a 20 μm electrode spacing while Figure 4.3B shows the electropherogram obtained with 10 μm electrode spacing. As can be seen in Figure 4.3A, the additional 10 micron spacing leads to

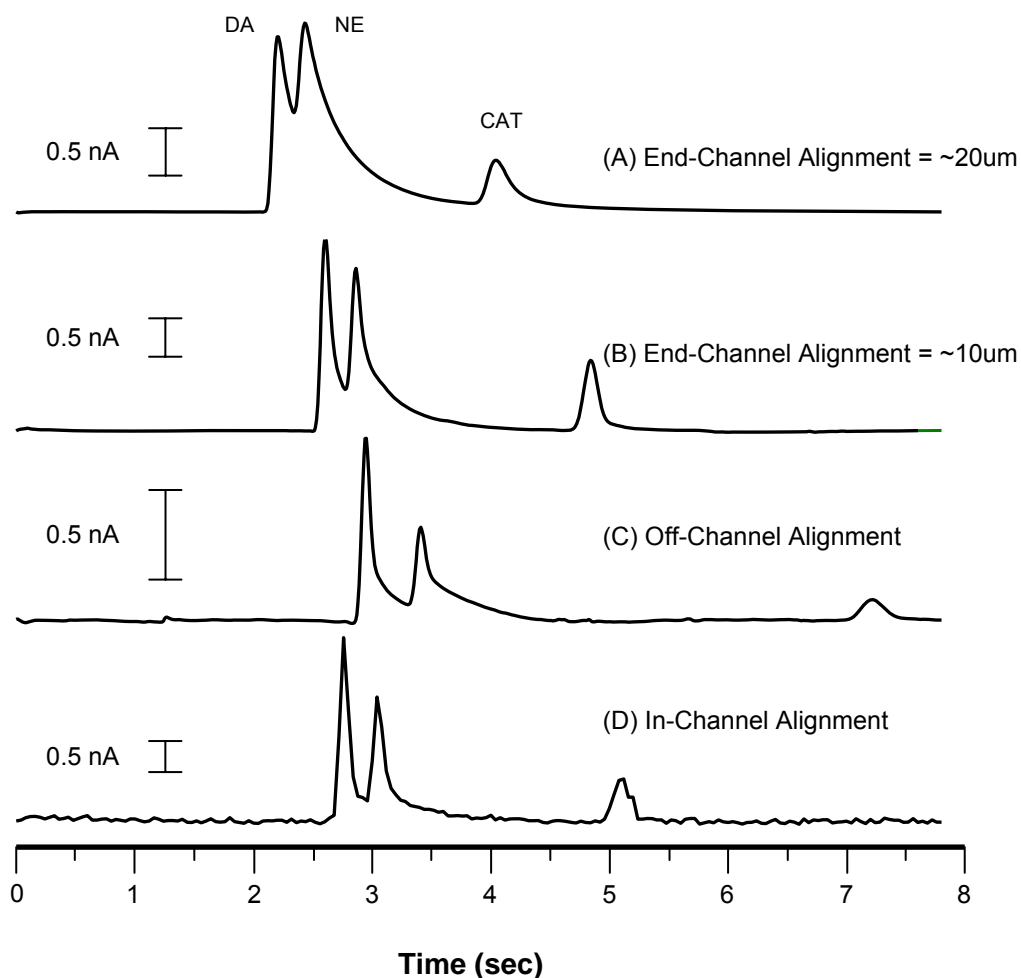


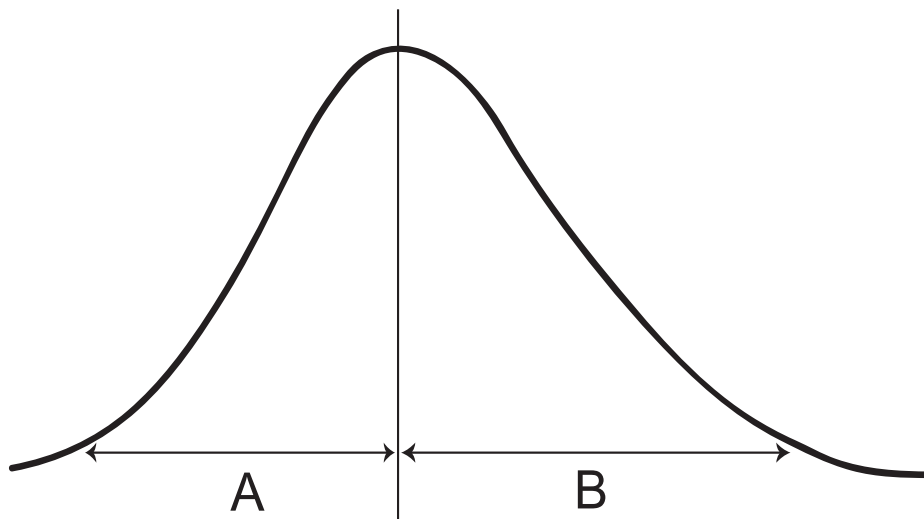
Figure 4.3. Effect of electrode alignment on resolution and peak shape. (A) PPF electrode with end-channel alignment $\sim 20 \mu\text{m}$ from the end of the separation channel; (B) carbon fiber electrode with end-channel alignment $\sim 10 \mu\text{m}$ from the end of the separation channel; (C) Pd electrode and decoupler with off-channel alignment; (D) PPF electrode with in-channel alignment. Separation conditions: 25 mM boric acid, pH 9.2; applied voltage +1400 V to B, +1200 V to S; 400 ms gated injection; $E_{\text{app}} = +900 \text{ mV}$ versus Ag/AgCl. All analytes were $100 \mu\text{M}$.

Table 4.1: Effect of Alignment on Resolution and Peak Shape*

	Rs¹	N²	H²(μm)	Skew²	Tailing Factor²
PPF End - Channel	0.65	379.0	92.3	3.6	2.3
Carbon Fiber End - Channel	0.70	1195	29.3	2.7	1.9
Palladium Off - Channel	0.89	3327	10.5	1.8	1.4
PPF In - Channel	0.91	5351	6.54	0.75	0.88

1: Determined using DA and NE peaks 2: Determined using CAT peak

* Calculated from Figure 4.3



$$\text{Skew} = \frac{B}{A}$$

$$\text{Tailing Factor} = \frac{A + B}{2A}$$

Figure 4.4. Peak skew and peak tailing factor were calculated using the equations shown above. The variables A and B were calculated as the distance from the peak apex to the shoulder of the peak at the baseline.

significant peak tailing and a considerable reduction of the resolution between DA and NE ($R_s = 0.65$ vs. $R_s = 0.7$). The inability to completely resolve NE from DA with the electrode placed 20 microns from the end of the channel (Fig. 4.3A) makes accurate quantitation of these two analytes difficult if not impossible. This illustrates how even small changes in the electrode alignment can directly affect the quality of analytical data.

A considerable improvement in resolution between DA and NE ($R_s = 0.89$) is observed when using off-channel alignment (Fig. 4.3C) compared to end-channel. Although the working electrode is placed directly in the channel minimizing peak dispersion due to dilution, DA and NE still exhibit a small degree of peak tailing due to the parabolic flow profile that forms between the decoupler and working electrode. This effect, as well as a significant shift in the migration time of catechol, is largely due to the change in flow dynamics from electroosmotic to hydrodynamic flow after the decoupler.

The results obtained from using an in-channel alignment are shown in Figure 4.3D. By placing the electrode directly in the separation channel, band broadening, peak tailing, and peak skew were significantly reduced. Even though the potentiostat had a maximum sampling rate of only 5 Hz, an increase in resolution between DA and NE ($R_s = 0.91$) was observed. An even larger resolution value would be expected with an increased sampling rate.

4.3.2 Comparison of Electrode Sensitivity

It is generally accepted that carbon-based materials offer superior analytical performance for EC detection of catecholamines. However, gold or platinum electrode materials have been shown to be useful for the detection of thiols and carbohydrates as well as catecholamines. Therefore, it is desirable to know exactly how the electrode material and alignment affect analytical performance. The sensitivities of the different electrodes and their alignments were determined for DA, NE, and CAT. Calibration curves were constructed over the concentration range of 0.75 to 500 μM for each analyte, electrode material, and electrode alignment. The slope of the line for each analyte (having a linear regression $R^2 = 0.99$ or better) was used to calculate the sensitivity. Since electrodes ranged in width from 20 to 50 μm , the sensitivity values were normalized to the largest electrode width used in the study (50 μm) to account for differences in electrode area which is explained in Table 4.2.

Normalized sensitivity values for all three analytes using a 600 ms injection time are listed in Table 4.3. As expected, DA gave the largest response of the three analytes, followed by NE and CAT, regardless of the electrode material used. The carbon fiber electrode, long considered the gold standard for carbon-based electrodes, exhibited very good sensitivity for dopamine (56.8 $\text{pA}/\mu\text{M}$). However, of all the electrode materials and alignments tested, the PPF electrode in an end-channel configuration exhibited the best sensitivity (72.0 $\text{pA}/\mu\text{M}$) for DA, a 26.7% increase in

Table 4.2: Normalization of Dopamine Sensitivity

	Electrode Width ¹ (μm)	Raw Electrode Sensitivity ² ($\text{pA}/\mu\text{m}$)	Normalized Electrode Sensitivity ³ ($\text{pA}/\mu\text{m}$)
PPF End-Channel	40	58	72
Carbon Fiber End-Channel	33	37.5	56.8
Palladium End-Channel	40	42	52.5
Palladium Off-Channel	50	12	12
Carbon Ink Off-Channel	20	8.1	20.2
Carbon Ink End-Channel	50	4.34	4.34

1: Electrode width was used for normalization since the separation channel was constant

2: Slope of the calibration curve for dopamine 3: Sensitivity corrected for electrode width

Table 4.2: The resulting sensitivity value for each electrode was normalized to an electrode width of $50 \mu\text{m}$ (which was the largest electrode used in the study). The width of the PDMS separation channel did not change throughout the experiment. Therefore, the width of the electrode is the only variable that would contribute to different electrode areas. Sensitivity values were calculated by multiplying sensitivity value for each electrode or configuration by 50 (the largest electrode width) then dividing by the width of the electrode used. Making the largest electrode width ($50 \mu\text{m}$) 1, and all smaller widths a fraction of that value.

Table 4.3: Normalized Sensitivity (pA/ μ M) for All Analytes

	<u>Dopamine</u>	<u>Norepinephrine</u>	<u>Catechol</u>
PPF End - Channel	72 \pm 2	44 \pm 1	15.03 \pm 0.04
Carbon Fiber End - Channel	56.8 \pm 0.1	45.1 \pm 0.9	18.3 \pm 0.3
Palladium End - Channel	52.5 \pm 0.3	41.1 \pm 0.3	10.67 \pm 0.09
Palladium Off - Channel	12 \pm 1	7.4 \pm 0.2	0.84 \pm 0.01
Carbon Ink Off - Channel	20.2 \pm 0.2	8.2 \pm 0.1	5.22 \pm 0.06
Carbon Ink End - Channel	4.34 \pm 0.02	2.28 \pm 0.02	0.418 \pm 0.003

sensitivity over the carbon fiber electrode. In addition, the PPF electrode was the only electrode tested that showed a large response for sub-second injections of nanomolar concentrations of analyte. Peaks were obtained for all three analytes at a concentration of 750 nM with $S/N > 3$ (Fig. 4.5). One surprising finding was that the sensitivity value for the end-channel Pd electrode was similar to that of the carbon fiber. Although Pd is normally thought of as an inferior electrode material for catecholamines, the sensitivity of the Pd electrode for DA was only 8% lower than that of the carbon fiber. Another unanticipated finding was that the Pd electrode exhibited significantly reduced sensitivity for all analytes when used in an off-channel detection scheme. This was unexpected because this configuration has been shown in the past to substantially reduce band broadening, leading to more efficient peaks, which should result in better sensitivity. This result was observed on multiple days with multiple electrodes (data not shown). The reason for the lower sensitivity is unclear. However, on several days, the portion of the Pd decoupler exposed to the electrophoresis channel exhibited visual signs of fouling. It is well known that catecholamines are susceptible to chemical degradation at high pH. The grounding of the separation voltage at the Pd cathode in the channel leads to the reductive electrolysis of H_2O , causing the formation of both hydrogen gas and hydroxide ions. It is possible that a high concentration of OH^- leads to analyte degradation at the surface of the palladium decoupler, reducing the amount of analyte that reaches the working electrode. Alternatively, the hydroxide ions produced at the decoupler could cause the formation of an oxide layer on the palladium working electrode, reducing

the effective working electrode area and the resulting current response [49, 50].

The carbon ink electrode showed an opposite trend, with off-channel detection providing better sensitivity. One potential reason is that carbon working electrodes are less likely to be affected by large changes in pH than their metal electrode counterparts. Another important factor is the dependence of analyte sensitivity on the carbon ink electrode fabrication process. Garcia and co-workers reported a reduction in sensitivity in EC detection with increasing carbon ink film thickness [51]. Using a carbon ink-coated gold wire, they observed that peak current (I_p) increased proportionally with the number of ink layers deposited. However, when more than 7 layers of ink were deposited ($\sim 1.0 \mu\text{m}$ total thickness), lower peak currents were obtained. The loss of signal and sensitivity was attributed to an increase in the resistance of the carbon ink film.

This phenomenon was also observed in our studies. It can be seen in Table 4.3 that carbon ink electrodes used in an off-channel configuration were more sensitive than those used end-channel. It has been shown that carbon ink electrodes are highly resistive and that this resistance is directly related to the amount of ink used for fabrication [52]. The electrode fabricated for end-channel use measured $50 \mu\text{m}$ wide, 8 mm long, and $16.1 \mu\text{m}$ thick, whereas the electrode used for off-channel detection was $20 \mu\text{m}$ wide, 2 mm long, and $0.8 \mu\text{m}$ thick. This is equal to a ~ 200 -fold increase in the amount of bulk electrode material and helps to explain the attenuation of signal observed with the end-channel carbon ink electrode (Fig. 4.5). Furthermore,

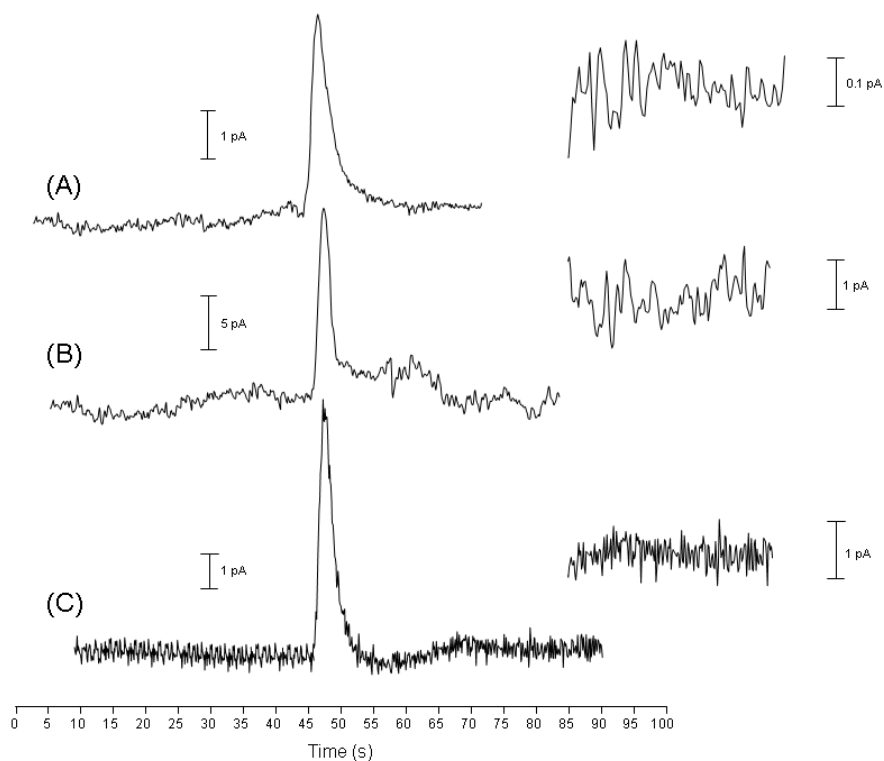


Figure 4.5. EC response of CAT at three different end-channel carbon electrodes. (A) $10\ \mu\text{M}$ at a carbon ink electrode; (B) $1.0\ \mu\text{M}$ CAT at a carbon fiber electrode; (C) $750\ \text{nM}$ CAT at a PPF electrode. An expanded view of the baseline noise is inset for each electropheroogram.

this demonstrates how seemingly small changes in fabrication can have dramatic effects on the analytical sensitivity of the resulting electrode.

4.3.3 Comparison of Limit of Detection

When evaluating the analytical performance of any detection scheme, it is important to consider not only sensitivity but also the limit of detection (LOD). Since LOD is calculated as a ratio of signal-to-noise (S/N), electrodes that do not exhibit a high degree of sensitivity but have low background noise can still yield low theoretical limits of detection. Conversely, electrodes that exhibit high sensitivity may also have a large amount of noise, leading to higher limits of detection. The theoretical LOD for each electrode material and electrode alignment was calculated. The average noise for each concentration examined was calculated from three separate measurements of the background noise. The resulting I_p for each analyte and concentration was divided by the average noise and used to calculate LOD at $S/N = 3$. Representative LOD values for each electrode material and alignment were determined by averaging the resulting LOD value generated by each concentration examined. Concentration and mass LOD values for all analytes, electrode materials, and alignments can be found in Table 4.4. Mass detection limits were calculated using an experimentally determined injection volume of 345.6 ± 16.7 pL (data not shown).

The PPF electrode not only exhibited the best sensitivity but outperformed all other electrodes by having the lowest LOD for all three analytes (Table 4.4). While

Table 4.4: Concentration (nM) and Mass (amol) LOD Values for All Analytes

	Dopamine		Norepinephrine		Catechol	
	Concentration (nM)	Mass (amol)	Concentration (nM)	Mass (amol)	Concentration (nM)	Mass (amol)
PPF End - Channel	73 ± 20	25 ± 8	110 ± 20	37 ± 8	200 ± 80	70 ± 30
Carbon Fiber End - Channel	300 ± 100	110 ± 50	300 ± 100	120 ± 40	700 ± 100	250 ± 40
Palladium End - Channel	400 ± 100	130 ± 50	500 ± 200	160 ± 60	1800 ± 600	600 ± 200
Palladium Off - Channel	370 ± 30	130 ± 10	680 ± 30	240 ± 10	4000 ± 1000	1400 ± 500
Carbon Ink Off - Channel	140 ± 30	49 ± 9	400 ± 100	140 ± 40	500 ± 200	170 ± 60
Carbon Ink End - Channel	290 ± 90	100 ± 30	500 ± 100	170 ± 40	3000 ± 1000	1000 ± 300

the pyrolyzed electrode material exhibited the largest response, it also benefited from fairly low background noise (averaging 0.85 pA peak-to-peak) as seen in Figure 4.5. Over the eight concentrations used in the experiment, the calculated LOD for DA averaged 73 ± 20 nM, with a best individual calculated LOD of 35 nM. Due to efficient decoupling of the separation voltage, the off-channel Pd electrode also benefited from low background noise, which resulted in a calculated LOD of 370 ± 30 nM.

Both carbon ink electrode configurations yielded calculated LODs (290 ± 90 nM for end channel; 140 ± 30 nM for off-channel) for DA that were similar to those of the carbon fiber and end-channel Pd electrode (30 ± 100 nM and 400 ± 100 nM, respectively). This finding seems to be contradictory to what one would expect, as the carbon ink electrodes were among the least sensitive electrodes tested (Table 4.3). However, the carbon ink electrodes exhibited the lowest noise of all the electrodes investigated (Fig. 4.5). Compared to more conductive materials such as Pd, the resistive electrode material leads to lower peak currents and decreased sensitivity. The increased resistivity also significantly reduces the peak-to-peak background noise (0.3 pA for carbon ink off-channel). The effects of the resultant I_p and baseline noise on the calculated LOD are illustrated in Figure 5. Despite the fact that the end-channel carbon ink electrode had the least amount of noise (Fig. 4.5A), the resulting I_p for a $10 \mu\text{M}$ CAT sample was smaller than that generated by a $1.0 \mu\text{M}$ or 750 nM CAT sample at a carbon fiber or PPF electrode (Fig. 4.5B and Fig. 4.5C respectively).

Therefore, because LOD is calculated as a ratio of the signal (peak height) to noise, the ink electrodes had calculated LODs similar to those of other electrode materials.

The calculated LODs in Table 4.4 were obtained by extrapolating the response obtained for the analytes of interest in the low micromolar range to a $S/N = 3$. Although all of these calculated LODs are reported to be in the nanomolar range, experimentally it was not possible to detect $1 \mu\text{M}$ DA with the carbon ink end-channel electrode as the potentiostat was not sensitive enough to detect the I_p generated at this concentration. However, dopamine was detectable at or below a $1 \mu\text{M}$ concentration for all the other electrode materials and configurations. The PPF electrode used in an end-channel alignment generated the best response for the detection of sub-micromolar concentrations of analytes. This is due to a combination of high sensitivity observed with the PPF electrodes and a small amount of background noise (0.85 nA). While the PPF electrodes were noisier than the carbon ink electrodes, the increased conductivity (reduced resistance) allowed the potentiostat to detect the change in current for lower concentration analytes. These results illustrate the importance of considering the LOD as well as the sensitivity of any particular electrode material and alignment. Understanding how both of these parameters can be affected by the electrode material or the electrode alignment is crucial to the success of any application of EC detection for microchip electrophoresis.

4.3.4 In-channel EC Detection

While used less frequently than end- or off-channel EC detection, in-channel detection offers many advantages. Placement of the electrode directly in the separation channel helps increase separation efficiency by limiting band broadening and peak skew. Preliminary experiments using the Pinnacle Technology wireless potentiostat illustrate the benefits of in-channel EC detection. As described earlier, the Pinnacle Technology isolated potentiostat was a prototype model that was limited to a 5 Hz sampling rate. Since its lower sampling rate restricted it from performing in a manner similar to other potentiostats used, it was not included in the direct comparison of sensitivity and LOD. However, many conclusions regarding the relationship between electrode alignment, peak shape, and analytical performance can still be made.

Using a PPF electrode in-channel, peak currents similar to those of the PPF electrode used in an end-channel configuration were observed (Fig. 4.3). However, since the prototype potentiostat was limited to a 5 Hz sampling rate, larger peak currents and a higher degree of sensitivity would be expected with an increased sampling rate. Alignment of the electrode directly in the separation channel mitigates the effects of band broadening and peak dispersion seen with end- or off-channel alignment. As seen in Table 4.1, the degree of peak skew for catechol was reduced by a factor of 2.4 over the off-channel alignment and a factor of 3.6 over the end-channel alignment. Peak tailing was also reduced by a factor of 1.9 over off-channel and 2.1 over end-channel alignment. This reduction in band broadening led to the

largest observed resolution between DA and NE ($R_s = 0.91$) compared to all other electrodes and alignments tested. Furthermore, since no decoupler is needed when using in-channel alignment, the detection scheme is less complicated than that for off-channel detection. In addition, one is not limited by the type of electrode material that can be used. This type of electrode alignment should prove very useful for many applications of microchip electrophoresis with EC detection.

4.4 Conclusions

The direct comparison of different electrode materials and electrode alignments for microchip electrophoresis with EC detection was described. General observations and comments on each electrode material and configuration can be found in Table 4.5. By comparing the influence of electrode material on EC response, it was determined that carbon-based electrode materials offered the greatest sensitivity for all three analytes. Of all materials and configurations examined, PPF electrodes used in an end-channel alignment offered the greatest sensitivity ($72.0 \text{ pA}/\mu\text{m}$) and lowest calculated LOD (35 nM) for DA. It was found that, when used in an end-channel alignment, Pd electrodes exhibited an EC response similar to that of carbon fiber electrodes. This was an interesting result as carbon fiber electrodes are generally considered to exhibit superior performance over metal electrodes for the detection of organic analytes. However, lower than expected analyte sensitivity values were obtained when Pd was used for off-channel EC detection. It is postulated that this could be due to sample degradation at the decoupler that precedes the working

Table 4.5: Qualitative Assessment of Microchip Performance

	Analytical Parameters			Fabrication Procedure			Remarks
	Sensitivity ¹	Limit of Detection ²	Noise ³	Process	Cost	Use of Hazardous Chemicals ⁴	
PPF End - Channel	Best	Best	Low	Simplest	Moderate	No	Requires fused silica substrate; high temperature furnace
Carbon Fiber End - Channel	Good	Fair	Fair	Simple	Inexpensive	No	Requires skill to embed carbon fiber into PDMS substrate
Palladium End - Channel	Good	Fair	High	Complex	Expensive	Yes	Deposition system required; use of expensive or rare materials
Palladium Off - Channel	Poor	Fair	Fair	Complex	Expensive	Yes	Deposition system required; use of expensive or rare materials
Carbon Ink Off - Channel	Fair	Good	Lowest	Simple	Inexpensive	Yes	Electrode size is limited by PDMS aspect ratio; thick films can be highly resistive
Carbon Ink End - Channel	Poor	Fair	Lowest	Simple	Inexpensive	No	Electrode size is limited by PDMS aspect ratio; thick films can be highly resistive

1: Slope of the calibration curve 2: Calculated for S/N=3 3: Based on average peak-to-peak baseline noise 4: Use of HF and/or aqua regia solutions

electrode. Despite being less sensitive, comparable LOD values for this electrode were obtained due to the lower noise provided by efficient decoupling of the separation voltage from the working electrode.

Experiments using an in-channel electrode alignment significantly reduced the amount of band broadening observed in the other electrode alignment schemes. Compared to end- and off-channel alignment, this led to a decrease in peak skew and peak tailing with increased resolution and plate number. With an improved sampling rate (>5 Hz), the authors believe that the in-channel alignment would have provided the best sensitivity and detection limits as well. This detection scheme will be investigated in future experiments involving the separation and detection of catecholamine neurotransmitters. Taken collectively, these results illustrate the dramatic effect that both electrode material and electrode alignment can have on EC response in microfluidic devices and the resulting quality of analytical data.

4.5 References

- [1] Harrison, D. J., Manz, A., Fan, Z., Ludi, H., Widmer, H. M., *Analytical Chemistry* 1992, *64*, 1926-1932.
- [2] Manz, A., Graber, N., Widmer, H. M., *Sensors and Actuators B* 1990, *1*, 244-248.
- [3] Manz, A., Harrison, D. J., Verpoorte, E., Fettingner, J. C., Ludi, H., Widmer, H. M., *Journal of Chromatography* 1992, *593*, 253-258.
- [4] Ohno, K.-i., Tachikawa, K., Manz, A., *Electrophoresis* 2008, *29*, 4443-4453.
- [5] Harrison, D. J., Fluri, K., Seiler, K., Fan, Z., Effenhauser, C. S., Manz, A., *Science* 1993, *261*, 895-897.
- [6] Jacobson, S. C., Hergenroder, R., Koutny, L. B., Ramsey, J. M., *Analytical Chemistry* 1994, *66*, 1114-1118.
- [7] Legendre, L. A., Bienvenue, J. M., Roper, M. G., Ferrance, J. P., Landers, J. P., *Analytical Chemistry* 2006, *78*, 1444-1451.
- [8] Landers, J. P., Editor, *Capillary and Microchip Electrophoresis and Associated Microtechniques*, 2008.
- [9] Vandaveer IV, W. R., Pisas-Farmer, S. A., Fischer, D. J., Frankenfeld, C. N., Lunte, S. M., *Electrophoresis* 2004, *25*, 3528-3549.
- [10] Pisas, S. A., Fogarty, B. A., Huynh, B. H., Lacher, N. A., Carlson, B., Martin, R. S., Vandaveer IV, W. R., Kutter, J. P., Fintschenko, Y. (Eds.), *Separation Methods in Microanalytical Systems*, Marcel Dekker, New York 2004.
- [11] Johnson, M. E., Landers, J. P., *Electrophoresis* 2004, *25*, 3513-3527.
- [12] Huynh, B. H., Fogarty, B. A., Nandi, P., Lunte, S. M., *Journal of Pharmaceutical and Biomedical Analysis* 2006, *42*, 529-534.
- [13] Li, M. W., Martin, R. S., *Analyst* 2008, *133*, 1358-1366.
- [14] Garcia, C. D., Henry, C. S., *Bio-MEMS* 2007, 265-297.
- [15] Castano-Alvarez, M., Fernandez-Abedul, M. T., Costa-Garcia, A., *Comprehensive Analytical Chemistry* 2007, *49*, 827-872.
- [16] Martin, R. S., *Methods in Molecular Biology* 2006, *339*, 85-112.
- [17] West, J., Becker, M., Tombrink, S., Manz, A., *Analytical Chemistry* 2008, *80*, 4403-4419.
- [18] Coltro, W. K. T., da Silva, J. A. F., Carrilho, E., *Electrophoresis* 2008, *29*, 2260-2265.
- [19] Noblitt, S. D., Henry, C. S., *Analytical Chemistry* 2008, *80*, 7624-7630.
- [20] Holcomb, R. E., Kraly, J. R., Henry, C. S., *Analyst* 2009, *134*, 486-492.
- [21] Kuhnline, C. D., Gangel, M. G., Hulvey, M. K., Martin, R. S., *Analyst* 2006, *131*, 202-207.
- [22] Vickers, J. A., Henry, C. S., *Electrophoresis* 2005, *26*, 4641-4647.
- [23] Amatore, C., Arbault, S., Bouton, C., Drapier, J.-C., Ghandour, H., Koh, A. C. W., *ChemBioChem* 2008, *9*, 1472-1480.
- [24] Huang, X., Zare, R. N., Sloss, S., Ewing, A. G., *Analytical Chemistry* 1991, *63*, 189-192.
- [25] Martin, R. S., Ratzlaff, K. L., Huynh, B. H., Lunte, S. M., *Analytical Chemistry* 2002, *74*, 1136-1143.

- [26] Wallingford, R. A., Ewing, A. G., *Analytical Chemistry* 1987, 59, 1762-1766.
- [27] Osbourn, D. M., Lunte, C. E., *Analytical Chemistry* 2003, 75, 2710-2714.
- [28] Wu, C.-C., Wu, R.-G., Huang, J.-G., Lin, Y.-C., Chang, H.-C., *Analytical Chemistry* 2003, 75, 947-952.
- [29] Lacher, N. A., Lunte, S. M., Martin, R. S., *Analytical Chemistry* 2004, 76, 2482-2491.
- [30] Hebert, N. E., Kuhr, W. G., Brazill, S. A., *Electrophoresis* 2002, 23, 3750-3759.
- [31] Lacher, N. A., Garrison, K. E., Martin, R. S., Lunte, S. M., *Electrophoresis* 2001, 22, 2526-2536.
- [32] McCreery, R. L., Cline, K. K., in: Kissinger, P. T., Heineman, W. R. (Eds.), *Laboratory Techniques in Electroanalytical Chemistry*, Marcel Dekker, New York 1996, pp. 293-332.
- [33] Zachek, M. K., Hermans, A., Wightman, R. M., McCarty, G. S., *J. Electroanalytical Chemistry* 2008, 614, 113-120.
- [34] Chesney, D. J., *Laboratory Techniques in Electroanalytical Chemistry, 2nd Edition. Edited by Peter T. Kissinger (Purdue University) and William R. Heineman (University of Cincinnati)*, 1996.
- [35] Gawron, A. J., Martin, R. S., Lunte, S. M., *Electrophoresis* 2001, 22, 242-248.
- [36] Kovarik, M. L., Torrence, N. J., Spence, D. M., Martin, R. S., *Analyst* 2004, 129, 400-405.
- [37] Liu, C., Li, X., Lu, G., *Huaxue Yanjiu Yu Yingyong* 2005, 17, 443-447.
- [38] Mecker, L. C., Martin, R. S., *Electrophoresis* 2006, 27, 5032-5042.
- [39] Kim, J., Song, X., Kinoshita, K., Madou, M., White, R., *J. Electrochem. Soc.* 1998, 145, 2314-2319.
- [40] Ranganathan, S., McCreery, R., Majji, S. M., Madou, M., *Journal of The Electrochemical Society* 2000, 147, 277-282.
- [41] Fischer, D. J., Vandaveer, W. R. I. V., Grigsby, R. J., Lunte, S. M., *Electroanalysis* 2005, 17, 1153-1159.
- [42] Martin, R. S., Gawron, A. J., Lunte, S. M., Henry, C. S., *Analytical Chemistry* 2000, 72, 3196-3202.
- [43] Madou, M. J., *Fundamentals of microfabrication: The science of minaturization*, CRC Press 2002.
- [44] McDonald, J. C., Duffy, D. C., Anderson, J. R., Chiu, D. T., Wu, H., Schueller, O. J. A., Whitesides, G. M., *Electrophoresis* 2000, 21, 27-40.
- [45] Hulvey, M. K., Genes, L. I., Spence, D. M., Martin, R. S., *Analyst* 2007, 132, 1246-1253.
- [46] Hulvey, M. K., Martin, R. S., *Analytical and Bioanalytical Chemistry* 2009, 393, 599-605.
- [47] Mecker, L. C., Martin, R. S., *Analytical Chemistry* 2008, 80, 9257-9264.
- [48] Spence, D. M., Torrence, N. J., Kovarik, M. L., Martin, R. S., *Analyst* 2004, 129, 995-1000.
- [49] Genesca, J., Victori, L., *Reviews on Coatings and Corrosion*. 1981, 4, 325-348.
- [50] Burke, L. D., Roche, M. B. C., *Journal of Electroanalytical Chemical Interfacial Electrochemistry* 1985, 186, 139-154.

- [51] Ding, Y., Ayon, A., Garcia, C. D., *Analytica Chimica Acta* 2007, 584, 244-251.
- [52] Grennan, K., Killard, A. J., Smyth, M. R., *Electroanalysis* 2001, 13, 745-750.

Chapter 5

Part I: Conclusion and Direction of Future Research

5.1 Conclusion of Part I

The original goal of the work performed for this part of this dissertation was the development of analytical methodology for the analysis of catecholamine neurotransmitters (NTs) by microchip electrophoresis with electrochemical (EC) detection. Neurotransmitters such as dopamine (DA), epinephrine (Epi), and norepinephrine (NE) are routinely analyzed when investigating complex neurological pathways or causes of neurodegenerative diseases. One of the most widely used analytical tools for this purpose is microchip electrophoresis with EC detection [1-3]. Microchip electrophoresis is an analytical technique capable of analyzing small sample volumes with high temporal resolution. In addition, electrochemistry offers the ability to miniaturize and integrate detection electrodes while maintaining a high degree of sensitivity.

Much of this work focused on the fabrication and characterization of the novel carbon-based electrode material, pyrolyzed photoresist. The fabrication of pyrolyzed photoresist film (PPF) electrodes was optimized for use in microchip electrophoresis was described. Following fabrication, the analytical performance of the electrodes was characterized using catecholamine NTs. In addition, the performance of several standard electrode materials was determined and directly compared to that of the PPF electrodes.

Chapter 3 describes the original work performed to fabricate and characterize the PPF electrodes [4]. Photoresist was patterned via standard photolithographic techniques and pyrolyzed using a high-temperature furnace. The analytical

performance of the newly developed electrodes was examined using the model analytes DA, catechol (CAT), and ascorbic (AA). Parameters such as linearity, sensitivity, and limit of detection (LOD) were determined and directly compared to the performance of a carbon fiber electrode. It was observed that the PPF electrodes behaved in a similar manner to the carbon fiber electrode. Both electrodes produced similar sensitivity values and LODs. However, the carbon fiber must be manually placed in a PDMS microchannel which can be time consuming and labor intensive.

One major advantage of the PPF electrode is that it is fabricated using photolithography. Therefore, the electrode size, shape, and geometry can be precisely controlled by the fabrication process. In addition, many other microchip components can be made using the same procedures. This reduces the time spent in the microfabrication facility and helps to promote the construction of a fully integrated device. The use of dual-electrode EC detection was also demonstrated through the fabrication of two electrodes fabricated in a serial configuration. This mode of detection offers enhanced selectivity for electrochemically reversible analytes. This work produced the first published report of PPF electrodes used in a dual-electrode format for EC detection with microchip electrophoresis [4].

Chapter 4 expands the scope of electrode comparison demonstrated in chapter 3. The effects of the electrode material as well as electrode alignment on analytical performance were examined. Carbon-based electrode materials such as carbon fiber (CF), carbon ink, and pyrolyzed carbon as well as palladium (Pd) metal electrodes were directly compared. In addition, the effect of electrode alignment on analytical

performance was also investigated. Analytical parameters such as resolution, sensitivity, and limit of detection were determined for end-, in-, and off-channel electrode alignments as well as the different electrode materials. These analytical parameters were determined through the separation and EC detection of DA, NE, and catechol (CAT) mixtures.

It was determined that a PPF electrode used in an end-channel configuration out performed all other electrode materials and alignments. The PPF electrode yielded the highest sensitivity and lowest limit of detection (LOD) for all analytes tested. Because end-channel alignment is the easiest to implement, this combination of electrode material and alignment resulted in the best performing and most user friendly EC detection mode examined. Although there are many published reports detailing the use of these electrodes and alignments, there are none that perform a side-by-side comparison. Therefore, there were a few surprising findings. One unexpected result was that off-channel detection was much less sensitive than end-channel alignment when directly comparing Pd electrodes. Off-channel EC detection has been shown to substantially reduce band broadening, leading to more efficient peaks, which should result in better sensitivity. However on several days, the portion of the Pd decoupler exposed to the electrophoresis channel exhibited visual signs of fouling. This result was observed on multiple days with multiple electrodes. Despite reduced sensitivity, placing the detection electrode directly in the channel resulted in greater separation efficiency (resolution) than end-channel alignment. Band broadening was reduced which lead to a greater separation between the closely

migrating species DA and NE. Overall, the added time and expense required to fabricate electrodes for off-channel detection makes this mode of EC detection less attractive than simple end-channel alignment.

Another unexpected result was that the end-channel Pd and CF electrodes had very similar performance. The CF electrode has long been considered the gold standard for carbon-based electrodes while metal electrodes are generally not considered to be ideal for the detection of catecholamine NTs. However, data analysis showed that these two electrode materials differed by only ~8% in terms of sensitivity. This result demonstrates that very little analytical performance is lost while taking advantage of a microfabricated Pd electrode.

5.2 Future Research Directions

Although the first reports of miniaturized electrophoretic devices appeared almost two decades ago, the field of microchip electrophoresis with EC detection is still evolving. Numerous microchip substrates, electrode materials, and configurations have been explored which has allowed researchers to utilize miniaturized devices for a multitude of applications. Because these microfluidic devices are fabricated from a handful of raw materials, there are a seemingly infinite number of possibilities for their design and use. There are a few possible areas that could be pursued which advance this area of research and this dissertation. One of these involves the use of longer separation channels for the separation of closely related species. Another area of research in our lab that can be improved is the on-chip analysis of single cells. Finally, continued work towards the miniaturization and

integration of supporting instrumentation will lead to the development of a truly portable system with the possibility of onsite or on-animal use.

5.2.1 Serpentine Separation Channels

One of the drawbacks of using a simple “T” microchip configuration is that the separation channel is relatively short (3-5 cm) [5-6]. Because most analytes have fast migration times through these short channels, resolving closely related species can be problematic. One strategy commonly used to increase resolution is to increase the separation length before the analytes are detected [7]. Due to the small footprint, this can be difficult in miniaturized devices. Recently, Ramsey and Culbertson have described the fabrication and characterization of long separation channels for microchip electrophoresis [8-10]. The authors describe the use of serpentine separation channels with incorporated asymmetric tapered turns (Fig. 5.1). The increased separation length increases peak capacity while the tapered turns decrease the amount of band broadening associated with the “racetrack” effect [11-12].

This strategy has been shown to be quite effective at separating a large number of closely related species. However, all of the reports detailing the use of serpentine channels have used laser induced fluorescence (LIF) for detection. Currently, there is only one published report describing the use of a serpentine separation channel with EC detection [13]. Bowen *et al.* described the use of a Pd decoupler for the off-channel detection of DA and NE. The authors report a dramatic improvement in separation efficiency and plate number as a result of the increased separation length. Although the authors employed off-channel alignment, end-

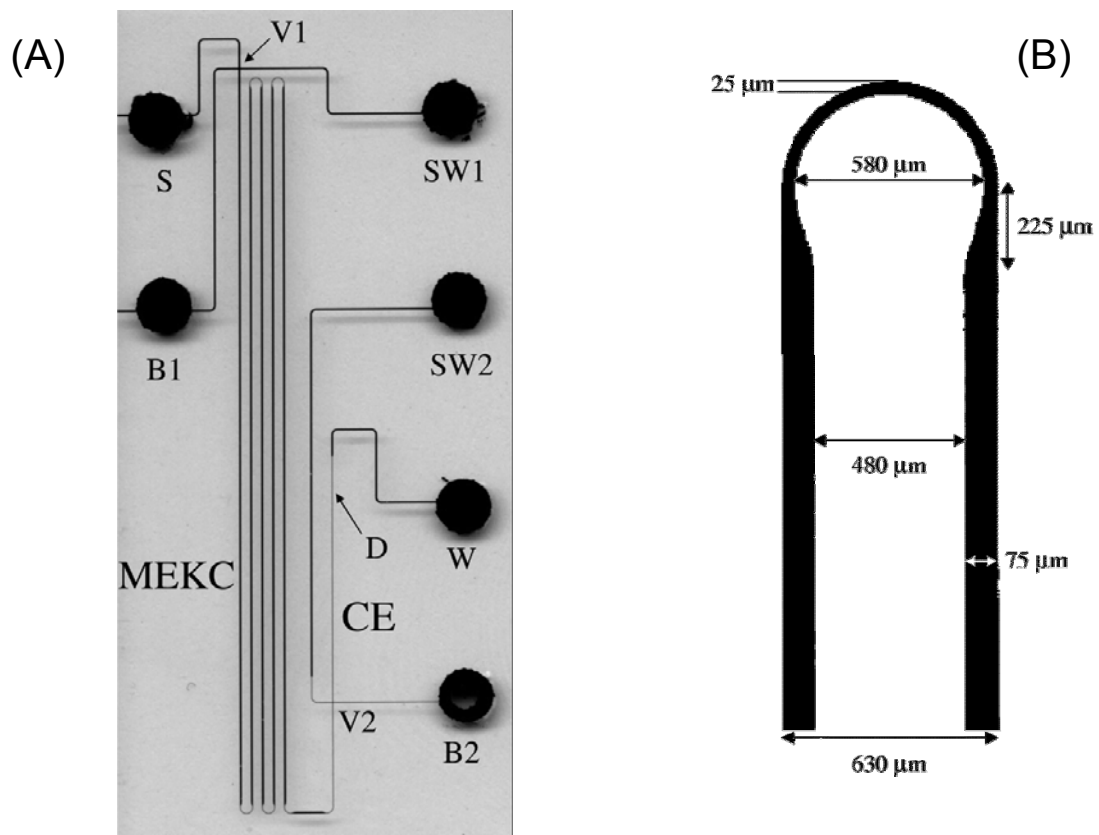


Figure 5.1: Microchip with serpentine channels. (A) Microchip with serpentine channels for two-dimensional separations. Injections for the first-dimension separation were made at valve 1 (V1) and valve 2 (V2) for the second-dimension. (B) Expanded view of the optimized asymmetric turn profile with dimensions included. Reprinted with permission from [8].

channel detection could just as easily be used. A microchip with serpentine channels and EC detection would be a very valuable tool for many applications.

One application our lab has recently investigated is the EC determination of CBI-derivatives of the amino arginine (Arg) and its methylated isomers N-monomethyl arginine (NMMA), N-N-dimethylarginine (NDMA), asymmetric dimethylarginine (ADMA), and symmetric dimethylarginine (SDMA). Arginine is a substrate for a family of nitric oxide synthase proteins which produce nitric oxide (NO). The methylated arginine species act as inhibitors of this process. The accurate determination of these species in blood is important for the administration of proper treatment for underdeveloped lungs in premature and newborn infants [14-15]. Because these species only differ by the weight or location of one methyl group, they are very hard to separate by microchip electrophoresis. Therefore, the use of a long separation channel would aid the separation of these closely related species aiding the identification of each marker in clinical samples.

5.2.2 Single Cell Analysis

Microfluidic electrophoresis devices with EC detection have been used for a variety of applications. Some of these research topics include neurochemistry, disease pathology, and cellular assays. In many instances, the samples are obtained from cells in culture and must be prepared off-line prior to being analyzed on-chip. Not only does this require more time and effort but it potentially introduces human error. Moreover, many of the physiological processes investigated require the use of a population of cells. However, the chemical events which occur on short timescales

(e.g. kinase cascades or receptor signaling) may not be fully elucidated when analyzing a population average. In addition, many cancers originate from a single cell. Therefore, finding the rare mutations in a population of cells that indicate the inception of a disease must be done on a cell by cell basis [16].

Analyzing the contents or analytes of interest from a single cell can be a very challenging task. The sample volume is extremely small which requires a sensitive and selective detection technique. In addition, the cells must be manipulated in such a way that their normal function is not disrupted. In many ways, the microfluidic platform is ideally suited for the analysis of single cells. Since multiple processes are routinely integrated on one device [17-19], cell culture, cell handling, and lysis can easily be performed prior to analysis. Moreover, because microfluidic devices have very small internal volumes, cell contents will not be significantly diluted after the cells are lysed. While our lab has experience with many of these functions, the integration of all the necessary processes on a single chip has not been performed.

Recently, our lab has investigated the production of peroxynitrite (ONOO^-) from macrophages stimulated in culture. Peroxynitrite is a strong oxidizing agent that is produced in cells from the reaction of superoxide (O_2^-) and nitric oxide (NO). Elevated levels of peroxynitrite can lead to oxidative stress and has been shown to damage cellular proteins, DNA, and lead to cell death [20-22]. Preliminary experiments were performed off-line to determine the feasibility of determining the amount of ONOO^- produced from a single macrophage. One method of estimating the amount of ONOO^- produced is by analyzing nitrate which is one of the reaction

products. The Griess reaction was utilized to indirectly measure the amount of ONOO^- produced from a population of cells in culture. It was determined that each cell produced an average of ~ 500 pmol of nitrate. Because this was an *in vitro* assay, significant dilution occurred. If a single cell were analyzed on-chip, dilution could be minimized so that the ONOO^- concentration would be easily detectable. This preliminary work indicates that it is possible to detect ONOO^- produced from a single cell, but significant work must be done to incorporate the many other processes on a single chip.

Price and Culbertson have outlined the necessities for single cell analysis [16] and have demonstrated this ability using fluorescently labeled cell contents [23]. Figure 5.2 illustrates the various processes that must be incorporated to successfully analyze single cells. The proposed microchip contains distinct areas for cell culture, cell sorting, as well as reagent loading or introduction. Most importantly, cells are lysed at the intersection of the sample and separation channels. This allows for the lysis of cells and separation of their contents. Many of these processes have been separately investigated in our lab; however, it would be beneficial for future work to incorporate all of these processes on a single microfluidic device. For our immediate goals, optimization of each of these tasks would make it possible to quantitate the amount of peroxynitrite produced from a single cell. In the long term, this single cell analysis platform could easily be applied to a variety of applications such as cancer screening, drug delivery, or proteomic analysis.

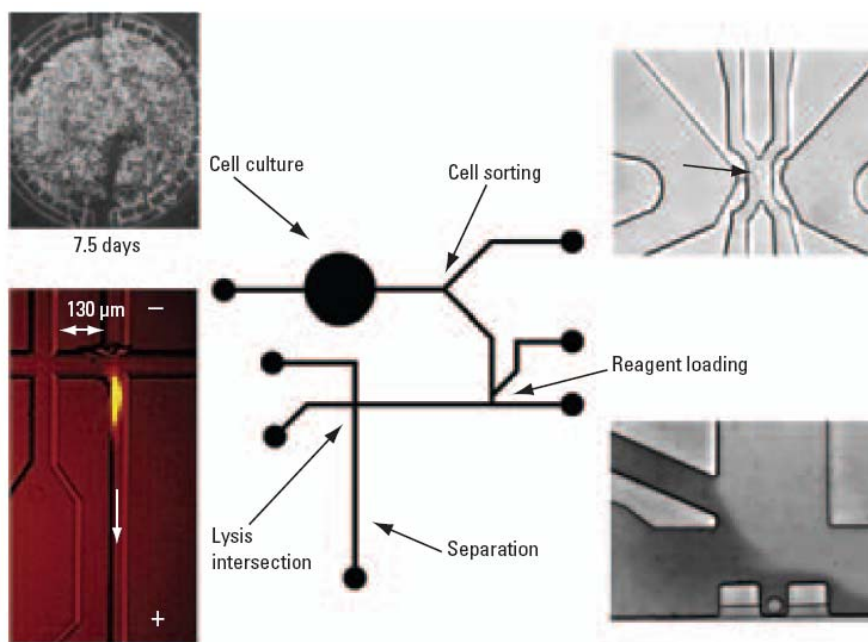


Figure 5.2: Schematic of an idealized single cell analysis device showing the multiple integrated functions. Reprinted with permission from [16].

5.2.3 Miniaturization and Integration of Supporting Instrumentation

The miniaturization of microfluidic devices has greatly advanced in the past decade, much of which is the result of progress in microfabrication techniques. Many research groups have demonstrated the use of devices with an extremely small footprint [24-26], however much of the supporting instrumentation used is still on the macroscale. To a large extent, the high voltage power supply (HVPS) used for application of the separation voltage and the potentiostat used for electrochemical measurements are very large and bulky. The miniaturization of these components is crucial for the realization of a truly self-contained micro total analysis system (μ -TAS).

Our lab has been working with Pinnacle Technology, Inc., which is a biomedical firm in Lawrence KS, to design and develop miniaturized instrumentation. One of the first collaborations sought to develop a miniaturized, wireless potentiostat for in-channel amperometric detection. Pinnacle Technologies had previously developed a wireless potentiostat used for *in vivo* voltammetry measurements of NTs in rats. One of our first tasks was to modify this potentiostat for use as an in-channel amperometric detector for microchip electrophoresis. To account for shifts in half wave potential, Pinnacle was able to modify the circuit design to allow the application of voltages as high as 2.0 V. Because the entire device is wireless and powered by a battery, it can be used as an electrically isolated or “floating” potentiostat for in-channel detection. Measuring only 2.5 cm by 3.0 cm, the finished device is not much larger than a standard U.S. quarter. This is much smaller than the

commonly used electrophoresis microchips which makes integration into a single unit possible. Some preliminary data that was taken using this device was presented in chapter 4. However, this potentiostat had a maximum sampling rate of only 5 Hz. Future improvements of this device should include faster data acquisition to improve the quality of the resulting data.

We are also working with Pinnacle Technologies to develop a miniaturized HVPS unit. Prototype versions of this device measure only 5 cm by 2.5 cm and are capable of delivering up to 2000 V. The end goal of this collaboration is the development of a project termed “lab on a sheep”. In the near future, the miniaturized potentiostat will be married with the HVPU as well as the electrophoresis microchip to create a self-contained, portable device (Fig 5.3). The final device will integrate microdialysis sampling, microchip electrophoresis, and EC detection. It will then be used to monitor NTs sampled through a microdialysis probe implanted in a sheep. Because the entire device must be placed on a sheep and run autonomously, the development of a small, portable, self-contained device is crucial for the success of the project. Not only will this improve upon the capabilities of our lab, but it will advance the field of μ -TAS as a whole.

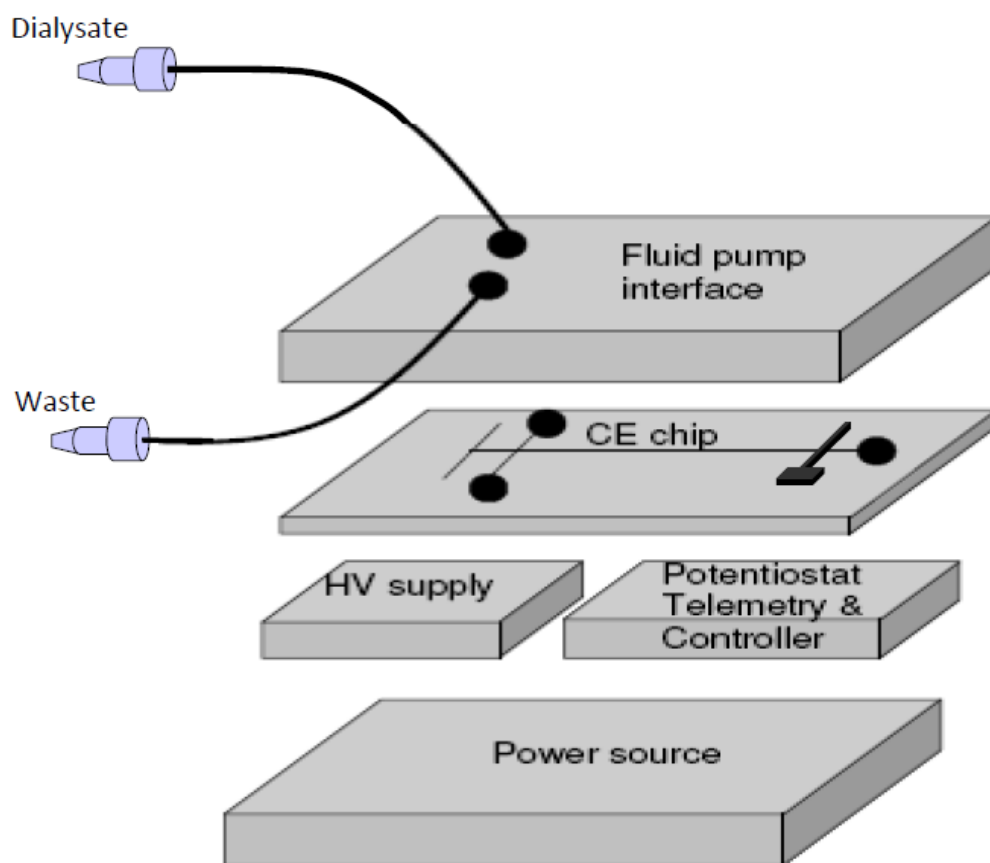


Figure 5.3: Proposed fully integrated μ -TAS device for on-line, on-animal, in vivo microdialysis sampling with in-channel EC detection. The device consists of miniaturized and integrated power source, HV power supply, potentiostat, microchip with integrated in-channel PPF electrode, and fluidic interface. When assembled, the entire device measures only 2.5" long, 1.5" wide, by 1.5" tall.

5.3 References

- [1] Vandaveer IV, W. R., Pasas-Farmer, S. A., Fischer, D. J., Frankenfeld, C. N., Lunte, S., M., *Electrophoresis* 2004, 25, 3528-3549.
- [2] Gawron, A. J., Martin, R. S., Lunte, S. M., *Electrophoresis* 2001, 22, 242-248.
- [3] Lacher, N. A., Lunte, S. M., Martin, R. S., *Analytical Chemistry* 2004, 76, 2482-2491.
- [4] Fischer, D. J., Vandaveer, W. R. I. V., Grigsby, R. J., Lunte, S. M., *Electroanalysis* 2005, 17, 1153-1159.
- [5] Noblitt, S. D., Henry, C. S., *Analytical Chemistry* 2008, 80, 7624-7630.
- [6] Pasas, S. A., Lacher, N. A., Davies, M. I., Lunte, S. M., *Electrophoresis* 2002, 23, 759-766.
- [7] Landers, J. P., Editor, *Capillary and Microchip Electrophoresis and Associated Microtechniques*, 2008.
- [8] Ramsey, J. D., Jacobson, S. C., Culbertson, C. T., Ramsey, J. M., *Analytical Chemistry* 2003, 75, 3758-3764.
- [9] Roman, G. T., McDaniel, K., Culbertson, C. T., *Analyst* 2006, 131, 194-201.
- [10] Roman, G. T., Carroll, S., McDaniel, K., Culbertson, C. T., *Electrophoresis* 2006, 27, 2933-2939.
- [11] Jacobson, S. C., Hergenroder, R., Koutny, L. B., Warmack, R. J., Ramsey, J. M., *Analytical Chemistry* 1994, 66, 1107-1113.
- [12] Zubritsky, E., *Analytical Chemistry* 2000, 72, 687A-690A.
- [13] Bowen, A. L., Martin, R. S., *Electrophoresis* 2009, 9999, NA.
- [14] Truog, W. E., *Expert Opinion on Pharmacotherapy* 2007, 8, 1505-1513.
- [15] Gibson, R. L., Berger, J. I., Redding, G. J., Standaert, T. A., Mayock, D. E., Truog, W. E., *Pediatric Research* 1994, 36, 776-783.
- [16] Price, A. K., Culbertson, C. T., *Analytical Chemistry* 2007, 79, 2614-2621.
- [17] West, J., Becker, M., Tombrink, S., Manz, A., *Analytical Chemistry* 2008, 80, 4403-4419.
- [18] Vickers, J. A., Henry, C. S., *Biological Applications of Microfluidics* 2008, 435-450.
- [19] Sato, K., Kitamori, T., *Handbook of Capillary and Microchip Electrophoresis and Associated Microtechniques (3rd Edition)* 2008, 1013-1019.
- [20] Suvorava, T., Kojda, G., *Biochimica et Biophysica Acta, Bioenergetics* 2009, 1787, 802-810.
- [21] Muller, G., Morawietz, H., *Antioxidants & Redox Signaling* 2009, 11, 1711-1731.
- [22] Radi, R., *Archives of Biochemistry and Biophysics* 2009, 484, 111-113.
- [23] Culbertson, C. T., *Methods Mol. Biol.* 2006, 339, 203-216.
- [24] Pai, R. S., Walsh, K. M., Crain, M. M., Roussel, T. J., Jr., Jackson, D. J., Baldwin, R. P., Keynton, R. S., Naber, J. F., *Analytical Chemistry* 2009, 81, 4762-4769.
- [25] Haerberle, S., Zengerle, R., *Lab on a Chip* 2007, 7, 1094-1110.

[26] Fercher, G., Smetana, W., Vellekoop, M. J., *Electrophoresis* 2009, 30, 2516-2522.

Chapter 6

Capillary Electrophoresis Methods for Protein Analysis

6.1 Introduction

During the past few decades, advances in molecular biology have provided tremendous insight into the structure, function, and interaction between immeasurable numbers of biologically relevant molecules. These interactions, which include the function and regulation of DNA, RNA, as well as protein expression, are critical to understanding the roles these biological systems play in health and human disease. By determining the nature and extent of these relationships, effective treatments for diseases including Alzheimer's, Huntington's, AIDS, and many forms of cancer may be developed more easily.

While researchers have a variety of methods for the analysis of proteins at their disposal, electrophoretic methods of analysis remain the most popular. Gel electrophoresis techniques such as polyacrylamide gel electrophoresis (PAGE), sodium dodecyl sulfate polyacrylamide gel electrophoresis (SDS-PAGE) and Western blot analysis are arguably the world's most widely utilized analysis methods for protein analysis [1]. Their popularity is due, in part, to the fact that these techniques are incredibly reliable, robust, and well characterized. The latter two techniques use SDS-PAGE for separation but differ in the method of detection. In both, cross-linked polyacrylamide gels separate denatured proteins according to the length of their polypeptide chain or their molecular weight (MW) [2]. In SDS-PAGE, protein samples are mixed with an excess of SDS and heated to 100 °C. This serves to denature the proteins and impart a uniform negative charge. Because SDS binds to proteins at a constant weight ratio of 1.4 g SDS to 1 g of protein, all protein species

have a negative charge, similar mass-to-charge ratios, and may then be separated by MW. Because small proteins can more easily traverse the porous gel matrix than large proteins, a sized-based migration is achieved with the electrophoretic mobilities of these proteins being a linear function of the logarithm of their MW [3-5].

While SDS-PAGE and Western blot analysis employ similar separation methods, visualization of the protein bands is achieved by different means. SDS-PAGE commonly utilizes either Coomassie Brilliant Blue or silver staining to allow visualization of the separated proteins; however, other detection methods such as fluorescence or chemiluminescence have been described [6-8]. Coomassie Brilliant Blue R-250, the most widely used protein stain, is an anionic dye which binds nonspecifically to denatured proteins. The dye can be incorporated into the bands of protein in the gel while simultaneously being fixed. Excess dye is then removed through a washing step and protein bands can be subsequently visualized. The limit of detection for Coomassie depends on the particular protein of interest. Typical LODs range from 50-100 ng, however LODs as low as 3 ng using bovine serum albumin (BSA) as a model protein have been reported.

An alternative to Coomassie is silver staining which was introduced by Switzer *et al.* in 1979. This technique remains very popular and is a very sensitive tool for protein visualization with a detection limit down to the 0.3 – 10 ng range [9]. Detection relies on the binding of silver ions to the amino acid side chains, primarily the sulfhydryl and carboxyl groups of the protein. Reduction of the silver ions to metallic silver results in the ability to visualize bands in the gel [10]. A comparative

analysis of the sensitivity of a variety of silver staining procedures has been described [11], however silver staining protocols can be divided into two general categories: silver amine or alkaline methods and silver nitrite or acidic methods. In general, silver amine or alkaline methods are more sensitive because of a lower background but require more extensive and time-consuming procedures. Staining methods utilizing acidic silver nitrate protocols are faster but are less sensitive. Each protocol has a distinct set of advantages and disadvantages regarding analysis time, sensitivity, and cost but are generally more sensitive than Coomassie staining.

While Coomassie and silver stains are the most popular, other methods of protein visualization do exist. Recently, Meier and co-workers detailed the development of a fluorescent prestain for use in SDS-PAGE [12]. The authors describe a fluorogenic amino-reactive label which has an absorbance maximum at 503 nm and emission at 602 nm [13]. Using a short 30 min prestain before separation, detection limits of 65, 62, 160, 182, and 314 pg were achieved for glutamate dehydrogenase (GDH), carbonic anhydrase (CA), bovine serum albumin (BSA), lactate dehydrogenase (LDH), and glycophosphorylase (GP) respectively. When an overnight prestain was investigated, these detection limits were reduced by more than half which resulted in LODs of 16, 31, 20, 45, and 109 pg, respectively.

As described earlier, Western blot analysis is similar to SDS-PAGE but differs in the manner of protein visualization. Once proteins have been separated by gel electrophoresis, the proteins are transferred to a membrane where they are probed using antibodies specific to the target protein [14-15]. By taking advantage of the

specificity of antibody-antigen binding, this additional step adds a very high degree of selectivity to the assay. The probing procedure can be performed in either one or two steps. Most often the probing process is performed in two steps due to the ease of producing secondary (2°) antibodies (Fig 6.1). This not only gives researchers additional flexibility when performing the assay, but it also provides a degree of signal amplification to yield better detection limits. Despite these benefits, a one step probing process can be advantageous. The addition of only one antibody reduces cost, reagent consumption, and time required for analysis. Recent advancements in recombinant technology have led to the production to a variety of high quality monoclonal antibodies and have resulted in the one step process becoming more popular. Depending on which procedure is employed, detection of the protein bands are performed through a reporter conjugated to the 1° or 2° antibody (one or two-step procedure, respectively). Many commonly used detection methods utilize enzyme reporters for colorimetric or chemiluminescent detection, radioisotopes for radioactive detection, or a fluorophore for fluorescent detection.

Although SDS-PAGE and Western blot analysis are among the most commonly used separation techniques for protein analysis, slab gel electrophoresis generally suffers from long analysis times and low efficiencies while being labor intensive and difficult to automate. An attractive alternative to these methods is capillary electrophoresis (CE). Since the first report by Jorgenson *et al.* in 1981 [16-18], capillary zone electrophoresis (CZE) has proven to be a powerful separation technique for the analysis of a variety of biologically relevant analytes. In addition,

the development of new analytical techniques has made the analysis of ever decreasing amounts of material possible [19-22]. In addition to CZE, many different variations of CE have been developed which include: micellar electrokinetic chromatography (MEKC), capillary gel electrophoresis (CGE), microchip electrophoresis (ME), two-dimensional electrophoresis (2-D CE), isoelectric focusing (IEF), and affinity capillary electrophoresis (ACE). Previous reviews of the analysis of proteins by CE are available [23-28], however this review will focus on the recent developments in the use of each of these electrophoretic techniques. In addition, specific examples will be provided which highlight the advantages of each technique.

6.2 Modes and Methods of Capillary Electrophoresis

6.2.1 Sample Preparation

6.2.1.1 Preconcentration

In many instances it is advantageous or even necessary to preconcentrate low-abundance analytes prior to analysis by CE. Regardless of the analysis technique, the ability to detect a given analyte is dictated by the concentration of material in the cross-sectional area of the capillary as it passes over the detector. For example, in ultraviolet (UV) detection, the absorbance of light (A) is directly proportional to three terms as given by the Beer-Lambert law (Eq. 6.1)

$$A = \epsilon bc \qquad \text{Eq. 6.1}$$

The molar absorptivity, ϵ , is an intrinsic property of the analyte, the second term, b , is the path length of the medium; in CE this term is small (usually 25 - 100 μm) and

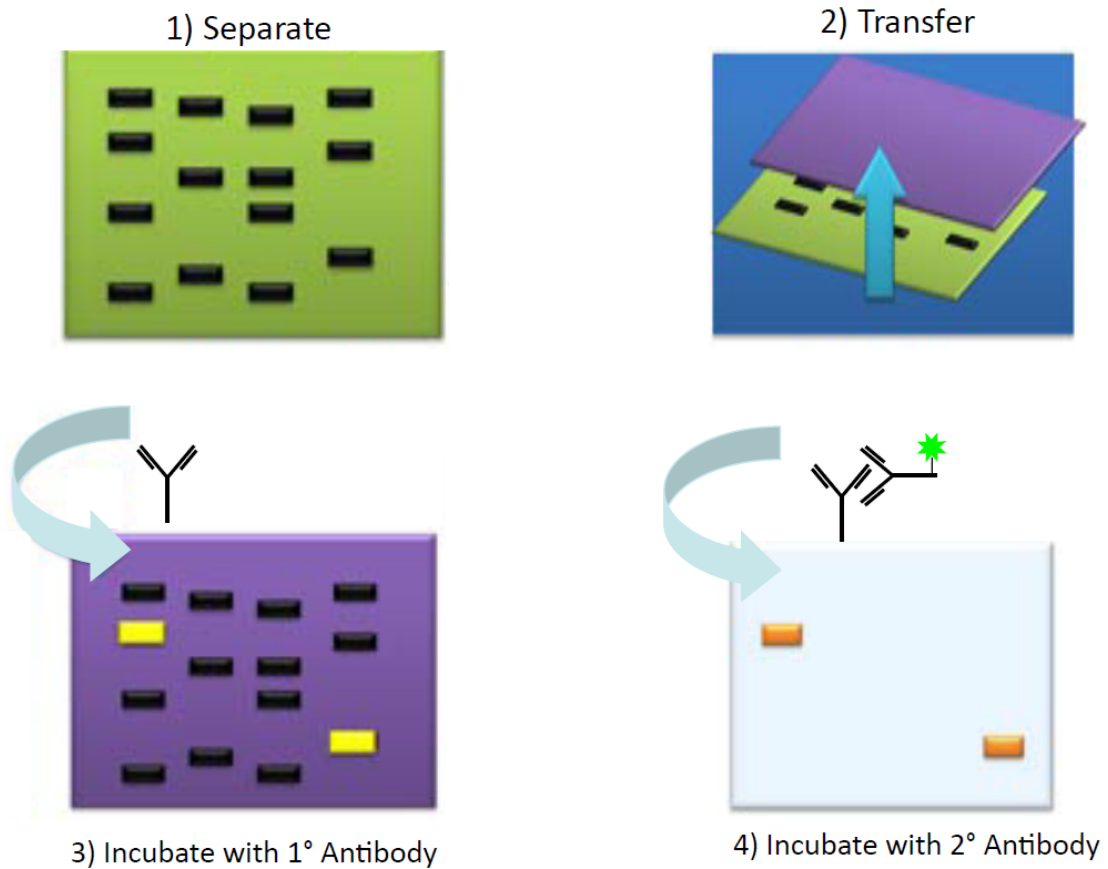


Figure 6.1: Depiction of the steps involved in a two-step probing protocol used for Western blot analysis. (1) Proteins are separated using SDS-PAGE, (2) proteins are transferred to a membrane, (3) a primary antibody is incubated with the membrane, (4) a secondary antibody with a conjugated reported is incubated with the membrane prior to detection.

cannot easily be changed without impacting the resolution of the separation process. Therefore, manipulation of the third term, c , the concentration of the analyte of interest, has been a topic of significant interest [29].

Various methods of either offline or online sample enrichment for proteins have been developed for use in CE and have been previously reviewed [29-32]. Wu and co-workers described the in-capillary preconcentration of proteins using a cellulose acetate (CA) coated porous joint [33]. The authors were able to preconcentrate proteins by applying a voltage between the inlet of the capillary and the porous CA joint. Preconcentration was achieved because the protein ions migrated to the porous joint but could not pass through it, while the buffer ions could pass easily through the joint. After preconcentrating, the separation voltage was applied across the two ends of the capillary and normal CE was carried out. Preconcentration factors of 65, 155, 705, and 800 were achieved for cytochrome *c*, lysozyme, ribonuclease, and chymotrypsinogen, respectively. A combination of field-amplified stacking (FAS) and non-uniform field CE was described by Yang and co-workers. Field-amplified stacking uses buffers with differing conductivities to create gradients in ionic conductivity (and therefore electric field) inside the capillary. Typically, a buffer of low conductivity is placed before a buffer of high conductivity. When the separation voltage is applied, non-uniform electromigration of analytes will cause a preconcentration effect at the interface of these two zones. Preconcentration factors as high as 30 were achieved for metoprolol and propranolol [34]. Lin *et al.* described an electric field gradient focusing (EFGF) technique for use in CE [35].

EFGF uses an electric field gradient and a hydrodynamic flow to form two counteracting forces to focus proteins in order of electrophoretic mobility. Focusing occurs at points where the protein electrophoretic migration velocities are equal and opposite to the hydrodynamic flow velocity. Using BSA as a model analyte, the authors were able to achieve a preconcentration factor as high as 15,000 which resulted in a concentration limit of detection as low as 30 pM even while using UV absorbance detection.

Analyte preconcentration methods have been developed for use in microchip electrophoresis as well. Several excellent reviews are available on this topic [36-37]. Xu and co-workers described a microchip gel electrophoresis (μ CGE) method with electrokinetic injection with transient isotachopheresis (termed electrokinetic supercharging, EKS), on a single channel chip. Using UV absorbance detection, the authors were able to reduce the lower limit of detectable concentration (LLDC) by a factor of 30-40 for phosphorylase b, albumin, ovalbumin, carbonic anhydrase, trypsin inhibitor, and α -lactalbumin achieving an average LLDC of 270 ng/mL. Ramsey and co-workers developed a multi-channel, glass microchip capable of preconcentrating fluorescently labeled ovalbumin by a factor of \sim 600 [38]. The proteins were concentrated using a porous silica membrane between adjacent microchannels which allowed the passage of buffer ions but excluded larger migrating analytes. Concentrated analytes were then injected in the separation channel for analysis where concentrations as low as 100 fM were detected.

In a novel approach, Wooley and co-workers developed a microchip with an incorporated phase-changing sacrificial material for interfacing microfluidics with ion-permeable membranes to create on-chip preconcentrators [39]. Imprinted microchannels in a poly(methyl methacrylate) (PMMA) substrate were filled with a liquid that solidifies at room temperature. Then, a methacrylate-based monomer solution is placed over the channel and polymerized to form a rigid semipermeable membrane. When the sacrificial liquid is melted and removed, the open channel interfaces with the polymer membrane. Electric field gradient focusing (EFGF) was used to enrich fluorescently labeled peptides by a factor >150 and R-phycoerythrin (R-PE) by a factor of ~10,000.

6.2.1.2 Derivatization

The sensitive detection of protein species in capillary and microchip electrophoresis typically involves the use of laser induced fluorescence (LIF) detection. While UV absorbance remains a popular detection method, the small path lengths prohibit the sensitive detection of low levels of analyte. Therefore, derivatization is typically necessary for sensitive LIF detection of protein species. Proteins can be labeled off-line or on-line using either covalent or noncovalent binding. While a multitude of fluorophores with a variety of derivatization chemistries exist, some of the most popular covalent derivatizing agents include FITC (fluorescein isothiocyanate) [40-41], BODIPY (boron-dipyrromethene) [42-44], 5-TAMRA (5-carboxytetramethylrhodamine) [45-46], and the Alexa Fluor family of dyes [22, 47-50].

Craig and co-workers recently described the development and use of a novel type of amino-reactive reagent [51]. The two dyes, Py-1 and Py-6, are fluorogenic dyes which consist of a pyrylium group attached to small aromatic moieties. Human serum albumin (HSA) was used as a test compound to determine analytical sensitivity when employing CE-LIF. After a 60 min labeling reaction in boric acid (BA), the Py-1 label produced a LOD of 6.5 ng/mL (98 pM) while the Py-6 label produced a LOD of 1.2 ng/mL (18 pM). The utility of these compounds as fluorogenic labels was demonstrated through the separation of Py-6 labeled HSA, lipase, myoglobin, and immunoglobulin G (IgG). Not only did these novel fluorogenic reagents prove to be sensitive and easy to use, the reaction chemistry does not change the overall charge of the protein. Therefore if incomplete labeling of lysine residues occurs, the formation of a series of products for a given protein will not be observed in the electropherogram.

Another fluorogenic derivatization agent that is gaining popularity for protein analysis is naphthalene-2,3-dicarboxaldehyde (NDA). Originally described for the derivatization of amino acids and small peptides by Stobaugh *et al.*, fluorescent 1-cyanobenz(f)isoindole (CBI) derivatives are formed through the reaction of NDA and cyanide ion (CN⁻) in the presence of primary amines [52-54]. More recently, Chiu and co-workers demonstrated its use for the derivatization and detection of several proteins using CE with light-emitting diode induced fluorescence detection (LEDIF) [55]. The authors employed a sieving matrix which allowed for the stacking of the NDA derivatized proteins based on differences in viscosity and electric field. The

analysis was completed in less than three minutes and resulted in LODs of 2.41, 0.59, 0.61, and 4.22 nM for trypsin inhibitor, HSA, β -lactoglobulin, and lysozyme, respectively.

An attractive alternative to covalent derivatization involves the use of noncovalent dyes. In many cases the use of these types of dyes helps to avoid the complications associated with covalent modification while still providing the benefits of fluorescence detection. Landers and co-workers have demonstrated the use of a fluorescent dye that interacts in a hydrophobic nature with protein-SDS complexes [56]. Importantly, this dye fluoresces significantly only when bound to SDS-protein complexes but not when bound to SDS micelles. In their first report, the authors showed that the commercially available fluorogenic dye NanoOrange could simply be added to the separation buffer prior to performing size-based electrophoresis. As the denatured protein-SDS complexes migrate through the capillary, the complexes were dynamically labeled on-column for subsequent LIF detection. This method was shown to be capable of separating eight protein size standards in less than 13 min. The technique was then transferred to the microchip format where the separation of all eight proteins was accomplished in less than 4 min. However, the detection limits were comparable to those using UV detection (1×10^{-5} M). The authors continued to optimize the separation conditions, and in a later report attributed the poor sensitivity to a high background signal caused by the separation buffer that was used [57]. By optimizing the separation buffer and using an excess of dye for labeling, sensitivity was improved by at least 2 orders of magnitude with a LOD of 500 ng/mL for BSA.

6.2.2 Detection Methods

6.2.2.1 Ultraviolet Absorbance

The predominant detection method for use in CE is UV absorbance detection. UV detection is a universal detection which is incredibly easy to perform and robust. However, one of UV detection's principal limitations is the rather poor concentration detection limits achievable. Stemming from the small path lengths of fused silica capillaries, these limits typically range from 10^{-5} to 10^{-7} M depending on the analyte [58]. In an effort to improve detection limits by increasing the optical path length, Z-shape [59-62] and bubble-shape [63-65] flow cell configurations have been developed. These however, are expensive, fragile, and often result in poor separation efficiencies.

Rather than trying to increase sensitivity by increasing the optical path, many researchers have instead chosen to develop grid or area imaging UV detectors [66-67]. Urban and co-workers describe the development of a UV area detector capable of imaging multiple windows in a looped capillary [68]. When applied to an electrophoretically mediated microanalysis assay (EMMA) to determine substrate specificity of tyramine oxidase, this detection method provided the authors with more information than single point detection and allowed the observation of reaction products in real time.

6.2.2.2 Laser Induced Fluorescence

LIF is the most sensitive detection method for low abundance proteins, providing the analyte of interest has been labeled with an appropriate fluorophore. Several excellent reviews are available which discuss the details of experimental setup and fundamentals of LIF detection [69-72]. Recently, Aspinwall and co-workers reported the utilization of a high power UV light-emitting diode for fluorescence detection (UV-LED-IF) in CE [73]. The 365 nm UV-LED was used for the detection of a number of compounds including: neurotransmitters (NTs), amino acids (AAs), peptides, and proteins that had been derivatized with o-phthalaldehyde/ β -mercaptoethanol (OPA/ β -ME). Native fluorescence detection of several polyaromatic hydrocarbons (PAHs) were also accomplished with detection limits ranging from 10 nM to 1.3 μ M. Detection limits of 28 and 47 nM were achieved for derivatized BSA and myoglobin, respectively in less than 2 min.

Most LIF systems employ a photomultiplier tube (PMT) to convert photons into current for the detection of emitted light. These detectors are extremely sensitive to ultraviolet and visible wavelengths and are capable of multiplying incident light by as much as 100 million times. However, PMTs are not very sensitive to the red and near-infrared wavelengths. Another type of detector that is becoming increasingly popular is the avalanche photodiode array detector. These detectors are a semiconducting analog to PMTs which use the photoelectric effect to convert photons into current. In addition, they are sensitive to a broader range of incident light and are

capable of single photon detection. Therefore, extremely low limits of detection and high sensitivity can result when they are used as detectors for CE-LIF.

Dovich and co-workers recently described the evaluation of the fluorogenic reagent Chromeo P465 for the analysis of proteins [74]. This reagent was used to label the model compounds ovalbumin, α -lactalbumin, and α -chymotrypsinogen. Sub-micellar SDS buffers were used for separation while detection was performed using a 473 nm laser for excitation and an avalanche photodiode (APD) detector. While the authors concluded that Chromeo P465 was not an optimal fluorescent reagent, concentration and mass detection limits for α -lactalbumin were found to be 24 pM and 15 zmol, respectively.

In a subsequent paper, Dovich's group investigated the use of Chromeo P540 dye for the analysis of protein standards and protein homogenates from Barrett's esophagus cells [75]. Isoelectric focusing (IEF) was used for separation and a 532 nm diode-pumped solid-state laser with an APD were used for LIF detection. To help reduce the background signal, ampholytes were photobleached using high-power photodiodes. The authors report that this reduced the noise in the blank by an order of magnitude. A concentration LOD of 520 ± 25 fM and a mass LOD of 150 ± 15 zmol was achieved for the model compound β -lactoglobulin. These detection limits were due to the excellent quantum efficiency of the fluorophore, but more importantly to the extreme sensitivity of the APD detector.

6.2.2.3 Mass Spectrometry

The large scale investigation of protein structure and function has led to the exponential growth in the use of mass spectrometry (MS) for proteomics research. In the early days of CE-MS, many believed that the separation power of MS would be sufficient for the complete analysis of proteins [28]. This prediction has been proven to be unfounded and the use of CE as a powerful separation technique prior to analysis by MS continues to be of great interest. Soft ionization techniques such as electrospray ionization (ESI) and matrix-assisted laser desorption ionization (MALDI) are commonly used in combination with CE. The use of both ESI [76-78] and MALDI [79-82] with CE has been reviewed previously [83].

Typically a sheath flow interface is used to deliver analytes to the MS interface. Mao and co-workers described the development of a sheath flow nanoelectrospray (nES) for microchip electrophoresis coupled to MS [84]. The interface consisted of a glass microchip interfaced with a fused silica capillary. This capillary was connected to a stainless steel tube using a mixing tee and was responsible for delivering the sheath flow liquid. The flow rate of the sheath liquid was optimized for the detection of several glycopeptides and glycoproteins. The authors achieved a detection limit between 2 and 5 fM for the peptide YGGFLR in less than 2 min.

While a sheath flow is generally used, a sheathless interface can be used if the EOF is sufficient for analyte delivery [85-87]. Several sheathless electrosprays have been developed for glass [88] and polymer microchips [89-90]. As seen in Figure

6.2, Ramsey and co-workers described the fabrication and characterization of a fully integrated glass microfluidic device for performing high-efficiency microchip electrophoresis coupled to ESI-MS [91]. The device utilized the corner of the glass microchip as the electrospray emitter (6.2 C). Because the ESI is performed directly from the corner of the rectangular chip, the use of external pressure sources or the insertion of capillary spray tips was not necessary.

The performance of the chip was evaluated for the separation and detection of the peptides methionine-enkephalin, leucine-enkephalin, angiotensin II, neurotensin, bradykinin, and thymopentin using a 20.5 cm long channel. All peptides but neurotensin and bradykinin were baseline resolved in less than 3 min, which equated to an efficiency of approximately 1,000,000 plates/m. Because only 2.5 pg of each peptide was injected for analysis, the microchip-MS device proved to be highly sensitive as well. The ability of the device to separate and detect proteins was also investigated. A mixture of horse skeletal myoglobin, horse heart cytochrome c, and bovine pancreas ribonuclease A (each at a concentration of 200 $\mu\text{g/mL}$) was separated and detected in less than 4.5 min. It was determined that the separation efficiency of each protein peak was greater than 280,000 theoretical plates which equated to ~ 1.3 million plates/m.

6.2.3 Methods of Surface Modification

While traditional capillary electrophoresis is performed in fused silica glass capillaries, the materials used to make microchips are quite varied. Glass and silica substrates were used to fabricate the earliest microchip devices [92-94], however

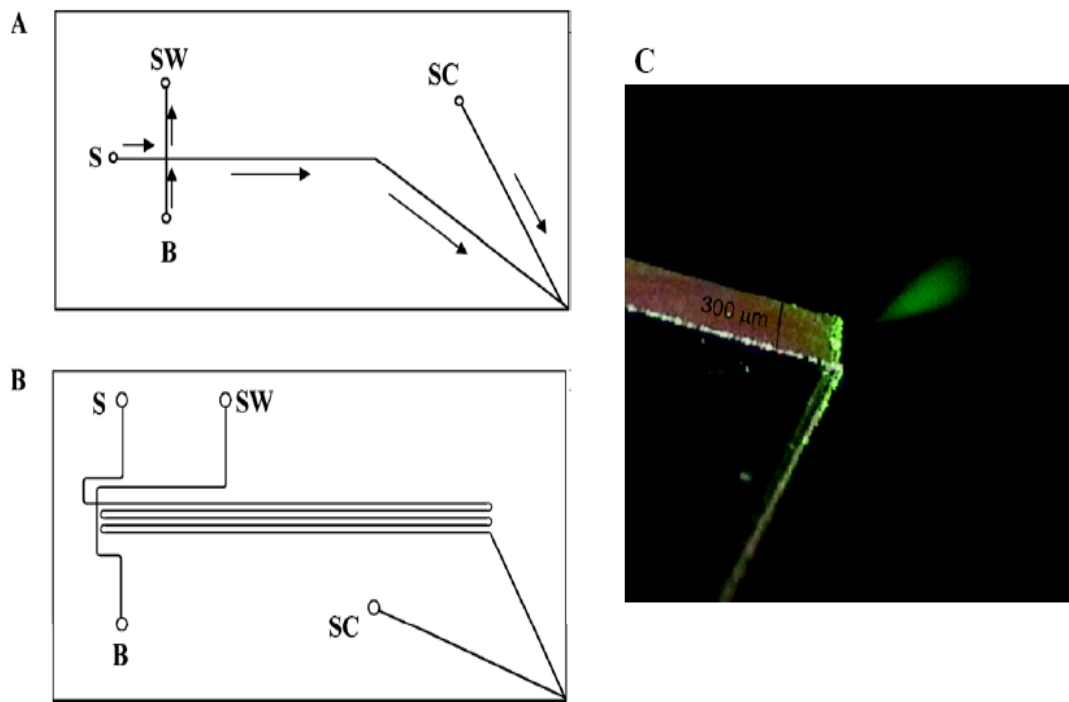


Figure 6.2: Schematic diagrams of the short-channel (A) and the long-channel (B) CE-ESI-MS chips. The length of the separation channel (measured from the injection cross to the outlet) was 4.7 cm for the short-channel chip and 20.5 cm for the long-channel chip. For both chips, the channels were all 75 μm wide at full width and 10 μm deep. The turns in the serpentine pattern of the long-channel chip were asymmetrically tapered to reduce band broadening. The reservoirs are labeled S (sample), B (buffer), SW (sample waste), and SC (side channel). The direction of electroosmotic fluid flow is indicated by the arrows in (A); (C) Image of the electrospray plume generated from the corner of a CE-ESI-MS chip acquired with a CCD camera. The plume was illuminated with a 3-mW, diode-pumped, solid-state laser. The liquid being sprayed was 50/50 (v/v) methanol/water with 0.2% acetic acid. The voltages applied to the microchip reservoirs raised the potential at the spray tip to 3.5 kV above that of the mass spectrometer inlet and caused the liquid to be pumped out of the chip at a flow rate of 40 nL/min. Reprinted with permission from [91].

various polymeric materials such as polydimethylsiloxane (PDMS) [95-96], poly(methyl methacrylate) (PMMA) [97-98], polystyrene (PS) [99-100], polycarbonate (PC) [101-102], polyethylene terephthalate (PET/PETG) [103-104], polyimide (PI) [105-106], polyester [107-108], and polyurethane methacrylate (PUMA) [109-110]. Unfortunately, analyte adsorption is typically observed regardless of the material used. This is especially true for large biomolecules which can interact through a combination of electrostatic and hydrophobic interactions. Not only is separation efficiency diminished but a loss of analyte is observed.

To prevent these adverse effects, the substrate surface of the separation device can be treated prior to analysis. Both dynamic and static surface modification strategies are commonly employed. Dynamic coatings typically consist of neutral polymers or ionic surfactants which are most often added to the background electrolyte (BGE). While these types of modifications are easy to apply, they do not eliminate surface adsorptions completely. Static coatings are much better at eliminating analyte adsorption; however because they are typically covalently attached to the surface, their preparation is much more time consuming. Therefore, each technique has a unique set of advantages, disadvantages, and application specific utility.

6.2.3.1 Dynamic Wall Coating

A variety of dynamic coatings have been used for capillary and microchip electrophoresis in an effort to modify the EOF and/or reduce analyte adsorption.

Some of these include: aliphatic polyamines [111-112], polyelectrolyte multilayers (PEMS) [113], phospholipid bilayer coatings [114], barium borate [115], self-assembled monolayers [116-117], polymers [118-121], successive multiple ionic-polymer layers (SMIL) [122], and ionic surfactant coatings [96, 123-128]. Dynamic modification of the capillary or microchip electrophoresis wall using ionic surfactants is by far the most popular method of reducing analyte adsorption. Not only are the reagents inexpensive and readily available but they can simply be incorporated into the separation buffer prior to analysis. In addition, these surfactants can be added in concentrations above or below the critical micelle concentration (CMC) to affect the separation mechanism (as in MEKC) [129]. Furthermore, the use of cationic surfactants such as dodecyl trimethylammonium bromide (DTAB) or cetyl trimethylammonium bromide (CTAB) can effectively reverse the EOF in both glass and polymeric devices [130-131].

Recently, Wu and co-workers described the use of a polyvinylamine compound to modify a capillary for CE-MS analysis [132]. Lupamin, a high molecular weight linear polyvinylamine (PVAm) polymer was used for modification. The capillaries were flushed with a solution of Lupamin (1%) in DDH₂O for 6 hours, followed by washing for 20 min with DDH₂O. This polymer physically adsorbed to the inner wall by strong electrostatic interaction and formed an entangled positively charged layer on the surface. Not only did the authors report a highly stable coating that was able to reverse and stabilize the EOF, peak shape and separation efficiency were also improved for the separation of several basic proteins.

The use of n-dodecyl- β -D-maltoside (DDM) in combination with SDS to suppress adhesion and enhance protein separation in PDMS microchips was recently reported by Zare *et al.* [133]. The effects of this dynamic coating on the EOF and separation of several proteins were investigated. The separation of the immunocomplexes between the mouse monoclonal anti-FLAG M1 antibody (M1) and the transmembrane protein, β_2 adrenergic receptor (β_2 AR) was optimized. It is known that DDM and SDS form negatively charged mixed micelles which can be used for MEKC. Furthermore, the low CMC value of these mixed micelles allows the use of SDS at non-denaturing concentrations and allows the analysis of proteins in their native state. This aspect was utilized for the separation of photosynthetic protein-chromophore complexes derived from *Synechococcus* cells without dissociation or denaturation.

Mohamadi and co-workers have described the combination of methylcellulose (MC) and polysorbate 20 (PS-20) for the separation of proteins using non-denaturing electrophoresis in PMMA microchips [134]. The concentrations of both modifiers were investigated in relation to their effects on EOF, electrophoretic mobility, and analyte adsorption. It was determined that a minimum concentration of 0.005% MC and 0.01 % PS-20 was necessary for successful separation of FITC-labeled BSA, trypsin inhibitor, and amyloglucosidase. At concentrations above 0.02% PS- 20 the electrophoresis was prone to failure.

6.2.3.2 Static Wall Coating

A variety of covalent surface modifications have been reported for capillary and microchip electrophoresis and have been reviewed recently [135]. Because covalent modifications often begin with the formation of a reactive wall surface, the modification strategy is unique to the particular type of substrate material being used. The modification of fused silica capillaries or glass microchips typically exploit silane chemistry or the strong physical interactions between compounds such as poly(ethylene oxide) PEO, poly(ethylene glycol) PEG, polyacrylamide (PAAm), or poly(vinyl alcohol) PVP [136-141].

Formation of reactive surfaces on PDMS often begins with exposure to plasma oxidation, corona discharge, or UV light [129, 142]. Once the PDMS has been activated it can then be exposed to alternate functionalities either using silanization [143-145], atom-transfer radical polymerization for modification by PAAm [146-147], or radiation-induced graft polymerization for modification by a variety of acrylic acid derivatives [148-150]. An alternate strategy to produce PEG-modified PDMS microchips was recently described by Lee *et al.* [151]. Instead of modifying the PDMS surface after fabricating the PDMS substrate, the authors chose to modify the PDMS mixture itself. PDMS, PEG, and methyl methacrylate (MMA) were mixed, cast against a Si wafer, and cured using heat and UV exposure. The authors observed dramatic differences in separation quality, EOF, reproducibility, and resistance to protein adsorption when the ratios of starting materials were varied.

Investigations of permanent surface modification techniques for PMMA substrates have not received nearly the attention that PDMS materials have. This may be due to the challenging microfabrication procedures required for rigid materials such as PMMA or simply due to the fact that it is a less popular substrate material than PDMS. Henry and co-workers described the modification of PMMA chips involving an aminolysis reaction [152]. Ethylenediamine and propylenediamine were mixed with n-butyl lithium to produce very reactive intermediates (i.e., n-lithiodiaminoethane and n-lithiodiaminopropane). These intermediates were then uniformly cast on a PMMA surface which had been cleaned with isopropyl alcohol. After a short incubation period the reaction was quenched with DDIH_2O , leaving layer of amine groups on the surface of the PMMA substrate.

Zangmeister and Tarlov have described the use of a UV/ozone modification strategy for PMMA. Pretreatment with UV/ozone, allows the reaction between the polymer and 3-methacryloxypropyltrimethoxysilane which can then be grafted on the surface. The authors reported a dramatic decrease in contact angle measurements and an increase of ~ 2.5 fold in device lifetime. Lee *et al.* have described an atom-transfer radical polymerization reaction to graft PEG on the surface of PMMA chips [153]. This procedure resulted in an increase of column efficiency and reproducibility of migration time of approximately 1 order of magnitude.

Wang and co-workers described the modification of PMMA substrates through a bulk modification process [154]. In this process, the primary monomer (MMA) was mixed with a chain modifier and a UV photoinitiator prior to fabrication.

After exposure to UV radiation to initiate polymerization, the solution was poured into a mold containing the desired features and allowed to solidify.

6.2.4 Capillary Zone Electrophoresis

The use of electrophoresis in open tubes as a separation technique was first described by Tiselius in 1937 [155-157]. He determined that sample components migrated in a direction and rate determined by their charge and mobility in the presence of an electric field. His work in this area of separation science earned him the Nobel Prize in chemistry in 1948. One of the major limitations to this type of electrophoresis in large-bore open tubes stemmed from thermal diffusion and convection caused by Joule heating. The field of capillary electrophoresis was revolutionized by Jorgenson *et al.*, who first described the use of small fused silica capillaries (25 - 75 μm internal diameter) which limited these effects [17-18]. His work helped to better define many of the fundamental aspects of CZE such as EOF, analyte migration velocity, separation efficiency (Eq. 6.2), and resolution (Eq. 6.3).

In CZE, the number of theoretical plates (N) is directly proportional to the electrophoretic mobility (μ_{ep}) of the analyte and the applied voltage (V) while being inversely proportional to the diffusion coefficient (D) of the analyte.

$$N = \frac{\mu_{\text{ep}}V}{2D} \quad \text{Eq. 6.2}$$

The resolution (R_s) between two species is proportional to the difference in electrophoretic mobility of two analytes ($\Delta\mu_{\text{ep}}$) and the square root of the number of

theoretical plates (N) while being inversely proportional to the electrophoretic mobility (μ_{ep}) of the analyte and the electroosmotic flow (μ_{eof}).

$$R_s = \frac{1}{4} \left(\frac{\Delta\mu_{ep}\sqrt{N}}{\mu_{ep} + \mu_{eof}} \right) \quad \text{Eq. 6.3}$$

Since these initial reports, capillary zone electrophoresis (CZE) has become the most widely utilized CE mode due to its versatility and simplicity of operation. Because the capillary is filled only with a buffer or BGE, it is also the most fundamentally simple form of CE. Separation occurs because analytes will migrate at different velocities in the presence of an electric field. The combination of the electrophoretic mobility of the analyte and the electroosmotic flow (EOF) generated inside the capillary provide efficient separations of both anionic and cationic analytes based on their mass-to-charge ratio. Neutral analytes are not influenced by the electric field and migrate with the EOF.

CZE has been utilized for a variety of applications which include the analysis of ions [98, 158], small molecules [20, 59-60], DNA [95, 105], amino acids [73, 159-160], peptides [69, 78], and proteins [27-28, 44, 136]. From equation 6.2, the popularity of CZE for the separation of macromolecules and proteins is evident. This equation shows that large analytes such as DNA and proteins, which have small diffusion coefficients (10^{-10} - 10^{-12} m^2s^{-1}), will exhibit less dispersion than small molecules ($\sim 10^{-9}$ m^2s^{-1}) and will result in more efficient separations. However, the separation of closely related, or highly basic proteins can present a problem. From

equation 6.3, it follows that maximum resolution is achieved when the electrophoretic and electroosmotic mobilities are similar in magnitude but opposite in sign. Unless two closely related proteins have vastly different electrophoretic mobilities, resolution will suffer. Therefore, CZE can be very effective for the separation of many different proteins, providing they are not closely related in charge, size, or molecular weight. In these cases, the selectivity (the relative order of migration) of the separation can be influenced to improve resolution. In CZE, selectivity is most easily changed through modifications of the separation buffer. Factors such as buffer type, pH, ionic strength, or the use of additives can dramatically influence resolution.

A specific example of how changes in the BGE can influence the resolution between closely related proteins is illustrated in the following section. Calmodulin (CaM) is a calcium binding protein expressed in all eukaryotic cells, but is found in the highest abundance in the brain [161-162]. It is a multifunctional protein that is involved in neuronal development, synaptic plasticity, learning and memory, as well as intercellular communication and regulation [163-168]. Since CaM has been target of chemotherapeutic drugs in the past [169-170], our lab sought the development of a CaM-based CE assay for the detection of cancer biomarkers.

Preliminary investigations involved the analysis of a sample of T34C CaM developed in the lab of Dr. Carey Johnson. Figure 6.3 shows the electropherogram of a 1 mg/mL sample analyzed by CZE and detected at 214 nm using a 25 mM boric acid (BA) pH 9.2 separation buffer. Rather than obtaining a single peak for the purified sample, multiple unresolved peaks were observed. In an effort to increase

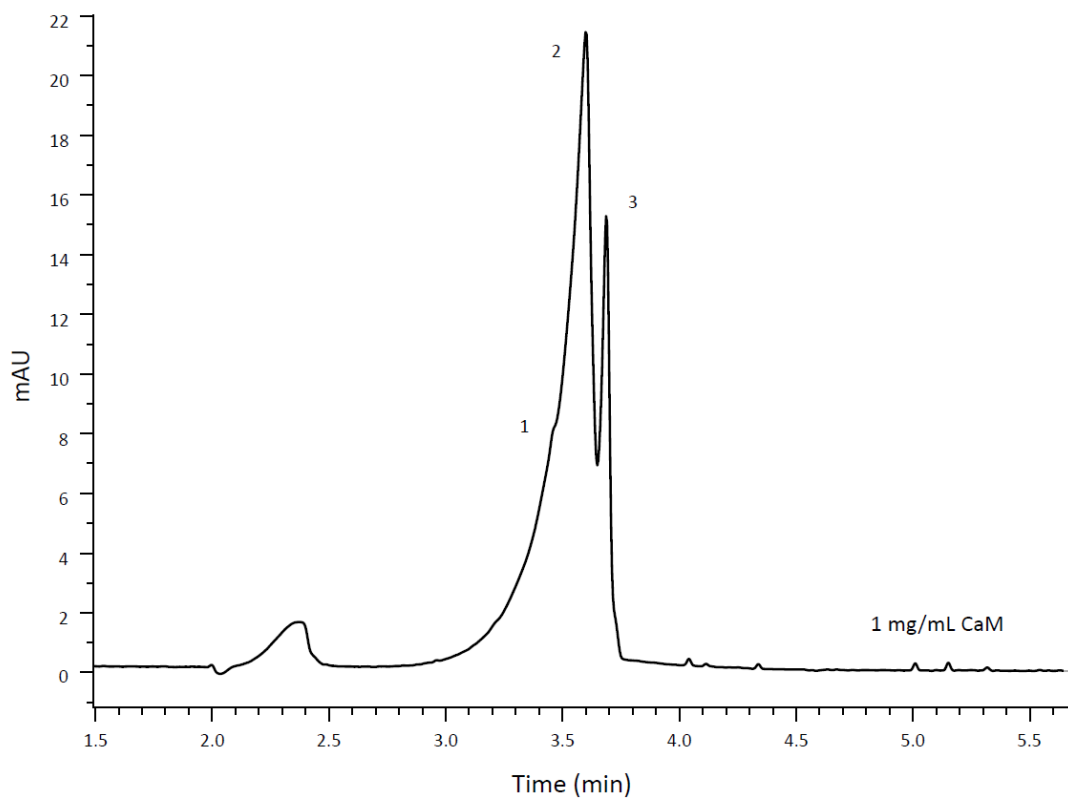


Figure 6.3: Separation of: 1.0 mg/mL calmodulin (CaM) by CZE with UV detection at 214 nm; Separation conditions: 25 mM boric acid, pH 9.2, 500 V/cm, 5.0 s injection at 0.5 psi.

the resolution between these species, a variety of different separation buffers were investigated. A 10 mM phosphate buffer pH 7.5 (Fig 6.4) and a 10 mM Tris buffer with 1 mM Ca^{2+} pH 7.5 (Fig 6.5) was examined for the separation of a variety of CaM concentrations. It can be seen that the use of the phosphate buffer slightly improved the resolution between the co-migrating analytes. However, baseline resolution was achieved with the tris buffer. Tris-based buffers are known to reduce the EOF in CZE which not only resulted in better resolution but increased migration times as well.

Although baseline resolution of these three species was achieved, the presence of three species was an unanticipated result. This protein sample had been purified prior to analysis through hydrophobic interaction chromatography (HIC) and analysis by MALDI had confirmed the presence of a single protein (data not shown). It was hypothesized that this CaM cysteine mutant was undergoing oxidation to form a dimeric species. To investigate this theory, a mixture of 0.25 mg/mL CaM and 0.01% (v/v) hydrogen peroxide in 10 mM Tris, 1 mM Ca^{2+} pH 7.5 was prepared and immediately analyzed by CZE. This solution was allowed to react while injections were performed every 30 min thereafter.

The results of the oxidation study can be seen in Figure 6.6. It was observed that the first peak in the electropherogram had completely disappeared and that the electropherograms of the oxidized samples remain unchanged between 30 and 60 min. These results indicate that peak number one represents the monomeric form of CaM while peak number 2 represents the formation of CaM dimers through disulfide

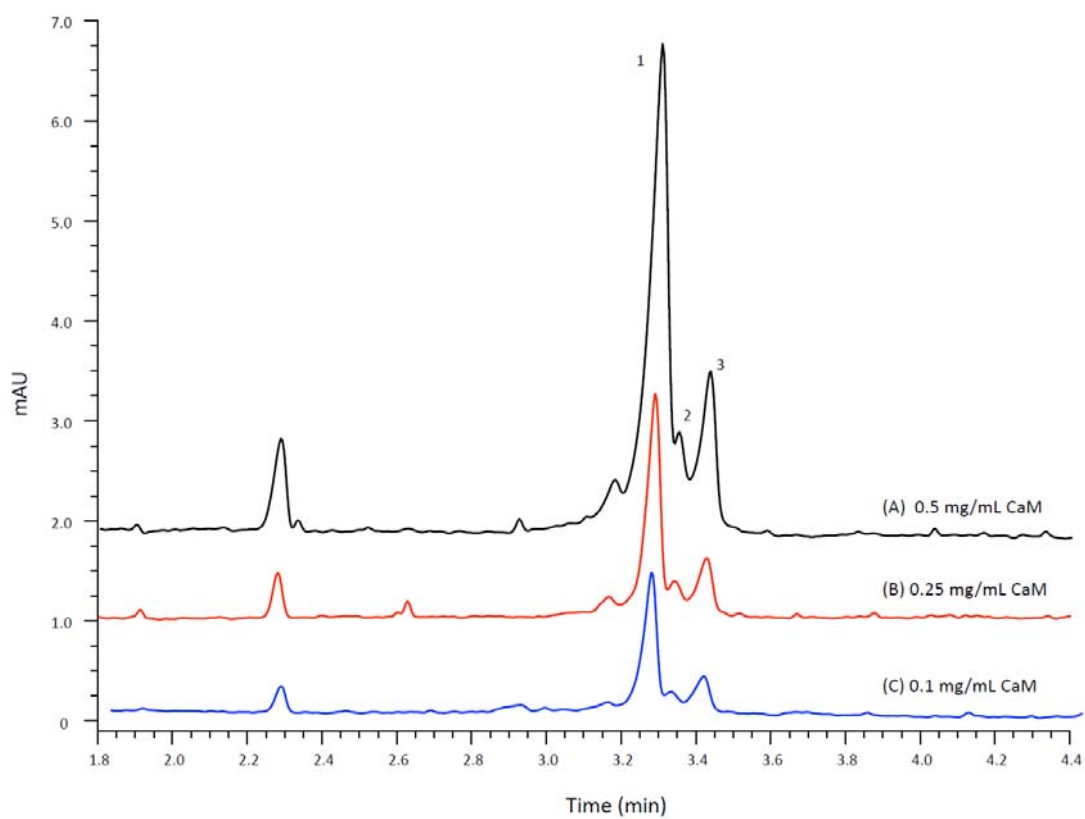


Figure 6.4: Separation of: (A) 0.5 mg/mL calmodulin (CaM); (B) 0.25 mg/mL CaM; (B) 0.10 mg/mL CaM by CZE with UV detection at 214 nm; Separation conditions: 10 mM phosphate, pH 7.5, 500 V/cm, 5.0 s injection at 0.5 psi.

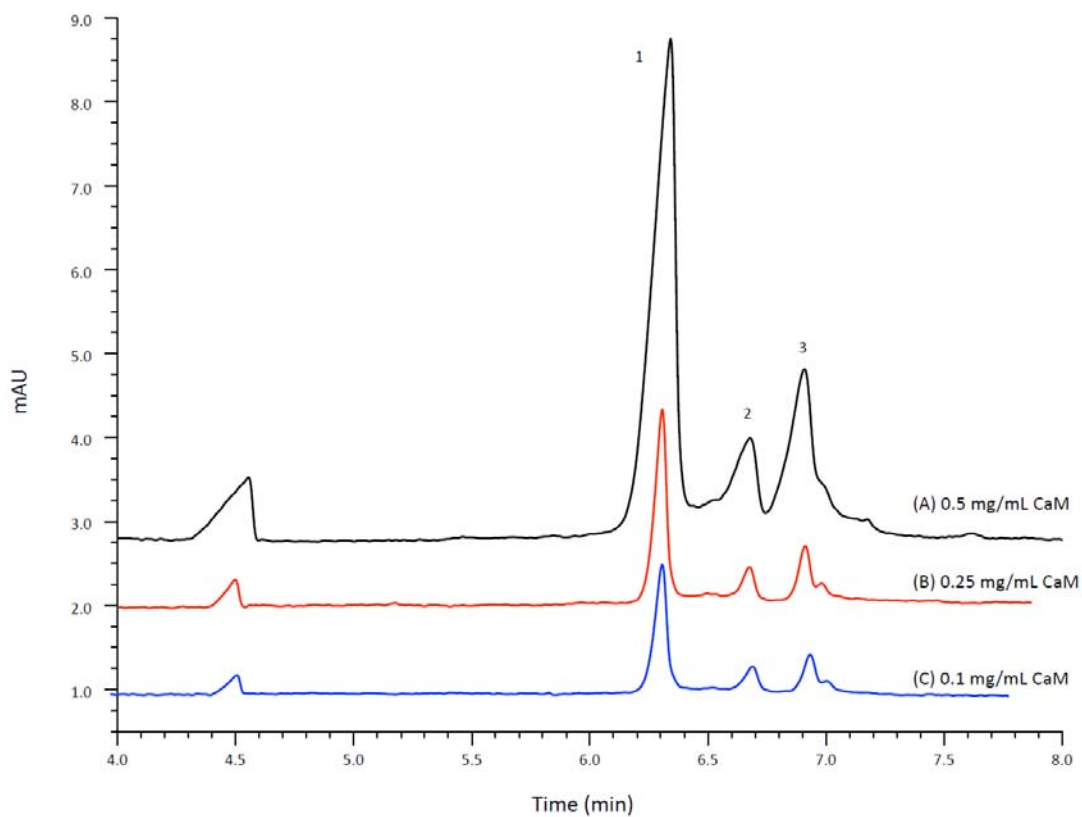


Figure 6.5: Separation of: (A) 0.5 mg/mL calmodulin (CaM); (B) 0.25 mg/mL CaM; (C) 0.10 mg/mL CaM by CZE with UV detection at 214 nm; Separation conditions: 10 mM tris, 1.0 mM CaCl₂ pH 7.5, 500 V/cm, 5.0 s injection at 0.5 psi.

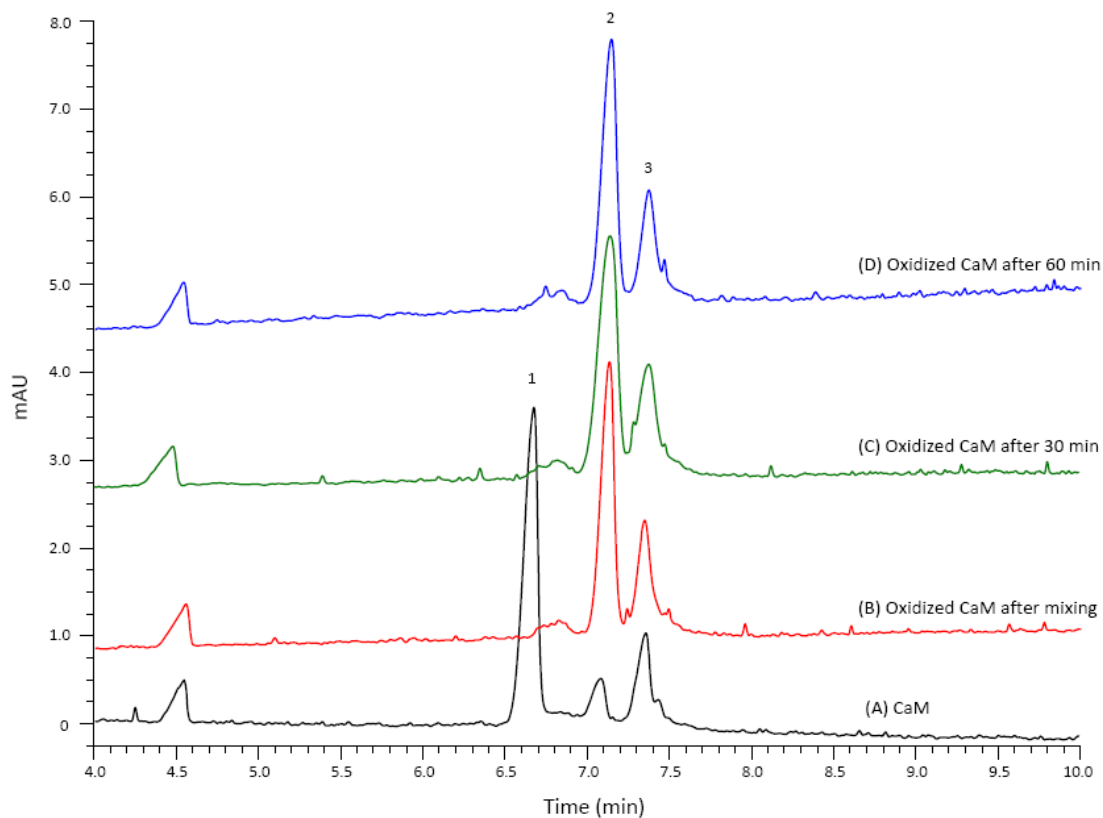


Figure 6.6: Time course oxidation study utilizing T34C CaM. (A) 0.25 mg/mL calmodulin (CaM); (B) 0.25 mg/mL CaM with 0.01% (v/v) H₂O₂ analyzed immediately after mixing; (C) 0.25 mg/mL CaM with 0.01% (v/v) H₂O₂ analyzed 30 min after mixing; (D) 0.25 mg/mL CaM with 0.01% (v/v) H₂O₂ analyzed 60 min after mixing by CZE with UV detection at 214 nm; Peak assignments are as follows: (1) CaM monomer, (2) CaM dimer, (3) CaM aggregate. Separation conditions: 10 mM tris, 1.0 mM CaCl₂ pH 7.5, 500 V/cm, 5.0 s injection at 0.5 psi.

linkages. The shape of peak 3 did not change throughout the experiment so the identity of this species was not evident; however, it was hypothesized that it represented an aggregated form of CaM. Because the formation of disulfide linkages is reversible, an excess of the reducing agent 2-mercaptoethanol (β -ME) was added to the sample and analyzed. Figure 6.7 shows the results from this experiment which produced a single peak corresponding to the reduced form of CaM.

Although CZE has been routinely used for the separation of proteins, the results obtained from this experiment illustrate the versatility of the method. As mentioned before, analytes are separated based on their mass-to-charge ratio. However, the mass-to-charge ratio of CaM monomer and the CaM homodimer are identical. The mass of the protein doubled as did the total charge, so the ratio remained constant. Separation of the monomer and dimer was only achieved because of differences in hydrodynamic radius. The physical size of the dimeric species was twice as large which reduced its electrophoretic mobility enough to result in baseline separation. In addition, separation was achieved only after an appropriate separation buffer was selected. Taken collectively, these factors illustrate the simplicity, versatility, and capability of CZE as a separation method.

6.2.5 Micellar Electrokinetic Chromatography

An alternate form of capillary electrophoresis, micellar electrokinetic chromatography (MEKC), is a hybrid of CE and chromatography. Originally described by Terabe in 1984, this separation mode has become widely popular [171-172]. Not only is it easily employed, it is the only electrophoretic technique capable

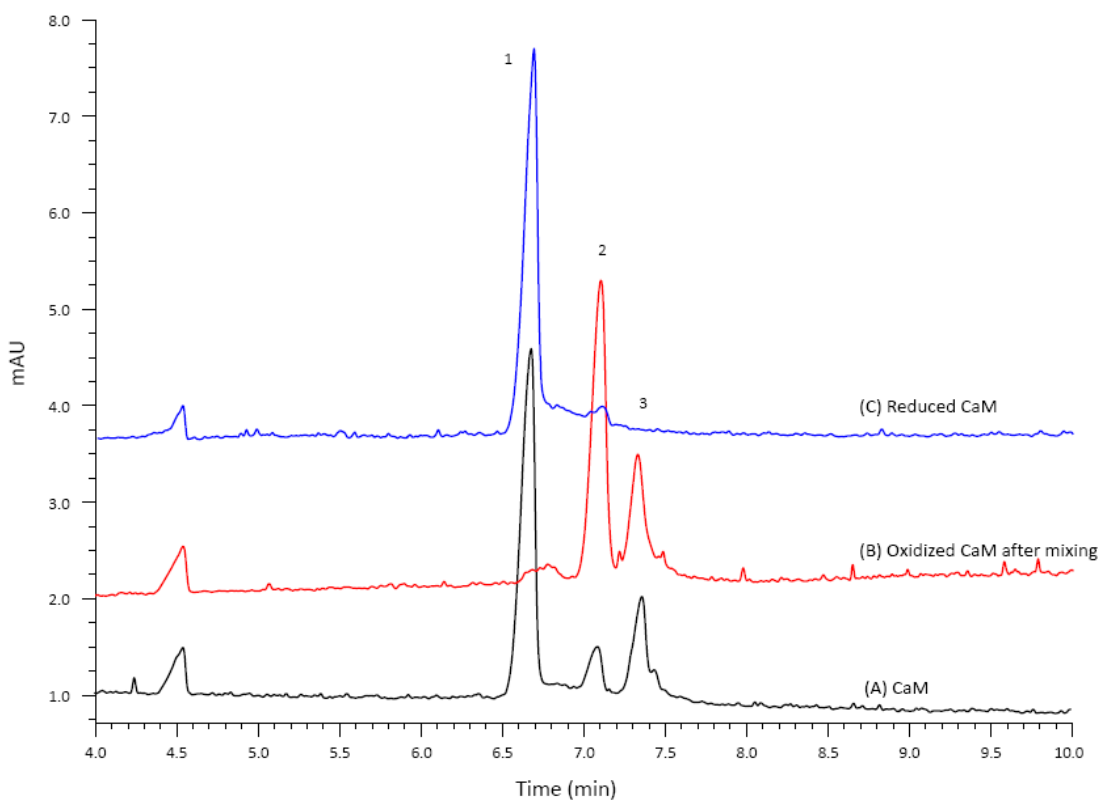


Figure 6.7: Oxidation and reduction study of T34C CaM. (A) 0.25 mg/mL calmodulin (CaM); (B) 0.25 mg/mL CaM with 0.01% (v/v) H_2O_2 analyzed immediately after mixing; (C) 0.25 mg/mL CaM with 2% 2-mercaptoethanol (v/v) analyzed 30 min after mixing by CZE with UV detection at 214 nm; Separation conditions: 10 mM tris, 1.0 mM CaCl_2 pH 7.5, 500 V/cm, 5.0 s injection at 0.5 psi

of separating charged as well as neutral analytes. The separation of neutral analytes is possible through the use of surfactants which are in concentrations at or above their CMC. As its name implies, the formation of micelles allows the partitioning of analytes in and out of the micelle in a similar manner to liquid chromatography. It was Terabe himself who described the interaction as a “moving stationary phase” [173].

The surfactants used in MEKC typically are charged as are the micelles which they create. Anionic surfactants such as SDS move in the opposite direction of the EOF; however, the EOF is faster than the migration velocity of the micelles. Therefore, the analytes which partition in and out of the micelles, as well as the micelles themselves, are eventually swept past the detector. The separation of charged species in MEKC is influenced by the electrophoretic mobility as well as interaction with the micelle. However, the separation of neutral analytes is only influenced by its partitioning in and out of the micelle. For this reason, MEKC is most often used on small hydrophobic analytes. Nevertheless, MEKC has been used for a variety of analytes some of which include: ionic compounds [174-175], chiral compounds [176-178], phenols [179-180], steroids [181-183], vitamins [184-185], pharmaceuticals [186-188], biogenic amines [189-192], amino acids [129, 193-195], nucleotides [196-198], DNA [199-200], RNA [201-202], peptides [203-205]. MEKC has been used for both capillary and microchip electrophoresis, and several reviews detail the design and execution of experiments for both of these formats [206-210].

MEKC has been used to a lesser extent for the separation of proteins. Many

of the surfactants commonly used for MEKC cause denaturation which prohibits native state analysis. In addition, the large size of proteins prevents efficient partitioning in and out of the micelle during short analysis times. This aspect is clearly evident when MEKC was used to separate the same CaM sample which was discussed in Section 6.2.4. Figure 6.8 shows the separation of CaM using a 10 mM Tris, 25 mM SDS, pH 7.5 buffer with detection at 214 nm. While many different buffer additives were investigated, little to no separation was observed with any combination examined. Because the CaM migration in MEKC is longer than that observed in using CZE, it is evident that CaM does indeed interact with the negatively charged SDS micelle. However, this interaction does not lead to a more efficient separation. Instead, CaM monomer and dimer interacted in a very similar fashion which led to co-migration and a loss of resolution.

While separation of CaM by MECK was not ideal for this application, MEKC has been used for the separation of proteins for many other applications. Glavac and co-workers recently described the development of a capillary MEKC-UV method for the identification of proteins in urine [211]. Proteinuria is characterized by increased levels of excreted proteins in urine, and is an indication of renal or urinary tract disease. The authors reported a fast and simple procedure for urine sample preparation without the need for pretreatment. The method was employed for the detection of albumin (ALB), hemoglobin (Hg), and myoglobin (MYO) in less than 20 min. Detection limits of 115, 234, and 124 ng/mL were achieved for ALB, Hg, and

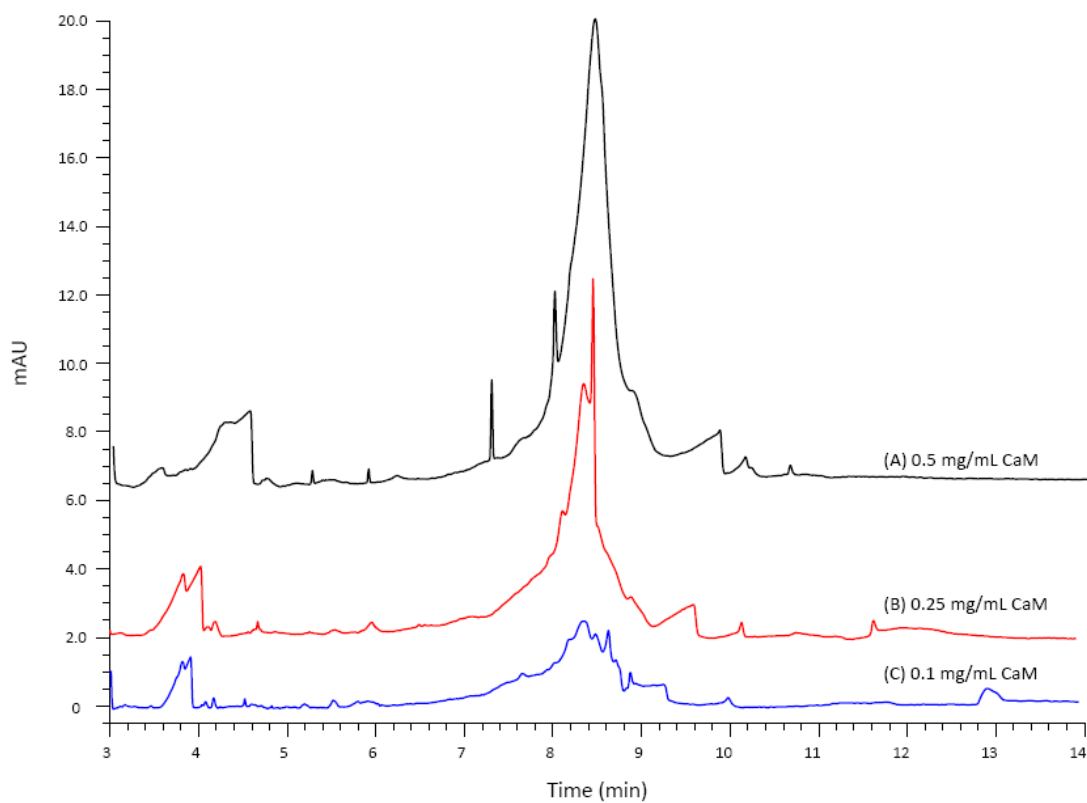


Figure 6.8: Separation of: (A) 0.05 mg/mL calmodulin (CaM); (B) 0.25 mg/mL CaM; (C) 0.10 mg/mL CaM by MEKC with UV detection at 214 nm; Separation conditions: 10 mM tris, 25 mM SDS, pH 7.5, 500 V/cm, 5.0 s injection at 0.5 psi

MYO, respectively which is suitable for the detection of physiologically relevant levels of protein in urine.

Roman and co-workers have used microchip MEKC for the analysis of fluorescently labeled proteins and homogenates from *E. coli* [212]. They presented work on both short straight channels (3.0 cm) and long serpentine channels (25 cm) in PDMS. Once buffer conditions were optimized for the separation of cytochrome *c*, lysozyme, ribonuclease A, MYO, and α -lactalbumin (Fig 6.9 A), relationships between separation efficiency, resolution, and length of separation were investigated. It was determined that longer separation channels produced larger plate numbers which increased linearly with respect to separation length (Fig 6.9 B). However, resolution reached an asymptotic value after only 7 cm.

Shadpour and Soper developed a two-dimensional separation method using a combination of capillary gel electrophoresis (CGE discussed in section 6.2.6) and MEKC in PMMA microchips [213]. Effluents from the first separation dimension were transferred into an orthogonal channel for the second dimension separation (Fig. 6.10) every 0.5 s. Because several of the proteins used had similar molecular weights, they were not completely resolved in the first separation dimension. However, once they were transferred to the second channel for separation by MEKC, all species were resolved. The complete separation process was completed in ~12 min and provided a peak capacity of ~1000.

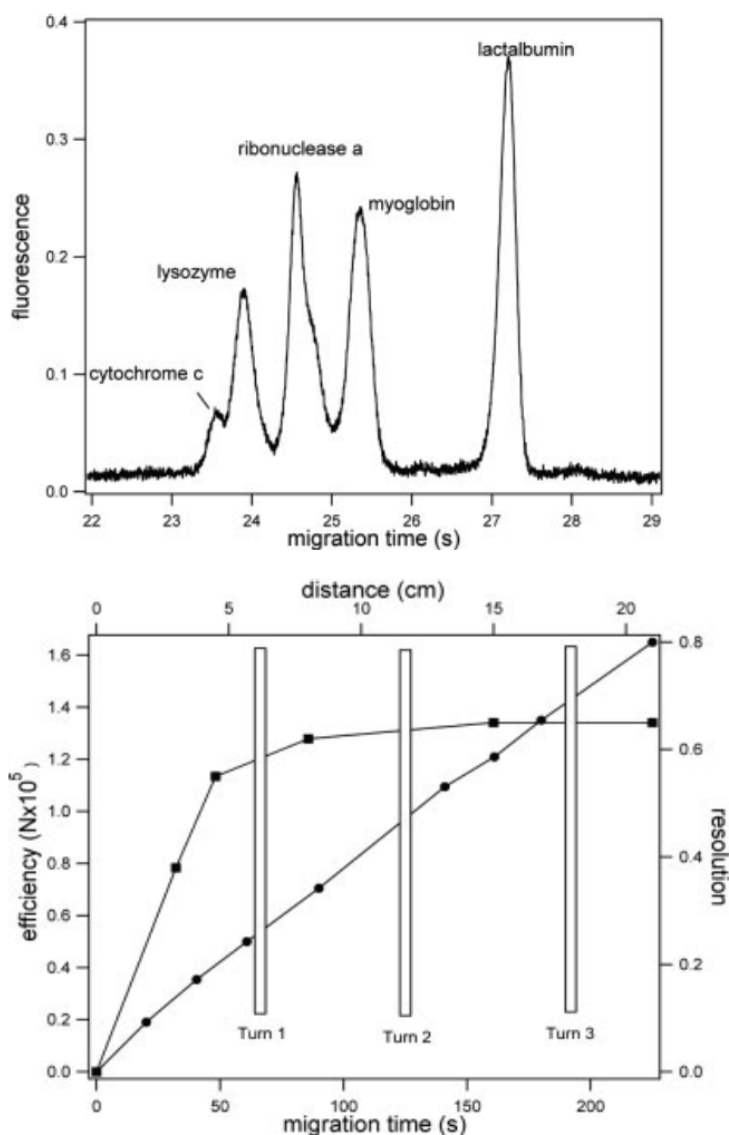


Figure 6.9: (A) Electropherogram of lysozyme, cytochrome c, myoglobin, ribonuclease A, and α -lactalbumin. device: cross channel PDMS chip with a 4.0 cm PDMS separation channel detected at 3.0 cm with a field strength of 650 V/cm; (B) Separation efficiency of BSA-AF and resolution between myoglobin-AF and BSA-AF as a function of both separation distance and time. Buffer: 25 mM SDS, 10 mM sodium borate, and 20% ACN; analytes: standard proteins diluted 1:100 from labeling cocktail; device, serpentine chip with field strength of 150 V/cm. Closed circles represent efficiency vs. migration time. Closed squares represent resolution vs. migration distance. Reprinted with permission from [212].

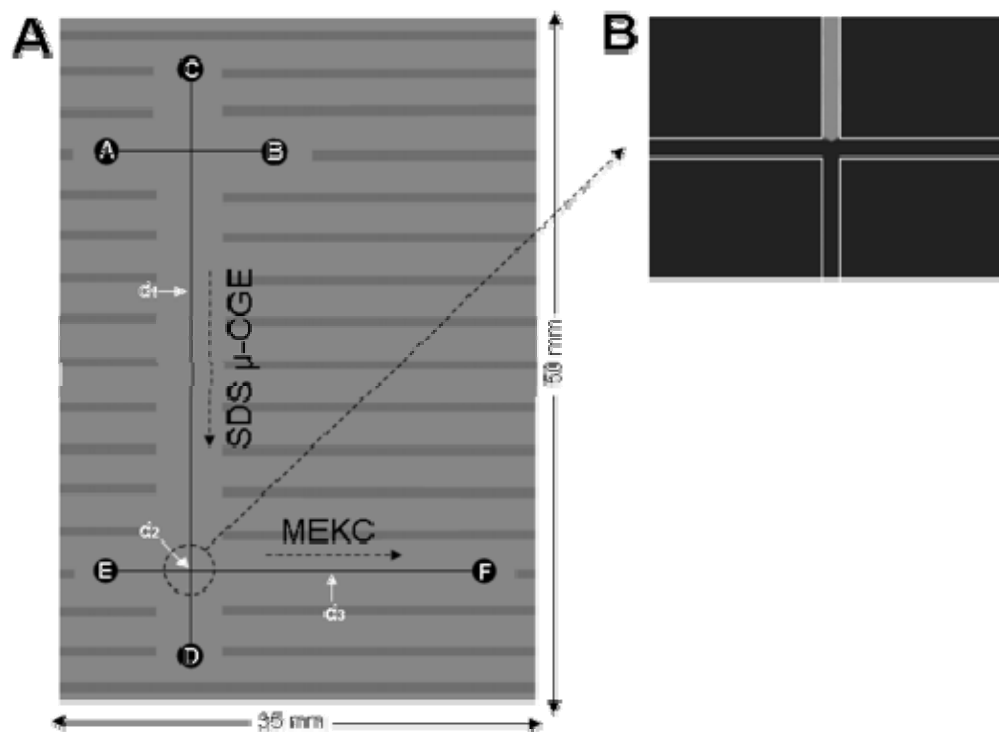


Figure 6.10: (A) Geometrical layout of the microelectrophoresis chip used for 1D and 2D separations. The chip was fabricated using hot embossing from a brass master into PMMA: with a channel width of 20 μm and a channel depth of 50 μm . Solution reservoirs: (A) sample reservoir, (B) sample waste reservoir, (C) SDS μ -CGE buffer reservoir, (D) SDS μ -CGE buffer waste reservoir, (E) MEKC buffer reservoir, and (F) MEKC buffer waste reservoir. (B) Fluorescence image of the sieving matrix/MEKC interface at the intersection of the SDS μ -CGE and MEKC dimensions. The fluorescence was generated by seeding the sieving matrix with fluorescein. Reprinted with permission from [213].

6.2.6 Capillary Gel Electrophoresis

Over the past decade, there has been increased popularity in the use of capillary gel electrophoresis (CGE) as an automated instrumental approach to classical slab gel electrophoresis [214-215]. The initial work on CE separations using a gel matrix, was performed using cross-linked polyacrylamide gel-filled capillaries [216]. Later work focused on the use of replaceable non-cross-linked polymer networks which were capable of separating protein-SDS complexes on the basis of their size [217-219]. While this technology has transitioned from cross-linked gels to entangled polymer networks, the term “capillary gel electrophoresis” is still commonly used. However, other terms such as CE-SDS, CE-SDS nongel sieving matrix, or CE-polymeric network separations have been used to describe this technique. In the absence of a consensus on the naming of this method, it will be referred to as capillary gel electrophoresis (CGE) in this dissertation.

Regardless of the name it is called, the mechanism by which the technique achieves a separation is identical. As analytes migrate through the capillary, they are forced to move through a polymeric network which acts as a molecular sieve. As analytes move through and interact with the network, their migration becomes hindered. Large analytes will be restricted to a greater extent than smaller analytes which have an easier time fitting through the polymer matrix. In this manner, a size-based separation is achieved for protein-SDS complexes.

CGE is directly comparable to slab gel electrophoresis techniques such as SDS-PAGE because the separation mechanisms are virtually identical. However,

CGE offers a rapid, sensitive, and quantitative method for the analysis of biomolecules. In addition, detection is done on-capillary, the instruments are typically automated, and the small volumes of capillaries allow the for the analysis of very small sample volumes. For these reasons, CGE is widely used as a characterization technique as well as for purity determination for many protein therapeutics in the pharmaceutical industry [220-224].

Although this technique has gained widespread popularity in recent years, there has been limited technical information available concerning the systematic optimization and implementation of CGE methods. However, several technical publications [225-227] as well as reviews for a variety of applications have been published in recent years [228-229]. A direct comparison between SDS-PAGE and CGE was made by Guttman and Nolan [230]. They used 65 different proteins to characterize and evaluate performance, precision, efficiency, and ease of use for both methods. Rustandi *et al.* described the many different applications for which CGE is being used in the development of biopharmaceutical antibody-based therapeutics [231].

Michels and co-workers described the development of a fluorescent derivatization method for proteins prior to analysis by CGE [232]. They described a fast and improved sample preparation method for the trace identification of impurities in recombinant monoclonal antibody production using CGE-LIF. A recent publication by Blazek and Caldwell sought to compare two commonly used CGE instruments in the pharmaceutical industry [233]. They directly compared the

Beckman Coulter ProteomeLab (a traditional instrument) with the Agilent 2100 Bioanalyzer, which utilizes lab-on-a-chip technology. The authors reported shorter analysis times, as well as more reproducible migration times and peak area calculations when using the lab-on-a-chip based technology.

Because CGE offers many advantages over SDS-PAGE for the size-based separation of proteins, this technique was utilized for the ongoing CaM project discussed in the previous sections. The first step in the development a suitable CGE assay involved the evaluation of size-based protein separations. An optimized separation of a typical molecular weight standard by CGE with UV detection can be seen in Figure 6.11 A. Protein MW standards ranging from 5 to 116 kDa were separated in less than 20 min. Incomplete resolution was achieved between the α -subunit (2.5 kDa) and β -subunit (3.5 kDa) of insulin because the type of CGE matrix used for this experiment (BioRad CE-SDS separation buffer) was not formulated to resolve such closely related species. However, other formulations exist for this purpose. To confirm peak identity, a 33 $\mu\text{g/mL}$ sample of BSA was added to the MW standard (Fig 6.11 B).

When compared to SDS-PAGE, analysis by CGE-UV has several advantages. The time required for analysis was reduced from ~ 24 hr to ~ 20 min, sample and reagent volumes were decreased, while sensitivity was increased. Table 6.1 shows both the concentration and mass sensitivity of this assay using UV detection at 214 nm. It can be seen that the mass LOD achieved using CGE-UV is approximately one order of magnitude less than standard Coomassie staining. In addition, Figure

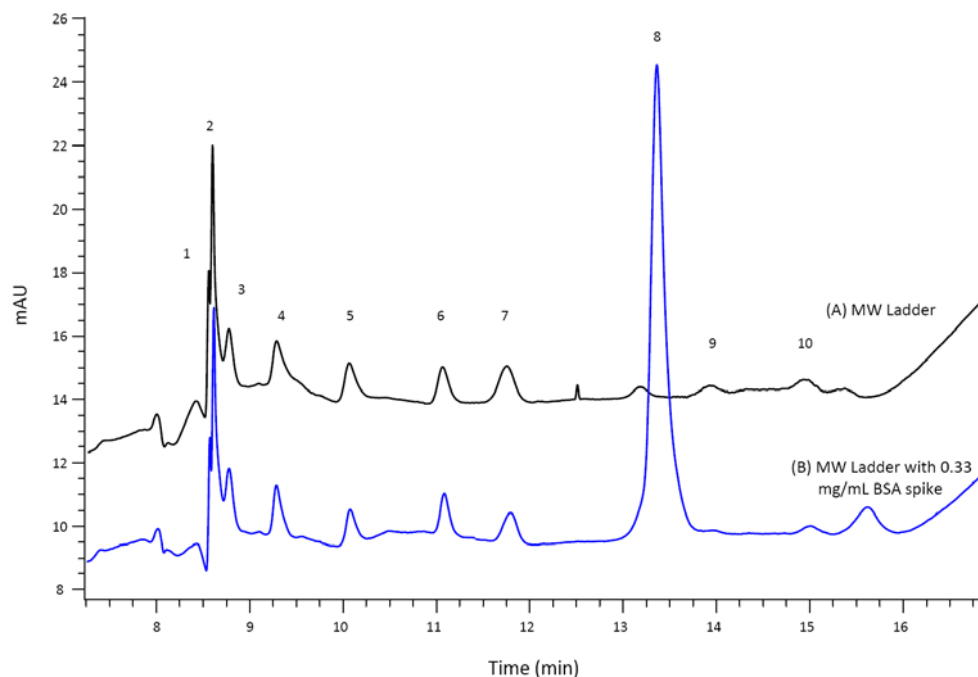


Figure 6.11: Separation of: (A) Mark 12 molecular weight ladder from Invitrogen; (B) Mark 12 molecular weight ladder from Invitrogen spiked with 0.33 mg/mL BSA by CGE with UV detection at 214 nm. Peak assignments are as follows: (1) insulin α -chain 2.5 kD, (2) insulin β -chain 3.5 kD, (3) aprotinin 6 kD, (4) lysozyme 14.4 kD, (5) trypsin inhibitor 21.5 kD, (6) carbonic anhydrase 31 kD, (7) glutamic dehydrogenase 55.4 kD, (8) bovine serum albumin 66.3 kD, (9) phosphorylase B 97.4 kd, (10) β -galactosidase 116 kD; Separation conditions: BioRad CE-SDS protein separation buffer, -500 V/cm, 20.0 s electrokinetic injection at -250 V/cm.

Table 6.1: Concentration and Mass Sensitivity of CGE-UV

Protein	Original Concentration ($\mu\text{g/mL}$)	Assay Concentration Sensitivity ($\mu\text{g/mL}$)	Assay Mass Sensitivity (ng)
Insulin (α & β)	224	112	5.6
Aprotinin	76	38	1.9
Lysozyme	50	25	1.25
Trypsin Inhibitor	64	32	1.6
Carbonic Anhydrase	44	22	1.1
Lactate Dehydrogenase	80	40	2.0
Glutamic Dehydrogenase	120	60	3.0
BSA	40	20	1.0
Phosphorylase B	70	35	1.75
B-Galactosidase	40	20	1.0

Table 6.1: Values were determined from figure 6.11.

6.12 demonstrates the ability of CGE to determine the MW of proteins. In CGE, the inverse of the electrophoretic mobility of the protein-SDS complex is proportional to the log of the apparent molecular size of the complex. Because the molecular size is proportional to the MW of the polypeptide backbone, a linear relationship is observed.

Two other related proteins were analyzed using the same CGE-UV method. Endothelial nitric oxide synthase (eNOS) and myosin light chain kinase (MLCK) are two calmodulin binding proteins (CaMBPs) which served as model compounds. Figure 6.13 shows the separation of 1 mg/mL MLCK and Fig. 6.14 shows the separation of 1 mg/mL eNOS using the optimized CGE method. Both figures contain an overlaid image of the same sample which had been analyzed by SDS-PAGE. It can be seen that both analysis images yield very similar results. The protein bands visualized in SDS-PAGE are present in the CGE electropherogram. However, CGE offers a few advantages. The sample volume used for SDS-PAGE was 25 μ L while CGE injected less than 300 nL for analysis. In addition, the ~24 hr analysis time required for SDS-PAGE was reduced to less than 30 min for CGE.

To examine the capability of CGE to separate a complex mixture of proteins, a sample containing 0.25 mg/mL each of CaM (16.8 kDa), MLCK (65 kDa), BSA (66 kDa), and eNOS (120 kDa) was prepared and analyzed by this method. As observed in Figure 6.15, all but two species were resolved. BSA and MLCK have molecular weights of 66 and 65 kDa, respectively, and were not able to be resolved. In addition, the MLCK and eNOS samples were not fully purified which led to an even greater

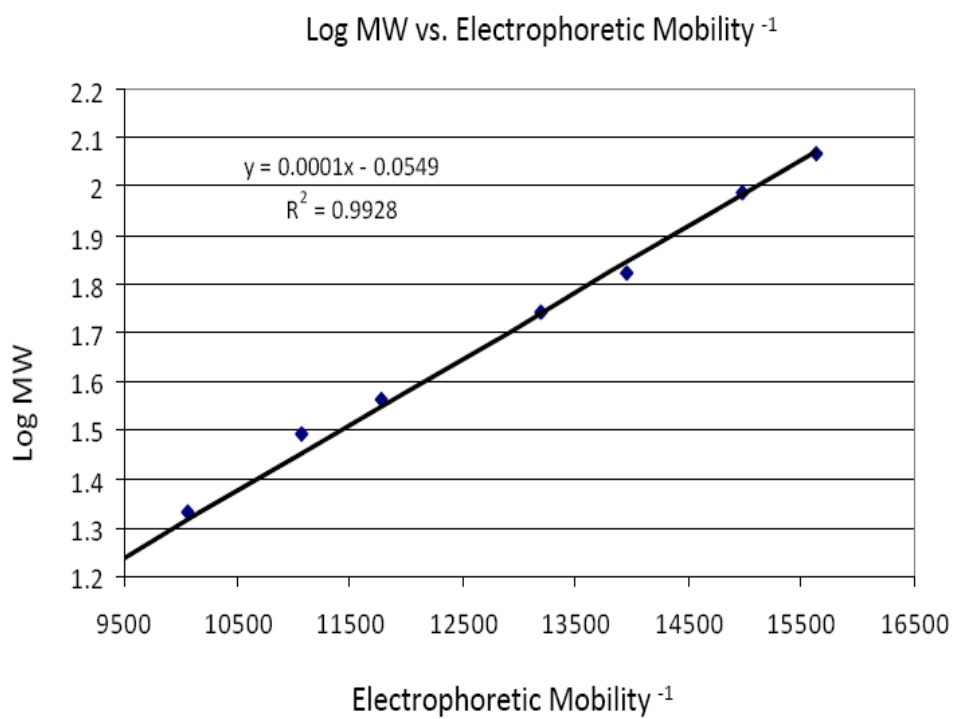


Figure 6.12: Linear relationship observed between the log of the molecular weight and the inverse electrophoretic mobility. Values for MW and electrophoretic mobility were taken from the electropherogram depicted in Figure 6.11.

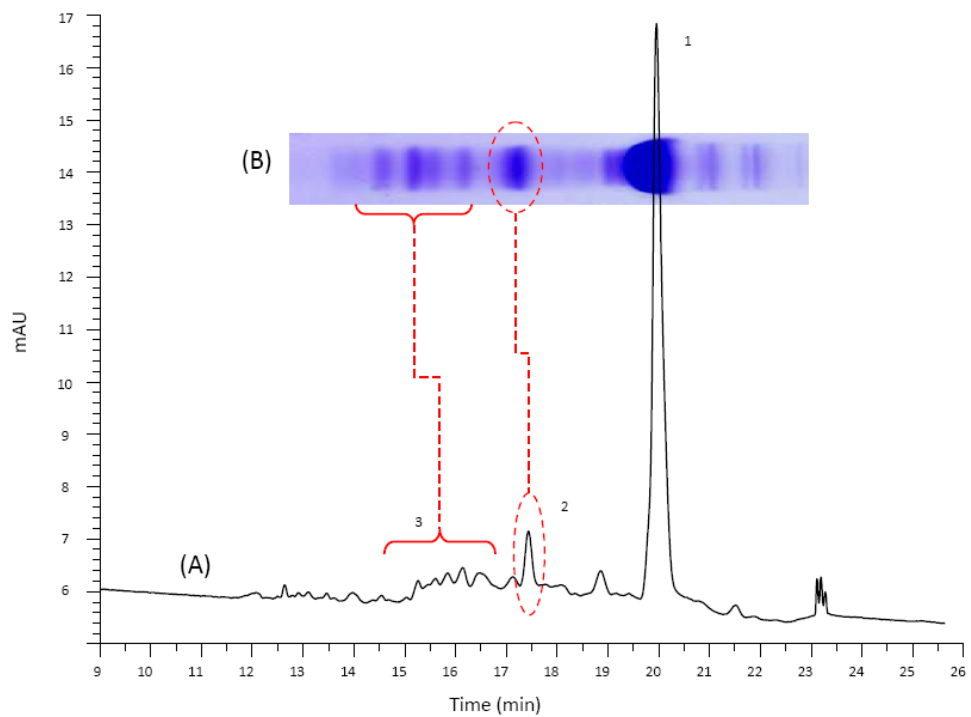


Figure 6.13: (A) 1.0 mg/mL MLCK separated by CGE with UV detection at 214 nm; (B) 880 µg/mL MLCK separated by SDS-PAGE with Coomassie staining: BioRad CE-SDS protein separation buffer, -500 V/cm, 20.0 s electrokinetic injection at -250 V/cm.

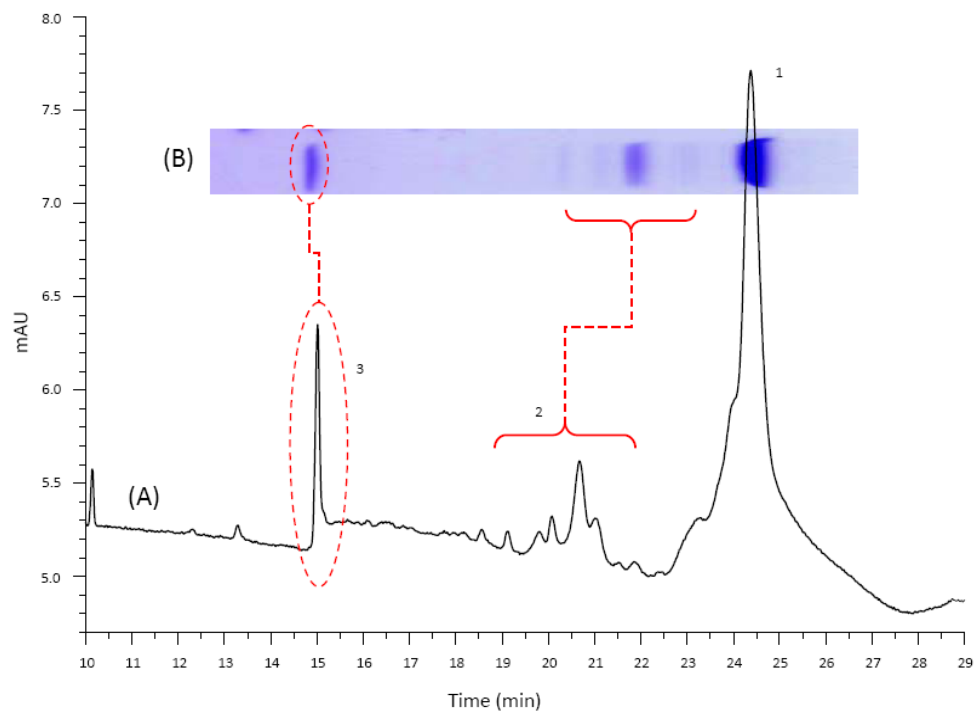


Figure 6.14: (A) 1.0 mg/mL eNOS separated by CGE with UV detection at 214 nm; (B) 360 µg/mL MLCK eNOS separated by SDS-PAGE with Coomassie staining: BioRad CE-SDS protein separation buffer, -500 V/cm, 20.0 s electrokinetic injection at -250 V/cm.

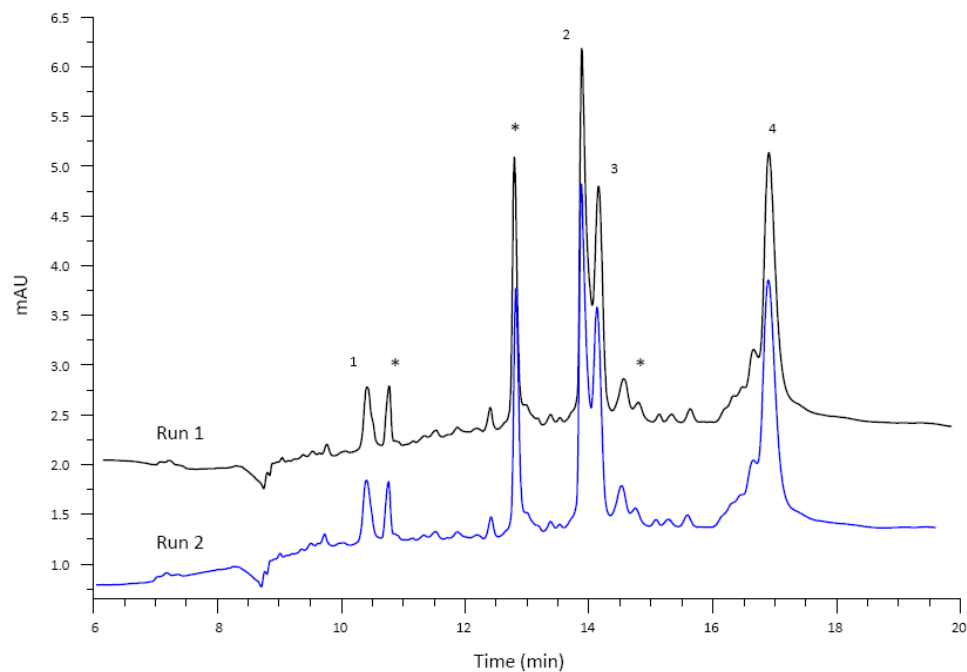


Figure 6.15: Replicate injections of a mixture of model proteins separated by CGE with UV detection at 214 nm. All proteins were at 0.25 mg/mL and peak assignments are as follows: (1) calmodulin 16 kD, (2) MLCK 65 kD (3) bovine serum albumin 66.3 (4) eNOS 120 kD, (*) indicates impurity from eNOS and MLCK samples. Separation conditions: BioRad CE-SDS protein separation buffer, -500 V/cm, 20.0 s electrokinetic injection at -250 V/cm.

sample complexity and the appearance of unidentified peaks. However, a size-based separation of the mixture was achieved.

This separation method was then transferred to the microchip to perform microchip gel electrophoresis with LIF detection (μ CGE-LIF). A simple “T” channel design fabricated in an all-glass microchip, employing a cross-T injection scheme was used for analysis (Fig. 6.16). LIF detection was performed using 488 nm while emission was collected at 520 nm. Figure 6.17 shows three replicate injections of 500 nM CaM which had been selectively labeled with Oregon Green. Using this analysis technique, a 12.5 nM limit of detection (LOD) at S/N=3 of was achieved. Because only ~125 nL of sample was injected for analysis, the mass LOD was determined to be ~2.65 pg. Figure 6.18 shows three replicate injections of 500 nM MLCK (which had been conjugated to cyan fluorescent protein), and Figure 6.19 shows three replicate injections of 250 nM CaM and MLCK. It is worth noting that the first injection in Figures 6.17 - 6.19 shows a diminished peak height. This is a result of the type of injection scheme utilized for microchip analysis. Because the sample must migrate across the “T” intersection, additional time is needed to completely fill the channel. The intersection was not completely filled until after the first injection, but remains filled for subsequent injections. Nevertheless, these results demonstrate the utility of μ CGE analysis for the size-based separation of proteins, the excellent sensitivity that can be achieved when using LIF detection, as well as a dramatic reduction in the time required for analysis.

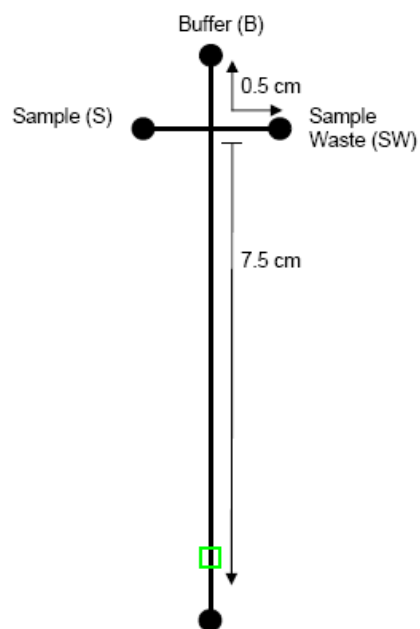


Figure 6.16: Schematic of the all-glass microchip used for μ CGE-LIF. All channels were 80 μm wide at full width and 22 μm deep. LIF detection was performed 5 mm from the end of the separation channel and is indicated by a square.

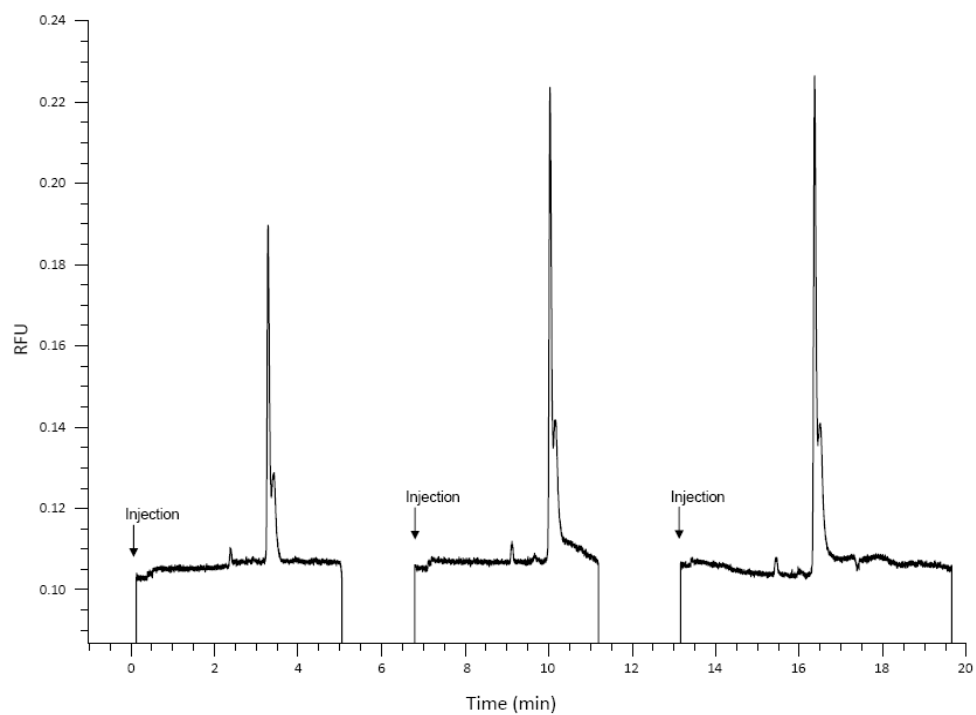


Figure 6.17: Three replicate injections of 500 nM Oregon Green labeled CaM separated by μ CGE with LIF detection using an all glass microchip. Separation conditions: BioRad CE-SDS protein separation buffer, -500 V/cm, 10.0 s electrokinetic injection at -500 V/cm.

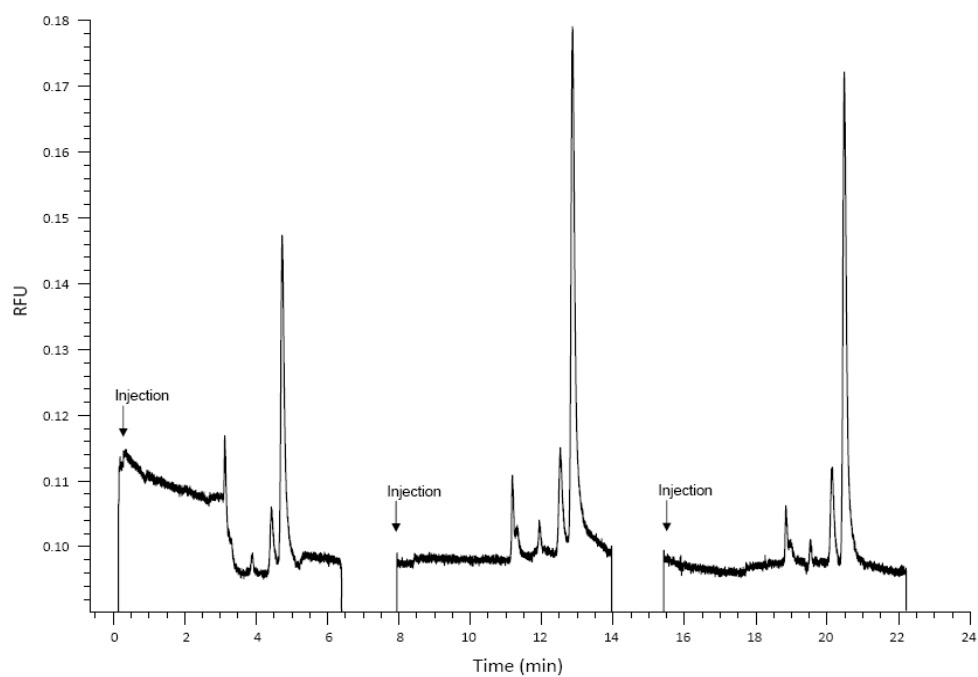


Figure 6.18: Three replicate injections of 500 nM MLCK protein separated by μ CGE with LIF detection using an all glass microchip. Separation conditions: BioRad CE-SDS protein separation buffer, -500 V/cm, 10.0 s electrokinetic injection at -500 V/cm.

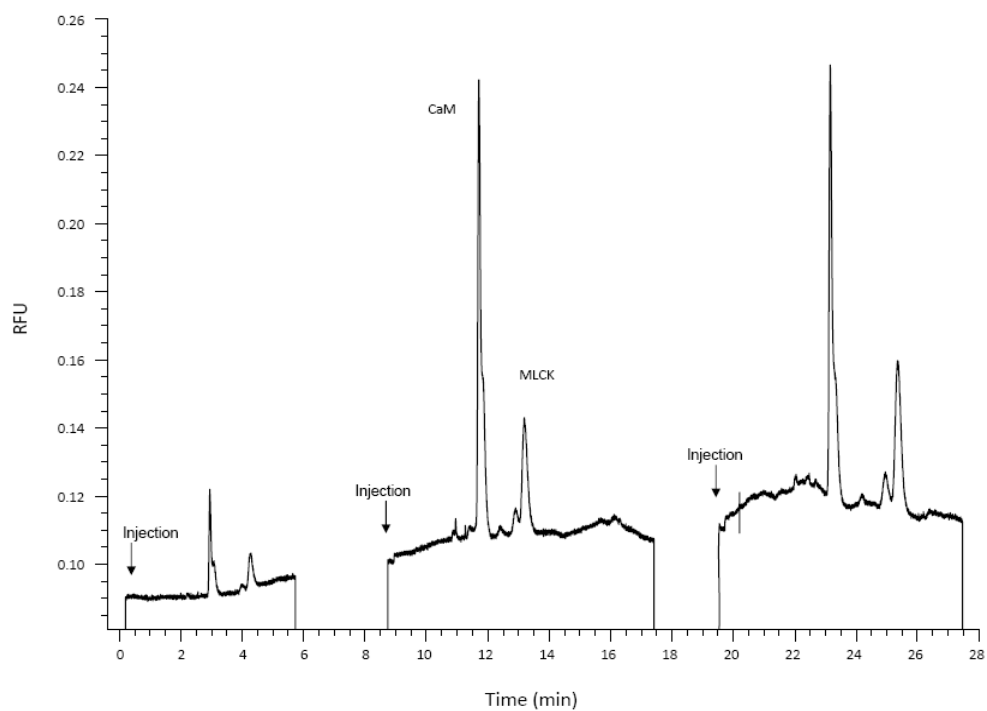


Figure 6.19: Three replicate injections of a mixture of 250 nM each Oregon Green labeled CaM and MLCK protein separated by μ CGE with LIF detection using an all glass microchip. Separation conditions: BioRad CE-SDS protein separation buffer, -500 V/cm, 10.0 s electrokinetic injection at -500 V/cm.

6.3 Special Electrophoretic Techniques

6.3.1 Isoelectric Focusing

Isoelectric focusing (IEF) is a powerful separation technique that focuses proteins into sharp zones according to their isoelectric point (pI). The first publications regarding this work arose from the work of Kolin in 1954 [234]. A pH gradient formed between highly acidic and highly basic buffers was used to separate hemoglobin and cytochrome c. However, it was not until Svensson and Vesterberg introduced the concept of carrier ampholytes (CAs) that IEF was seen as a viable analytical tool [235-236]. Carrier ampholytes are amphoteric compounds with closely spaced pIs which will form a reproducible pH gradient in the presence of an electric field. This technology was used for almost two decades as an analytical and preparatory tool for protein separations, until Righetti *et al.* introduced the use of the immobilized pH gradient (IPG) [237-238]. An analog to ampholytes, he termed these immobilines because they consisted of amphoteric monomer containing an acrylate backbone which can be later polymerized. This technique became the predominant method for IEF because it resulted in higher resolution, better buffering capacity, and increased sample loading capacity. IPG strips are still commonly used today and are available from many commercially available sources.

Shortly after Jorgenson's seminal work involving CZE, Hjerten and Zhu adapted the use of small bore capillaries for use in IEF [239]. Termed capillary isoelectric focusing (cIEF), they described the use of carrier ampholytes to focus proteins followed by hydrodynamic or electrokinetic mobilization of proteins past a

single point detector. The field of cIEF has matured in parallel with CE instrumentation and has become a popular technique due to advantages of speed, automation, and precision. However, the major drawbacks of cIEF are associated with the mobilization procedure. Chemical mobilization requires long analysis times and hydrodynamic mobilization can lead to band broadening and decreased separation efficiency. To overcome many of the problems associated with mobilization, several research groups and instrument manufacturers have developed whole-column imaging detection techniques [66-67, 240]. Instead of moving the solution past the detector, the detector is moved along the length of the capillary. This type of detection has been adapted for UV as well as LIF detection in both capillaries as well as microchip devices. The use of both capillary and microchip IEF with UV and LIF detection has been detailed previously in several excellent reviews [241-244].

Kitagawa and co-workers have described the use of a microchip-based whole-channel imaging system with UV detection [245]. They reported the separation of four model proteins in 130 s in a 2.5 cm quartz microchip. Yao *et al.* reported the use of a multichannel microchip device with whole-column LIF detection using an organic LED for excitation [246]. The authors were able to focus proteins in ~30 s using a field strength of 700 V/cm. Under optimized conditions they reported a LOD of ~600 ng/mL for R-phycoerythrin which equates to a mass LOD of ~45 pg.

The most common application of cIEF is for the analysis of therapeutic proteins produced by recombinant DNA technology [247]. Vlckova and co-workers

detailed the analysis of three therapeutic proteins: hirudin, erythropoietin, and bevacizumab [248]. The analysis of these proteins by conventional cIEF (Beckman Coulter Proteomelab) was compared to analysis by microchip ICE using the Shimadzu MCE-2010 microchip station. They found that both systems were able to accurately determine the correct pI, however the microchip system required extensive optimization of separation conditions. Apostol and co-workers at Amgen recently evaluated the use of cIEF for the detection and quantitation limits of antibody purity [249]. Several different techniques were suggested by the International Conference on Harmonization (ICH) to assess the LOD and limit of quantitation (LOQ) for an antibody purity determination. The authors evaluated five different approaches using cIEF to determine the purity of several different monoclonal antibodies and found all techniques to be satisfactory according to the ICH guidelines. These results were validated by independent analysis, which illustrated the utility and versatility of cIEF for the biopharmaceutical industry and research community as a whole.

6.3.2 Affinity Capillary Electrophoresis

At the heart of essentially all biological functions are molecular recognition events that underlie all mechanisms that are essential to life. At a cellular level, all functions in the human body depend on protein-protein, protein-small molecule, protein-nucleic acid, or other intermolecular interactions. While there are a variety of techniques to investigate and measure affinity parameters of these interactions, one method that has been shown to be an effective and versatile analytical method is affinity capillary electrophoresis (ACE). The first reports of the use of ACE for the

investigation of molecular interactions were published by the Whitesides group in 1992 [250-252].

Since then, many interactions including protein-protein [253-255], protein-antibody [50, 256], protein-ligand [257-258], receptor-ligand [257, 259-260], protein-peptide [261-262], protein-DNA [263-265], and protein-drug [257, 259, 266] have been reported. In addition several reviews of the implementation and application of ACE have been published [259, 267-269]. Because of the many inherent advantages of microchip and lab-on-a-chip devices, the use of ACE in the microfluidic format (MC-ACE) has become more widespread and has also been previously detailed [270-273].

In general, there are three different methods in which ACE can be employed. In the first type, the two species which are being investigated (i.e. receptor and ligand) are mixed prior to separation by electrophoresis. This type of ACE is advantageous when the k_{on} (association rate constant) and k_{off} (disassociation rate constant) of the binding pair is slow. Therefore, premixing is often required to ensure formation of the complex. An alternate method of performing ACE involves placing the receptor (or ligand) in the separation buffer. As the ligand (or receptor) migrates through the capillary, the complex is formed and a shift in mobility is observed. The change in mobility and the concentration of ligand used to elicit the change in migration can be correlated to an affinity constant through Scatchard (or other) type of analysis. In the third type of ACE, the receptor is immobilized on a solid support and a solution containing the ligand is flowed through the capillary for capture. Typically,

the receptor is immobilized in the capillary lumen or on beads which are inserted in the capillary. In this manner, low abundance analytes can be selectively captured and enriched prior to analysis. In addition, sample cleanup, desalting, or removal of unwanted species can be achieved. Due to the progress of lab-on-a-chip technology, this technique has become quite popular. The inherent advantages of microfluidics has allowed the integration of several processes on a single device which allows for automation, high throughput sampling, and the analysis of extremely small volumes of sample with a high degree of sensitivity.

Kalish and Phillips recently demonstrated this third type of ACE through the application of immunoaffinity for the measurement of several secreted cytokines by cultured astrocytes [22]. Antibodies directed against the analytes of interested were first immobilized inside a fused silica capillary. Fluorescently derivatized sample was introduced into the capillary to allow binding, then an elution buffer was introduced to release the analytes for separation and detection by LIF (Fig. 6.20). Ten different cytokines and chemokines were sampled using microdialysis and separated and detected in less than 20 min. The ACE system was found to have a LOD of approximately 100 ag/mL, however all analytes were found to be in the low pg/mL range.

While monoclonal antibodies are most often utilized for ACE experiments, the use of artificial biomimetic receptors such as aptamers and molecularly-imprinted polymers (MIPs) are gaining popularity. A review by Giovannoli and co-workers

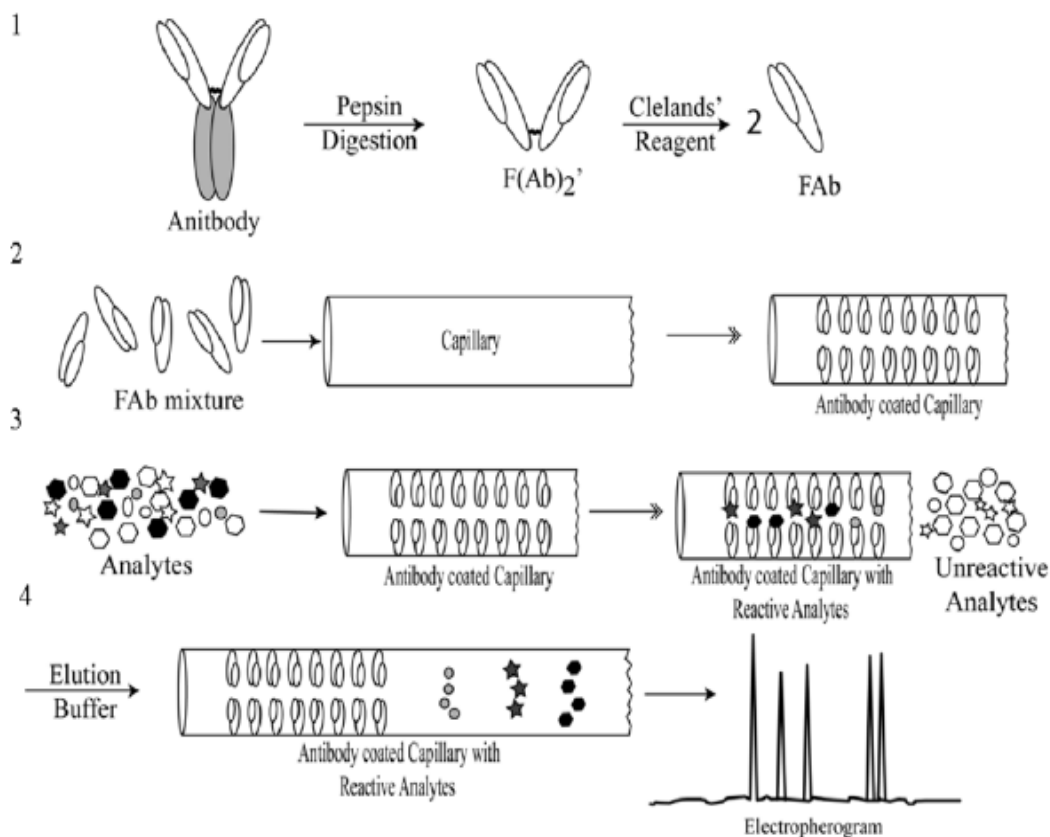


Figure 6.20: Illustration of the preparation of an immunoaffinity capillary and steps of an immunoaffinity assay. Step 1: The antibody is digested by pepsin digestion, yielding the $F(Ab)_2'$ fragment, which is further reduced by Cleland's reagent to 2 Fab fragments. Step 2: The antibody fragments are loaded by capillary action into the derivatized capillary. Step 3: The AlexaFluor labeled analytes are introduced into the capillary and bind to the immobilized antibody. Nonreactive analytes are removed. Step 4: An elution buffer is introduced into the capillary, breaking the antibody analyte bond and releasing the analytes, which separate and are detected as an electropherogram. Reprinted with permission from [22].

describes the use of DNA, RNA, short single-stranded DNA (ssDNA) and ss(RNA) as well as a variety of MIPs for applications of ACE [274].

6.4 Applications of Capillary and Microchip Electrophoresis

6.4.1 Analysis of Brain and Cerebrospinal Proteins

The elucidation of neurochemical pathways is a subject matter that has received a tremendous amount of attention. The development of more sensitive and robust analytical tools has facilitated the investigation of a variety of neurologically significant proteins and enhanced our understanding of many neurodegenerative diseases.

Schmerr utilized an immunoaffinity approach in combination with CZE-LIF for the detection of Scrapie in sheep [275]. Scrapie in sheep and goats is a progressive, neurodegenerative disease of the central nervous system (CNS) caused by a prion protein (PrP). Traditional assays are lengthy, require relatively large amounts of starting material, and lack sensitivity. The use of CZE dramatically reduced the time required for analysis and LIF resulted in a highly sensitive method of detection. Ed Yeung's group has also developed a CE-based noncompetitive immunoassay for PrP in scrapie-infected sheep [276]. A dynamic range of 0.2 to 2 $\mu\text{g/mL}$ and a LOD of ~ 6 ng/mL was reported. The analytical method was then successfully applied for the analysis of blood samples from infected sheep.

The neurochemical mechanisms underlying Alzheimer's disease are not well understood and have been the focus of intense research in the past two decades. Alper and Schmidt recently reported a CE-based method for the evaluation of

amyloid beta (A β) proteolysis [277]. Multiple clearance mechanisms are hypothesized to regulate physiological levels of A β . Insulin-degrading enzyme (IDE) is thought to be one of the principal enzymes responsible for regulation, however relatively few methods exist for studying IDE activity *in vitro*. The authors reported the development of a CE-based method amenable to kinetic analysis of proteolysis. In addition, it was determined that A β -mediated proteolysis was significantly inhibited by the presence of alternate IDE substrates. Once A β is cleaved from its precursor protein, it is known to aggregate *in vivo* and form neuronal plaques [278-279]. Sabella and co-workers have described a CE-based method to monitor the aggregation of A β *in vitro* [280]. CZE-UV was used to monitor the steps of A β nucleation and the dynamics involved in the formation of aggregates. This simplistic CE-based approach allowed the sensitive and rapid analysis of samples with minimal reagent volume.

As described earlier, CE-based separations coupled to MS detection has become an important tool for proteomics research. Fang *et al.* has described the use of CZE-based multidimensional separations with ESI-MS detection for the characterization of the mouse brain mitochondrial proteome [281]. Mitochondria have a multitude of essential intracellular responsibilities, and their dysfunction has been implicated in a number of neurodegenerative diseases [282-283]. Therefore, the identification of the proteins involved in disease pathology is essential. The high resolving power of 2-D electrophoresis allowed the detection of ~12,000 tryptic

peptides and the identification of 1705 unique proteins in synaptic mitochondria isolated from mouse brain.

Not only are intercellular proteins of great interest, proteins and peptides secreted into cerebrospinal fluid are routinely used for disease identification. Zuberovic and co-workers recently described a CE-based method interfaced to an off-line MALDI-TOF/TOF MS for the detection of cerebrospinal fluid proteins [284]. During separation, the CE eluate was directly fractionated onto a pre-spotted MALDI plate where one spot was deposited every 6 s which corresponded to a volume of ~300 nL. Following separation, spots were analyzed by MALDI-TOF/TOF MS/MS analysis. This analysis was performed on samples collected from patients with traumatic brain injury (TBI) during recovery. A total of 43 proteins were identified which correlated with previously published protein profiles characteristic of patients recovering from TBI. The use of this type of method demonstrated the effectiveness of CE-based proteomic analysis for the identification of clinically significant proteins in human cerebrospinal fluid.

6.4.2 Analysis of Proteins in Blood and Urine

Although cerebrospinal and brain proteins have been the focus of intense research, human serum and urine are the two bodily fluids that are most frequently analyzed for proteins. These fluids can be obtained through less invasive procedures and can give information about the function of many organs. Because of this, the development of sensitive, high throughput CE-based separation methods are highly valuable.

Human plasma is a highly complex body fluid which contains dissolved proteins, glucose, clotting factors, hormones, and minerals. In addition, proteins such as albumin, α -glycoprotein, and lipoproteins bind to many drugs which cause a reduction in bioavailability and efficacy. Because of this, it is of great importance to quantify the nature and extent of drug-plasma binding during the process of drug development. Capillary electrophoresis has been used for the identification and optimization of drug candidates for preclinical development. Several anti-cancer gallium(III) complexes were examined to determine the degree of binding to albumin and transferrin in order to determine the drug's distribution pathways [285]. CE has also been utilized to determine the extent to which many drugs bind serum proteins including: platinum group anticancer metallodrugs [286], ruthenium based anti-cancer drugs [287], antitumor indazolium derivatives [288], theophylline [289], and several fluoroquinolone antibiotics [290]. Aarong and Trajkovska exploited the intrinsic fluorescence of many commonly used anticancer drugs to perform trace analysis of plasma concentrations using CE-LIF [291]. An extensive characterization of the interaction between many different beta blockers and phenothiazines with serum proteins was performed by Gomez *et al.* [292].

Recently Nguyen and Moini described the development of a CE-MS method for the determination of several protein-protein and protein-metal complexes in blood [293]. The authors reported a dynamic range of approximately 3 orders of magnitude for the detection of carbonic anhydrase I complexed with its zinc cofactor, carbonic

anhydrase II complexed with its zinc cofactor, and hemoglobin A; a tetramer formed by two α - β -subunits and four heme groups.

The analysis of urine is a vital part of routine clinical diagnostics. Routine urinalysis can provide information about renal, hepatic, and pancreatic function as well as urinary tract and prostate health. A review by Pisitkun highlights the importance of using urinalysis for routine use as well as for the discovery of important biomarkers [294]. Theodorescu, and co-workers described the use of CE-MS analysis for the diagnosis of urothelial carcinoma. They analyzed the urine from 33 healthy volunteers and 46 patients suffering from bladder cancer and developed a statistical model capable of predicting the presence of cancer.

This same group described the development of a CE-MS method for the identification of biomarkers specific for prostate cancer in urine samples [295]. After developing a proteomic profile for the disease biomarkers, the authors reported the ability to correctly identify cancerous from noncancerous samples with 96% accuracy. A CZE method for the determination of Bence Jones protein in urine has been described by Mussap and co-workers [296]. Bence Jones protein is a monoclonal globular protein found in the blood or urine which can indicate a variety of maladies including bone marrow cancer, renal failure, and lytic bone disease. Traditional analysis is done by agarose gel electrophoresis which is time consuming and requires a large sample volume. The authors analyzed 350 24 hr urine samples and compared their newly developed technique to standard analysis. A LOD of 1.2 mg/mL and analysis times of less than 25 min was reported.

6.5 Conclusions

This review has focused on the application of capillary electrophoresis-based analytical methods for the analysis of proteins. Since the first reports almost two decades ago, the development and application of CE to a variety of biochemical processes has been extensively researched and developed. Much of this progress is owed to the development of radically improved CE instrumentation and detection systems. Due to its ease of operation, versatility, and excellent resolving power, the analysis of proteins by CE has helped revolutionize our understanding of myriad biochemical interactions.

6.6 References

- [1] Deyl, Z., Editor, *Journal of Chromatography Library, Vol. 18B: Electrophoresis. A Survey of Techniques and Applications, Pt. B: Applications*, 1983.
- [2] Shapiro, A. L., Vinuela, E., Maizel, J. V., Jr., *Biochemical and biophysical research communications* 1967, 28, 815-820.
- [3] Rothe, G. M., Purkhanbaba, H., *Electrophoresis (Weinheim, Fed. Repub. Ger.)* 1982, 3, 43-48.
- [4] Neville, D. M., Jr., *Journal of Biological Chemistry* 1971, 246, 6328-6334.
- [5] Poduslo, J. F., Rodbard, D., *Analytical Biochemistry* 1980, 101, 394-406.
- [6] Xiong, X., Ouyang, J., Zhai, S., Baeyens, W. R. G., *TrAC, Trends in Analytical Chemistry* 2009, 28, 961-972.
- [7] Alba, F. J., Bartolome, S., Bermudez, A., Daban, J.-R., *Methods in molecular biology (Clifton, N.J.)* 2009, 536, 407-416.
- [8] Dunn, M. J., *Protein Protocols Handbook (2nd Edition)* 2002, 287-293.
- [9] Switzer, R. C., III, Merril, C. R., Shifrin, S., *Analytical Biochemistry* 1979, 98, 231-237.
- [10] Merril, C. R., *Nature* 1990, 343, 779-780.
- [11] Sorensen, B. K., Hojrup, P., Ostergard, E., Jorgensen, C. S., Enghild, J., Ryder, L. R., Houen, G., *Analytical Biochemistry* 2002, 304, 33-41.
- [12] Meier, R. J., Steiner, M.-S., Duerkop, A., Wolfbeis, O. S., *Analytical Chemistry* 2008, 80, 6274-6279.
- [13] Wetzl, B. K., Yarmoluk, S. M., Craig, D. B., Wolfbeis, O. S., *Angewandte Chemie, International Edition* 2004, 43, 5400-5402.
- [14] Burnette, W. N., *Analytical Biochemistry* 1981, 112, 195-203.
- [15] Mousseau, D. D., Rao, V. L. R., *Neuromethods* 1999, 34, 167-191.
- [16] Jorgenson, J. W., Lukacs, K. D., *HRC & CC, Journal of High Resolution Chromatography and Chromatography Communications* 1981, 4, 230-231.
- [17] Jorgenson, J. W., Lukacs, K. D., *Analytical Chemistry* 1981, 53, 1298-1302.
- [18] Jorgenson, J. W., Lukacs, K. D., *Science* 1983, 222, 266-272.
- [19] Effenhauser, C. S., Bruin, G. J. M., Paulus, A., *Electrophoresis* 1997, 18, 2203-2213.
- [20] Woods, L. A., Roddy, T. P., Paxon, T. L., Ewing, A. G., *Analytical Chemistry* 2001, 73, 3687-3690.
- [21] Woods, L. A., Powell, P. R., Paxon, T. L., Ewing, A. G., *Electroanalysis* 2005, 17, 1192-1197.
- [22] Kalish, H., Phillips, T. M., *Journal of Separation Science* 2009, 32, 1605-1612.
- [23] Dolnik, V., *Electrophoresis* 1997, 18, 2353-2361.
- [24] Dolnik, V., *Electrophoresis* 1999, 20, 3106-3115.
- [25] Dolnik, V., Hutterer, K. M., *Electrophoresis* 2001, 22, 4163-4178.
- [26] Hutterer, K., Dolnik, V., *Electrophoresis* 2003, 24, 3998-4012.
- [27] Dolnik, V., *Electrophoresis* 2006, 27, 126-141.
- [28] Dolnik, V., *Electrophoresis* 2008, 29, 143-156.

- [29] Burgi, D. S., Giordano, B. C., *Handbook of Capillary and Microchip Electrophoresis and Associated Microtechniques (3rd Edition)* 2008, 413-427.
- [30] Monton, M. R. N., Terabe, S., *Journal of Chromatography, B: Analytical Technologies in the Biomedical and Life Sciences* 2006, 841, 88-95.
- [31] Shihabi, Z., *Current Pharmaceutical Analysis* 2006, 2, 9-15.
- [32] Lin, C.-H., Kaneta, T., *Electrophoresis* 2004, 25, 4058-4073.
- [33] Wu, X.-Z., Umeda, R., *Analytical and Bioanalytical Chemistry* 2005, 382, 848-852.
- [34] Yang, L., He, Y. Z., Gan, W. E., Lin, X. Q., Zhao, Y. Q., Qu, Q. S., *Journal of Chromatography, A* 2001, 932, 13-20.
- [35] Lin, S. L., Tolley, H. D., Lee, M. L., *Chromatographia* 2005, 62, 277-281.
- [36] Breadmore, M. C., Thabano, J. R. E., Dawod, M., Kazarian, A. A., Quirino, J. P., Guijt, R. M., *Electrophoresis* 2009, 30, 230-248.
- [37] Sueyoshi, K., Kitagawa, F., Otsuka, K., *Journal of Separation Science* 2008, 31, 2650-2666.
- [38] Foote, R. S., Khandurina, J., Jacobson, S. C., Ramsey, J. M., *Analytical Chemistry* 2005, 77, 57-63.
- [39] Kelly, R. T., Li, Y., Woolley, A. T., *Analytical Chemistry* 2006, 78, 2565-2570.
- [40] Sun, X., Yang, W., Pan, T., Woolley, A. T., *Analytical Chemistry* 2008, 80, 5126-5130.
- [41] Wu, Z., Zhen, Z., Jiang, J.-H., Shen, G.-L., Yu, R.-Q., *Journal of the American Chemical Society* 2009, 131, 12325-12332.
- [42] Welder, F., McCorquodale, E. M., Colyer, C. L., *Electrophoresis* 2002, 23, 1585-1590.
- [43] Yang, P., Whelan, R. J., Jameson, E. E., Kurzer, J. H., Argetsinger, L. S., Carter-Su, C., Kabir, A., Malik, A., Kennedy, R. T., *Analytical Chemistry* 2005, 77, 2482-2489.
- [44] Jameson, E. E., Cunliffe, J. M., Neubig, R. R., Sunahara, R. K., Kennedy, R. T., *Analytical Chemistry* 2003, 75, 4297-4304.
- [45] Michels, D. A., Brady, L. J., Guo, A., Balland, A., *Analytical Chemistry* 2007, 79, 5963-5971.
- [46] Salas-Solano, O., Tomlinson, B., Du, S., Parker, M., Strahan, A., Ma, S., *Analytical Chemistry* 2006, 78, 6583-6594.
- [47] Yu, W., Li, Y., Deng, C., Zhang, X., *Electrophoresis* 2006, 27, 2100-2110.
- [48] Liu, J., Lee, M. L., *Electrophoresis* 2006, 27, 3533-3546.
- [49] Phillips, T. M., Wellner, E., *Journal of Chromatography, A* 2006, 1111, 106-111.
- [50] Guzman, N. A., Blanc, T., Phillips, T. M., *Electrophoresis* 2008, 29, 3259-3278.
- [51] Craig, D. B., Wetzl, B. K., Duerkop, A., Wolfbeis, O. S., *Electrophoresis* 2005, 26, 2208-2213.
- [52] De Montigny, P., Stobaugh, J. F., Givens, R. S., Carlson, R. G., Srinivasachar, K., Sternson, L. A., Higuchi, T., *Analytical Chemistry* 1987, 59, 1096-1101.
- [53] Lunte, S. M., Wong, O. S., *Current Separations* 1990, 10, 19-25.

- [54] Shou, M., Smith, A. D., Shackman, J. G., Peris, J., Kennedy, R. T., *Journal of Neuroscience Methods* 2004, *138*, 189-197.
- [55] Chiu, T.-C., Tu, W.-C., Chang, H.-T., *Electrophoresis* 2008, *29*, 433-440.
- [56] Jin, L. J., Giordano, B. C., Landers, J. P., *Analytical Chemistry* 2001, *73*, 4994-4999.
- [57] Giordano, B. C., Jin, L., Couch, A. J., Ferrance, J. P., Landers, J. P., *Analytical Chemistry* 2004, *76*, 4705-4714.
- [58] Culbertson, C. T., Jorgenson, J. W., *Analytical Chemistry* 1998, *70*, 2629-2638.
- [59] Mainka, A., Baechmann, K., *Journal of Chromatography, A* 1997, *767*, 241-247.
- [60] Fernandez, C., Egginger, G., Wainer, I. W., Lloyd, D. K., *Journal of Chromatography, B: Biomedical Applications* 1996, *677*, 363-368.
- [61] Moring, S. E., Reel, R. T., van Soest, R. E. J., *Analytical Chemistry* 1993, *65*, 3454-3459.
- [62] Bruin, G. J. M., Stegeman, G., Van Asten, A. C., Xu, X., Kraak, J. C., Poppe, H., *Journal of Chromatography* 1991, *559*, 163-181.
- [63] Djordjevic, N. M., Widder, M., Kuhn, R., *Journal of High Resolution Chromatography* 1997, *20*, 189-192.
- [64] Hempel, G., *Electrophoresis* 2000, *21*, 691-698.
- [65] Xue, Y., Yeung, E. S., *Analytical Chemistry* 1994, *66*, 3575-3580.
- [66] Fang, X., Tragas, C., Wu, J., Mao, Q., Pawliszyn, J., *Electrophoresis* 1998, *19*, 2290-2295.
- [67] Urban, P. L., Bergstroem, E. T., Goodall, D. M., Narayanaswamy, S., Bruce, N. C., *Analyst* 2007, *132*, 979-982.
- [68] Urban, P. L., Goodall, D. M., Carvalho, A. Z., Bergstrom, E. T., Van Schepdael, A., Bruce, N. C., *Journal of Chromatography, A* 2008, *1206*, 52-63.
- [69] Lacroix, M., Poinot, V., Fournier, C., Couderc, F., *Electrophoresis* 2005, *26*, 2608-2621.
- [70] Garcia-Campana, A. M., Taverna, M., Fabre, H., *Electrophoresis* 2007, *28*, 208-232.
- [71] Lin, Y.-W., Chiu, T.-C., Chang, H.-T., *Journal of Chromatography, B: Analytical Technologies in the Biomedical and Life Sciences* 2003, *793*, 37-48.
- [72] Johnson, M. E., Landers, J. P., *Electrophoresis* 2004, *25*, 3513-3527.
- [73] Hapuarachchi, S., Janaway, G. A., Aspinwall, C. A., *Electrophoresis* 2006, *27*, 4052-4059.
- [74] Swearingen, K. E., Dickerson, J. A., Turner, E. H., Ramsay, L. M., Wojcik, R., Dovichi, N. J., *Journal of Chromatography, A* 2008, *1194*, 249-252.
- [75] Ramsay, L. M., Dickerson, J. A., Dada, O., Dovichi, N. J., *Analytical Chemistry* 2009, *81*, 1741-1746.
- [76] Klampfl, C. W., *Electrophoresis* 2006, *27*, 3-34.
- [77] Simpson, D. C., Smith, R. D., *Electrophoresis* 2005, *26*, 1291-1305.
- [78] Monton, M. R. N., Terabe, S., *Analytical Sciences* 2005, *21*, 5-13.
- [79] McGown, L. B., *Aptamers in Bioanalysis* 2009, 229-249.
- [80] Stutz, H., *Electrophoresis* 2005, *26*, 1254-1290.
- [81] Wehr, T., *LCGC North America* 2003, *21*, 974,976,978,980,982.

- [82] Huck, C. W., Bakry, R., Huber, L. A., Bonn, G. K., *Electrophoresis* 2006, 27, 2063-2074.
- [83] Schmitt-Kopplin, P., Englmann, M., *Electrophoresis* 2005, 26, 1209-1220.
- [84] Mao, X., Chu, I. K., Lin, B., *Electrophoresis* 2006, 27, 5059-5067.
- [85] Issaq, H. J., Janini, G. M., Chan, K. C., Veenstra, T. D., *Journal of Chromatography, A* 2004, 1053, 37-42.
- [86] Janini, G. M., Chan, K. C., Conrads, T. P., Issaq, H. J., Veenstra, T. D., *Electrophoresis* 2004, 25, 1973-1980.
- [87] Wu, Y.-T., Chen, Y.-C., *Analytical Chemistry* 2005, 77, 2071-2077.
- [88] Yue, G. E., Roper, M. G., Jeffery, E. D., Easley, C. J., Balchunas, C., Landers, J. P., Ferrance, J. P., *Lab on a Chip* 2005, 5, 619-627.
- [89] Dahlin, A. P., Wetterhall, M., Liljegren, G., Bergstroem, S. K., Andren, P., Nyholm, L., Markides, K. E., Bergquist, J., *Analyst* 2005, 130, 193-199.
- [90] Svedberg, M., Pettersson, A., Nilsson, S., Bergquist, J., Nyholm, L., Nikolajeff, F., Markides, K., *Analytical Chemistry* 2003, 75, 3934-3940.
- [91] Mellors, J. S., Gorbounov, V., Ramsey, R. S., Ramsey, J. M., *Analytical Chemistry* 2008, 80, 6881-6887.
- [92] Manz, A., Harrison, D. J., Verpoorte, E., Fettinger, J. C., Ludi, H., Widmer, H. M., *Journal of Chromatography* 1992, 593, 253-258.
- [93] Manz, A., Graber, N., Widmer, H. M., *Sensors and Actuators B* 1990, 1, 244-248.
- [94] Harrison, D. J., Manz, A., Fan, Z., Ludi, H., Widmer, H. M., *Analytical Chemistry* 1992, 64, 1926-1932.
- [95] Effenhauser, C. S., Bruin, G. J. M., Paulus, A., Ehrat, M., *Analytical Chemistry* 1997, 69, 3451-3457.
- [96] Duffy, D. C., McDonald, J. C., Schueller, O. J. A., Whitesides, G. M., *Analytical Chemistry* 1998, 70, 4974-4984.
- [97] Martynova, L., Locascio, L. E., Gaitan, M., Kramer, G. W., Christensen, R. G., MacCrehan, W. A., *Analytical Chemistry* 1997, 69, 4783-4789.
- [98] Galloway, M., Stryjewski, W., Henry, A., Ford, S. M., Llopis, S., McCarley, R. L., Soper, S. A., *Analytical Chemistry* 2002, 74, 2407-2415.
- [99] Barker, S. L. R., Tarlov, M. J., Canavan, H., Hickman, J. J., Locascio, L. E., *Analytical Chemistry* 2000, 72, 4899-4903.
- [100] Barker, S. L. R., Ross, D., Tarlov, M. J., Gaitan, M., Locascio, L. E., *Analytical Chemistry* 2000, 72, 5925-5929.
- [101] Liu, Y., Ganser, D., Schneider, A., Liu, R., Grodzinski, P., Krutchinina, N., *Analytical Chemistry* 2001, 73, 4196-4201.
- [102] Vreeland, W. N., Locascio, L. E., *Analytical Chemistry* 2003, 75, 6906-6911.
- [103] Henry, A. C., Waddell, E. A., Shreiner, R., Locascio, L. E., *Electrophoresis* 2002, 23, 791-798.
- [104] Malmstadt, N., Yager, P., Hoffman, A. S., Stayton, P. S., *Analytical Chemistry* 2003, 75, 2943-2949.
- [105] Giordano, B. C., Ferrance, J., Swedberg, S., Huhmer, A. F. R., Landers, J. P., *Analytical Biochemistry* 2001, 291, 124-132.

- [106] Yin, H., Killeen, K., Brennen, R., Sobek, D., Werlich, M., Van de Goor, T., *Analytical Chemistry* 2005, 77, 527-533.
- [107] Fiorini, G. S., Lorenz, R. M., Kuo, J. S., Chiu, D. T., *Analytical Chemistry* 2004, 76, 4697-4704.
- [108] Xu, W., Uchiyama, K., Shimosaka, T., Hobo, T., *Journal of Chromatography, A* 2001, 907, 279-289.
- [109] Kuo, J. S., Zhao, Y., Ng, L., Yen, G. S., Lorenz, R. M., Lim, D. S. W., Chiu, D. T., *Lab on a Chip* 2009, 9, 1951-1956.
- [110] Kuo, J. S., Ng, L., Yen, G. S., Lorenz, R. M., Schiro, P. G., Edgar, J. S., Zhao, Y., Lim, D. S. W., Allen, P. B., Jeffries, G. D. M., Chiu, D. T., *Lab on a Chip* 2009, 9, 870-876.
- [111] Ullsten, S., Zuberovic, A., Wetterhall, M., Hardenborg, E., Markides, K. E., Bergquist, J., *Electrophoresis* 2004, 25, 2090-2099.
- [112] Hardenborg, E., Zuberovic, A., Ullsten, S., Soderberg, L., Heldin, E., Markides, K. E., *Journal of Chromatography, A* 2003, 1003, 217-221.
- [113] Liu, Y., Fanguy, J. C., Bledsoe, J. M., Henry, C. S., *Analytical Chemistry* 2000, 72, 5939-5944.
- [114] Yang, T., Jung, S.-y., Mao, H., Cremer, P. S., *Analytical Chemistry* 2001, 73, 165-169.
- [115] Mendieta, M. E., Antonioli, P., Righetti, P. G., Citterio, A., Descroix, S., Sebastiano, R., *Electrophoresis* 2006, 27, 4016-4024.
- [116] Meagher, R. J., Seong, J., Laibinis, P. E., Barron, A. E., *Electrophoresis* 2004, 25, 405-414.
- [117] Jiang, T.-F., Gu, Y.-L., Liang, B., Li, J.-B., Shi, Y.-P., Ou, Q.-Y., *Analytica Chimica Acta* 2003, 479, 249-254.
- [118] Ullsten, S., Soederberg, L., Folestad, S., Markides, K. E., *Analyst* 2004, 129, 410-415.
- [119] Zuberovic, A., Ullsten, S., Hellman, U., Markides, K. E., Bergquist, J., *Rapid Communications in Mass Spectrometry* 2004, 18, 2946-2952.
- [120] Simo, C., Elvira, C., Gonzalez, N., San Roman, J., Barbas, C., Cifuentes, A., *Electrophoresis* 2004, 25, 2056-2064.
- [121] Gonzalez, N., Elvira, C., San Roman, J., Cifuentes, A., *Journal of Chromatography, A* 2003, 1012, 95-101.
- [122] Kitagawa, F., Kamiya, M., Okamoto, Y., Taji, H., Onoue, S., Tsuda, Y., Otsuka, K., *Analytical and Bioanalytical Chemistry* 2006, 386, 594-601.
- [123] Ocvirk, G., Munroe, M., Tang, T., Oleschuk, R., Westra, K., Harrison, D. J., *Electrophoresis* 2000, 21, 107-115.
- [124] Youssef Badal, M., Wong, M., Chiem, N., Salimi-Moosavi, H., Harrison, D. J., *Journal of Chromatography A* 2002, 947, 277-286.
- [125] Liu, Q., Li, Y., Tang, F., Ding, L., Yao, S., *Electrophoresis* 2007, 28, 2275-2282.
- [126] Wang, A.-J., Xu, J.-J., Chen, H.-Y., *Analytica Chimica Acta* 2006, 569, 188-194.

- [127] Baryla, N. E., Melanson, J. E., McDermott, M. T., Lucy, C. A., *Analytical Chemistry* 2001, 73, 4558-4565.
- [128] Righetti, P. G., Gelfi, C., Verzola, B., Castelletti, L., *Electrophoresis* 2001, 22, 603-611.
- [129] Roman, G. T., McDaniel, K., Culbertson, C. T., *Analyst* 2006, 131, 194-201.
- [130] Frankenfeld, C. N., Rosenbaugh, M. R., Fogarty, B. A., Lunte, S. M., *Journal of Chromatography, A* 2006, 1111, 147-152.
- [131] Lucy, C. A., Underhill, R. S., *Analytical Chemistry* 1996, 68, 300-305.
- [132] Wu, Y., Xie, J., Wang, F., Chen, Z., *Journal of Separation Science* 2008, 31, 814-823.
- [133] Huang, B., Kim, S., Wu, H., Zare, R. N., *Analytical Chemistry* 2007, 79, 9145-9149.
- [134] Mohamadi, M. R., Mahmoudian, L., Kaji, N., Tokeshi, M., Baba, Y., *Electrophoresis* 2007, 28, 830-836.
- [135] Liu, J., Lee, M. L., *Electrophoresis* 2006, 27, 3533-3546.
- [136] Iki, N., Yeung, E. S., *Journal of Chromatography, A* 1996, 731, 273-282.
- [137] He, Y., Yeung, E. S., *Journal of Proteome Research* 2002, 1, 273-277.
- [138] Hjerten, S., *Journal of Chromatography* 1985, 347, 191-198.
- [139] Bousse, L., Mouradian, S., Minalla, A., Yee, H., Williams, K., Dubrow, R., *Analytical Chemistry* 2001, 73, 1207-1212.
- [140] Belder, D., Deege, A., Husmann, H., Koehler, F., Ludwig, M., *Electrophoresis* 2001, 22, 3813-3818.
- [141] Verzola, B., Gelfi, C., Righetti, P. G., *Journal of Chromatography, A* 2000, 874, 293-303.
- [142] Makamba, H., Kim, J. H., Lim, K., Park, N., Hahn, J. H., *Electrophoresis* 2003, 24, 3607-3619.
- [143] Wang, B., Chen, L., Abdulali-Kanji, Z., Horton, J. H., Oleschuk, R. D., *Langmuir* 2003, 19, 9792-9798.
- [144] Wang, B., Abdulali-Kanji, Z., Dodwell, E., Horton, J. H., Oleschuk, R. D., *Electrophoresis* 2003, 24, 1442-1450.
- [145] Wang, B., Oleschuk, R. D., Horton, J. H., *Langmuir* 2005, 21, 1290-1298.
- [146] Xiao, D., Van Le, T., Wirth, M. J., *Analytical Chemistry* 2004, 76, 2055-2061.
- [147] Xiao, D., Zhang, H., Wirth, M., *Langmuir* 2002, 18, 9971-9976.
- [148] Hu, S., Ren, X., Bachman, M., Sims, C. E., Li, G. P., Allbritton, N., *Electrophoresis* 2003, 24, 3679-3688.
- [149] Hu, S., Ren, X., Bachman, M., Sims, C. E., Li, G. P., Allbritton, N. L., *Analytical Chemistry* 2004, 76, 1865-1870.
- [150] Hu, S., Ren, X., Bachman, M., Sims, C. E., Li, G. P., Allbritton, N., *Analytical Chemistry* 2002, 74, 4117-4123.
- [151] Sun, X., Li, D., Lee, M. L., *Analytical Chemistry* 2009, 81, 6278-6284.
- [152] Henry, A. C., Tutt, T. J., Galloway, M., Davidson, Y. Y., McWhorter, C. S., Soper, S. A., McCarley, R. L., *Analytical Chemistry* 2000, 72, 5331-5337.
- [153] Liu, J., Pan, T., Woolley, A. T., Lee, M. L., *Analytical Chemistry* 2004, 76, 6948-6955.

- [154] Wang, J., Muck, A., Jr., Chatrathi, M. P., Chen, G., Mittal, N., Spillman, S. D., Obeidat, S., *Lab on a Chip* 2005, 5, 226-230.
- [155] Tiselius, A., *Biochemical Journal* 1937, 31, 313-317.
- [156] Tiselius, A., *Journal of Experimental Medicine* 1937, 65, 641-646.
- [157] Tiselius, A., *Transactions of the Faraday Society* 1937, 33, 524-531.
- [158] Coltro, W. K. T., Lunte, S. M., Carrilho, E., *Electrophoresis* 2008, 29, 4928-4937.
- [159] Legendre, B. L., Jr., Moberg, D. L., Williams, D. C., Soper, S. A., *Journal of Chromatography A* 1997, 779, 185-194.
- [160] Huynh, B. H., Fogarty, B. A., Nandi, P., Lunte, S. M., *Journal of Pharmaceutical and Biomedical Analysis* 2006, 42, 529-534.
- [161] Deckel, A. W., Elder, R., Fuhrer, G., *NeuroReport* 2002, 13, 707-711.
- [162] Means, A. R., Dedman, J. R., *Nature* 1980, 285, 73-77.
- [163] Wayman, G. A., Lee, Y.-S., Tokumitsu, H., Silva, A., Soderling, T. R., *Neuron* 2008, 59, 914-931.
- [164] Manabe, T., *Brain and Nerve* 2008, 60, 707-715.
- [165] Swulius, M. T., Waxham, M. N., *Cellular and Molecular Life Sciences* 2008, 65, 2637-2657.
- [166] Cheung, W. Y., *Science (New York, N.Y.)* 1980, 207, 19-27.
- [167] Cheung, W. Y., *Harvey lectures* 1983, 79, 173-216.
- [168] Kennedy, M. B., *Trends in Neurosciences* 1989, 12, 417-420.
- [169] Hait, W. N., Lazo, J. S., *Journal of clinical oncology : official journal of the American Society of Clinical Oncology* 1986, 4, 994-1012.
- [170] Hait, W. N., *Anti-Cancer Drug Design* 1987, 2, 139-149.
- [171] Terabe, S., Otsuka, K., Ichikawa, K., Tsuchiya, A., Ando, T., *Analytical Chemistry* 1984, 56, 111-113.
- [172] Terabe, S., Otsuka, K., Ando, T., *Analytical Chemistry* 1985, 57, 834-841.
- [173] Terabe, S., Ozaki, H., Otsuka, K., Ando, T., *Journal of Chromatography* 1985, 332, 211-217.
- [174] Nishi, H., Tsumagari, N., Terabe, S., *Analytical Chemistry* 1989, 61, 2434-2439.
- [175] Ma, L., Kang, J., *Journal of Separation Science* 2008, 31, 888-892.
- [176] Otsuka, K., Terabe, S., *Journal of Chromatography* 1990, 515, 221-226.
- [177] Otsuka, K., Terabe, S., *Methods in Molecular Biology* 2004, 243, 355-363.
- [178] Herrero, M., Ibanez, E., Martin-Alvarez Pedro, J., Cifuentes, A., *Analytical Chemistry* 2007, 79, 5071-5077.
- [179] Ong, C. P., Ng, C. L., Chong, N. C., Lee, H. K., Li, S. F. Y., *Journal of Chromatography* 1990, 516, 263-270.
- [180] Otsuka, K., Terabe, S., Ando, T., *Journal of Chromatography* 1985, 348, 39-47.
- [181] Shen, S., Li, Y., Wakida, S.-i., Takeda, S., *Environmental Monitoring and Assessment* 2009, 153, 201-208.
- [182] Silva, C. A., Pereira, E. A., Micke, G. A., Farah, J. P. S., Tavares, M. F. M., *Electrophoresis* 2007, 28, 3722-3730.

- [183] Kartsova, L. A., Bessonova, E. A., *Journal of Analytical Chemistry* 2007, 62, 68-75.
- [184] Nishi, H., Tsumagari, N., Kakimoto, T., Terabe, S., *Journal of Chromatography* 1989, 465, 331-343.
- [185] Pedersen-Bjergaard, S., Naess, O., Moestue, S., Rasmussen, K. E., *Journal of chromatography A* 2000, 876, 201-211.
- [186] Nishi, H., Tsumagari, N., Kakimoto, T., Terabe, S., *Journal of Chromatography* 1989, 477, 259-270.
- [187] Nishi, H., Terabe, S., *Electrophoresis* 1990, 11, 691-701.
- [188] Rabel, S. R., Stobaugh, J. F., *Pharmaceutical research* 1993, 10, 171-186.
- [189] Kartsova, L. A., Ganzha, O. V., *Journal of Analytical Chemistry* 2009, 64, 518-523.
- [190] Tseng, H.-M., Barrett, D. A., *Journal of Chromatography A* 2009, 1216, 3387-3391.
- [191] Powell, P. R., Paxon, T. L., Han, K.-A., Ewing, A. G., *Analytical Chemistry* 2005, 77, 6902-6908.
- [192] Hapuarachchi, S., Janaway, G. A., Aspinwall, C. A., *Electrophoresis* 2006, 27, 4052-4059.
- [193] Iadarola, P., Ferrari, F., Fumagalli, M., Viglio, S., *Electrophoresis* 2008, 29, 224-236.
- [194] Hogan, B. L., Lunte, S. M., Stobaugh, J. F., Lunte, C. E., *Analytical Chemistry* 1994, 66, 596-602.
- [195] Xu, B., Feng, X., Xu, Y., Du, W., Luo, Q., Liu, B.-F., *Analytical and Bioanalytical Chemistry* 2009, 394, 1911-1917.
- [196] Ruta, J., Perrier, S., Ravelet, C., Roy, B., Perigaud, C., Peyrin, E., *Analytical Chemistry* 2009, 81, 1169-1176.
- [197] Zanone, C., Chiarelli, L. R., Valentini, G., Perani, E., Annovazzi, L., Viglio, S., Iadarola, P., *Electrophoresis* 2004, 25, 3270-3276.
- [198] Elisabeth, P., Yoshioka, M., Sasaki, T., Senda, M., *Journal of Chromatography, A* 1998, 806, 199-207.
- [199] Savard, J. M., Grosser, S. T., Schneider, J. W., *Electrophoresis* 2008, 29, 2779-2789.
- [200] Wang, W., Zhou, L., Wang, S., Luo, Z., Hu, Z., *Talanta* 2008, 74, 1050-1055.
- [201] Cornelius, M. G., Schmeiser, H. H., *Electrophoresis* 2007, 28, 3901-3907.
- [202] Geldart, S. E., Brown, P. R., *Journal of Chromatography A* 1998, 828, 317-336.
- [203] Wu, Y., Xie, J., Wang, F., Chen, Z., *Journal of Separation Science* 2009, 32, 437-440.
- [204] Kasicka, V., *Electrophoresis* 2008, 29, 179-206.
- [205] Huang, J., Kang, J., *Journal of Chromatography, B: Analytical Technologies in the Biomedical and Life Sciences* 2007, 846, 364-367.
- [206] Foley, J. P., *Analytical Chemistry* 1990, 62, 1302-1308.
- [207] Terabe, S., *Annual Review of Analytical Chemistry* 2009, 2, 99-120.
- [208] Silva, M., *Electrophoresis* 2009, 30, 50-64.

- [209] Terabe, S., *Handbook of Capillary and Microchip Electrophoresis and Associated Microtechniques (3rd Edition)* 2008, 109-133.
- [210] Kitagawa, F., Otsuka, K., *Journal of Separation Science* 2008, 31, 794-802.
- [211] Glavac, N. K., Injac, R., Kreft, S., *Chromatographia* 2009, 70, 1473-1478.
- [212] Roman, G. T., Carroll, S., McDaniel, K., Culbertson, C. T., *Electrophoresis* 2006, 27, 2933-2939.
- [213] Shadpour, H., Soper, S. A., *Analytical Chemistry* 2006, 78, 3519-3527.
- [214] Salas-Solano, O., Felten, C., *Separation Science and Technology* 2008, 9, 401-424.
- [215] Hunt, G., Nashabeh, W., *Analytical Chemistry* 1999, 71, 2390-2397.
- [216] Cohen, A. S., Karger, B. L., *Journal of Chromatography* 1987, 397, 409-417.
- [217] Widhalm, A., Schwer, C., Blaas, D., Kenndler, E., *Journal of Chromatography* 1991, 549, 446-451.
- [218] Wu, D., Regnier, F. E., *Journal of Chromatography* 1992, 608, 349-356.
- [219] Ganzler, K., Greve, K. S., Cohen, A. S., Karger, B. L., Guttman, A., Cooke, N. C., *Analytical Chemistry* 1992, 64, 2665-2671.
- [220] Hunt, G., Nashabeh, W., *Analytical Chemistry* 1999, 71, 2390-2397.
- [221] Wehr, T., *LCGC North America* 2005, 23, 676, 678-681.
- [222] Hunt, G., Nashabeh, W., *Analytical Chemistry* 1999, 71, 2390-2397.
- [223] Lee, H. G., *Journal of Immunological Methods* 2000, 234, 71-81.
- [224] Quigley, W. W. C., Dovichi, N. J., *Analytical Chemistry* 2004, 76, 4645-4658.
- [225] Han, M., Phan, D., Nightlinger, N., Taylor, L., Jankhah, S., Woodruff, B., Yates, Z., Freeman, S., Guo, A., Balland, A., Pettit, D., *Chromatographia* 2006, 64, 335-342.
- [226] Schure, M. R., Murphy, R. E., Klotz, W. L., Lau, W., *Analytical Chemistry* 1998, 70, 4985-4995.
- [227] Schaeper, J. P., Sepaniak, M. J., *Electrophoresis* 2000, 21, 1421-1429.
- [228] Cooper, J. W., Wang, Y., Lee, C. S., *Electrophoresis* 2004, 25, 3913-3926.
- [229] Salas-Solano, O., Felten, C., *Separation Science and Technology* 2008, 9, 401-424.
- [230] Guttman, A., Nolan, J., *Analytical Biochemistry* 1994, 221, 285-289.
- [231] Rustandi, R. R., Washabaugh, M. W., Wang, Y., *Electrophoresis* 2008, 29, 3612-3620.
- [232] Michels, D. A., Brady, L. J., Guo, A., Balland, A., *Analytical Chemistry (Washington, DC, United States)* 2007, 79, 5963-5971.
- [233] Blazek, V., Caldwell, R. A., *International Journal of Food Science and Technology* 2009, 44, 2127-2134.
- [234] Kolin, A., *Journal of Chemical Physics* 1954, 22, 1628-1629.
- [235] Svensson, H., *Acta Chemica Scandinavica* 1961, 15, 325-341.
- [236] Vesterberg, O., Svensson, H., *Acta Chemica Scandinavica* 1966, 20, 820-834.
- [237] Bjellqvist, B., Ek, K., Righetti, P. G., Gianazza, E., Goerg, A., Westermeier, R., Postel, W., *Journal of Biochemical and Biophysical Methods* 1982, 6, 317-339.
- [238] Gianazza, E., Dossi, G., Celentano, F., Righetti, P. G., *Journal of Biochemical and Biophysical Methods* 1983, 8, 109-133.

- [239] Hjerten, S., Zhu, M. D., *Journal of Chromatography* 1985, 346, 265-270.
- [240] Mao, Q., Pawliszyn, J., *Journal of Biochemical and Biophysical Methods* 1999, 39, 93-110.
- [241] Sommer, G. J., Hatch, A. V., *Electrophoresis* 2009, 30, 742-757.
- [242] Kilar, F., *Electrophoresis* 2003, 24, 3908-3916.
- [243] Silvertand, L. H. H., Torano, J. S., van Bennekom, W. P., de Jong, G. J., *Journal of Chromatography A* 2008, 1204, 157-170.
- [244] Shimura, K., *Electrophoresis* 2009, 30, 11-28.
- [245] Kitagawa, F., Aizawa, S., Otsuka, K., *Analytical Sciences* 2009, 25, 979-984.
- [246] Yao, B., Yang, H., Liang, Q., Luo, G., Wang, L., Ren, K., Gao, Y., Wang, Y., Qiu, Y., *Analytical Chemistry* 2006, 78, 5845-5850.
- [247] Salas-Solano, O., Felten, C., *Separation Science and Technology* 2008, 9, 401-424.
- [248] Vlckova, M., Kalman, F., Schwarz, M. A., *Journal of Chromatography A* 2008, 1181, 145-152.
- [249] Apostol, I., Miller, K. J., Ratto, J., Kelner, D. N., *Analytical Biochemistry* 2009, 385, 101-106.
- [250] Chu, Y. H., Avila, L. Z., Biebuyck, H. A., Whitesides, G. M., *Journal of Medicinal Chemistry* 1992, 35, 2915-2917.
- [251] Carpenter, J. L., Camilleri, P., Dhanak, D., Goodall, D., *Journal of the Chemical Society, Chemical Communications* 1992, 804-806.
- [252] Chu, Y. H., Whitesides, G. M., *Journal of Organic Chemistry* 1992, 57, 3524-3525.
- [253] Kiessig, S., Thuncke, F., *Drugs and the Pharmaceutical Sciences* 2003, 128, 211-241.
- [254] Pierceall, W. E., Zhang, L., Hughes, D. E., *Methods in Molecular Biology (Totowa, NJ, United States)* 2004, 261, 187-197.
- [255] Nguyen, A., Moini, M., *Analytical Chemistry* 2008, 80, 7169-7173.
- [256] Phillips, T. M., Wellner, E. F., *Electrophoresis* 2007, 28, 3041-3048.
- [257] Zavaleta, J., Chinchilla, D., Gomez, A., Silverio, C., Azad, M., Gomez, F. A., *Methods in Molecular Biology* 2008, 384, 647-660.
- [258] Gomez, F. A., Avila, L. Z., Chu, Y.-H., Whitesides, G. M., *Analytical Chemistry* 1994, 66, 1785-1791.
- [259] Azad, M., Kaddis, J., Villareal, V., Hernandez, L., Silverio, C., Gomez, F. A., *Methods in Molecular Biology* 2004, 276, 153-168.
- [260] Zhang, L.-W., Ding, L., Zhang, X.-X., *Analytical and Bioanalytical Chemistry* 2007, 387, 2833-2841.
- [261] Yang, P., Whelan, R. J., Mao, Y., Lee, A. W. M., Carter-Su, C., Kennedy, R. T., *Analytical Chemistry* 2007, 79, 1690-1695.
- [262] Saito, K., Yokoyama, S., Hirota, H., *Peptide Science* 2005, 41st, 201-202.
- [263] Gong, M., Nikcevic, I., Wehmeyer, K. R., Limbach, P. A., Heineman, W. R., *Electrophoresis* 2008, 29, 1415-1422.
- [264] Krylov, S. N., *Aptamers in Bioanalysis* 2009, 183-212.
- [265] Linscheid, M. W., *Drugs and the Pharmaceutical Sciences* 2003, 128, 243-264.

- [266] Wan, H., Bergstroem, F., *Journal of Liquid Chromatography & Related Technologies* 2007, 30, 681-700.
- [267] Liu, X., Dahdouh, F., Salgado, M., Gomez, F. A., *Journal of Pharmaceutical Sciences* 2009, 98, 394-410.
- [268] Moser, A. C., Hage, D. S., *Electrophoresis* 2008, 29, 3279-3295.
- [269] Zavaleta, J., Chinchilla, D., Brown, A., Ramirez, A., Calderon, V., Sogomonyan, T., Gomez, F. A., *Current Analytical Chemistry* 2006, 2, 35-42.
- [270] Vlckova, M., Stettler, A., Schwarz, M., *Journal of Liquid Chromatography & Related Technologies* 2006, 29, 1047-1076.
- [271] Kuehn, A., Kiessig, S., Thunecke, F., *Drugs and the Pharmaceutical Sciences* 2003, 128, 303-327.
- [272] Gong, M., Nikcevic, I., Wehmeyer, K. R., Limbach, P. A., Heineman, W. R., *Electrophoresis* 2008, 29, 1415-1422.
- [273] Stettler, A. R., Krattiger, P., Wennemers, H., Schwarz, M. A., *Electrophoresis* 2007, 28, 1832-1838.
- [274] Giovannoli, C., Baggiani, C., Anfossi, L., Giraudi, G., *Electrophoresis* 2008, 29, 3349-3365.
- [275] Schmerr, M. J., Goodwin, K. R., Cutlip, R. C., *Journal of Chromatography A* 1994, 680, 447-453.
- [276] Yang, W.-C., Schmerr, M. J., Jackman, R., Bodemer, W., Yeung, E. S., *Analytical Chemistry* 2005, 77, 4489-4494.
- [277] Alper, B. J., Schmidt, W. K., *Journal of Neuroscience Methods* 2009, 178, 40-45.
- [278] Nordberg, A., *European journal of nuclear medicine and molecular imaging* 2008, 35 Suppl 1, S46-50.
- [279] Mucke, L., *Nature* 2009, 461, 895-897.
- [280] Sabella, S., Quaglia, M., Lani, C., Racchi, M., Govoni, S., Caccialanza, G., Calligaro, A., Bellotti, V., De Lorenzi, E., *Electrophoresis* 2004, 25, 3186-3194.
- [281] Fang, X., Wang, W., Yang, L., Chandrasekaran, K., Kristian, T., Balgley, B. M., Lee, C. S., *Electrophoresis* 2008, 29, 2215-2223.
- [282] Greaves, L. C., Turnbull, D. M., *Biochimica et Biophysica Acta, General Subjects* 2009, 1790, 1015-1020.
- [283] Wallace, D. C., Fan, W., *Genes & Development* 2009, 23, 1714-1736.
- [284] Zuberovic, A., Wetterhall, M., Hanrieder, J., Bergquist, J., *Electrophoresis* 2009, 30, 1836-1843.
- [285] Rudnev, A. V., Foteeva, L. S., Kowol, C., Berger, R., Jakupec, M. A., Arion, V. B., Timerbaev, A. R., Keppler, B. K., *Journal of Inorganic Biochemistry* 2006, 100, 1819-1826.
- [286] Polec-Pawlak, K., Abramski, J. K., Semenova, O., Hartinger, C. G., Timerbaev, A. R., Keppler, B. K., Jarosz, M., *Electrophoresis* 2006, 27, 1128-1135.
- [287] Hartinger, C. G., Hann, S., Koellensperger, G., Sulyok, M., Groessl, M., Timerbaev, A. R., Rudnev, A. V., Stingeder, G., Keppler, B. K., *International Journal of Clinical Pharmacology and Therapeutics* 2005, 43, 583-585.

- [288] Timerbaev, A. R., Rudnev, A. V., Semenova, O., Hartinger, C. G., Keppler, B. K., *Analytical Biochemistry* 2005, *341*, 326-333.
- [289] Zhou, D., Wang, H., Li, F., *Zhongguo Yaoke Daxue Xuebao* 2005, *36*, 36-39.
- [290] Sun, H., He, P., *Chromatographia* 2008, *68*, 969-975.
- [291] Aaron, J.-J., Trajkovska, S., *Current Drug Targets* 2006, *7*, 1067-1081.
- [292] Martinez-Gomez, M. A., Sagrado, S., Villanueva-Camanas, R. M., Medina-Hernandez, M. J., *Electrophoresis* 2006, *27*, 3410-3419.
- [293] Nguyen, A., Moini, M., *Analytical Chemistry* 2008, *80*, 7169-7173.
- [294] Pisitkun, T., Johnstone, R., Knepper, M. A., *Molecular and Cellular Proteomics* 2006, *5*, 1760-1771.
- [295] Theodorescu, D., Fliser, D., Wittke, S., Mischak, H., Krebs, R., Walden, M., Ross, M., Eltze, E., Bettendorf, O., Wulfing, C., Semjonow, A., *Electrophoresis* 2005, *26*, 2797-2808.
- [296] Mussap, M., Ponchia, S., Zaninotto, M., Varagnolo, M., Plebani, M., *Clinical Biochemistry* 2006, *39*, 152-159.

Chapter 7

Development of an Electrophoretic Immunoaffinity Assay for myc-Tagged Proteins: Application to Mutant Huntingtin Protein

(Journal of Neuroscience Methods, In preparation)

7.1 Introduction

Huntington's disease (HD) is an autosomal dominant neurodegenerative disorder that affects an estimated 30,000 people in the United States alone [1]. Named for George Huntington, the physician who first described the illness in 1872, HD is also called Huntington's chorea which refers to the involuntary, jerky movements that develop in later stages of the disorder. The clinical symptoms of HD are associated with mental as well as physical impairment. Physical symptoms include loss of coordination and balance, slurred speech, and development of involuntary movements. Cognitive abilities such as judgment and memory are also diminished, which ultimately leads to dementia.

HD is one of nine disorders caused by an abnormal, and unstable CAG trinucleotide-repeat in the gene encoding the huntingtin protein [2]. Although huntingtin protein is ubiquitously expressed, the striatum and cortex regions of the brain are selectively vulnerable to neurodegeneration and atrophy [3]. Amino-terminal fragments of mutant huntingtin protein (mHtt) containing an expanded glutamine repeat have been shown to form insoluble deposits in neurons in these brain regions [4]. Although mutant huntingtin protein is an approx 350 kilodalton (kDa) protein that is largely cytosolic in nature, the subcellular locations of these deposits are dependent on the size of the protein. Full length mHtt and smaller fragments have been shown to accumulate in the plasma membrane, mitochondria, Golgi, nucleus, endoplasmic reticulum (ER), and axon terminals [5-12].

Wild type huntingtin, which contains <35 N-terminal poly-glutamine repeats, is expressed in all humans and causes no symptoms of the disease. Individuals with an intermediate number of glutamine repeats (36–39) have been shown to exhibit incomplete penetrance. This means that some individuals will develop HD whereas others will not. Those with 40 or more glutamine repeats have been shown to exhibit HD with full penetrance and progressively worse symptoms with the number of repeats [13]. In addition, there is an inverse relationship between the number of glutamine repeats and the age of onset of disease symptoms. A greater number of repeats results in a decreased age of onset and increased severity of symptoms.

While much is known about the huntingtin protein itself and the multiple cellular components with which it associates, very little is known about the normal function(s) of huntingtin and the neurotoxic function(s) of mutant huntingtin. There has been much debate as to whether the expression of mHtt causes a toxic loss-of-function or a toxic gain-of-function. However, since the discovery of the gene that causes HD in 1993, much of the research indicates that neurodegeneration is caused by a toxic gain-of-function. Some of the proposed mechanisms associated with a neurotoxic gain-of-function include transcriptional modulation [14-17], protein aggregation [18-21], and excitotoxicity [22-23]. Transgenic mouse models expressing either full length or truncated versions of mHtt have been shown to produce neuropathology resembling the human disorder and have helped provide support for the toxic gain-of-function hypothesis [24]. Furthermore, recent research has implicated the excitatory amino acids glutamate and aspartate in the

neurodegeneration associated with HD. The upregulation and excessive activation of N-methyl-D-aspartate (NMDA) receptors has been shown to lead to the excitotoxic death of medium-sized spiny striatal neurons in mouse models of HD [25-27].

Although the majority of the findings are consistent with a toxic gain-of-function, there is also evidence that neurodegeneration in HD is caused by a toxic loss-of-function. For example, the expression and transport of brain-derived neurotrophic factor (BDNF) has been shown to require Htt. However, Zuccato *et al.* has demonstrated that BDNF expression and trafficking within neurons is impaired in mouse models of HD [28]. In addition, Deckel and co-workers have demonstrated widespread disturbances in many calcium-dependent proteins in a mouse model of HD [29]. The authors determined that the expression levels of Ca⁺²-calmodulin (CaM) dependent phosphodiesterase, calcineurin, CaM kinase II, CaM kinase IV, and neuronal nitric oxide synthase (nNOS) are all decreased in late-state HD. CaM-kinases are signaling proteins that regulate a variety of processes including the transcription factor CREB (cyclic AMP response element binding protein) and CREM (cyclic AMP response element modulator). nNOS is an enzyme responsible for the synthesis of nitric oxide (NO) which is a potent signaling molecule involved in long term potentiation (LTP) [30-31], neurotransmission [32-34], and cerebral blood flow [35-37]. Therefore, it is believed that the dysregulation and diminished expression levels of these essential proteins contribute to the neurodegenerative effects observed in HD.

While many research labs have dedicated vast amounts of resources to investigate this disease, a definitive cure remains elusive. The majority of published reports have investigated the molecular pathways of HD through the isolation, detection, or quantitation of huntingtin protein. Some of the most popular analysis methods include gel electrophoresis [38-39], immunoblotting [5, 40-42], immunofluorescence [5, 43-45], and HPLC with MS detection, [46-48]. Although these analysis methods can be sensitive, highly selective, and are well characterized, they are often time consuming and labor intensive. Traditional Western blot analysis uses large volumes of reagents and solutions and may take as long as 36 hr to yield results. In addition, many gradient elution methods for HPLC are as long as 2 hr for complex protein samples. Capillary electrophoresis (CE) is high throughput method which has been shown to be ideally suited for the separation of protein mixtures [49-51]. Surprisingly, no published reports exist which describe the use of CE for the detection of huntingtin protein. The only application of CE for the investigation of HD demonstrated the separation of oligonucleotides for the determination of CAG repeats [52-53].

The present study describes the development and evaluation of capillary and microchip electrophoresis methodology with laser induced fluorescence (LIF) detection for the detection of mutant huntingtin protein. Two separate, but related, analytical strategies were developed for the determination of mHtt isolated from cells in culture. Naphthalene 2,3-dicarboxaldehyde (NDA) was employed to derivatize mHtt with a fluorescent label for direct LIF detection. Alternatively, an

immunoaffinity technique was developed through the use of a fluorescently labeled monoclonal antibody (mAb) specific for myc-tagged proteins. The utility of this method was demonstrated through the analysis of mutant huntingtin protein expressed in cells culture. Both of these methodologies were developed and optimized for CE as well as microchip electrophoresis. The results obtained from these experiments were directly compared to those obtained using conventional Western blot analysis. Analytical parameters such as selectivity, sensitivity, limit of detection (LOD) are directly compared. In addition, factors such as reagent and sample consumption, time of analysis, and ease of implementation are discussed.

7.2 Materials and Methods

7.2.1 Materials and Reagents

The following chemicals were used as received: Fluorescein isothiocyanate-labeled mouse anti-myc monoclonal antibody, Novex tricine 10x running buffer, OptiMEM reduced serum medium, fetal bovine serum, and Lipofectamine Plus (Invitrogen, Carlsbad, CA, USA); bicinchoninic acid (BCA) protein assay (Pierce, Rockford, IL, USA); bis-acrylamide, glycerol, glycine, bromophenol blue (2% solution in ethanol), 2-mercaptoethanol (BME), tetramethylethylenediamine (TEMED), 0.1% Tween 20 and 20x tris-buffered saline (TBS) (AMRESCO, Solon, OH, USA); sodium dodecyl sulfate (SDS), ammonium persulfate (APS), methanol (MeOH), 2-propanol (IPA), acetone, 30% H₂O₂, H₂SO₄, HNO₃, and HCl (Fisher Scientific, Fairlawn, NJ, USA); non-fat dry milk (Best Choice, Kansas City, KS,

USA); nitrocellulose membrane (BioRad, Hercules, CA, USA); horseradish peroxidase-conjugated goat, anti-mouse antibody (Jackson ImmunoResearch, West Grove, PA, USA); enhanced chemiluminescence (ECL) Western blotting detection reagents (Amersham Biosciences, Piscataway, NJ, USA); 75 μm internal diameter (i.d.) x 365 μm outside diameter (o.d.) fused silica capillary tubing (Polymicro Technologies, Phoenix, AZ, USA); SU-8 10 negative photoresist and SU-8 developer (MicroChem Corp., Newton, MA, USA); 100 mm and 127 mm Si wafers (Silicon, Inc., Boise, ID, USA); Sylgard 184 (Ellsworth Adhesives, Germantown, WI, USA); naphthalene 2,3-dicarboxaldehyde (NDA) (Molecular Probes, Eugene, OR, USA); sodium cyanide, NaCl, MgCl_2 , tergitol-type NP-40 (NP-40), EDTA, protease inhibitor cocktail, formic acid, acetonitrile, 1 N NaOH, boric acid (BA), urea, trizma base (Tris), and Kodak Biomax XAR film (Sigma-Aldrich, St. Louis, MO, USA). In addition, the following were utilized: 1 mL syringes and Pt wire (22 gauge) (Fisher Scientific, Fairlawn, New Jersey, USA); 0.22 μm Teflon filters (Osmonics, Inc., Minnetonka, MN, USA); 18.2 M Ω water (Millipore, Kansas City, MO, USA).

7.2.2 Cell Culture System

The culture human embryonic kidney (HEK) 293T cells and transfection with mutant Huntington (mHtt) has been described previously [40]. Briefly, in the presence of 5% CO_2 at 37 °C, HEK-293T cells were grown in OptiMEM reduced serum medium containing nonessential amino acids, antimycotic, antibiotic agents, and 10% fetal bovine serum. Cells were grown to 80% to 90% confluency and

transfected with one of two vectors using Lipofectamine Plus. An empty vector was used to create a vector control (VC) cell population, while the N-terminal huntingtin fragment containing 148 polyglutamine repeats (htt-N63-148Q) was used to create the mutant huntingtin transfected cell population. The huntingtin vector also contained a sequence coding for the myc-tag amino acid sequence EQKLISEEDL. Forty-eight hours after transfection cells were harvested using a sterilized cell scraper and resuspended in lysis buffer containing 50 mM Tris-HCl, pH 8.8, 100 mM NaCl, 5 mM MgCl₂, 0.05% NP-40, 1 mM of EDTA, and 1:1000 protease inhibitor mixture. To ensure complete cell lysis, the cell mixture was allowed to react for 30 min on ice. Following the determination of the protein concentration by BCA assay, samples containing three different protein quantities were prepared. Cell lysates containing 200, 400, and 800 μ g of total protein from both the VC and mHtt transfected cells were loaded into separate microcentrifuge tubes. Insoluble fractions were prepared by centrifuging the cell lysates at 12,000 x g for 5 minutes. The supernatant was then removed and stored until further use. The pellet was then resuspended in 95% formic acid and incubated at 37 °C until dissolved (~40 minutes). Formic acid was then removed using a rotary speed vacuum [54]. The pellets were then resuspended in 150 μ L of buffer (10 mM Tris-HCl, 140 mM NaCl, pH 7.5) and sonicated (Fisher ultrasonic homogenizer, 130 watts, 20 kHz, amp 30%, 5 sec \times 20 pulses) until the pellet was completely dissolved. Samples were stored at -80 °C until the day of use.

7.2.3 Immunoblot Procedure

Proteins were separated on a 12% sodium dodecyl sulfate-polyacrylamide gel which was prepared according to Table 7.1. For immunoblots, the following sample volumes were used: 40 μL of insoluble mHtt, 16 μL soluble mHtt, and 6 μL of molecular weight (MW) marker. Gels were run at 200 V for approximately 1 to 1.5 hr or until the MW marker reached the bottom of the gel. Following electrophoresis, the gels were transferred to a container and washed in transfer buffer (2:7:1 MeOH, 18.2 M Ω H₂O, and 10x transfer buffer respectively) for 10 min with mild agitation to remove excess SDS. The 10x transfer buffer solution consisted of 250 mM Tris-base and 1.92 M glycine in 18.2 M Ω H₂O. Subsequently, the gel was brought into contact with a nitrocellulose membrane, placed in an electrophoresis module assembly and proteins were transferred to the membrane through the application of 100 V for 2 hr.

Following transfer, the nitrocellulose membrane was placed in a container and incubated in blotto solution (5 % non-fat dry milk, 0.1% Tween 20, 1x TBS) on a shaker to block non-specific interactions. After 1 hr, the blotto solution was removed and primary (1^o) antibody was added to the membrane. For all data reported, the 1^o antibody used was a mouse anti-myc monoclonal antibody (mAb) directed against the amino acid sequence EQKLISEEDL which was diluted 1:1000 in antibody buffer (1% non-fat dry milk, 0.1% Tween 20, 1x TBS buffer). The membrane and antibody were incubated overnight at 4 °C with mild agitation to promote binding. The next morning, the antibody solution was removed and the membrane was washed three times for 5 min each in wash buffer (0.1% Tween 20, 1x TBS buffer) to remove

Table 7.1: Materials Needed to Make Resolving Gel			
Reagent	Volume (mL) Needed to Make <i>N</i>		
	1.5 mm Gels		
	1	2	4
18.2 MΩ water	0.95	0.19	0.38
10 M Urea	4.8	9.5	19
40% Acrylamide	3.13	6.25	12.5
2 M Tris, pH 8.7	1.88	3.75	7.5
10% SDS	0.1	0.2	0.4
10% APS	0.05	0.1	0.2
TEMED	0.004	0.008	0.016
Total Volume	10	20	40

excess (unbound) 1° mAb. The membrane was then incubated with goat, anti-mouse secondary (2°) antibody conjugated to horseradish peroxidase for 1 hr at room temperature on a shaker. Signal was detected using enhanced chemiluminescence Western blotting detection reagents which were allowed to react with the 2° for exactly 1.0 min. In a dark room, Kodak XAR film was then placed over the membrane for exposure and detection of the protein bands.

7.2.4 Sample Preparation

7.2.4.1 Sample Derivatization Using NDA/CN⁻

The use of naphthalene 2,3-dicarboxaldehyde (NDA) and cyanide ion (CN⁻) in the presence of primary amines has previously been shown to yield fluorescent 1-cyanobenz(f)isoindole (CBI) derivatives [55-57]. This fluorogenic reaction was utilized to derivatize the samples collected from both the VC and mHtt transfected cells. The reaction was accomplished by adding 5.0 μL of the desired sample to 2.5 μL of 14 mM NDA in 100% acetonitrile (ACN), 5.0 μL of 10 mM NaCN in 50 mM boric acid (BA) pH 9.2, and 5.0 μL of 25 mM BA pH 9.2 in a microcentrifuge tube. After mixing, the reaction was carried out in the dark for 20 min at room temperature. After 20 min, samples for electrophoresis were prepared by performing a 1:10 dilution of the reaction mixture in the appropriate separation buffer.

7.2.4.2 Immunoaffinity Sample Preparation

The antibody used for immunoaffinity experiments was similar to the 1° mAb used for immunoblots, except it had been conjugated to fluorescein isothiocyanate (FITC) by the manufacturer. It was also directed against the amino acid sequence EQKLISEEDL and had a concentration of 1.09 mg/mL when received. Standards ranging from 5.45 to 21.8 $\mu\text{g/mL}$ were prepared by diluting the stock mAb solution in 10 mM Tris, pH 7.5. FITC labeled anti-myc was also mixed with the protein samples obtained from cell culture. Samples were prepared by mixing 10 μL of the desired protein sample with FITC labeled 1° mAb and dilution to the final concentration with 10 mM Tris, pH 7.5 in a microcentrifuge tube. The sample was allowed to react at room temperature (RT) for 30 min with gentle agitation and an additional 30 min with no agitation. All samples were prepared the day of use.

7.2.5 Capillary Electrophoresis with Laser Induced Detection

A Beckman Coulter P/ACE MDQ equipped with a 488 nm laser induced fluorescence module and detector were used for all conventional capillary electrophoresis (CE) experiments. The separations were performed using a 60 cm total length fused silica capillary with an i.d. of 75 μm . A 2 mm detection window was made at 50 cm by removing the polyimide coating using a Window Maker (Microsolv). Each day, the capillary was conditioned by flushing with 0.1 N HCl, MeOH, 0.1 N NaOH, 18.2 M Ω H₂O, and buffer for 10 min each. The capillary was rinsed between each run by flushing the same solutions for 5 min each. The buffer

solutions used for experimentation are discussed in the results and discussion sections. During the experiment, samples were stored at 4 °C and injections were performed at 10 psi for 10 sec. Unless otherwise noted, a 20 kV separation voltage and a capillary temperature of 25 °C were used for all experiments. Signals were collected at 8 Hz and analyzed using the accompanying software (32 Karat).

7.2.6 Microchip Electrophoresis with Laser Induced Detection

7.2.6.1 Microchip Fabrication

The fabrication of PDMS-based microfluidic devices has been described previously [58-61]. SU-8 10 negative photoresist (for electrophoresis channels) was spin coated on a 100 mm silicon (Si) wafer using a Cee 100 spincoater (Brewer Science, Rolla, MO, USA). SU-8 10 was spun at 500 rpm for 5 s, then 2100 rpm for 30 s. A design containing the desired structures was created using AutoCad LT 2004 (Autodesk, Inc., San Rafael, CA, USA) and transferred to a transparency film at a resolution of 50,000 dpi (Infinite Graphics Inc., Minneapolis, MN, USA). Following the manufacturer's recommended prebake process, the appropriate negative film mask was placed over the coated wafer, brought into hard contact, and exposed to a near-UV flood source at 21.5 mW/cm² (ABM, San Jose, CA, USA) using the suggested exposure dose.

Following the UV exposure, the wafer was postbaked and allowed to cool to room temperature. The wafers were then developed in SU-8 developer, rinsed with IPA, and dried under nitrogen. A final hard-curing bake was performed at 175°C for

2 h. The thickness of the raised photoresist, which corresponded to the depth of the PDMS channels, was measured with a surface profiler (Alpha Step-200, Tencor Instruments, Mountain View, CA, USA). PDMS microstructures were made by casting a 10:1 mixture of PDMS elastomer and curing agent, respectively, against the silicon master. After curing at 75°C for at least 1.5 h, the PDMS was removed from the master, yielding the desired negative relief pattern. Holes for the reservoirs were created in the polymer with a biopsy punch while fluid inlets were produced with a 20 gauge Luer stub.

Two different configurations were used for the experiments reported. For experiments utilizing NDA derivatized protein samples, a gated serpentine design was utilized (Fig 7.1 A). The width and depth of these electrophoresis microchannels were 40 μm and 20 μm , respectively. For immunoaffinity experiments, a simple “T” device containing a 5.5 cm separation channel (from the T intersection to the end of the separation channel) and 0.5 cm side arms was used for all studies reported (Fig. 7.1 B). The width of the separation channel was 40 μm , the width of the side arms were 10 μm , while the depth of all microchannels was 20 μm . In addition, it is worth noting that the bottom PDMS layer was made to a thickness of approximately 5 mm.

Regardless of the microchannel configuration used, fabrication of the final device was completed in the same manner. All-PDMS microchips were constructed using a semi-cure process previously reported [62]. A 10:1 mixture of PDMS elastomer and curing agent, respectively, was poured on a blank 127 mm Si wafer. After curing for ~10 min at 95 °C, the fully cured PDMS layer containing the

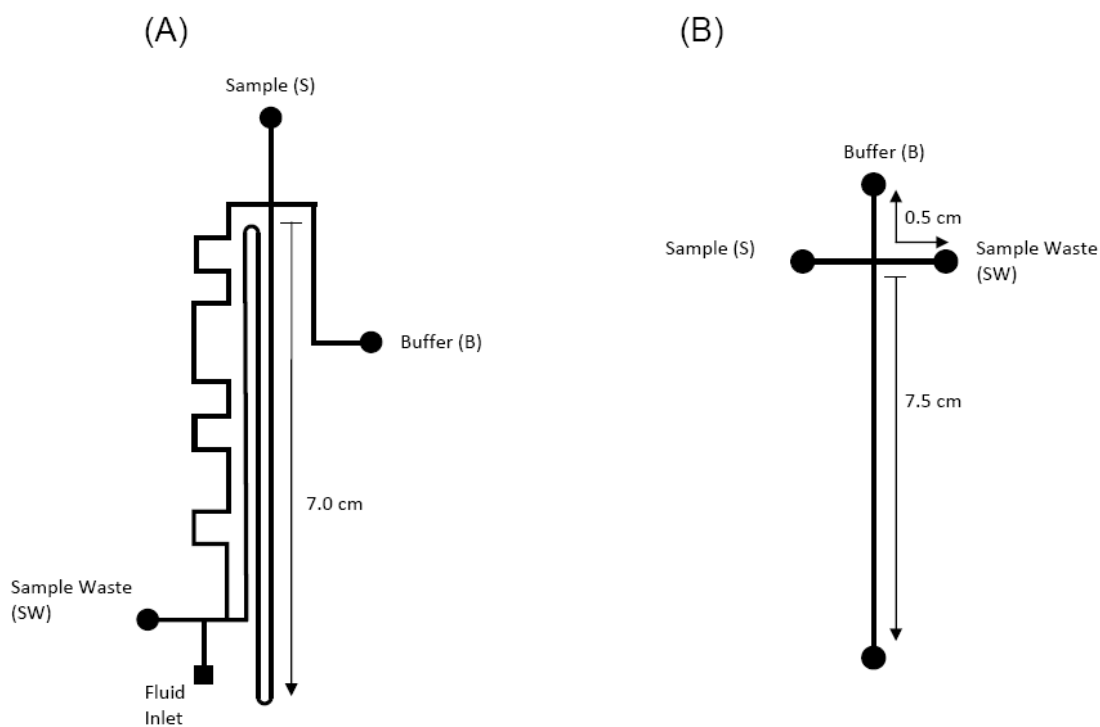


Figure 7.1: Schematic of the two types of all-PDMS microchips used for microchip electrophoresis with LIF detection. (A) Gated serpentine microchip used for NDA derivatized samples, (B) Simple “T” microchip used for immunoaffinity experiments. Channel dimensions are given in the text.

electrophoresis channels were brought into conformal contact and placed back into an 85 °C oven for 2 h.

7.2.6.2 Electrophoresis Procedure for NDA Derivatized Samples

Electrophoresis was carried out in unmodified PDMS microchannels using a programmable Jenway Microfluidic Power Supply (Dunlow, Essex, U.K.). The electrophoresis buffer used for experiments with NDA derivatized protein samples was 25 mM boric acid, 100 μ M SDS, pH 9.2. The buffer was degassed (Fisher Ultrasonic Cleaner, Fisher Scientific) and filtered with a 0.22 μ m cellulose acetate (CA) filter before use. A 20 gauge stainless steel pin connected to fluorinated ethylene propylene (FEP) tubing and a 1 mL syringe was fitted into the fluid inlet on the chip. A syringe pump (CMA 300, North Chelmsford, MA, USA) set to a flow rate of 25 μ L min⁻¹ was used to fill the microchannels and were flushed for 10 min before use.

Electrophoresis was performed by applying +5000 V at the buffer reservoir (B), +1200 V) at the sample reservoir (S), and -5000 V at the sample waste (SW) reservoir. For all data presented, a gated injection method was used for introduction of the sample plug and was achieved by floating the high voltage at the buffer reservoir for the duration of the injection before returning it to +5000 V. Unless otherwise noted, an injection time of 1.0 s was employed for all data presented.

7.2.6.3 Electrophoresis Procedure for Immunoaffinity Experiments

Electrophoresis was carried out in unmodified PDMS microchannels using a programmable Jenway Microfluidic Power Supply (Dunlow, Essex, U.K.). The electrophoresis buffer used for immunoaffinity experiments was 25 mM boric acid, pH 9.2. The buffer was degassed (Fisher Ultrasonic Cleaner, Fisher Scientific) and filtered with a 0.22 μm CA filter before use. The PDMS channels were flushed with buffer for 3-5 min with buffer by applying a vacuum. Electrophoresis was carried by utilizing a modified “cross T” injection and separation technique which is also termed “simplest injection” by Manz *et al.* [63]. Injection was accomplished by applying 500 V to the sample reservoir (S) for 10 s while the sample waste (SW) and detection reservoir were grounded. Following injection, the high voltage (HV) was removed and placed in the buffer reservoir. The separation was initiated by applying +5000 V to the buffer reservoir while the detection reservoir was held at ground.

7.2.6.4 Laser Induced Detection for Microchip Electrophoresis

Laser induced fluorescence (LIF) detection was performed using an epi-fluorescent microscope (Nikon TE 2000). The finished microchip device was placed on a single microscope cover glass (Gold Seal cover glass #3334), positioned on the microscope stage, and secured in place. Incident light was provided by a 100 W mercury lamp connected to the microscope by a fiber optic cable. This broadband light then passed through the appropriate excitation and emission filters as well as dichroic mirrors that had been installed in the internal carousel. Studies involving the

detection of FITC were performed using a FITC filter cube (B1-E) obtained from Nikon. For the detection of CBI derivatives, a custom-built cube containing a 25 mm diameter z442/10X clean-up filter, 25 mm diameter 510hq/50m band-pass emission filter, 25.5 × 36 mm laser dichroic filter, and transmission filter hq510/50m (Chroma, Rockingham, VT, USA) was used. Incident light was focused on the separation channel using a 40x objective and a photomultiplier tube, (PMT) (Hamamatsu, Bridgewater, NJ, USA) which was aligned to the microscope side port, collected light emitted from the sample. Data was acquired at 10 Hz using a preamplifier (Stanford Research Systems, Sunnyvale, CA, USA) and analog-to-digital converter (DA-5, Bioanalytical Systems) using Chromgraph software. Electropherograms were analyzed using Origin 5.0 software.

7.3 Results and Discussion

Western blot analysis, or immunoblotting, is one of the most robust and selective protein analysis techniques available to researchers. Protein mixtures are separated by SDS polyacrylamide gel electrophoresis (SDS-PAGE) based on MW. Separated proteins are then transferred to a membrane where they are probed using antibodies specific to the target protein [64-65]. The success of Western blotting is dependent on the quality of the antibody used to probe the protein of interest and how specific it is for this protein. The prevalence and specificity of Western blot analysis has been greatly advanced with the development of recombinant DNA technology. Currently, there are a variety of commercial sources that offer tens of thousands of

extremely pure, high quality monoclonal antibodies (mAb) for use in immunoblot analysis. Because this technique offers excellent specificity for a wide range of target proteins, Western blot analysis was chosen as the starting point for the current studies. The results obtained from the immunoblot procedure served as a platform for the development of a selective, sensitive, and high-throughput novel analytical method employing capillary and microchip electrophoresis. In addition, the results obtained from future studies can be compared to those obtained using this standard analysis method.

7.3.1 Detection of mHtt by Immunoblotting

The samples collected from both VC and mHtt transfected cells were analyzed by Western blot analysis and are shown in Figure 7.2. Lanes 1 through 3 of the gel contain the 200, 400, and 800 μg samples prepared from the insoluble fraction of VC cells, respectively. Lane 4 contains the MW marker, while lanes 5 through 7 contain the 200, 400, and 800 μg samples prepared from the insoluble fraction of mHtt transfected cells, respectively. Lane 8 is empty, lane 9 contains the supernatant taken from the 800 μg VC cell lysate, and lane 10 contains the supernatant from the 800 μg mHtt transfected cell lysate.

Because an empty vector was used a negative control, mHtt was not expressed in VC cells. Therefore, mHtt is not detected in the samples prepared from either the insoluble fraction (lanes 1-3) or the soluble fraction (lane 9) of the VC cells. However, mHtt is clearly visible in both the insoluble fraction (lanes 5-7) and the

Western Blot Analysis

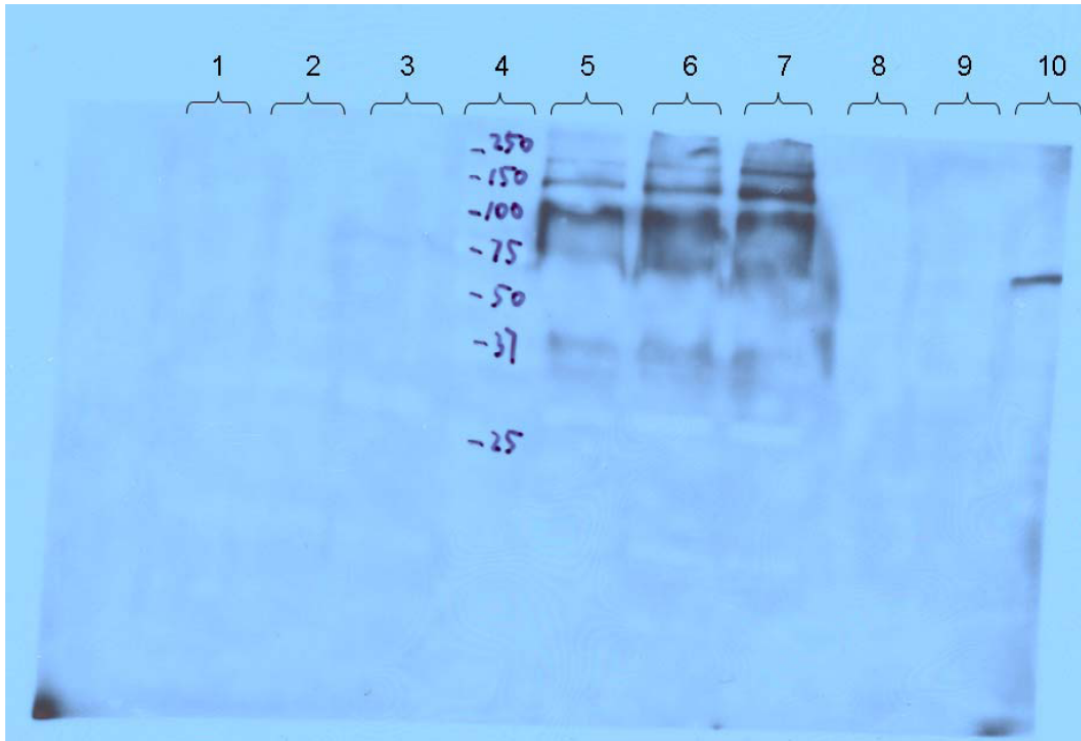


Figure 7.2: Western blot analysis of vector control (VC) and mutant huntingtin (mHtt) transfected cells. Analysis conditions are given in the text. Lane contents are as follows: (1) 200 μg insoluble VC, (2) 400 μg insoluble VC, (3) 800 μg insoluble VC, (4) molecular weight markers, (5) 200 μg insoluble mHtt, (6) 400 μg insoluble mHtt, (7) 800 μg insoluble mHtt, (8) no sample (blank), (9) 800 μg VC supernatant (soluble), (10) 800 μg mHtt supernatant (soluble).

soluble fraction (lane 10) of the transfected cells. In addition, the response for the 200, 400, and 800 μg samples behaves in a dose-dependent manner. Although the same total volume was loaded for each sample (40 μL), the protein bands are increasingly darker because of increasingly higher protein concentration in each sample. Another important observation is the marked difference between the mHtt observed in the insoluble *versus* the soluble fraction. The mHtt detected in the soluble fraction shows a single, homogeneous population of monomeric huntingtin protein at ~ 65 kDa. However, the mHtt detected in the insoluble fraction shows several protein bands of higher MW. Since the antibody used in the immunoblot is specific for the myc-tag on the huntingtin protein, these bands cannot be any other endogenous proteins found in the cell lysate. Rather, they must be high MW aggregates of mHtt.

Huntingtin with an expanded glutamine repeat has been shown to aggregate *in vivo*. This is due in part, to the fact that mHtt is a substrate of the enzyme transglutaminase (TG) [66-69]. Transglutaminases (EC2.3.2.13) are a family of enzymes that form extensively cross-linked, and generally insoluble, protein polymers which facilitates the formation/stabilization of huntingtin-containing aggregates [40, 66, 70]. TGs can catalyze the formation of an ϵ -(γ -glutamyl) lysine bond between the γ -carboxy group of a glutamine residue and the ϵ -amino group of a lysine residue [71]. While TG was not co-transfected with mHtt, HEK cells have been shown to express endogenous TG at sufficient levels to cross-link mHtt [44].

Therefore, the high MW bands observed in Figure 7.2 represent covalently linked dimers, trimers, and high order multimers of mHtt.

One drawback of utilizing an immunoblot for detection of huntingtin protein is that the protein cannot be directly quantified. While the total protein content of the samples was determined by the BCA assay, mHtt was only isolated and not purified. Since the cell lysate contained many other cellular proteins, the exact amount of mHtt is unknown. Furthermore, since there are no commercially available sources of mHtt standards, a calibration curve cannot be constructed. Therefore, densitometry cannot be utilized to quantify the amount of mHtt. Because of these factors, the results of the immunoblot procedure are only qualitative in nature. The only two conclusions that can be made are whether mHtt is absent or present in the sample and the MW of the corresponding protein bands.

7.3.2 Detection of NDA Derivatized mHtt

A major challenge associated with developing a CE-based analytical method for the determination of mHtt is the choice of an appropriate detection method. While ultraviolet (UV) absorbance is easily adapted to CE, it is not very sensitive. Due to the very small path lengths of microfluidic channels, it is even less sensitive when used for microchip electrophoresis. Therefore, UV detection is rarely used for trace analysis of proteins. Fluorescence detection is an alternative on-column detection technique which provides a high degree of sensitivity and selectivity. The fluorogenic reagent 2,3-dicarboxaldehyde (NDA) has previously been shown to be an

effective derivatization agent for amino acids (AA) and peptides [55, 72]. The reaction of NDA (in excess) with cyanide ion (CN^-) in the presence of primary amines was used for derivatization at pH 9.2.

7.3.2.1 Capillary Electrophoresis with Laser Induced Fluorescence

The AA sequence of mHtt that was used for this study has only two possible reaction sites which helps to reduce the heterogeneity of reaction products. In addition to the N-terminus of the protein, the myc-tag AA sequence contains a lysine (K) residue which may be derivatized. Because the sample is derivatized in boric acid (BA) pH 9.2, 25 mM BA pH 9.2 was chosen as the background electrolyte (BGE) for separations. Many other separation buffers were tested but resulted in poor performance (data not shown). Figure 7.3 A and B shows the electropherogram resulting from the separation of NDA derivatized mHtt prepared from the insoluble fraction. At first glance it appears as if only two large peaks are observed. However, when the first peak is expanded (inset of Fig 7.3), a total of three unresolved species are observed. In an effort to improve the resolution between these species, the electroosmotic flow (EOF) was reduced through the addition of 10 mM Tris to the BGE (pH 9.0). As seen in Figure 7.3 B, this slightly increased the resolution between these three co-migrating species but did not result in baseline resolution. One prominent feature of the Tris modified buffer is the appearance of a very sharp peak (peak 3) on the tailing end of the first peak cluster. However, it is not clear what this

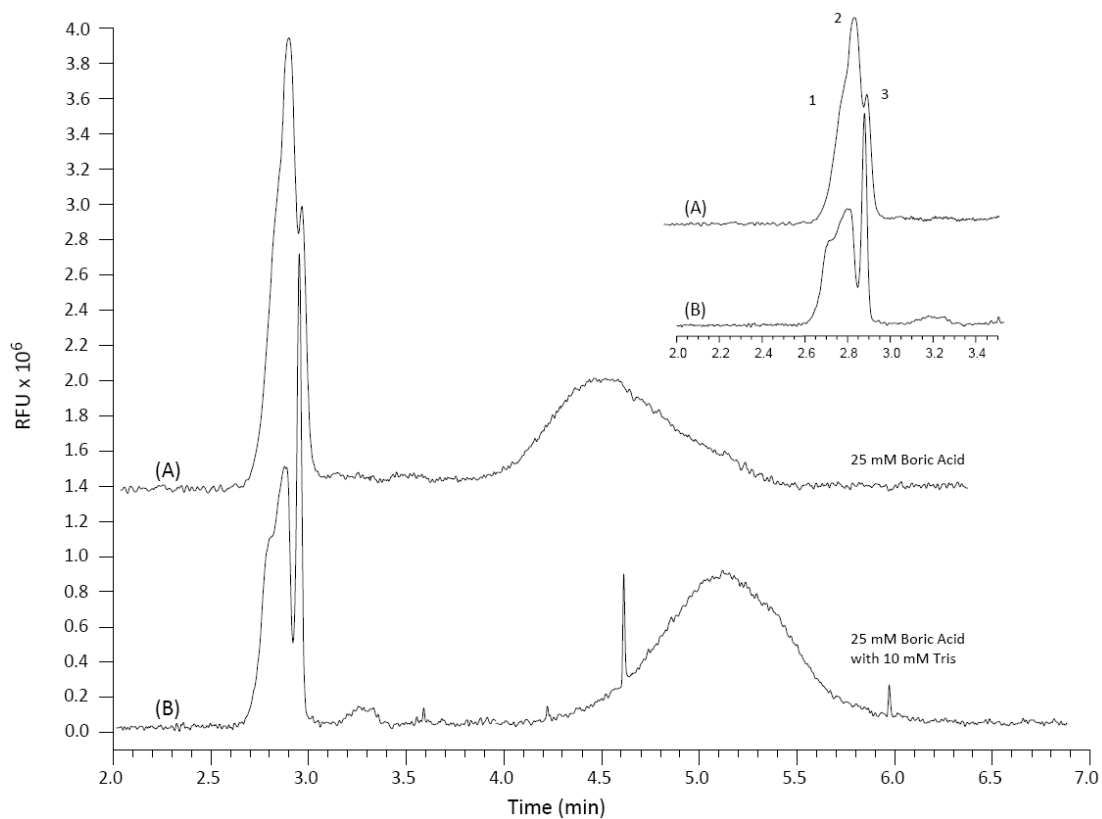


Figure 7.3: CE separation and LIF detection of 800 µg mHtt insoluble fraction of transfected cells which had been derivatized with NDA. Separation conditions: 75 µm i.d. capillary, 60 cm total length, 50 cm to detector, 488 nm excitation, 520 nm emission, 333 V/cm using (A) 25 mM boric acid pH 9.2, and (B) 25 mM boric acid, 10 mM Tris, pH 9.2.

peak represents. To obtain a better perspective, this result was compared to the insoluble fraction prepared from VC cells (Fig. 7.4). The electropherogram for the insoluble fraction derived from VC cells is similar, but it contains one fewer peak. Peak 3 is not present in the VC cell sample, but as can be seen in Figure 7.5, it is present in the soluble fraction of mHtt transfected cells.

Because the 3rd very sharp peak is present in the mHtt samples but not the VC samples, it is believed that this peak represents mHtt. However, drawing certain conclusions from this data is difficult. One common approach to identifying peaks is to spike a sample with a known analyte. In this case, it is not possible since there are no commercial sources of mHtt and it was not isolated to 100% purity in this study. Additionally, quantitation of mHtt is not possible either. This would require the construction of a calibration curve using pure mHtt itself or an analyte similar to mHtt which has comparable derivatization chemistry. Since neither is available, only qualitative conclusions can be made.

7.3.2.2 Microchip Electrophoresis with Laser Induced Fluorescence

Microfluidic devices have become increasingly popular since their introduction almost two decades ago [61, 73-76]. Microchip electrophoresis offers many advantages such as portability, high sample throughput, and reduced sample and reagent consumption. In addition, many popular microchip substrates have completely different surface chemistries than fused silica. Therefore, separations performed in microchips can yield noticeably different results than separations

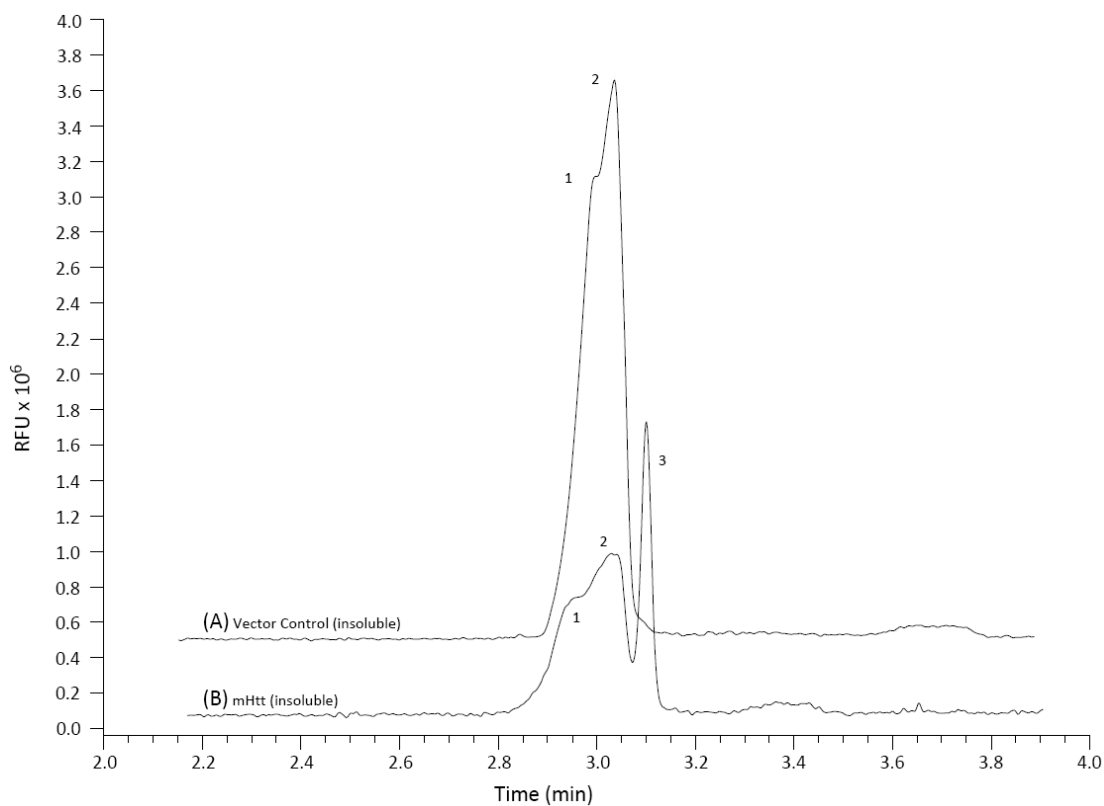


Figure 7.4: CE separation and LIF detection of (A) 800 μg mHtt insoluble fraction of vector control cells and (B) 800 μg insoluble fraction of mHtt transfected cells which had been derivatized with NDA. Separation conditions: 75 μm i.d. capillary, 60 cm total length, 50 cm to detector, 488 nm excitation, 520 nm emission, 333 V/cm using 25 mM boric acid, 10 mM Tris, pH 9.2.

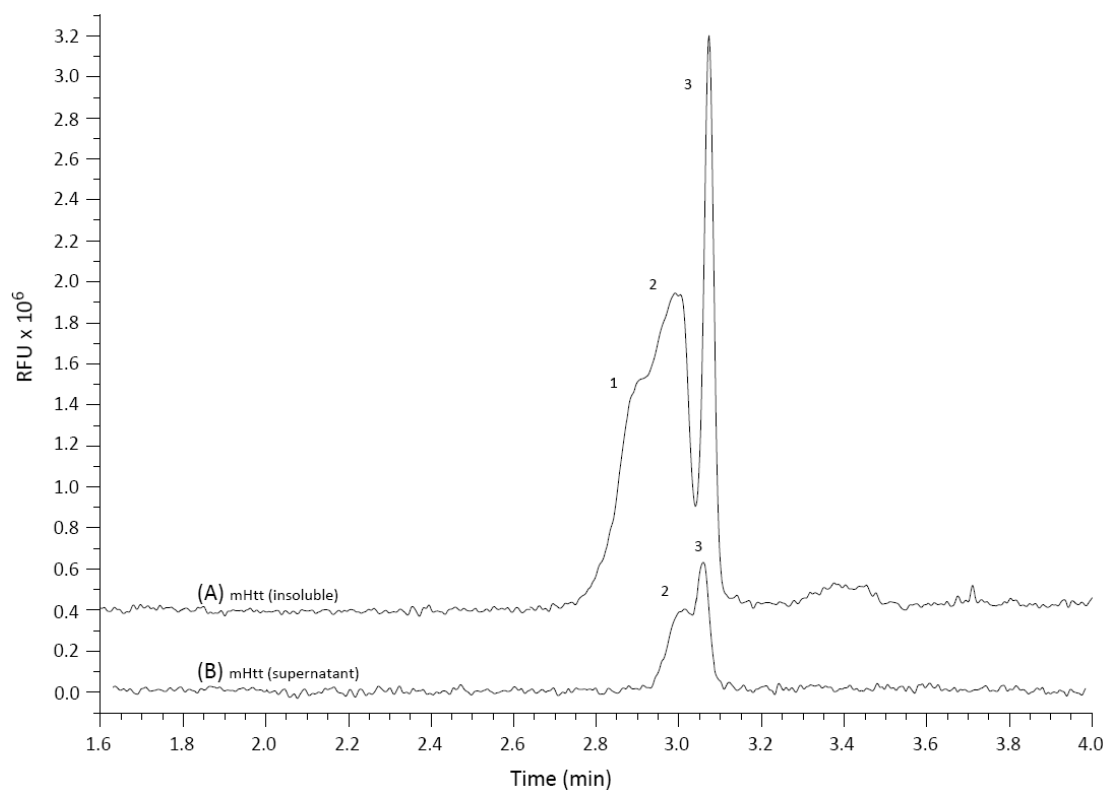


Figure 7.5: CE separation and LIF detection of (A) 800 μg mHtt insoluble fraction of mHtt transfected cells and (B) 800 μg supernatant of mHtt transfected cells which had been derivatized with NDA. Separation conditions: 75 μm i.d. capillary, 60 cm total length, 50 cm to detector, 488 nm excitation, 520 nm emission, 333 V/cm using 25 mM boric acid, 10 mM Tris, pH 9.2.

performed using CE. This effect was observed when NDA derivatized protein samples were analyzed using microchip electrophoresis. Despite have a shorter separation length than the CE experiments outlined in section 7.3.2.1 (13 cm vs. 50 cm), a greater degree of resolution is observed when an all-PDMS microchip is used for analysis. Figure 7.6 shows the separation of NDA derivatized mHtt prepared from the insoluble fraction. Baseline resolution is achieved for all analytes and four distinct peaks are observed. NDA derivatized mHtt from the soluble fraction was also analyzed (Fig. 7.7 A) and compared to mHtt from the insoluble fraction (Fig. 7.7 B). Similar to the results obtained using CE, only three peaks are observed in the soluble fraction.

However, much better resolution was achieved using microchip electrophoresis. Even though the separation length in the microchip was approximately one third as long as the capillary used for CE-LIF, the differences in surface chemistry resulted in vastly different separation characteristics. A distinct difference between the VC and mHtt transfected cells can be seen in Figure 7.8. A large shift in migration of the fourth peak is observed but is inconsequential. This shift to a longer migration time is most likely due to an inefficient injection or a diminishment of the EOF due to modification of the PDMS from analyte adsorption. The important result is that the third peak is clearly absent in the VC sample (Fig 7.8 A) but is present in the mHtt transfected sample (Fig. 7.8 B).

It is evident that the use of microchip electrophoresis provided a dramatic increase in resolution between the analytes. Moreover, this increased resolution

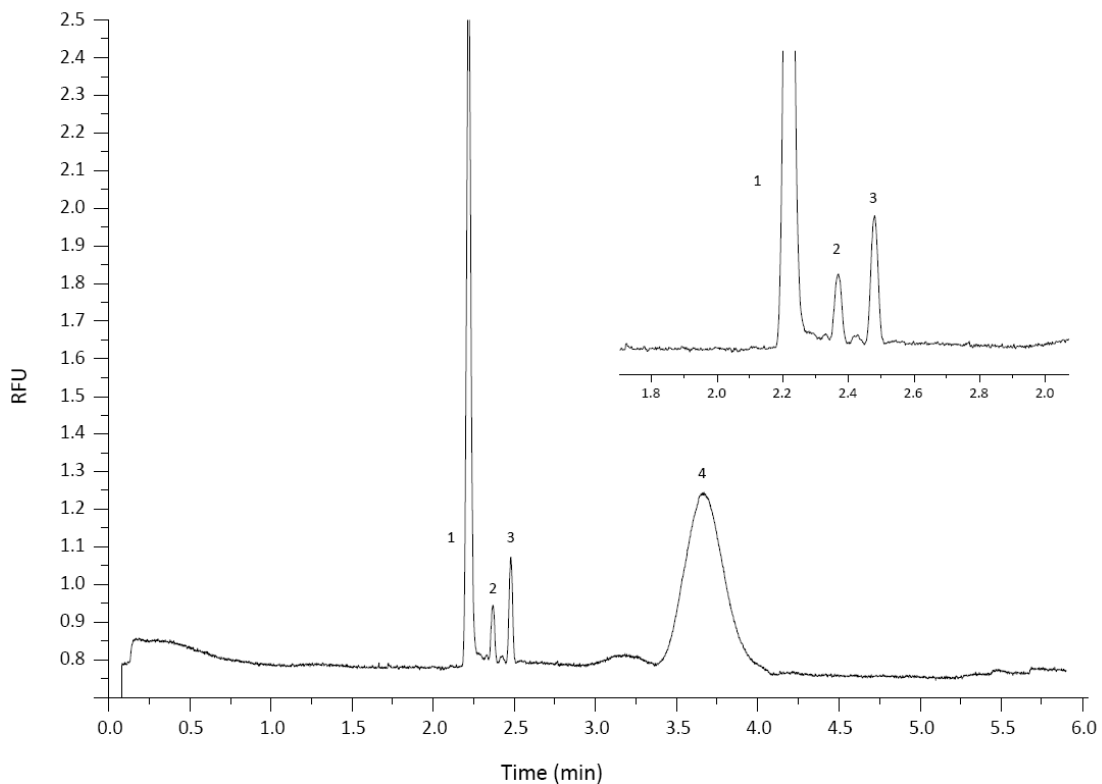


Figure 7.6: Microchip electrophoresis with LIF detection of 800 μg mHtt insoluble fraction of transfected cells which had been derivatized with NDA. Separation conditions: 21 cm total length, 13.5 cm to detector, 442 nm excitation, 490 nm emission, 500 V/cm using 25 mM boric acid, 100 μM SDS, pH 9.2.

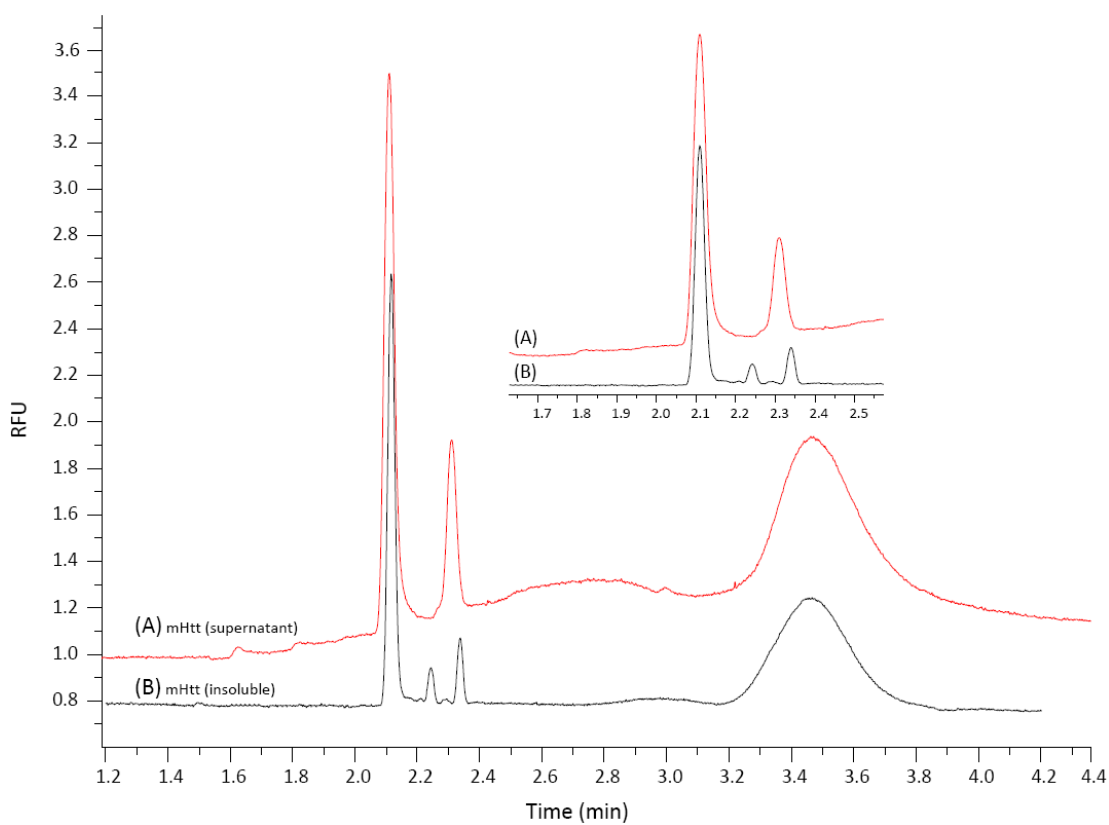


Figure 7.7: Microchip electrophoresis with LIF detection of (A) 800 μg mHtt supernatant of mHtt transfected cells and (B) 800 μg insoluble fraction of mHtt transfected cells which had been derivatized with NDA. Separation conditions: 21 cm total length, 13.5 cm to detector, 442 nm excitation, 490 nm emission, 500 V/cm using 25 mM boric acid, 100 μM SDS, pH 9.2.

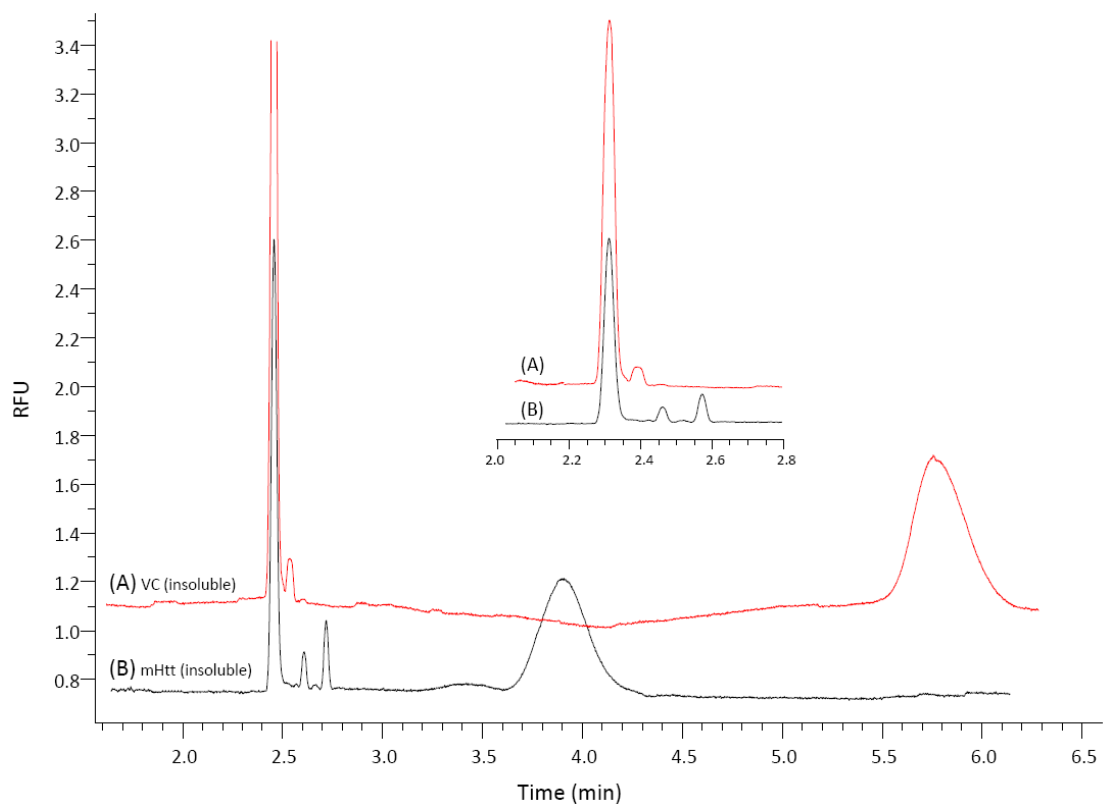


Figure 7.8: Microchip electrophoresis with LIF detection of (A) 800 μg mHtt insoluble fraction of vector control cells and (B) 800 μg insoluble fraction of mHtt transfected cells which had been derivatized with NDA. Separation conditions: 21 cm total length, 13.5 cm to detector, 442 nm excitation, 490 nm emission, 500 V/cm using 25 mM boric acid, 100 μM SDS, pH 9.2.

facilitated peak identification. Because it was present in both the supernatant and insoluble fraction of transfected cells, but absent in the VC cells, peak 3 in the electropherogram most likely corresponds to mHtt. However, because there are no purified standards, this peak cannot be conclusively identified. Moreover, quantitation is not possible and only qualitative conclusions can be made. Nonetheless, the use of microchip electrophoresis for the analysis of NDA derivatized samples does have some benefits. The time of analysis was reduced while analytical sensitivity was increased. In addition, the sample volume needed for analysis was greatly reduced. The amount of sample injected for conventional CE was ~ 90 nL while only ~800 pL was injected in the microchip.

7.3.3 Detection of mHtt using an Electrophoretic Immunoaffinity Assay

Because mHtt was not able to be conclusively identified and quantified using NDA derivatization, a more selective assay was developed. The highly specific antigen-antibody binding utilized in the immunoblot procedure was adapted for capillary and microchip electrophoresis. An immunoaffinity assay was developed for the determination of mHtt. Immunoaffinity is a commonly utilized technique that has previously been employed for the detection of a variety of analytes including cytokines [77], neuropeptides [78], and biomarkers [79]. Typical electrophoretic immunoaffinity assays immobilize the antibody to a solid support such as beads or the surface of a microreactor. However, that strategy is not utilized in the present study. Instead, both the antigen (myc-mHtt) and antibody (FITC labeled anti-myc

mAb) are free in solution. When allowed to react, the mAb and mHtt target protein will form a mAb-mHtt complex in a 1:1 stoichiometric ratio. Because the size, charge, and MW of the complex is different than unbound mAb, the two species will have different electrophoretic mobilities and can be easily separated. Therefore once a suitable calibration curve is constructed for the FITC-labeled mAb, the concentration of mHtt can be calculated by measuring the response of the mAb-mHtt complex.

7.3.3.1 Capillary Electrophoresis with Laser Induced Fluorescence

Standards of 21.8, 14.5, 10.9, 7.27, and 5.45 $\mu\text{g}/\text{mL}$ were prepared by performing a 1:50, 1:75, 1:100, 1:150 dilution respectively, of the FITC-labeled anti-myc mAb stock solution. These standards were injected and analyzed as previously described using CE-LIF (section 7.2.5). The response of these standards can be seen in Figure 7.9 and a calibration curve was constructed by plotting the resulting peak area vs. concentration (Fig. 7.10). As observed in Fig. 7.9, the peak corresponding to the FITC mAb is approximately one minute wide. This indicates a small degree of band broadening which is most likely due to hydrophobic and/or electrostatic interactions with the capillary wall. However, the most important result is that the response of the FITC-labeled mAb is linear with respect to concentration. To perform the immunoaffinity assay, 10 μL of the mHtt prepared from the 800 μg insoluble fraction was incubated with 10.9 $\mu\text{g}/\text{mL}$ FITC mAb and analyzed by CE-LIF. Two peaks are observed in Figure 7.11. Because it has a similar migration time

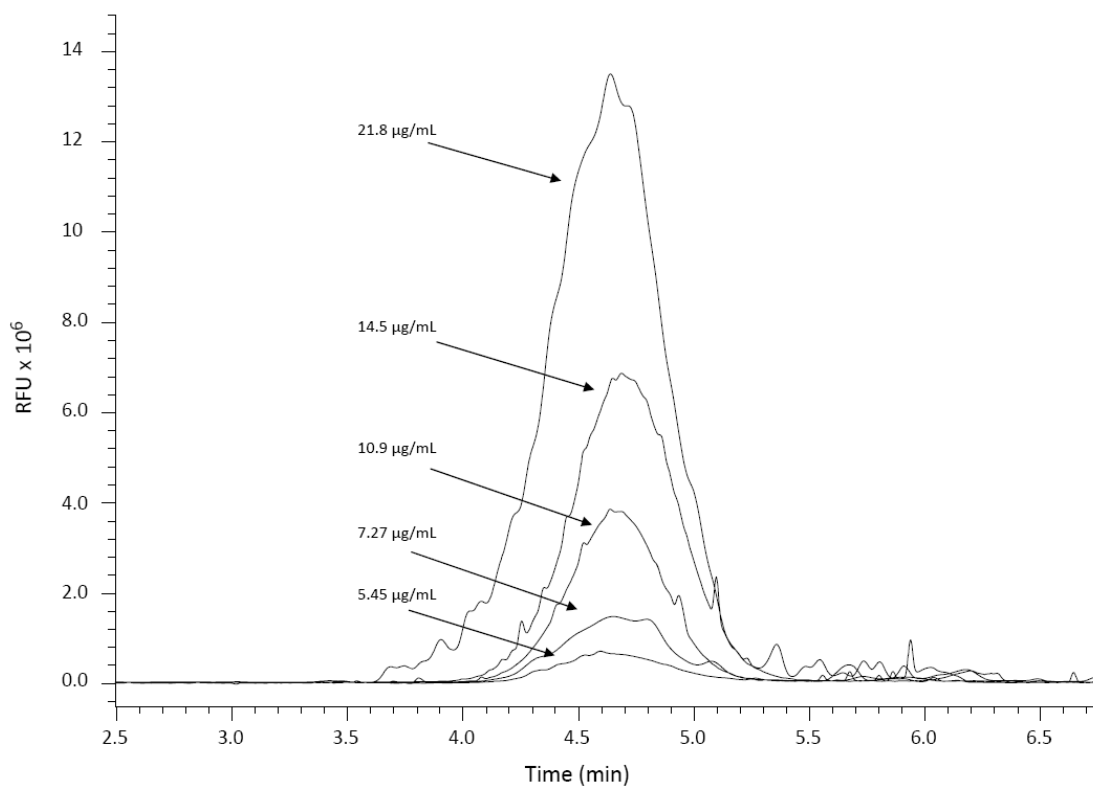


Figure 7.9: CE separation and LIF detection of standard solutions of FITC labeled anti-myc mAb. Separation conditions: 75 µm i.d. capillary, 60 cm total length, 50 cm to detector, 488 nm excitation, 520 nm emission, 333 V/cm using 25 mM boric acid pH 9.2.

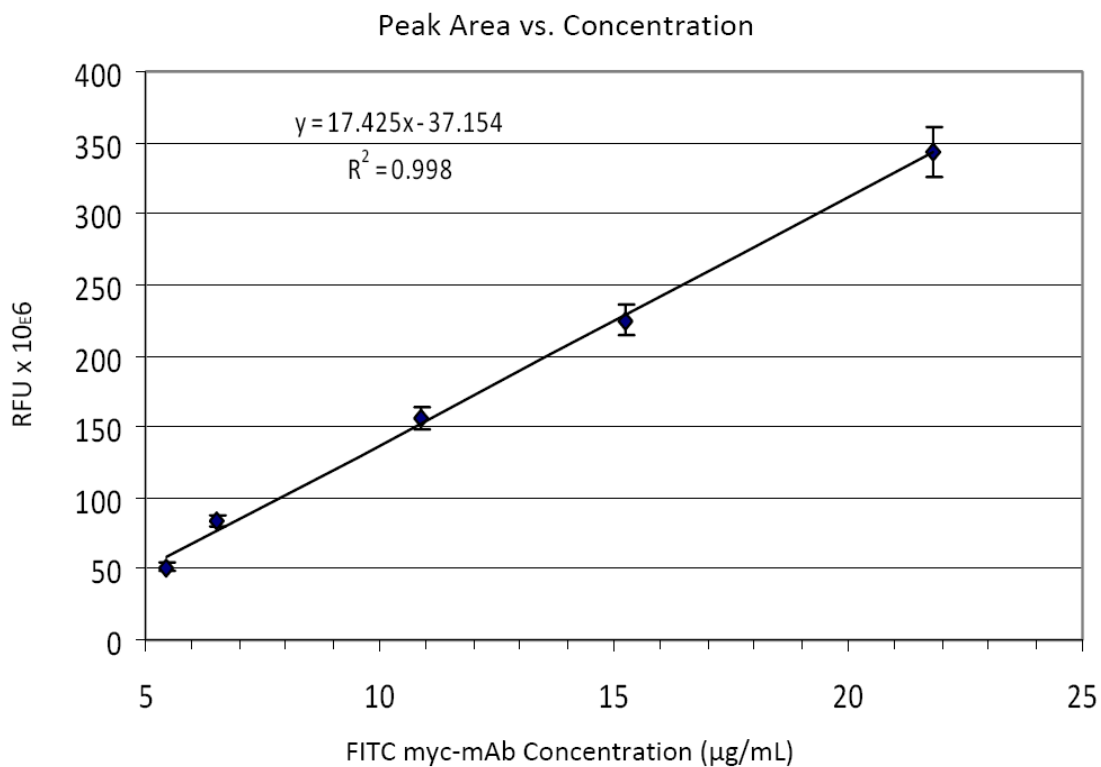


Figure 7.10: Calibration curve of the resulting peak area of the FITC labeled anti-myc mAb plotted *versus* the concentration. Data taken from figure 7.9.

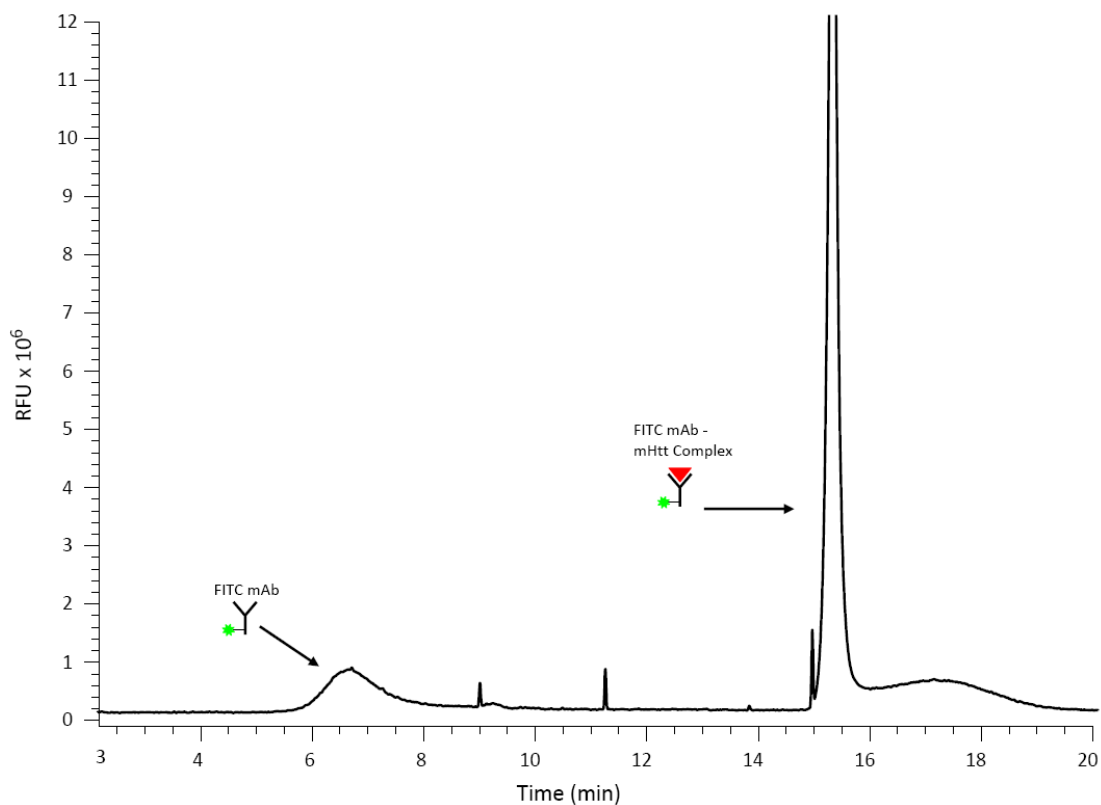


Figure 7.11: Electropherogram of the myc-tagged mHtt immunoassay performed using CE with LIF detection of 10.9 $\mu\text{g/mL}$ FITC anti-myc mAb incubated with 10 μL of the 800 μg insoluble fraction of mHtt transfected cells. Separation conditions: 75 μm i.d. capillary, 60 cm total length, 50 cm to detector, 488 nm excitation, 520 nm emission, 333 V/cm using 25 mM boric acid, 10 mM Tris, pH 9.2

as the standard solutions, the first peak corresponds to the unbound FITC-labeled mAb and second peak corresponds to the mAb-mHtt complex. As expected, the peak area of the free mAb is decreased by the formation of the mAb-mHtt complex and the much larger complex migrates more slowly than the free mAb (Fig 7.12). However, upon closer inspection of the second peak, significant tailing is observed. Although this feature was observed on multiple days with multiple samples, it is unclear what this shoulder represents. It is possible that the shoulder represents a mAb-mHtt complex with the high MW aggregates identified by immunoblotting. However, there is no conclusive method to make this determination.

7.3.3.2 Microchip Electrophoresis with Laser Induced Fluorescence

Microchip electrophoresis was also employed to analyze the same samples described in the previous section. Described in section 7.2.6, an all-PDMS microchip was used for analysis (Fig. 7.1 B). Much like the results obtained when the analysis of NDA derivatized samples was transferred from CE to microchip electrophoresis, noticeable differences in separation characteristics are observed in the immunoaffinity assay as well. Using conventional electrophoresis, a very broad peak was observed for the FITC-labeled mAb. However, a much narrower peak (only ~6 s wide) is observed using microchip electrophoresis (Fig. 7.13). A calibration curve was constructed using the same standard solutions described above (Fig. 7.14).

Similar to the results obtained using CE, the appearance of a second peak is observed after mHtt is incubated with FITC-labeled mAb (Fig. 7.15) which

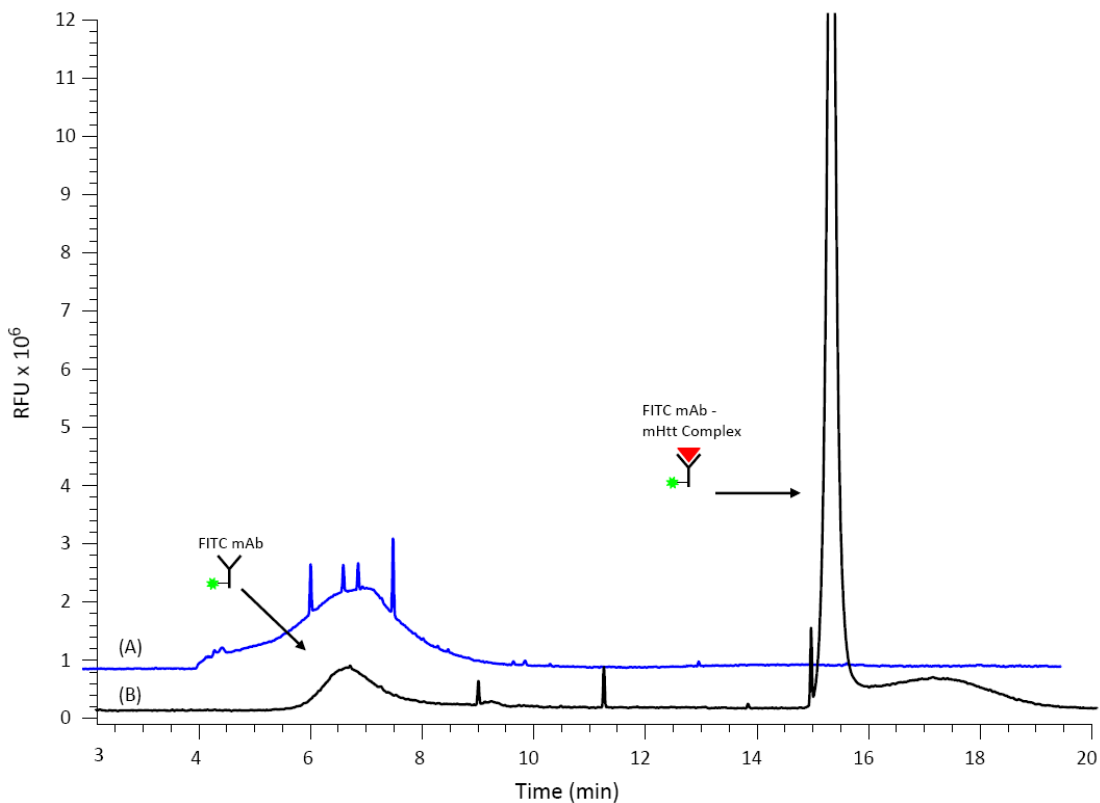


Figure 7.12: Electropherogram of the myc-tagged mHtt immunoassay performed using CE with LIF detection of (A) 10.9 $\mu\text{g}/\text{mL}$ FITC anti-myc mAb and (B) 10.9 $\mu\text{g}/\text{mL}$ FITC anti-myc mAb incubated with 10 μL of the 800 μg insoluble fraction of mHtt transfected cells. Separation conditions: 75 μm i.d. capillary, 60 cm total length, 50 cm to detector, 488 nm excitation, 520 nm emission, 333 V/cm using 25 mM boric acid, 10 mM Tris, pH 9.2.

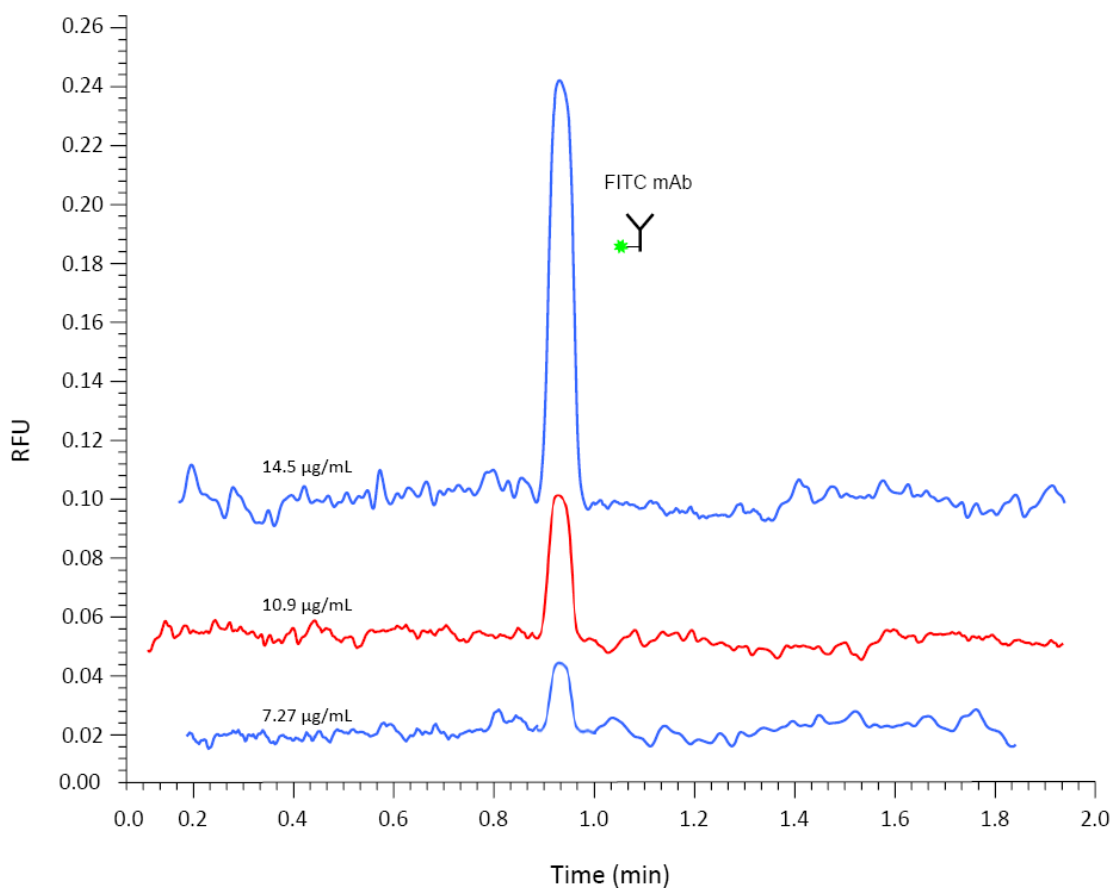


Figure 7.13: Microchip electrophoresis with LIF detection of standard solutions of FITC labeled anti-myc mAb. Separation conditions: 8 cm total length, 7.5 cm to detector, 488 nm excitation, 520 nm emission, 700 V/cm using 25 mM boric acid, pH 9.2.

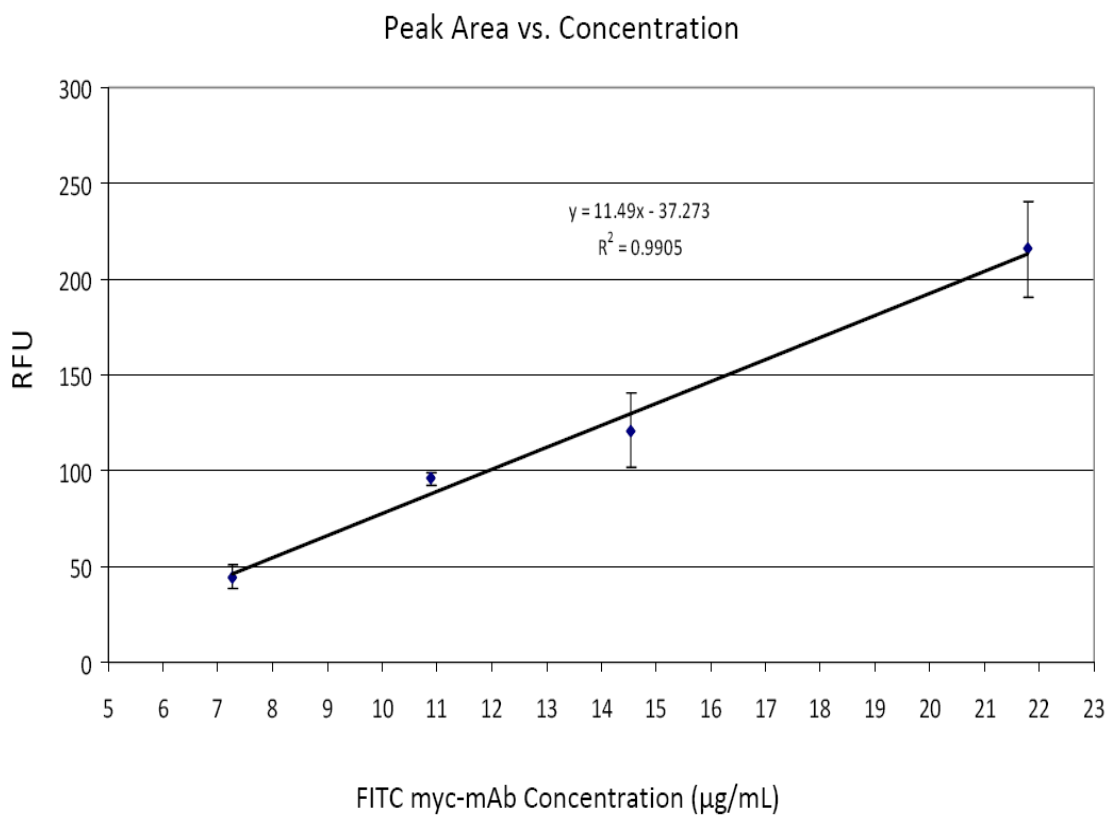


Figure 7.14: Calibration curve of the resulting peak area of the FITC labeled anti-myc mAb plotted *versus* the concentration. Data taken from figure 7.13.

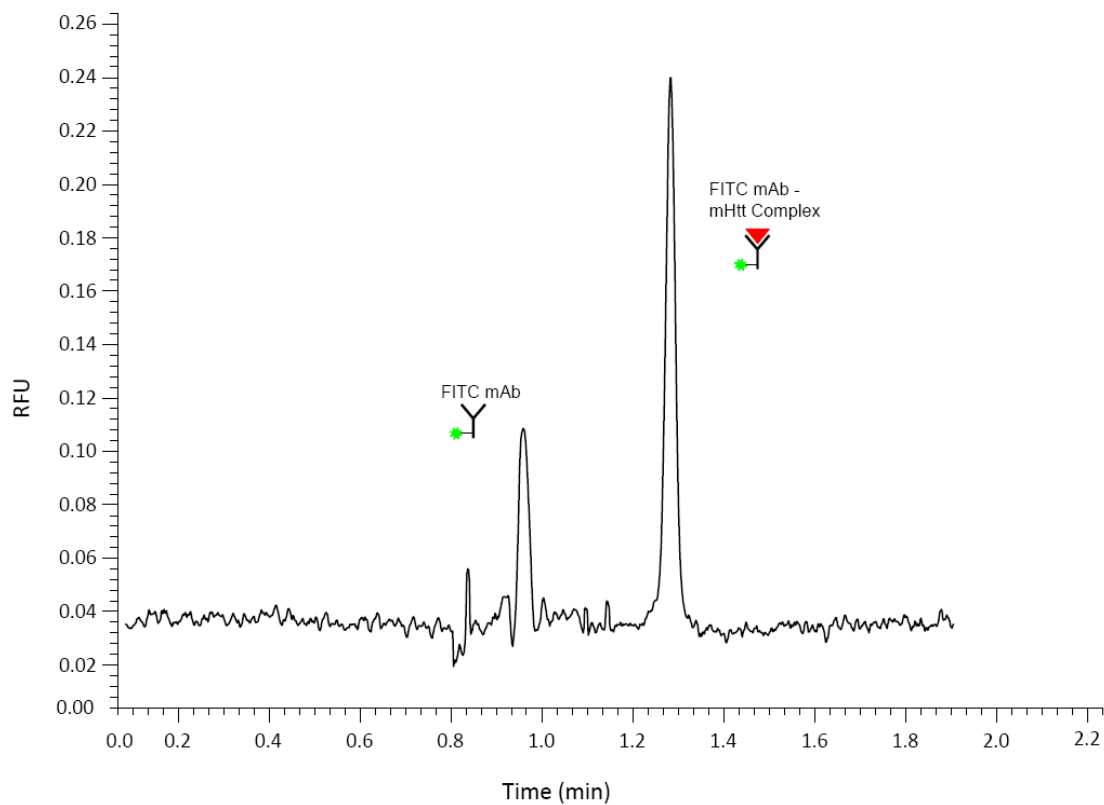


Figure 7.15: Electropherogram of the myc-tagged mHtt immunoassay performed using microchip electrophoresis with LIF detection of 10.9 $\mu\text{g/mL}$ FITC anti-myc mAb incubated with 10 μL of the 800 μg insoluble fraction of mHtt transfected cells. Separation conditions: 8 cm total length, 7.5 cm to detector, 488 nm excitation, 520 nm emission, 700 V/cm using 25 mM boric acid, pH 9.2.

corresponds to the mAb-mHtt complex. In addition, the peak area of the free mAb decreases when incubated with mHtt (Fig 7.16). However, unlike the results obtained using CE, the mAb-mHtt peak is very Gaussian in nature. No band broadening or tailing is observed. This result highlights how differences in the substrate's surface chemistry can have dramatic effects on the separation mechanism and resulting data.

More importantly, the amount of mHtt in the sample can be quantified. The number of moles of antibody in the mHtt-mAb complex can be determined from the calibration curve. Because the complex has a 1:1 stoichiometry, this also corresponds to the number of moles of mHtt. After accounting for the MW and injection volume, the concentration of mHtt in the sample was determined to be 2.64 $\mu\text{g/mL}$, which is in accordance with the values obtained from previous experiments (data not shown).

7.4 Conclusions: Comparison of Analytical Performance

The direct comparison of different analytical methodologies for the analysis of myc-tagged proteins, with a specific example utilizing mutant huntingtin protein was described. General observations and comments on each strategy can be found in Table 7.2. Analytical parameters such as sensitivity, selectivity, and limit of detection (LOD) were compared. In addition, factors such as reagent consumption, time of analysis, and ease of implementation were assessed. By comparing the ability of each technique to separate mHtt samples, it was determined that immunoblot provided the highest degree of separation. Because this technique relies on a cross-linked separation matrix, mHtt as well as several higher order aggregates were

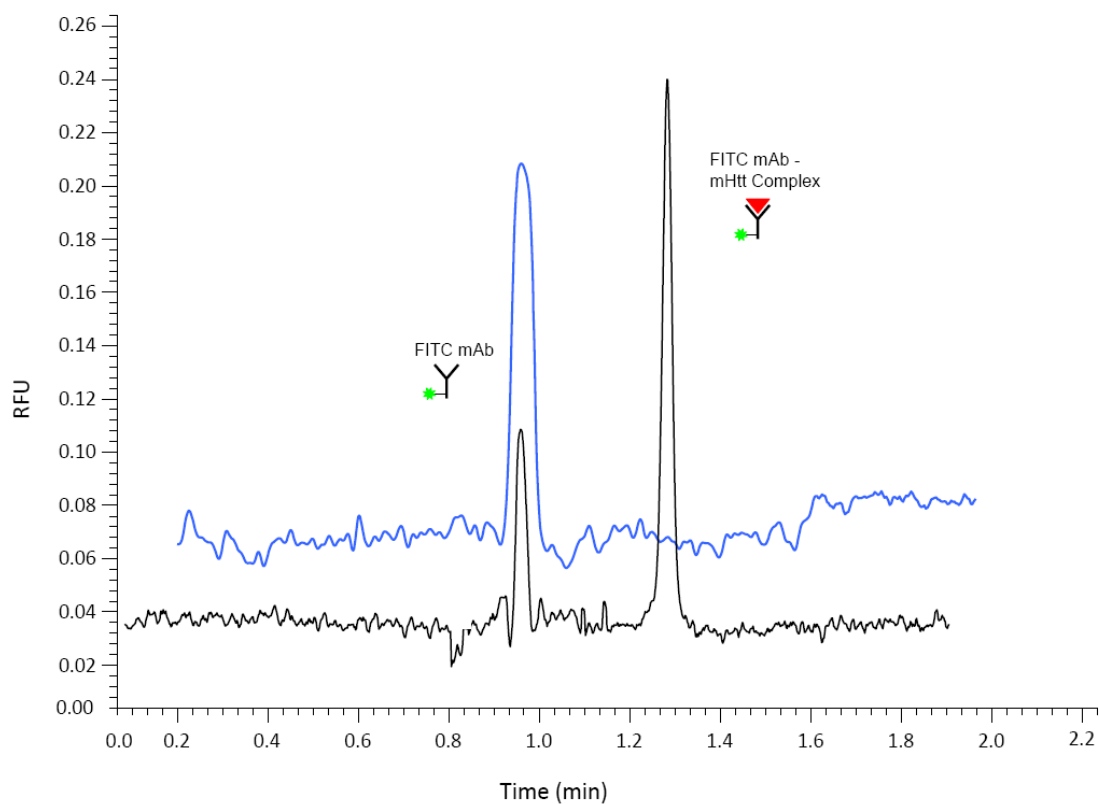


Figure 7.16: Electropherogram of the myc-tagged mHtt immunoassay performed using microchip electrophoresis with LIF detection of (A) 10.9 $\mu\text{g/mL}$ FITC anti-myc mAb and (B) 10.9 $\mu\text{g/mL}$ FITC anti-myc mAb incubated with 10 μL of the 800 μg insoluble fraction of mHtt transfected cells. Separation conditions: 8 cm total length, 7.5 cm to detector, 488 nm excitation, 520 nm emission, 700 V/cm using 25 mM boric acid, pH 9.2.

Table 7.2: Qualitative Comparison of Analytical Performance

	Western Blot	NDA Derivatization		Immunoaffinity	
		Capillary Electrophoresis	Microchip Electrophoresis	Capillary Electrophoresis	Microchip Electrophoresis
Time of Analysis (hr)	30 - 36	4	2	5	3
Reagent Volume Required (mL)	2000	15	5	15	5
Sample Volume Required (μ L)	40	5	5	10	10
Concentration Limit of Detection	ND	ND	ND	36 nM	36 nM
Mass Limit of Detection	High Nanogram	ND	ND	490 μ g	4.5 μ g
Quantitation Possible	No	No	No	Yes	Yes

observed. This result was not observed using either capillary or microchip electrophoresis. Both of these techniques utilized aqueous buffers for separation which could not provide adequate resolution between these species. This result stems from the fact that dimers and trimers of mHtt have the same mass-to-charge ratio and cannot be easily separated using this separation technique. Although there are alternate separation strategies to alleviate this problem, the buffer systems would hinder the analysis method in other ways. For example, various surfactants can be added to aqueous buffers in order to perform micellar electrokinetic chromatography (MEKC). However, the use of surfactants even at low concentrations has been shown to disrupt protein-protein interactions which would render an immunoaffinity assay ineffective. Alternatively, capillary gel electrophoresis (CGE) has been shown to be very effective at separating proteins based on MW. However, there is very little possibility of the mAb-mHtt complex staying intact while it traverses the porous gel matrix.

Despite their inability to separate mHtt aggregates, conventional and microchip electrophoresis have some advantages over immunoblotting. The time of analysis, reagent, and sample volume needed for analysis is greatly reduced. The immunoblot procedure required a total of 40 μL of sample, ~ 2 liters of reagents, and almost 30 hr to yield the final result. Including the time necessary for microchip fabrication and sample preparation, the immunoaffinity assay required only 10 μL of sample, ~ 5 mL of reagents, and yielded results in less than three hours. The separation of NDA

derivatized samples by microchip electrophoresis required only 5 μL of sample, less than 5 mL of reagents, and produced results in less than two hours.

Despite needing much less sample than the immunoblot, both capillary and microchip electrophoresis injected even less for analysis. An estimated 90 nL and 800 pL of sample was injected for capillary and microchip electrophoresis respectively. Even though these volumes are extremely small, the electrophoretic methods exhibited favorable sensitivity and limits of detection. The lowest concentration of FITC-labeled mAb that either electrophoretic method could detect was 5.45 $\mu\text{g}/\text{mL}$ which equates to a concentration of ~ 36 nM. However, each mol of mAb is labeled with two mols of FITC. Therefore, a FITC concentration of ~ 72 nM is what is really being detected. However when the injection volume of each method is considered, mass detection limits of ~ 490 pg and ~ 4.5 pg for capillary and microchip electrophoresis (respectively) were achieved. Taken collectively, these three different analytical methods have obvious advantages and disadvantages. The immunoblot procedure provides the best resolution of mHtt species, but requires the largest investment of reagents, time, and money. Both the conventional and microchip methods save a considerable amount of time and reagents but do not provide a complete separation. These methods also provide the opportunity to quantitate the amount of mHtt while the immunoblot procedure does not. However, microchip analysis is a non-standard technique which may lead to reduced precision. While each of these techniques has inherent advantages and disadvantages, four novel strategies for the separation and detection of mHtt were developed. Now, laboratories

which perform research into mechanisms of HD have alternate analytical strategies to achieve their desired goals.

7.5 References

- [1] Walker Francis, O., *Lancet* 2007, 369, 218-228.
- [2] Young, A. B., *Journal of Clinical Investigation* 2003, 111, 299-302.
- [3] Ferrante, R. J., Kowall, N. W., Richardson, E. P., Jr., *The Journal of neuroscience : the official journal of the Society for Neuroscience* 1991, 11, 3877-3887.
- [4] DiFiglia, M., Sapp, E., Chase, K. O., Davies, S. W., Bates, G., Vonsattel, J. P., Aronin, N., *Science* 1997, 277, 1990-1993.
- [5] Kegel, K. B., Sapp, E., Yoder, J., Cuiffo, B., Sobin, L., Kim, Y. J., Qin, Z.-H., Hayden, M. R., Aronin, N., Scott, D. L., Isenberg, G., Goldmann, W. H., DiFiglia, M., *Journal of Biological Chemistry* 2005, 280, 36464-36473.
- [6] Hackam, A. S., Singaraja, R., Wellington, C. L., Metzler, M., McCutcheon, K., Zhang, T., Kalchman, M., Hayden, M. R., *Journal of Cell Biology* 1998, 141, 1097-1105.
- [7] Kegel, K. B., Meloni, A. R., Yi, Y., Kim, Y. J., Doyle, E., Cuiffo, B. G., Sapp, E., Wang, Y., Qin, Z.-H., Chen, J. D., Nevins, J. R., Aronin, N., DiFiglia, M., *Journal of Biological Chemistry* 2002, 277, 7466-7476.
- [8] Rockabrand, E., Slepko, N., Pantalone, A., Nukala, V. N., Kazantsev, A., Marsh, J. L., Sullivan, P. G., Steffan, J. S., Sensi, S. L., Thompson, L. M., *Human Molecular Genetics* 2007, 16, 61-77.
- [9] Strehlow, A. N. T., Li, J. Z., Myers, R. M., *Human Molecular Genetics* 2007, 16, 391-409.
- [10] Caviston, J. P., Ross, J. L., Antony, S. M., Tokito, M., Holzbaur, E. L. F., *Proceedings of the National Academy* 2007, 104, 10045-10050.
- [11] Choo, Y. S., Johnson, G. V. W., MacDonald, M., Detloff, P. J., Lesort, M., *Human Molecular Genetics* 2004, 13, 1407-1420.
- [12] Orr, A. L., Li, S., Wang, C.-E., Li, H., Wang, J., Rong, J., Xu, X., Mastroberardino, P. G., Greenamyre, J. T., Li, X.-J., *Journal of Neuroscience* 2008, 28, 2783-2792.
- [13] Myers Richard, H., *NeuroRx : the journal of the American Society for Experimental NeuroTherapeutics* 2004, 1, 255-262.
- [14] Sugars, K. L., Rubinsztein, D. C., *Trends in Genetics* 2003, 19, 233-238.
- [15] Thomas, E. A., *Journal of Neuroscience Research* 2006, 84, 1151-1164.
- [16] Cha, J. H. J., *Trends in Neurosciences* 2000, 23, 387-392.
- [17] Luthi-Carter, R., Strand, A., Peters, N. L., Solano, S. M., Hollingsworth, Z. R., Menon, A. S., Frey, A. S., Spektor, B. S., Penney, E. B., Schilling, G., Ross, C. A., Borchelt, D. R., Tapscott, S. J., Young, A. B., Cha, J.-H. J., Olson, J. M., *Human Molecular Genetics* 2000, 9, 1259-1271.
- [18] Davies, S. W., Turmaine, M., Cozens, B. A., Difiglia, M., Sharp, A. H., Ross, C. A., Scherzinger, E., Wanker, E. E., Mangiarini, L., Bates, G. P., *Cell* 1997, 90, 537-548.

- [19] DiFiglia, M., Sapp, E., Chase, K. O., Davies, S. W., Bates, G., Vonsattel, J. P., Aronin, N., *Science* 1997, 277, 1990-1993.
- [20] Sapp, E., Penney, J., Young, A., Aronin, N., Vonsattel, J. P., DiFiglia, M., *Journal of neuropathology and experimental neurology* 1999, 58, 165-173.
- [21] Ross, C. A., *Cell* 2004, 118, 4-7.
- [22] DiFiglia, M., *Trends in Neurosciences* 1990, 13, 286-289.
- [23] Fan, M. M. Y., Raymond, L. A., *Progress in Neurobiology* 2007, 81, 272-293.
- [24] Rubinsztein, D. C., *Trends in Genetics* 2002, 18, 202-209.
- [25] Fernandes, H. B., Baimbridge, K. G., Church, J., Hayden, M. R., Raymond, L. A., *Journal of Neuroscience* 2007, 27, 13614-13623.
- [26] Zeron, M. M., Fernandes, H. B., Krebs, C., Shehadeh, J., Wellington, C. L., Leavitt, B. R., Baimbridge, K. G., Hayden, M. R., Raymond, L. A., *Molecular and Cellular Neuroscience* 2004, 25, 469-479.
- [27] Zeron, M. M., Hansson, O., Chen, N., Wellington, C. L., Leavitt, B. R., Brundin, P., Hayden, M. R., Raymond, L. A., *Neuron* 2002, 33, 849-860.
- [28] Zuccato, C., Ciammola, A., Rigamonti, D., Leavitt, B. R., Goffredo, D., Conti, L., MacDonald, M. E., Friedlander, R. M., Silani, V., Hayden, M. R., Timmusk, T., Sipione, S., Cattaneo, E., *Science* 2001, 293, 493-498.
- [29] Deckel, A. W., Elder, R., Fuhrer, G., *NeuroReport* 2002, 13, 707-711.
- [30] Huang, E. P., *Current Biology* 1997, 7, R141-R143.
- [31] Izumi, Y., Tokuda, K., Zorumski, C. F., *Hippocampus* 2008, 18, 258-265.
- [32] Prast, H., Philippu, A., *Progress in Neurobiology* 2001, 64, 51-68.
- [33] Pogun, S., Kuhar, M. J., *Annals of the New York Academy of Sciences* 1994, 738, 305-315.
- [34] Steinert, J. R., Kopp-Scheinpflug, C., Baker, C., Challiss, R. A. J., Mistry, R., Haustein, M. D., Griffin, S. J., Tong, H., Graham, B. P., Forsythe, I. D., *Neuron* 2008, 60, 642-656.
- [35] Toda, N., Ayajiki, K., Okamura, T., *Pharmacological Reviews* 2009, 61, 62-97.
- [36] Fabricius, M., Lauritzen, M., *American Journal of Physiology* 1994, 266, H1457-H1464.
- [37] Eibeshitz, E., Barbiro-Michaely, E., Mayevsky, A., *Proceedings of SPIE* 2009, 7280, 72801Y/72801-72801Y/72809.
- [38] Bao, J., Sharp, A. H., Wagster, M. V., Becher, M., Schilling, G., Ross, C. A., Dawson, V. L., Dawson, T. M., *Proceedings of the National Academy of Sciences* 1996, 93, 5037-5042.
- [39] Challapalli, K. K., Zabel, C., Schuchhardt, J., Kaindl, A. M., Klose, J., Herzel, H., *Electrophoresis* 2004, 25, 3040-3047.
- [40] Dudek, N. L., Dai, Y., Muma, N. A., *Journal of Neuropathology & Experimental Neurology* 2008, 67, 355-365.
- [41] Niclis, J. C., Trounson, A. O., Dottori, M., Ellisdon, A. M., Bottomley, S. P., Verlinsky, Y., Cram, D. S., *Reproductive BioMedicine Online* 2009, 19, 106-113.
- [42] Schilling, G., Savonenko, A. V., Klevytska, A., Morton, J. L., Tucker, S. M., Poirier, M., Gale, A., Chan, N., Gonzales, V., Slunt, H. H., Coonfield, M. L.,

- Jenkins, N. A., Copeland, N. G., Ross, C. A., Borchelt, D. R., *Human Molecular Genetics* 2004, *13*, 1599-1610.
- [43] Dorsman, J. C., Smoor, M. A., Maat-Schieman, M. L. C., Bout, M., Siesling, S., Van Duinen, S. G., Verschuuren, J. J. G. M., Den Dunnen, J. T., Roos, R. A. C., Van Ommen, G. J. B., *Philosophical Transactions of the Royal Society of London, Series B: Biological Sciences* 1999, *354*, 1061-1067.
- [44] Zainelli, G. M., Ross, C. A., Troncoso, J. C., Muma, N. A., *Journal of Neuropathology & Experimental Neurology* 2003, *62*, 14-24.
- [45] Muchowski, P. J., Ramsden, R., Nguyen, Q., Arnett, E. E., Greiling, T. M., Anderson, S. K., Clark, J. I., *Journal of Biological Chemistry* 2008, *283*, 6330-6336.
- [46] Hoffner, G., van der Rest, G., Dansette, P. M., Djian, P., *Analytical Biochemistry* 2009, *384*, 296-304.
- [47] Schilling, B., Gafni, J., Torcassi, C., Cong, X., Row, R. H., LaFevre-Bernt, M. A., Cusack, M. P., Ratovitski, T., Hirschhorn, R., Ross, C. A., Gibson, B. W., Ellerby, L. M., *Journal of Biological Chemistry* 2006, *281*, 23686-23697.
- [48] Liu, X., Miller, B. R., Rebec, G. V., Clemmer, D. E., *Journal of Proteome Research* 2007, *6*, 3134-3142.
- [49] Dolnik, V., *Electrophoresis* 2008, *29*, 143-156.
- [50] Dolnik, V., *Electrophoresis* 2006, *27*, 126-141.
- [51] Hempe, J. M., *Handbook of Capillary and Microchip Electrophoresis and Associated Microtechniques (3rd Edition)* 2008, 75-107.
- [52] Blanco, S., Suarez, A., Gandia-Pla, S., Gomez-Llorente, C., Antunez, A., Gomez-Capilla, J. A., Farez-Vidal, M. E., *Scandinavian Journal of Clinical and Laboratory Investigation* 2008, *68*, 577-584.
- [53] Williams, L. C., Hedge, M. R., Herrera, G., Stapleton, P. M., Love, D. R., *Molecular and Cellular Probes* 1999, *13*, 283-289.
- [54] Tang, T.-S., Tu, H., Chan, E. Y. W., Maximov, A., Wang, Z., Wellington, C. L., Hayden, M. R., Bezprozvanny, I., *Neuron* 2003, *39*, 227-239.
- [55] De Montigny, P., Stobaugh, J. F., Givens, R. S., Carlson, R. G., Srinivasachar, K., Sternson, L. A., Higuchi, T., *Analytical Chemistry* 1987, *59*, 1096-1101.
- [56] Lunte, S. M., Wong, O. S., *Current Separations* 1990, *10*, 19-25.
- [57] Shou, M., Smith, A. D., Shackman, J. G., Peris, J., Kennedy, R. T., *Journal of Neuroscience Methods* 2004, *138*, 189-197.
- [58] Madou, M., Lal, A., Schmidt, G., Song, X., Kinoshita, K., Fendorf, M., Zettl, A., White, R., *Proceedings - Electrochemical Society* 1997, *97-19*, 61-69.
- [59] Martin, R. S., Gawron, A. J., Lunte, S. M., Henry, C. S., *Analytical Chemistry* 2000, *72*, 3196-3202.
- [60] Landers, J. P., Editor, *Capillary and Microchip Electrophoresis and Associated Microtechniques*, 2008.
- [61] Vandaveer IV, W. R., Padas-Farmer, S. A., Fischer, D. J., Frankenfeld, C. N., Lunte, S., M., *Electrophoresis* 2004, *25*, 3528-3549.
- [62] Roman, G. T., McDaniel, K., Culbertson, C. T., *Analyst* 2006, *131*, 194-201.
- [63] Zhang, C.-X., Manz, A., *Analytical Chemistry* 2001, *73*, 2656-2662.

- [64] Burnette, W. N., *Analytical Biochemistry* 1981, *112*, 195-203.
- [65] Mousseau, D. D., Rao, V. L. R., *Neuromethods* 1999, *34*, 167-191.
- [66] Cooper, A. J. L., Sheu, K.-F. R., Burke, J. R., Strittmatter, W. J., Gentile, V., Peluso, G., Blass, J. P., *Journal of Neurochemistry* 1999, *72*, 889-899.
- [67] Karpuj, M. V., Garren, H., Slunt, H., Price, D. L., Gusella, J., Becher, M. W., Steinman, L., *Proceedings of the National Academy of Sciences of the United States of America* 1999, *96*, 7388-7393.
- [68] Kahlem, P., Green, H., Djian, P., *Molecular Cell* 1998, *1*, 595-601.
- [69] Gentile, V., Sepe, C., Calvani, M., Melone, M. A. B., Cotrufo, R., Cooper, A. J. L., Blass, J. P., Peluso, G., *Archives of Biochemistry and Biophysics* 1998, *352*, 314-321.
- [70] Green, H., *Cell* 1993, *74*, 955-956.
- [71] Folk, J. E., Finlayson, J. S., *Advances in Protein Chemistry* 1977, *31*, 1-133.
- [72] De Montigny, P., Riley, C. M., Sternson, L. A., Stobaugh, J. F., *Journal of Pharmaceutical and Biomedical Analysis* 1990, *8*, 419-429.
- [73] Madou, M. J., *Fundamentals of microfabrication: The science of minaturization*, CRC Press 2002.
- [74] Manz, A., Graber, N., Widmer, H. M., *Sens. Actuators B* 1990, *1*, 244-248.
- [75] Jacobson, S. C., Hergenroder, R., Koutny, L. B., Ramsey, J. M., *Analytical Chemistry* 1994, *66*, 1114-1118.
- [76] Ohno, K.-i., Tachikawa, K., Manz, A., *Electrophoresis* 2008, *29*, 4443-4453.
- [77] Kalish, H., Phillips, T. M., *Journal of Separation Science* 2009, *32*, 1605-1612.
- [78] Phillips, T. M., Wellner, E., *Journal of Chromatography A* 2006, *1111*, 106-111.
- [79] Guzman, N. A., Blanc, T., Phillips, T. M., *Electrophoresis* 2008, *29*, 3259-3278.

Chapter 8
Part II: Conclusion and Direction of Future Research

8.1 Conclusion of Part II

The goal of the work performed for this part of this dissertation was the development of analytical methodology for the analysis of proteins by conventional and microchip electrophoresis. While these techniques have been employed for the separation of proteins [1-6], Western blot analysis remains one of the most widely used methods of analysis [7-9]. As a play on the name of the technique for DNA detection developed earlier by Edwin Southern [10-11], the Western blot is a well characterized, robust, and highly selective method of analysis. For these reasons (and others) it is heavily relied upon by researchers from many different fields of study. However when compared to microchip and capillary electrophoresis, Western blot analysis requires much larger sample and reagent volumes as well as a longer time of analysis.

Much of the work in the second half of the dissertation focused on the development of analytical methods for the analysis of proteins using capillary and microchip electrophoresis. The separation and detection of complex protein mixtures was optimized using a variety of electrophoretic separation modes and detection strategies. The knowledge gained from these experiments was used to develop an electrophoretic immunoaffinity assay for the detection of myc-tagged huntingtin protein expressed in cell culture. Following optimization of the procedure, the performance of the newly developed technique was directly compared to Western blot analysis.

Chapter 6 is a review of many commonly used electrophoretic methods of protein analysis. Not only does this chapter provide many published reports, it also contains original work performed using calmodulin (CaM) and several calmodulin-binding proteins (CaMBPs). The performance of various techniques such as capillary zone electrophoresis (CZE), micellar electrokinetic chromatography (MEKC), and capillary gel electrophoresis (CGE) were evaluated for the separation of protein mixtures. In addition, techniques such as isoelectric focusing (IEF), affinity capillary electrophoresis (ACE), and 2-dimensional electrophoresis were discussed. In general, it was observed that CZE was an effective separation technique to efficiently separate complex protein mixtures. However, because the mass-to-charge ratio of the analyte governs the separation mechanism of CZE, proteins must have sufficiently different ratios for efficient separation. In some instances, this ratio can be manipulated by adjusting the pH, ionic strength, or type of separation buffer. Proper buffer selection can also be effective in minimizing adsorption of proteins to the capillary wall. These effects were demonstrated by the separation of genetically modified CaM. Through the optimization of the separation buffer, the separation of CaM monomer, dimer, and aggregates were achieved.

While not generally thought of as an effective separation mode for proteins, the use of MEKC in both conventional and microchip electrophoresis has been demonstrated [12-14]. Despite these reports, extensive optimization of different buffer combinations and additives failed to produce a suitable separation of the different CaM species. The use of MECK was also evaluated for the separation of

several calmodulin-binding proteins (CaMBPs); however, an effective separation was never achieved. Another separation method that was evaluated was capillary gel electrophoresis (CGE). This technique is best suited for the size-based separation of proteins. Much like slab-gel electrophoresis, CGE uses a polymeric network to separate denatured proteins based on molecular weight.

The separation of CaM and several CaMBPs using CGE was demonstrated using both conventional and microchip electrophoresis. In addition, parameters such as separation efficiency, sensitivity, and time of analysis were directly compared with SDS-PAGE. It was determined that CGE was able to provide almost identical data to that obtained using SDS-PAGE; however, analysis by CGE had many advantages. Analysis by SDS-PAGE required 25 μL of sample, ~ 1 L of reagents, and ~ 24 hr for analysis whereas CGE used only 10 μL of sample, ~ 15 mL of reagents, and ~ 25 min for analysis. Furthermore, quantitation has the potential for greater accuracy in CGE than densitometry used in many slab gel electrophoresis techniques. Taken collectively, the experiments performed using these three techniques demonstrate the difficulty associated with the separation and detection of proteins.

Chapter 7 builds upon the work performed in the previous chapter through the development of an immunoaffinity assay for the detection of myc-tagged mutant huntingtin protein expressed in cell culture. This goal of this chapter was to develop a sensitive and selective assay which would be a high-throughput alternative to Western blot analysis. Mutant huntingtin (mHtt) protein which was expressed in cell culture was analyzed by Western blot, capillary electrophoresis, and microchip

electrophoresis. Two different strategies were employed for analysis and directly compared to Western blot analysis. First, the fluorogenic reagent naphthalene 2,3-dicarboxaldehyde (NDA) was used to derivatize protein samples for analysis by both conventional and microchip laser induced fluorescence (LIF). The second strategy utilized an anti-myc, FITC-labeled monoclonal antibody for the development of an immunoaffinity assay. The analytical performance of each technique was assessed and directly compared. It was observed that derivatization with NDA was not able to provide conclusive results by which mHtt could be identified and quantified. This is due to the lack of a purified mHtt standard which is needed for peak identification and signal calibration. Therefore, the results obtained using this strategy are only qualitative in nature.

The results from the immunoaffinity assay were less ambiguous. Much like the Western blot, this technique employed an anti-myc monoclonal antibody (mAb) directed against the myc tag on the mHtt protein. Therefore, it had an extremely high degree of specificity. The antibody was also labeled with FITC which made detection by LIF sensitive as well. Because the mass-to-charge ratio of the mAb is different than that of the mAb-mHtt complex, the separation of these two species is easily achieved using CZE. Furthermore, the amount of mHtt in the sample could be quantified through the construction of a calibration curve consisting of known quantities of FITC-labeled mAb.

This immunoaffinity technique was used to analyze samples with both capillary and microchip electrophoresis. While both techniques yielded similar

results, it was observed that microchip electrophoresis provided superior performance. Separation using CE resulted in increased band broadening and lower efficiencies than microchip electrophoresis. This effect is most likely the result of interactions between the proteins and the surface of the fused silica capillary. Due to differences in surface chemistry, the PDMS microchip did not produce a large amount of band broadening. This resulted in higher efficiencies and better peak shape during analysis. It was observed that both separation techniques yielded the same concentration limit of detection (LOD) of 5.5 $\mu\text{g}/\text{mL}$. However, microchip electrophoresis injects ~ 100 -fold less sample than CE for analysis, which resulted in a mass LOD of ~ 4.5 pg *versus* ~ 490 pg for CE.

This result highlights another distinct advantage of this technique. The Western blot is not able to quantitate the amount of mHtt whereas the immunoaffinity approach can. On the other hand, one distinct advantage of the Western blot is the higher degree of resolving power. The Western blot revealed the presence of aggregated mHtt species. However because the mHtt monomer, dimer, and trimer have almost identical mass-to-charge ratios, CZE was not able to separate these species. In summary, each technique has a unique set of advantages and disadvantages. Microchip electrophoresis is much faster but less precise. Western blot analysis provides much better resolution but is much more labor intensive and time consuming. Depending on the goals of the experiment, microchip electrophoresis provides a new analytical tool that is available to researchers not only for the detection of mutant huntingtin protein but feasibly for any myc-tagged protein.

8.2 Future Research Directions

8.2.1 Immunoaffinity using an Alternate Fluorophore

The use of a fluorescent label in the immunoaffinity experiments resulted in a high degree of sensitivity and selectivity. Fluorescein isothiocyanate (FITC) labeled mAb was used because this product was commercially available. In addition, the supplier was the same vendor from which the antibody used for the Western blot was purchased. Because antibody quality varies between supplier and source, this helped reduce the degree of variability between experiments. Furthermore, the supplier had pre-labeled the antibody with FITC and performed size exclusion chromatography to remove any unreacted FITC dye which greatly reduced the amount of time needed for sample preparation.

While FITC is routinely used for fluorescence experiments [15-18], alternate fluorophores which have superior characteristics are available. Fluorescent dyes such as PE-Texas Red [19], Belgian red [20], and Oregon Green [21] have very similar spectral properties and are routinely used for LIF detection. Another type of fluorescent probe which has become very popular is the Alexa Fluor family of dyes. This family of dyes, which spans the visible to infrared spectrum, is routinely used as cell and tissue as well as protein and peptide labels [22-24]. As seen in Figure 8.1, these probes are routinely used because they are less pH sensitive, more photostable, and have greater quantum efficiencies than many other comparable dyes [25-28].

Because these fluorescent probes have superior qualities than FITC, analytical sensitivity would be enhanced if these dyes were used for immunoaffinity experiment

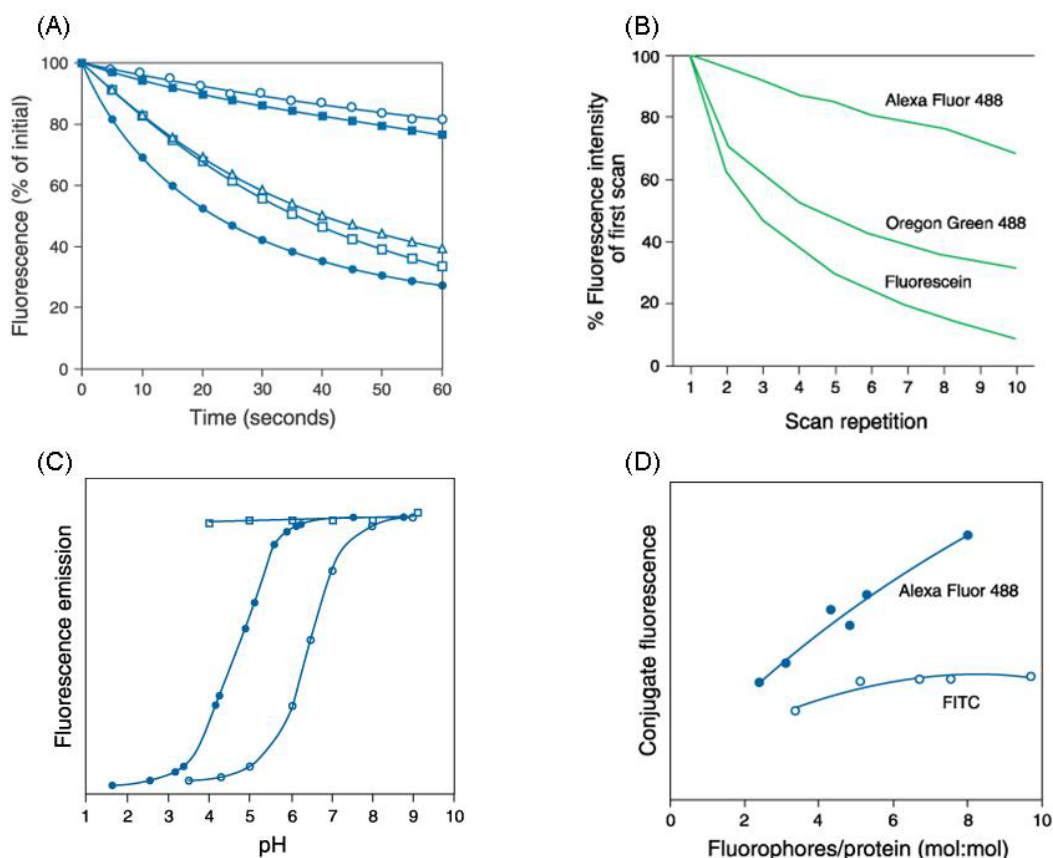


Figure 8.1: Comparison of the spectral properties of several fluorescein-based dyes and Alexa Fluor 488. (A) Comparison of the photostability of green fluorescent probes, (■) Oregon Green 514, (○) Alexa Fluor 488, (△) BODIPY, (□) Oregon Green 488, and (●) fluorescein; (B) resistance to photobleaching as a function of scan number; (C) comparison of the pH dependence of (●) Oregon Green 488, (○) carboxyfluorescein, and (□) Alexa Fluor 488; (D) comparison of the relative fluorescence of protein-fluorophore conjugates. Adapted with permission from refs [27-28].

instead of FITC. The enhanced quantum efficiency of Alexa Fluor would allow for expectedly lower concentration limits of detection. Guzman and Phillips have routinely labeled antibodies and target proteins for immunoaffinity experiments and have described a quick and simple procedure [24, 29-30]. To enhance durability, the intact antibody can be cleaved using pepsin to produce bivalent a F(ab)₂ fragment. Reduction with β-mercaptoethanol will produce identical monovalent Fab' fragments with a free sulfhydryl group at the opposite end. This free thiol can then be easily labeled with a variety of thiol-reactive dyes like Alexa Fluor 488 maleimide. This procedure could then be used to produce high quality fluorescent antibodies to improve the immunoaffinity experiment described in chapter 7.

8.2.2 Calmodulin Affinity Assay for Huntingtin Protein

One of the limitations of the mutant huntingtin isolation procedure outlined in chapter 7 was that the mHtt protein was not completely purified. Instead, the protein was merely isolated which required the downstream assay to include a high degree of specificity. However, if mHtt was completely purified, techniques such as derivatization with NDA would be more successful. Furthermore, there would be less interference and cross reactivity with other species in the sample when performing the immunoaffinity assay. One strategy that is commonly used to isolate proteins is affinity chromatography or affinity capture [31-34].

Huntingtin protein is also a known calmodulin-binding protein (CaMBP). Therefore, mHtt could be easily isolated using a CaM affinity assay. Several published reports detail the synthesis and use of a CaM affinity assay to isolate a

variety of CaMBPs [35-38]. This technique utilizes the high degree of specificity between CaM and target proteins and Ca²⁺-depending binding. Calmodulin is a ubiquitous signaling protein which can bind up to four Ca²⁺ ions. The binding of Ca²⁺ causes CaM to undergo a conformational change which increases its affinity for its target proteins. Affinity constants between 10⁻⁹ and 10⁻¹¹ M⁻¹ are observed for many CaMBPs. These two factors combined with the fact that CaM is known to interact with upwards of 300 different species make CaM affinity a popular choice for isolating many proteins of interest.

This approach would work well for the isolation of mHtt from cellular samples. The affinity procedure which has been previously described is shown in Figure 8.2 is fast and simple [39]. The lysate from cells that have been transfected with mHtt are incubated with CaM-agarose in a Ca²⁺ rich buffer. After incubating for a sufficient amount of time, the agarose-bound proteins are washed several times to remove excess cellular proteins and other non-CaMBPs. Proteins of interest are eluted using a buffer containing ethylene glycol tetraacetic acid (EGTA) and then collected for later analysis. Because there are a large number of CaMBPs in all cell types, this approach is not capable of purifying mHtt. However, this technique can dramatically decrease the amount of nonessential proteins and cellular debris and add additional degree of specificity in the development of an immunoaffinity assay.

Another potential application of this procedure is for the high throughput screening of peptides capable of interrupting the binding between CaM and mHtt. Muma and co-workers recently described a novel CaM construct capable of inhibiting

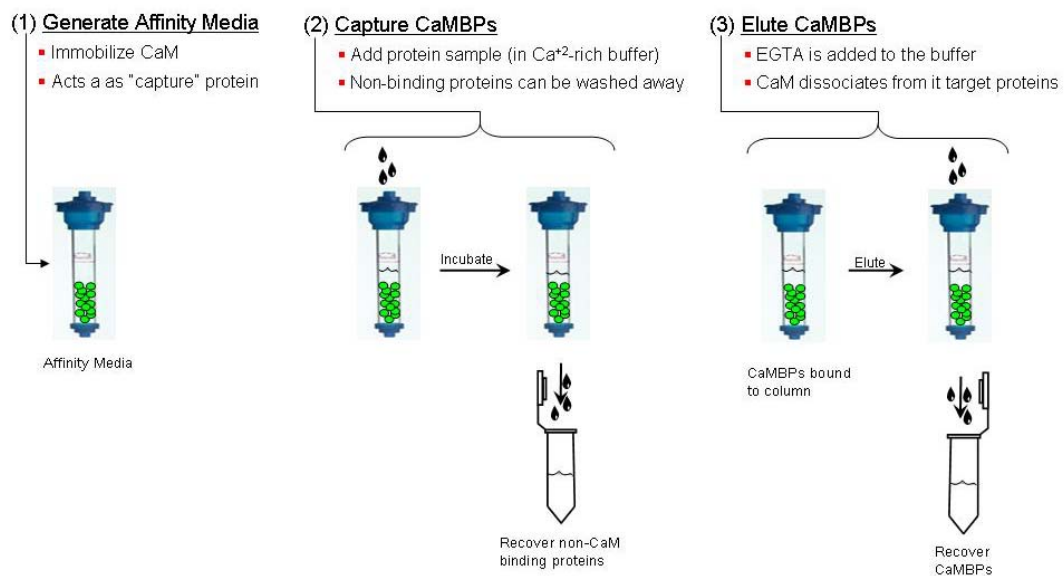


Figure 8.2: Calmodulin affinity assay protocol. (1) CaM is immobilized on a solid support and loaded into a column, (2) Calmodulin-binding proteins are captured due to Ca²⁺ dependent binding while non-CaMBPs are washed from the media, (3) CaMBPs are eluted from the media using a buffer containing EGTA.

the binding of CaM and mHtt *in vivo* [39]. The study examined the effects of small CaM fragments expressed in HEK cells expressing N-terminal mHtt as well as wild type CaM. Four different truncated versions of CaM were developed: the first 76 amino acids, the last 72 amino acids, 77 amino acids in the center (CaM-center), and the overlapping region of the last 72 amino acids and the CaM-center (CaM-overlap). The authors reported a 40% - 60% reduction in transglutaminase modified mHtt along with a 40% reduction in cytotoxicity. These results not only demonstrate the protective effects of disrupting the binding between mHtt and CaM, but point towards a potential therapeutic drug target.

Ongoing efforts have focused on the development of a small molecule or peptide capable of inhibiting his binding in the same manner as the CaM-overlap fragment. One of the major drawbacks of this strategy is the long analysis times associated with Western blot analysis. Therefore, the utilization of the CaM affinity assay in conjunction with microchip electrophoresis would provide a fast and simple analytical alternative to immunoblotting. Many smaller fragments of the CaM-overlap construct could be co-expressed with mHtt in cellular models. The cell lysates from each of these newly developed fragments could be subjected to the CaM affinity assay. Then analysis using the microchip immunoaffinity assay detailed in chapter 7 could be used to determine which CaM fragment was capable of inhibiting the binding between CaM and mHtt. This approach to screening of potential inhibitors would provide a higher-throughput analytical approach than standard Western blot analysis.

8.2.2 Photoaffinity Capture of Calmodulin-binding Proteins

One of the long term goals of this project is to be able to perform single cell analysis. As outlined in chapter 5, this goal requires many different components for success. A few of these components, such as off-line analysis of cellular analytes and the microfluidics involved in handling single cells are being actively pursued by current lab members. However, the ability to separate and detect mHtt in addition to other CaMBPs from a single cell has not been yet developed. One of the major challenges is the extremely small volume of a single cell. Because most mammalian cells contain between 10 fL and 1 pL, the CaM affinity assay described above is not a viable option for single cell analysis. An alternative to performing affinity chromatography is to capture proteins of interest using photoaffinity crosslinking. Crosslinking reagents have been used for the determination of three-dimensional structure, nearest neighbor relationships, and protein-protein interactions [40-43]. To effectively separate and detect mHtt, as well as other CaMBPs in single cells would require a photoaffinity strategy such as this.

The overall strategy would involve CaM which has been labeled with two different moieties and is shown in Figure 8.3. Calmodulin which was labeled with an optimized photo-reactive crosslinker as well as a fluorescent probe would serve two purposes. First, initiation of the crosslinking agent would result in the conjugation of CaM to its target proteins. Once crosslinked, the CaM-target complex could be separated by electrophoresis. Because CaM also contains a fluorescent probe, it could be easily detected using LIF. *In vitro* experiments are currently in progress in

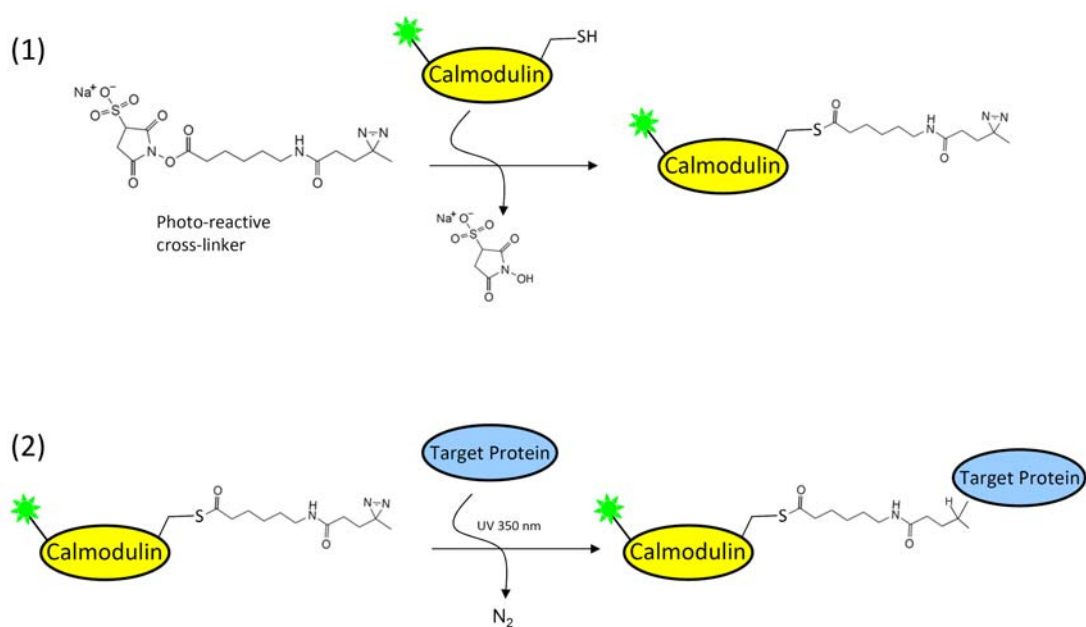


Figure 8.3: Schematic of the procedure for photo-reactive protein cross-linking. (1) The photo-reactive crosslinker reacts with fluorescently labeled calmodulin at a single cysteine residue in the protein. (2) After incubation with a protein mixture, calmodulin is cross-linked with its target protein(s) upon radiation with 350 nm UV light. Following cross-linking, the calmodulin-target protein complex can be separated and detected via LIF.

the laboratory of Carey Johnson at KU. His lab has previously described the development of a bi-functional CaM which contains two possible sites for derivatization [44-46]. CaM which was doubly labeled with two different fluorescent probes at opposite ends of the globular domains was used to demonstrate the existence of an unfolding intermediate. The current study has simply replaced one of the fluorophores with the crosslinking agent sulfo-NHS-LC-Diazirine (sulfo-LC-SDA). Incubation with endothelial nitric oxide synthase (eNOS), a known CaMBP, and irradiation with 320 nm light for 30 min resulted in efficient crosslinking as determined by Western blot analysis (data not shown). By transferring this approach to a separations-based method such as CE or microchip electrophoresis, CaM can be covalently linked to its binding partner and effectively detected using LIF. This strategy has an added benefit in that the researcher is not constrained by the separation conditions. If the CaM-target complex were not covalently linked, CZE would be the only possible separation mode. However since the two will not disassociate, other techniques such as MEKC or CGE could be employed which would be better suited for the analysis.

One of the main challenges associated with *in vivo* experimentation in single cells would be in delivering the modified CaM in the cell lumen. Unlike many FRET proteins such as green fluorescent protein (GFP) which can be expressed in the cell, doubly labeled CaM cannot. Therefore it must be delivered inside the cell by some mechanism. One strategy described by Ramsey *et al.* is the pinocytic loading of extracellular contents through the use of a hypertonic solution [47]. Initial

experiments in the lab of Chris Culbertson have successfully demonstrated the loading of Texas Red-labeled CaM into Jurkat cells. In this manner, doubly labeled CaM can be prepared and loaded into cells prior to the photoaffinity reaction and analysis. An alternative method which has been used extensively in cell biology is microinjection [48]. While this approach is not feasible for a large number of cells, a recent report by Jensen and co-workers has described the fabrication of a microfluidic chip capable of online microinjection [49]. This device is capable of cell handling, injection, and analysis. A slight modification of this strategy would be required for the photoaffinity experiments. The cells would need to be incubated in an additional reservoir so that the injected CaM could equilibrate inside the cell. By doing this, a more accurate representation of the proteins it associates with could be derived. Once all of these individual aspects are optimized, the goal of a single cell analysis system for the analysis of CaMBPs could be realized.

8.3 References

- [1] Chen, H., Fan, Z. H., *Electrophoresis* 2009, 30, 758-765.
- [2] Dolnik, V., *Electrophoresis* 2006, 27, 126-141.
- [3] Hempe, J. M., *Handbook of Capillary and Microchip Electrophoresis and Associated Microtechniques (3rd Edition)* 2008, 75-107.
- [4] Dolnik, V., *Electrophoresis* 2008, 29, 143-156.
- [5] Nagata, H., Tabuchi, M., Hirano, K., Baba, Y., *Electrophoresis* 2005, 26, 2687-2691.
- [6] Peng, Y., Pallandre, A., Tran, N. T., Taverna, M., *Electrophoresis* 2008, 29, 157-178.
- [7] Kegel, K. B., Meloni, A. R., Yi, Y., Kim, Y. J., Doyle, E., Cuiffo, B. G., Sapp, E., Wang, Y., Qin, Z.-H., Chen, J. D., Nevins, J. R., Aronin, N., DiFiglia, M., *Journal of Biological Chemistry* 2002, 277, 7466-7476.
- [8] Karpuj, M. V., Garren, H., Slunt, H., Price, D. L., Gusella, J., Becher, M. W., Steinman, L., *Proceedings of the National Academy of Sciences* 1999, 96, 7388-7393.
- [9] Kahlem, P., Green, H., Djian, P., *Molecular Cell* 1998, 1, 595-601.
- [10] Southern, E. M., *Journal of Molecular Biology* 1975, 98, 503-517.
- [11] Southern, E. M., *Biotechnology* 1992, 24, 122-139.
- [12] Xu, Y., Li, J., Wang, E., *Journal of Chromatography A* 2008, 1207, 175-180.
- [13] Roman, G. T., Carroll, S., McDaniel, K., Culbertson, C. T., *Electrophoresis* 2006, 27, 2933-2939.
- [14] Michels, D. A., Hu, S., Dambrowitz, K. A., Eggertson, M. J., Lauterbach, K., Dovichi, N. J., *Electrophoresis* 2004, 25, 3098-3105.
- [15] Meagher, R. J., Light, Y. K., Singh, A. K., *Lab on a Chip* 2008, 8, 527-532.
- [16] Wu, G., Li, Z., *Journal of Experimental Biology* 2009, 212, 2176-2182.
- [17] Wang, C., Prossnitz, E. R., Roy, S. K., *Endocrinology* 2008, 149, 4452-4461.
- [18] Wang, Q., Luo, G., Yeung, W. S. B., *Journal of Liquid Chromatography & Related Technologies* 1999, 22, 3129-3137.
- [19] Chen, X., Wu, H., Mao, C., Whitesides, G. M., *Analytical Chemistry* 2002, 74, 1772-1778.
- [20] Ferrari, B. C., Attfield, P. V., Veal, D. A., Bell, P. J., *Journal of Microbiological Methods* 2003, 52, 133-135.
- [21] Liyanage, M. R., Zaidi, A., Johnson, C. K., *Analytical Biochemistry* 2009, 385, 1-6.
- [22] Lee, S. B., Hassan, M., Fisher, R., Chertov, O., Chernomordik, V., Kramer-Marek, G., Gandjbakhche, A., Capala, J., *Clinical Cancer Research* 2008, 14, 3840-3849.
- [23] Sumner, J. P., Kopelman, R., *Analyst* 2005, 130, 528-533.
- [24] Phillips, T. M., Wellner, E., *Journal of Chromatography A* 2006, 1111, 106-111.

- [25] Berlier, J. E., Rothe, A., Buller, G., Bradford, J., Gray, D. R., Filanoski, B. J., Telford, W. G., Yue, S., Liu, J., Cheung, C.-Y., Chang, W., Hirsch, J. D., Beechem, J. M., Haugland, R. P., Haugland, R. P., *Journal of Histochemistry and Cytochemistry* 2003, *51*, 1699-1712.
- [26] Song, L., Hennink, E. J., Young, I. T., Tanke, H. J., *Biophysical Journal* 1995, *68*, 2588-2600.
- [27] Song, L., Hennink, E. J., Young, I. T., Tanke, H. J., *Biophysical Journal* 1995, *68*, 2588-2600.
- [28] Sjoeback, R., Nygren, J., Kubista, M., *Spectrochimica Acta, Part A: Molecular and Biomolecular Spectroscopy* 1995, *51A*, L7-L21.
- [29] Guzman, N. A., Phillips, T. M., *Analytical Chemistry* 2005, *77*, 60A-67A.
- [30] Kalish, H., Phillips, T. M., *Journal of Separation Science* 2009, *32*, 1605-1612.
- [31] Poetz, O., Hoeppe, S., Templin, M. F., Stoll, D., Joos, T. O., *Proteomics* 2009, *9*, 1518-1523.
- [32] Liang, S., Shen, G., Xu, X., Xu, Y., Wei, Y., *Current Proteomics* 2009, *6*, 25-31.
- [33] Arakawa, T., Kita, Y., Sato, H., Ejima, D., *Current Pharmaceutical Biotechnology* 2009, *10*, 456-460.
- [34] Roque, A. C. A., Lowe, C. R., *Methods in Molecular Biology* 2008, *421*, 1-21.
- [35] Sharma, R. K., *Journal of Biological Chemistry* 1990, *265*, 1152-1157.
- [36] Friedman, R. L., *Infection and Immunity* 1987, *55*, 129-134.
- [37] Ortega Perez, R., Irminger-Finger, I., Arrighi, J.-F., Capelli, N., van Tuinen, D., Turian, G., *European Journal of Biochemistry* 1994, *226*, 303-310.
- [38] Berggrd, T., Arrighi, G., Olsson, O., Fex, M., Linse, S., James, P., *Journal of Proteome Research* 2006, *5*, 669-687.
- [39] Dudek, N. L., Dai, Y., Muma, N. A., *Journal of Neuropathology & Experimental Neurology* 2008, *67*, 355-365.
- [40] Haberkant, P., van Meer, G., *Biological Chemistry* 2009, *390*, 795-803.
- [41] Robinette, D., Neamati, N., Tomer, K. B., Borchers, C. H., *Expert Review of Proteomics* 2006, *3*, 399-408.
- [42] Gimpl, G., Reitz, J., Brauer, S., Trossen, C., *Progress in Brain Research* 2008, *170*, 193-204.
- [43] De Meyts, P., *American Pharmaceutical Review* 2007, *10*, 63-66.
- [44] Johnson, C. K., *Biochemistry* 2006, *45*, 14233-14246.
- [45] Slaughter, B. D., Bieber-Urbauer, R. J., Johnson, C. K., *Journal of Physical Chemistry B* 2005, *109*, 12658-12662.
- [46] Slaughter, B. D., Unruh, J. R., Price, E. S., Huynh, J. L., Bieber Urbauer, R. J., Johnson, C. K., *Journal of the American Chemical Society* 2005, *127*, 12107-12114.
- [47] McClain, M. A., Culbertson, C. T., Jacobson, S. C., Allbritton, N. L., Sims, C. E., Ramsey, J. M., *Analytical Chemistry* 2003, *75*, 5646-5655.
- [48] Zhang, Y., Yu, L.-C., *BioEssays : news and reviews in molecular, cellular and developmental biology* 2008, *30*, 606-610.
- [49] Adamo, A., Jensen, K. F., *Lab on a Chip* 2008, *8*, 1258-1261.